MND-M-1814
REACTORS — POWER

PM-1 NUCLEAR POWER PLANT PROGRAM 3RD QUARTERLY PROGRESS REPORT 1 SEPTEMBER TO 30 NOVEMBER 1959

By
E. H. Smith
J. S. Sieg

March 1960
[TIS Issuance Date]

Nuclear Division
Martin Company
Baltimore, Maryland

UNITED STATES ATOMIC ENERGY COMMISSION
Technical Information Service

This report has been reproduced directly from the best available copy.

Printed in USA. Price $5.00. Available from the Office of Technical Services, Department of Commerce, Washington 25, D. C.

AEC Technical Information Service Extension
Oak Ridge, Tennessee

MND-M-1814

PM-1 Nuclear Power Plant Program

3RD QUARTERLY PROGRESS REPORT

1 September to 30 November 1959

Contract AT(30-1)-2345

Prepared By:

E. H. Smith

E. H. Smith

J. S. Sieg

J. S. Sieg

Approved By:

F. Hittman

F. Hittman
Project Manager

ABSTRACT

This report contains a description of the work accomplished during the third contract quarter (1 September to 30 November 1959) of Contract AT(30-1)-2345 between The Martin Company and the USAEC.

The objective of the contract is the design, development, fabrication, installation and initial testing and operation of a prepackaged air-transportable pressurized water reactor nuclear power plant, the PM-1. The specified output is 1 Mwe and 7 million Btu/hr of heat. The plant is to be operational by March 1962.

The principal efforts during the third project quarter were the furthering of the final design and preparation of specifications for some long-lead components. The entire power plant has been divided, for final design purposes, into 37 subsystems. The status of work on each subsystem at the close of the period is reported. A revised summary of design parameters is given, with flow diagrams of the primary and secondary systems. The most significant changes were in core design details and in the packaging and housing plan. A scheme for integral housing using the shipping containers for structural components was dropped, except for the decontamination package. The final design work will continue to be the main effort during the next report period.

Systems development work included preparations for full-scale structural testing of a test package, completion of the survey of incore instrumentation techniques, completion of development work on the reactor control and instrumentation system and further development of components for the steam generator, condenser and turbine generator which are not available commercially. The conclusions of the incore and control instrumentation work are summarized briefly.

Reactor development work included:

(1) Preparations for the flexible zero-power test (PMZ-1) program.

(2) Preparations for the revised fuel element irradiation test program.

(3) Continuation of reactor flow tests.

(4) Further work on the heat transfer test program, including evaluation and reporting of the seven-tube test section tests (SETCH-1) and design of a follow-up program and unit (SETCH-2).

(5) Completion of the single-tube test section program (STTS-2) and design of the follow-up STTS-3 and STTS-4 programs.

(6) Further work on the development and testing of magnetic jack-type control rod actuators.

Core fabrication commenced with delivery of the first batch of UO_2 and pilot runs of fuel element fabrication. Ultrasonic testing of selected pilot run fuel tubes was conducted. Work continued on study of control rod materials, UO_2 recovery techniques and boron analysis.

The Parametric Study Report, MND-M-1852, the Preliminary Hazards Summary Report, MND-M-1853, and the Preliminary Design Report (no number) were published during the period. For the preceding period, see MND-M-1813.

FOREWORD

This is the third quarterly progress report submitted to the U.S. Atomic Energy Commission under Contract AT(30-1)-2345. It covers the work accomplished by The Martin Company on the PM-1 Project for the period from 1 September through 30 November 1959.

CONTENTS

CONTENTS (continued)

CONTENTS (continued)

PROGRAM HIGHLIGHTS

1. The preliminary design of the PM-1 nuclear power plant was completed on schedule, submitted to the AEC for review and approved (Task 3).
2. The PM-1 hazards report was submitted to the AEC. (Task 17).
3. The Martin Company's packaging and housing plan for the PM-1 was presented in a Technical Memorandum (MND-M-1906) and reviewed by the AEC at a formal meeting on 29 October 1959. Changes in this area, resulting from this review, were made to the PM-1 program (Tasks 1 and 4).
4. The design of the PM-1 fuel element was established, UO_2 deliveries to The Martin Company were initiated and fuel element production for the critical experiment was begun (Tasks 2, 4 and 5).
5. As a result of a quarterly review meeting held on 15 October 1959, a redesigned version of the PM-1 core was approved for final design. (Task 4).
6. A recommendation to utilize 347 stainless steel as the PM-1 pressure vessel material was made to and approved by the AEC (Task 4).
7. A revised primary loop piping configuration and refueling procedure was completed and submitted to the AEC for approval.
8. A testing program was formulated for the air-steam condenser and was presented to and agreed to by, representatives of the AEC and Eglin Air Force Base. Construction of the test model was initiated (Task 1).
9. Design and hazards analysis work connected with the performance of the PM-1 critical experiments continued and neared completion. (Task 2).
10. A revised PM-1 program plan was submitted to and approved by the AEC.

INTRODUCTION

This is the third of 12 quarterly progress reports required by Contract AT(30-1)-2345 between The Martin Company and the USAEC.

During the third quarter, Tasks 1, 2, 4, 5, 11, 14, 15, 16 and 17 were active. Procurement of tubing for fabrication of the dummy core under Task 6 and initiation of procurement action under Task 7 were begun (not reported as yet). Task 13 will become active during the next quarter.

Blank Page

PM-1 NUCLEAR POWER PLANT DESIGN SUMMARY

A. REACTOR DESIGN CHARACTERISTICS

1. Overall Performance Data

Pressurizer water, nominal operating pressure (psia)	1300
Design pressure for heat transfer analysis (psia)	1200
Design pressure for structural analysis (psia)	1485
Average core coolant temperature, nominal (°F)	463
Reactor thermal power, nominal (megawatts)	9.37 ←
Reactor thermal power, design (megawatts)	10.31←
Core life, nominal (megawatt-year)	18.74←

2. Core Design Characteristics

Geometry, right circular cylinder (approximately)	
Diameter, average (inches)	23
Active length (inches)	30
Overall length (inches)	33-1/4←
Core structural material	Stainless steel
Fuel element data, tubular, cermet-type	
Outside diameter (inches)	0.500
Inside diameter (inches)	0.416
Clad thickness (inches)	0.006
*Clad material	AISI type 347 stainless steel, modified, 0.01 weight % Co, maximum, 0.02 weight % Ta, maximum
*U-235 loading/tube (grams)	$38.6^{+1.5}_{-0}$

* Denotes new items added to major plant parameters.
→ Denotes change in plant parameter from previous submission.

Number	727←
Meat composition, weight % UO_2	27.5
*Burnable poison element data, tubular, alloy-type	
Outside diameter (inches)	0.500
Clad thickness (inches)	0.006
Clad material	AISI type 347 stainless steel, modified, 0.01 weight % Co, maximum, 0.02 weight % Ta, maximum
Boron loading (natural) grams/tube in stainless steel alloy	$3.675 \begin{smallmatrix} + 0.184 \\ - 0.184 \end{smallmatrix}$
Number	75
*Control element data, Y-shaped, cermet-type	
Arm length--total overall from pickup ball centerline (inches)	38-3/8
--active (inches)	30
Arm width--total (inches)	3-7/8
--active poison (inches)	3-1/2
Arm thickness (inches)	5/16
Clad thickness(inches)	0.030
Clad material	AISI type 347 stainless steel, modified, 0.01 weight % Co, maximum 0.02 weight % Ta, maximum
Poison element	Eu_2O_3
Number	6

3. Core Heat Transfer Characteristics

Heat flux (Btu/ft^2-hr)	
Average	73,000←
Average coolant temperature (°F)	463

4. Reactor Hydraulic Characteristics

Coolant flow rate (gpm)	2125←

B. SYSTEMS DESIGN

1. General Plant

Reactor power output, nominal (megawatts)	9.37←
Steam generator power output, nominal (megawatts)	9.37←

Steam pressure, full power, minimum (psia) (saturated)	300
*Steam pressure, zero power, maximum (psia)	485
Steam quality, full power, maximum	1/4% moisture

2. Main Coolant System

Number of coolant loops	1
Coolant flow rate (gpm)	2125
Coolant system design pressure (psig)	1485
Coolant velocity in piping (main loop) (feet per second)	26
Coolant pipe size, main loop, (inches) nominal, Schedule 80	6
System basic material	
Reactor pressure vessel	AISI 347
Piping	AISI 316
Remainder	AISI 304
Main coolant pumps	
Pumps, number (canned rotor type)	1 ←
Steam generator	
Number of units	1
Design pressure (shell side) (approximately) (psi)	600
Type	Vertical with integral steam drum and separators
Temperature primary inlet, full power (approximately) (°F)	479
Temperature primary outlet, full power (approximately) (°F)	447
Temperature steam side outlet, full power (°F)	417
Access	Shell and tube side bolted
*Tube material	Inconel

3. Pressurizing and Pressure Relief System

Number of pressurizers	1
Type	Steam
Temperature, normal (°F)	577
Pressure, normal (psia)	1300
Pressure element (decreasing)	Water spray head
Pressure element (increasing)	Electric immersion heaters

* Denotes new items added to major plant parameters.
→ Denotes change in plant parameter from previous submission.

4. Coolant Purification and Sampling System

Number of purification loops	1
Purification device	Ion exchange resin
Inlet temperature to ion exchanger (maximum) (°F)	120←
Maintenance provisions	Recharge with fresh resin←

5. Primary Shield Water System

Primary shield water cooler	Air blast type
Purification loop	Ion exchange resin
Maintenance provisions	Recharge with fresh resin←

C. SECONDARY SYSTEM

1. General Plant

Steam flow, full power (lb/hr)	34,312←
*Steam flow, turbine, full power (straight condensing) (lb/hr)	26,253
*Steam flow to evaporator-reboiler, full load (lb/hr)	7859
Steam pressure, full power, dry and saturated, (psia)	300
Feedwater flow, full power (lb/hr)	34,512←
Rated gross electrical output, 0.8 pf(kw)	1250
Net electrical output, 0.8 pf (kw)	1000
Line voltage	4160/2400
Cycles	60
Phases	3
Auxiliary equipment voltage	480
Process heat, 6815 lb/hr of 35 psia dry and saturated steam (Btu/hr)	7×10^6
Design elevation (feet)	6500
Auxiliary power (approximately) (kw)	135

2. Turbine Generator Set

Type	Horizontal, single extraction turbine

* Denotes new items added to major plant parameters.
→ Denotes change in plant parameter from previous submission.

*Number of stages	5
Throttle pressure, full power (psia)	290
*Extraction steam pressure, full load (psia)	90
*Extraction steam flow, full load (lb/hr)	3224
Turbine steam exhaust conditions, full power	
Pressure (inches Hg abs)	9
Moisture (%)	12.2
Lube oil cooler, type	Air cooled
Turbine speed (rpm)	8050 ←
Generator rating (kva)	1562.5
Generator rating, 0.8 pf (exclusive of excitation power) (kw)	1250
Generator type	Salient pole
Generator speed (rpm)	1200

3. Condenser System

Number of units	2
Type	Direct air to steam
Duty--heat rejected, full load, per unit (Btu/hr)	10.1×10^6
*Design heat load per unit (Btu/hr)	10.4×10^6
*Tubes	Horizontal, finned aluminum

4. Feedwater System

Deaerator	
Type	Atomizing
Feedwater design flow (lb/hr)	37,912 ←
Design pressure (psia)	50
Oxygen removal guarantee (cc/liter remaining)	0.005
Storage (minutes)	5
Boiler feed pumps	
Number	2
Drivers	One steam driven, one electrical driven
Type	Vertical, centrifugal
Closed feedwater heaters	
Number	1
Type	Tube and shell, horizontal

* Denotes new items added to major plant parameters.
→ Denotes change in plant parameter from previous submission.

5. Auxiliaries

Evaporator Reboiler	
Capacity (lb/hr of 35 psia steam)	7500
Design pressure (psia)	65
Make-up water temperature (minimum) (°F)	40
Condensate return temperature (°F)	172←
Feedwater storage tank	
Capacity (approximately) (gal)	2100←
Turbine steam bypass system	
Type	Manual with de-superheater station
Auxiliary generator unit	
Type	Hi-speed diesel
Number	1
Capacity (kw)	150
Electrical characteristics	480 volts, 60 cps, 3 phase
Emergency power	
DC power source	Batteries
AC power source	2-unit MG set
*Capacity at 8-hour discharge rate (ampere-hour)	160

D. PACKAGING

*Number of shipping packages in basic plant (exclusive of housing and site preparation):

	Uncontained	Contained
Primary loop packages including waste disposal system	5	7
Secondary loop packages	8	8
Decontamination package	1	1

* Denotes new items added to major plant parameters.
→ Denotes change in plant parameter from previous submission.

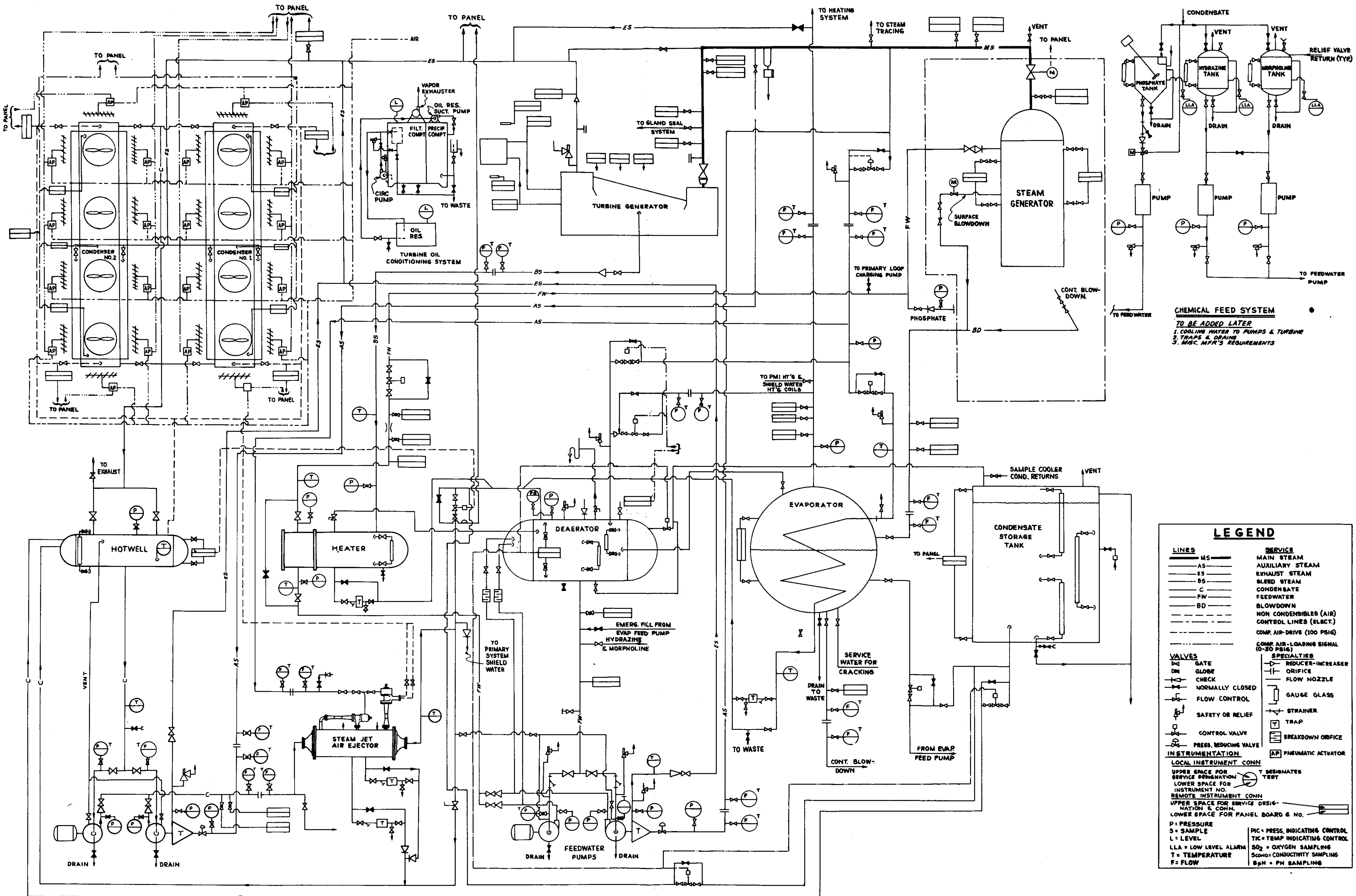

Fig. 2. Flow Diagram of Secondary System

I. TASK 1--PRELIMINARY DESIGN--SYSTEM DEVELOPMENT

Project Engineers--Subtasks 1.3: R. Akin; 1.2, 1.5: G. Zindler; 1.1, 1.6: C. Fox

A. SUBTASK 1.1--PACKAGE DEVELOPMENT AND TEST

J. Cosby, A. Layman

During the third quarter, planned objectives were to complete the final package test specifications, the detail test schedule and the final test package design. These were accomplished. In addition, the test program was modified to include changes which developed from a packaging and housing review meeting with the AEC at Germantown on 29 October 1959. Accordingly, the test program deals with shipping packages rather than the integral housing concept and incorporates the following tests on a full scale mockup of the Heat Transfer Apparatus Package*:

(1) Structural element tests to ultimate conditions.

(2) Handling and load tests of a mockup of the Heat Transfer Apparatus Package to limit conditions:

  (a) Hoisting tests.

  (b) Supporting skid at center and one end.

  (c) Supporting skid at ends.

  (d) Skid tie-down fitting tests.

(3) Impact and drop tests of the mockup of the Heat Transfer Apparatus Package to limit conditions (i.e., handling and simulated shipping loads):

  (a) Uniaxial impact tests.

  (b) Edge drop tests.

  (c) Corner drop tests.

(4) Weather protection tests of the mockup of the Heat Transfer Apparatus Package:

  (a) Snow load test.

  (b) Rain leakage test.

*Substantial changes have been made since the test program outlined in the second quarterly report was prepared.

(5) Static load and drop tests of the mockup of the Heat Transfer Apparatus Package using one insulated side as designed for the Decontamination Package:

(a) Hoisting of skid.

(b) Edge drop test.

(c) Corner drop test.

(6) Static load, impact and drop test of the mockup of the Heat Transfer Apparatus Package to ultimate conditions (i.e., simulated aircraft emergency landing loads):

(a) Vertical drop test (applied statically).

(b) Edge drop test.

(c) Corner drop test.

(d) Uniaxial impact.

(7) Vibration survey test on Heat Transfer Apparatus Package mockup.

As noted in the above listings, testing of the Heat Transfer Apparatus Package mockup includes two drop tests and one maximum bending test using one insulated side panel from the Decontamination Package. This is to ensure the structural adequacy of the insulated, integrally housed type of structure to be used in the Decontamination Package.

Test program objectives established for the coming quarter are:

(1) Design of the test apparatus and fixture will continue.

(2) Fabrication of the test fixtures will start.

(3) Test package fabrication will start.

B. SUBTASK 1.2--INCORE INSTRUMENTATION

J. Henry, R. Hradsky

The objectives of Subtask 1.2 are to evaluate methods for measuring fuel element temperature, coolant channel flow, local neutron flux and other operating core parameters of interest, and recommend the approach that would result in incorporation of certain of these methods into the design of a PM-1 instrumented core. The subtask was nearly complete at the end of the project quarter and will be entirely completed during the next quarter. A technical memorandum will be prepared to report the findings.

Evaluation of information compiled from The National Reactor Test Station, Idaho, and elsewhere has been completed. Based on knowledge of methods and analyses previously used, the most meaningful measurements which can be made for advance core design purposes in the PM-1 core are:

(1) Inside surface temperature of the fuel element.

(2) Coolant temperature along the fuel element.

(3) Coolant flow rates inside of fuel tube.

(4) Coolant flow rates outside of fuel element.

(5) Thermal neutron flux measurements.

1. Inside Surface Temperature of the Fuel Element

Three methods of installing thermocouples to obtain this measurement were devised. Only one of these methods was acceptable from the standpoint of reliability and economy. A description of the most promising method follows.

An accurate fuel element metal temperature measurement can be obtained by forcing the heat flow from the fuel to the outer surface of the fuel tube only. This unidirectional heat flow is obtained by blocking the coolant flow along the inside of the fuel tube. With the blocked internal coolant flow, the center of the fuel tube will operate at a constant temperature equal to the meat temperature. Therefore, a thermocouple attached to the inside cladding will provide an accurate, steady temperature reading.

To block the internal coolant channel, the inside of a special fuel tube is filled with powdered alumina. Alumina was selected as the filler because of its radiation stability and because it can be used at temperatures above the coolant water temperature of the reactor.

The thermocouple leads are welded to the inside clad of the fuel element and then led out to the end of the fuel tube through the alumina. To further increase the accuracy of the measurement, the thermocouple is preshaped so that the leads run normal to the surface at the point of attachment and into the alumina filler before bending parallel to the axis of the fuel tube. This places the first one-fourth inch (approximately) of the thermocouple lead along a path of essentially constant temperature and greatly reduces the effect of the thermocouple lead conducting heat away from the thermojunction.

Several thermocouples can be spaced along the internal cladding of the instrumented fuel tube. By placing the thermocouples in the alumina-filled center of the fuel element, sufficient space is available to permit using larger diameter (0.067 inch) thermocouple leads for more reliable operation.

The methods that were evaluated and rejected were:

(1) The installation of thermocouples inside the meat of the fuel element. This method was not acceptable because of uncertainties of the thermocouple location within the fuel in the fuel element.

(2) Use of a keyway on the outer clad of the inner surface and increasing the thickness of the outer clad. This method was not acceptable from an economic standpoint because of the cost of special swaging equipment required.

2. Coolant Temperature Along the Fuel Element

The method selected to measure this temperature was to utilize one of the three structural tubes in the center bundle. Thermocouples are inserted down through the inside of the tube from the outlet end and protrude through holes drilled in the tube at right angles to the axis of the tube. This will provide thermocouples in the coolant stream near the fuel element.

3. Coolant Flow Rates Inside of Fuel Element

Two methods to measure flow rates inside of a fuel element are discussed below:

(1) A flow tube can be inserted into one of the three structural tubes in the center bundle. Because the flow tube will be installed in one of the structural tubes instead of a fuel element, the actual flow characteristics will be slightly different. This difference can be determined by experiment and a correction factor can be applied. The effect of the flow tube on the actual flow rate can also be determined experimentally and a correction can be made. This is a widely used and successful method of flow rate measurement.

(2) The static-dynamic pressure tap method can be used. A structural tube in the center is used here also. In this method, small diameter tubing is fastened along the outside of the structural tube to a predetermined location and inserted through holes drilled into the structural tube.

Both methods (1) and (2) are considered feasible on the basis of this study.

4. Coolant Flow Rates Outside the Fuel Element

The selected method to acquire flow rate outside of the fuel element is as follows:

The static-dynamic pressure tap method would be used to obtain this measurement. The same structural tube could be used for the outside measurement as for the inside measurement. Small diameter tubing will be inserted into the structural tube from the outlet end and will protrude through holes drilled into the tube at right angles to the axis of the tube. This method of obtaining outside tube flow measurements will be used in the gross flow test.

5. Thermal Neutron Flux Measurements

Two possible methods of obtaining neutron flux measurements are as follows:

(1) Use of a neutron flux thimble containing activation wires. This method is considered impractical due to the lack of technical information on thimble design and the lack of any experience data as to the successful operations of these thimbles.

(2) Use of a miniature ion chamber. Due to the limited life of the ion chamber under high levels of neutron radiation, a method of inserting and withdrawing the chamber from the core is necessary. This would require an elaborate and expensive positioning mechanism to enable the chamber to be positioned precisely in the core. It would also require pressure vessel penetrations for access tubes to lower the chamber into the core, which would involve considerable core redesign. The ion chamber would be lowered into the core and the flux level would be indicated on a micromicroammeter. After the readings were taken, the chambers would be withdrawn from the core to an area of lower flux density. This method is presently being employed on the S-1-W core at Naval Reactor Facility, NRTS, Idaho, with good results. The miniature chamber being used is one developed by General Electric at their West Lynn Plant.

An alternate method of determining neutron flux is to measure decay gammas after reactor shutdown using a gamma-sensitive ion chamber or a scintillation counter. In this method, the chamber or counter would be inserted into the reactor core through an access port after reactor shutdown. The gamma level readings would then be used to calculate the average neutron flux level of the reactor during operation.

C. SUBTASK 1.3--SHIELDING MEASUREMENTS

This subtask has the objective of accomplishing the analysis of potential site shielding materials.

During the third project quarter, four core borings were selected from borrow area No. 2 at the PM-1 site*. Based on chemical and spectrographic analysis, this material was recommended for the back-fill material to be used around the PM-1 primary loop packages.

During the next quarter, activation analysis will be performed on borrow area No. 2 and borrow area No. 4 (plant site) samples at the MITR. If the activation analysis confirms the chemical data, borrow area No. 2 will be specified as the source of local shielding material at the site.

D. SUBTASK 1.5--INSTRUMENTATION AND CONTROL

G. Zindler

1. Research and Development Program

This subtask has the objective of developing an advanced, highly reliable instrumentation and control system which shall be easy to operate and maintain. The effort is subcontracted to the Stromberg-Carlson Corporation which is performing the development work and assembling the instrumentation specified by The Martin Company.

Work planned for this report period comprised:

(1) Completion by Stromberg-Carlson of their research and development efforts.

(2) Completion by Martin of the design of plant instrumentation and control (see Task 4).

The planned work was 90% completed during the quarter.

* See under Task 11 in the second quarterly progress report on the PM-1 program, MND-M-1813.

During the next project quarter:

(1) All efforts under the research and development program will be completed.

(2) A technical memorandum will be prepared, reporting the R&D program.

(3) The final design for instrumentation and control will be completed, incorporating appropriate findings of the R&D program.

During this reporting period, efforts continued on the Phase 2 (preparation and testing of breadboard models) portion of the instrumentation development program at Stromberg-Carlson. The major areas are the fabrication of models of the self-checking and fault monitoring systems and of the advanced reactor period measurement instrument. The breadboard models will serve to verify electronic circuit designs and demonstrate their operating features.

Tests to date indicate that the fault monitoring and self-checking systems will significantly reduce the time and skill required for the maintenance of the nuclear instrumentation. These systems will provide a "good-bad" type indication and location of faulty instrument modules. The operation of each of the major instruments will be continuously monitored in such a way as to warn the reactor operator of the instrument's deviation from normal operation in advance of complete failure.

The reactor period measurement instrument breadboard model was test operated at the Martin Critical Facility. Under test comparison with existing instruments, the new circuits indicate significant improvement in signal-to-noise ratio. This will result in a reduction of the number of instrument scrams during the startup phase of the PM-1.

2. Design of Instrumentation and Control System

As the individual instrument designs have been changed during the R&D program, efforts to integrate the new developments into the overall nuclear instrumentation system have followed. These include designing new modules and interconnecting the new circuits into existing control systems. In addition, cost comparisons are being prepared to ascertain the cost differential resulting from the changes.

At the completion of the R&D program, the inclusion of the improved items will be evaluated in terms of the relative cost. Each of the new developments is within a reasonable price range, considering the advantages gained. There also remains, following completion of the R&D program, final design of the developed instruments for field use.

E. SUBTASK 1.6--SECONDARY SYSTEM DEVELOPMENT

W. Koch, L. Hassell, R. Groscup, J. McNeil

The objective of this subtask is the development of components for the PM-1 Nuclear Power Plant Secondary System which are not commercially available.

Planned accomplishments during his period were:

(1) Completion of final steam generator basic design and final specifications (see discussion of Subsystem 6 under Task 4).

(2) Completion of the final condenser test model test procedure.

(3) Coordination of the condenser test model installation and test procedures with Eglin AFB personnel.

(40 Continuation of condenser model fabrication.

(5) Completion of control analysis work.

(6) Continuation of Secondary System design development with emphasis on the condenser and the turbine-generator.

(7) Completion of basic design and final, certified outline drawings for the switchgear and motor control center.

During the period, the following work was actually accomplished:

(1) Analysis of the feedwater control system was completed and is reported under Task 4, in this report.

(2) Westinghouse Corporation completed an analysis of the Secondary System during a 300-ekw step load change. This analysis includes the primary loop temperature transient resulting from the reference maneuver as furnished to Westinghouse by The Martin Company.

Following is the Summary of Conclusions portion of the Westinghouse Report*.

"Summary of Conclusions"

"The analysis of the secondary system during a 30% (300 kw) step load change yields the following conclusions:

(a) The worst condition of impact load will cause the steam pressure to dip 13 psi under the steady-state low pressure level. It might be possible to eliminate this pressure undershoot by using load "anticipation" feedback to reactor rod drive. However, this 13 psi pressure undershoot has such a minor effect on equipment size compared to the complication of rod drive feedback that it is undesirable.

(b) As a worst approximation (this worst condition exists when the condenser pressure control is inoperative during the transient), the condenser back pressure will increase by 5 inches of mercury above steady-state maximum.

(c) The voltage dip and recovery will meet the specifications through the use of the recommended magamp voltage regulator.

(d) No firm analytical conclusion can be reached concerning the type of speed regulation required. However, experience indicates that the speed regulation required can be met by use of the type EMM governor with reset and load anticipation from the 1250 kw generator." (See turbine control discussion under Task. 4.)

The analysis is presently being reviewed by Martin.

(3) The steam generator design (Westinghouse outline drawing, Fig. 1.1) and the Westinghouse draft of specification MN-7321 were completed, reviewed by Martin and accepted as complete (noted in Task 4, Subsystem 6, Part D).

(4) Design of the turbine generator unit (Westinghouse drawing, Fig. 1.2) continued and is now 90% complete. The design conditions are:

Rating:	1250 ekw
rpm:	8050/1200
Throttle pressure:	290 psia (saturated)
First stage:	90 psia, 1150 Btu/lb
Exhaust:	9 -in. Hg abs, 1007 Btu/lb

*"Martin PM-1 Secondary Plant Analysis," Report No. 10A, 19 October 1959.

Throttle flow (corrected to straight condensing at 1250 kw): 23,550 lb/hr.

The turbine expansion curves for 4/4, 3/4 and 1/2 loads were completed and are shown in Fig. 1.3.

(5) The certified outline drawings (Fig. 1.4) of the 30,000-square foot air cooled condenser were completed and are being reviewed by Martin.

(6) The 26,000-square foot condenser model fabrication by Westinghouse was started and is now 70% complete. Figure 1.5 shows the condenser model at 30% completion. Figure 1.6 is a perspective sketch of the condenser model.

(7) The entire condenser program was reviewed with AEC personnel at Germantown on 25 September 1959, and the test program was reviewed with Climatic Laboratory personnel at Eglin AFB, Florida, on 10 November 1959. The test program plan is essentially the same as reported last quarter and is complete with the exception of the detailed testing procedures from Westinghouse to be completed during the next quarter.

One additional test was added: Using the condenser bank with all fans off, close the two sections of louvers nearest the steam inlet and open the third set to a fully open position. Allow only enough steam flow into the condenser to maintain 9 inches Hg abs pressure. Check for freezing conditions in the open-louver tube bank area when a 100-mph wind is blowing across this tube bank section.

During the course of the above test, the operation of the dampers will be observed over a wide range of conditions, and the adequacy of the control system will be determined. Rate of damper operation may be varied by changing the supply air pressure. Several transients will be run to determine the required response time of the damper operators.

During the period that the climatic chamber is between +70 and -65° F, several tests will be conducted in order to anticipate any problems which may arise at the more severe ambient temperatures. Steady-state tests will be conducted at ambients of 0, -25 and -45° F. There will also be at least one startup at each of the above temperatures. This series of tests is intended to indicate the adequacy of the design at 70° F as well as at -65° F. During the course of testing, the problem of possible freezing at low ambients will certainly be encountered, and "bugs" in the system will have to be eliminated as the test program progresses.

(8) The design of the switchgear and motor control center is 80% complete and is to be completed next quarter with the submittal of certified outline drawings and wiring diagrams.

The following progress is anticipated in the next quarter:

(1) The condenser model will be completed and shipped to Eglin AFB, Florida.

(2) The condenser test will begin at the Climatic Laboratory, Eglin AFB.

(3) The certified outline drawings of the turbine-generator, switchgear and motor control center will be completed.

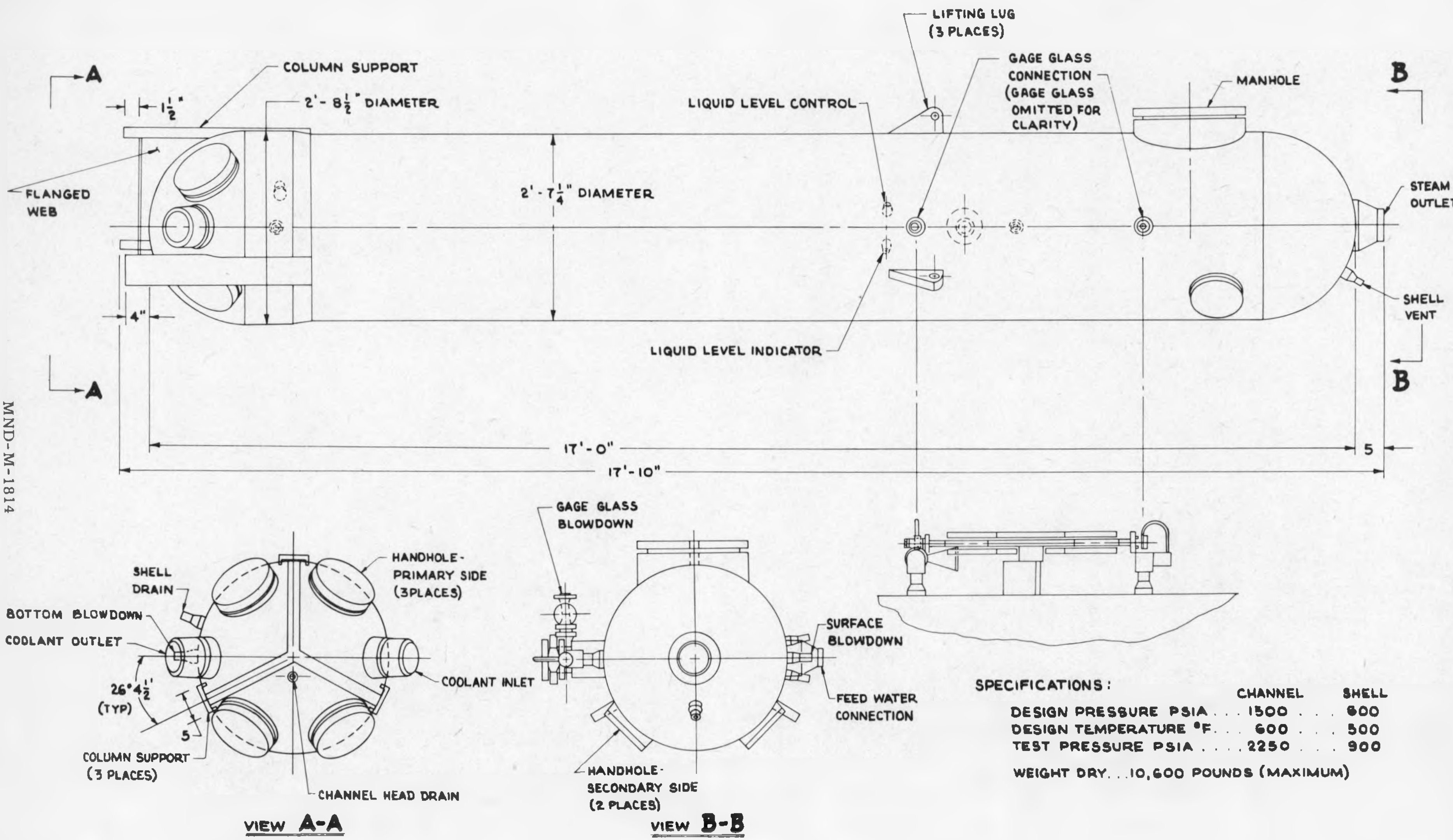

Fig. 1.1. Steam Generator

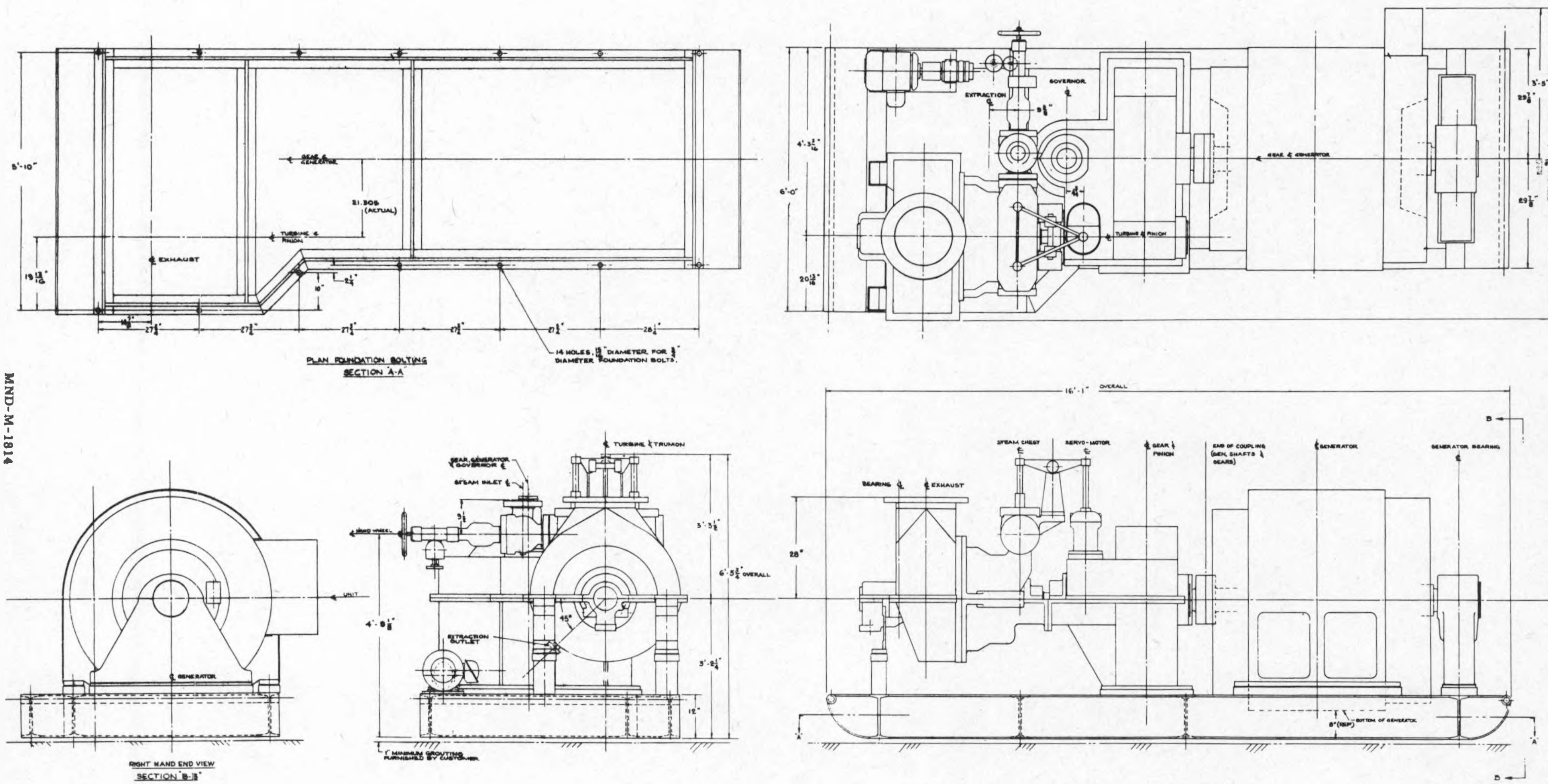

Fig. 1.2. Turbine and Generator Unit

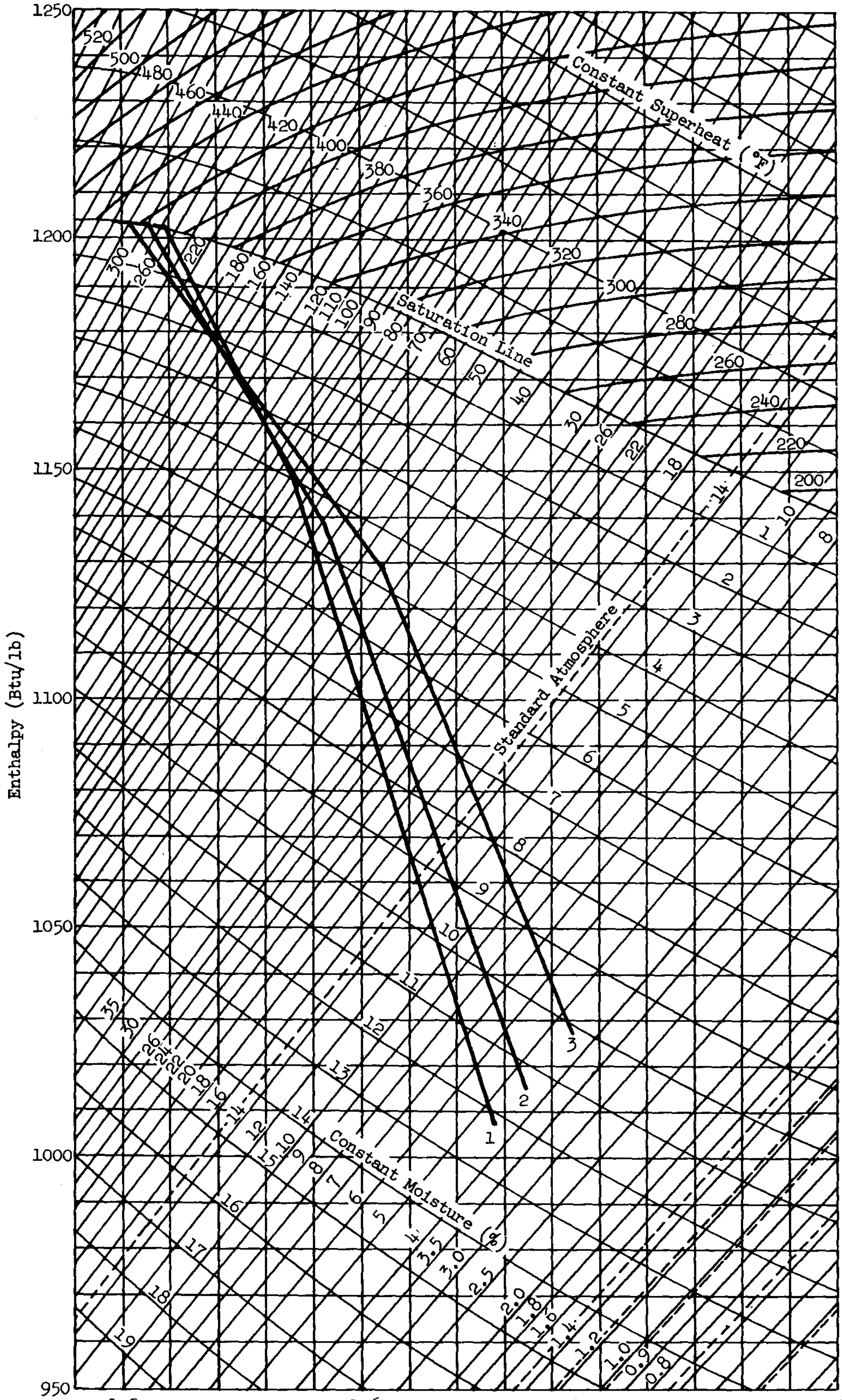

Rating: 1250 kw RPM 8050/1200
Steam generator pressure: 300 psia
Steam generator temperature: F D&S
Absolute exhaust pressure: 9-in. Hg (psi)

(straight condensing)

Expansion line	1	2	3
Load (kw)	1,250	938	625
Throttle flow (lb/hr)	23,553	18,649	13,701

Fig. 1.3. Mollier Chart, Turbine Expansion Lines

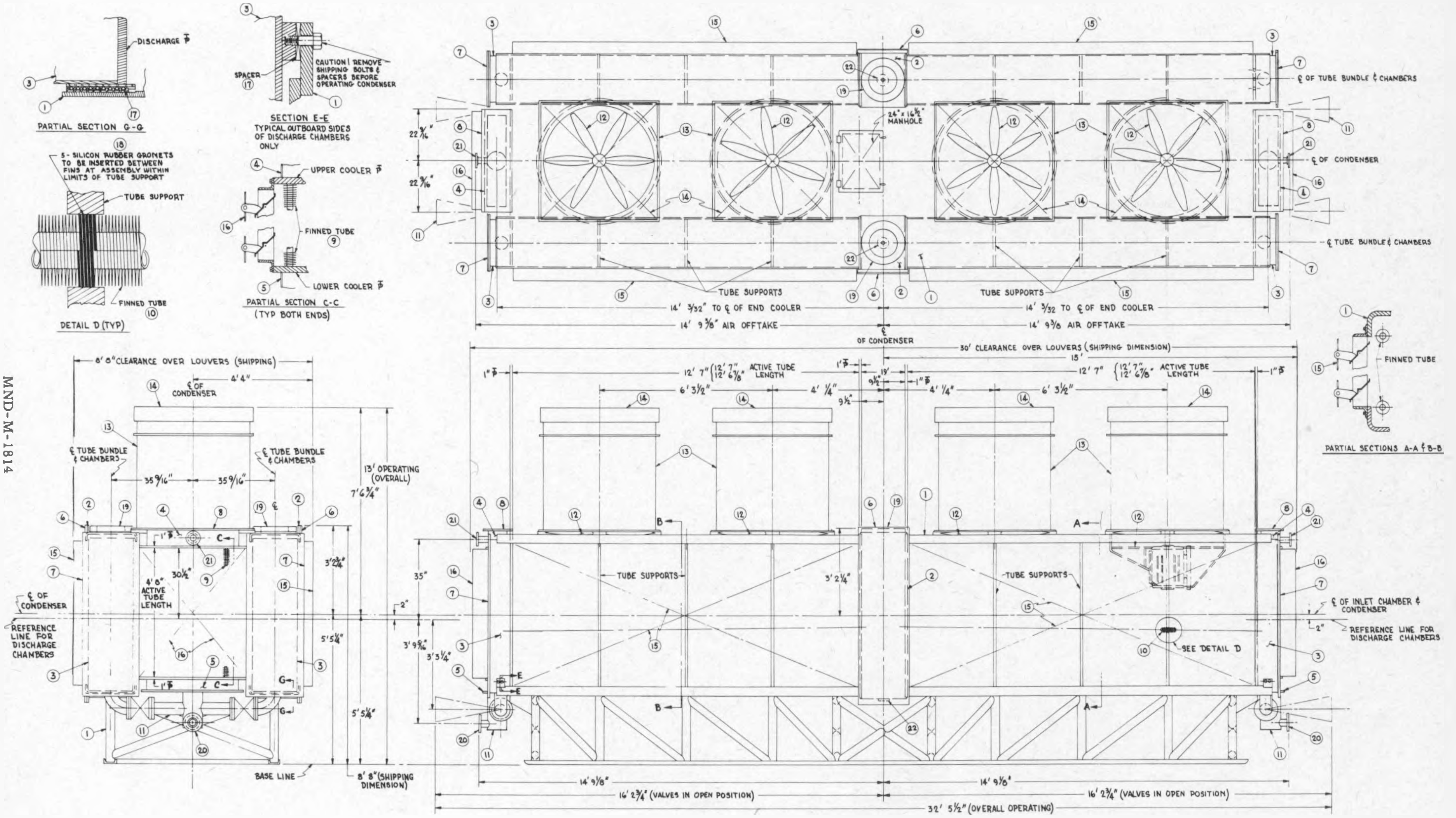

Fig. 1.4. Condenser Assembly

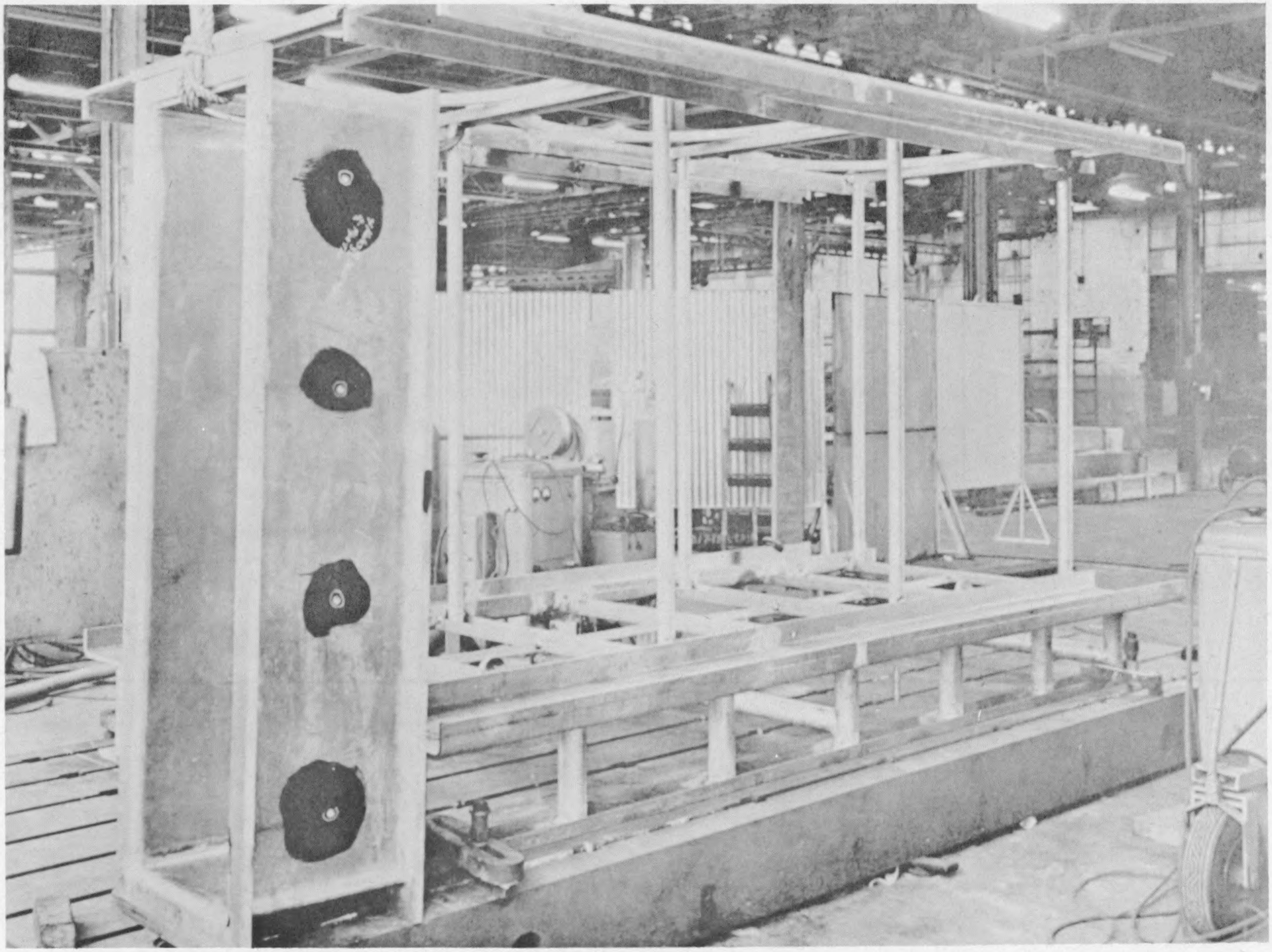

Fig. 1.5. Condenser Model (30% complete)

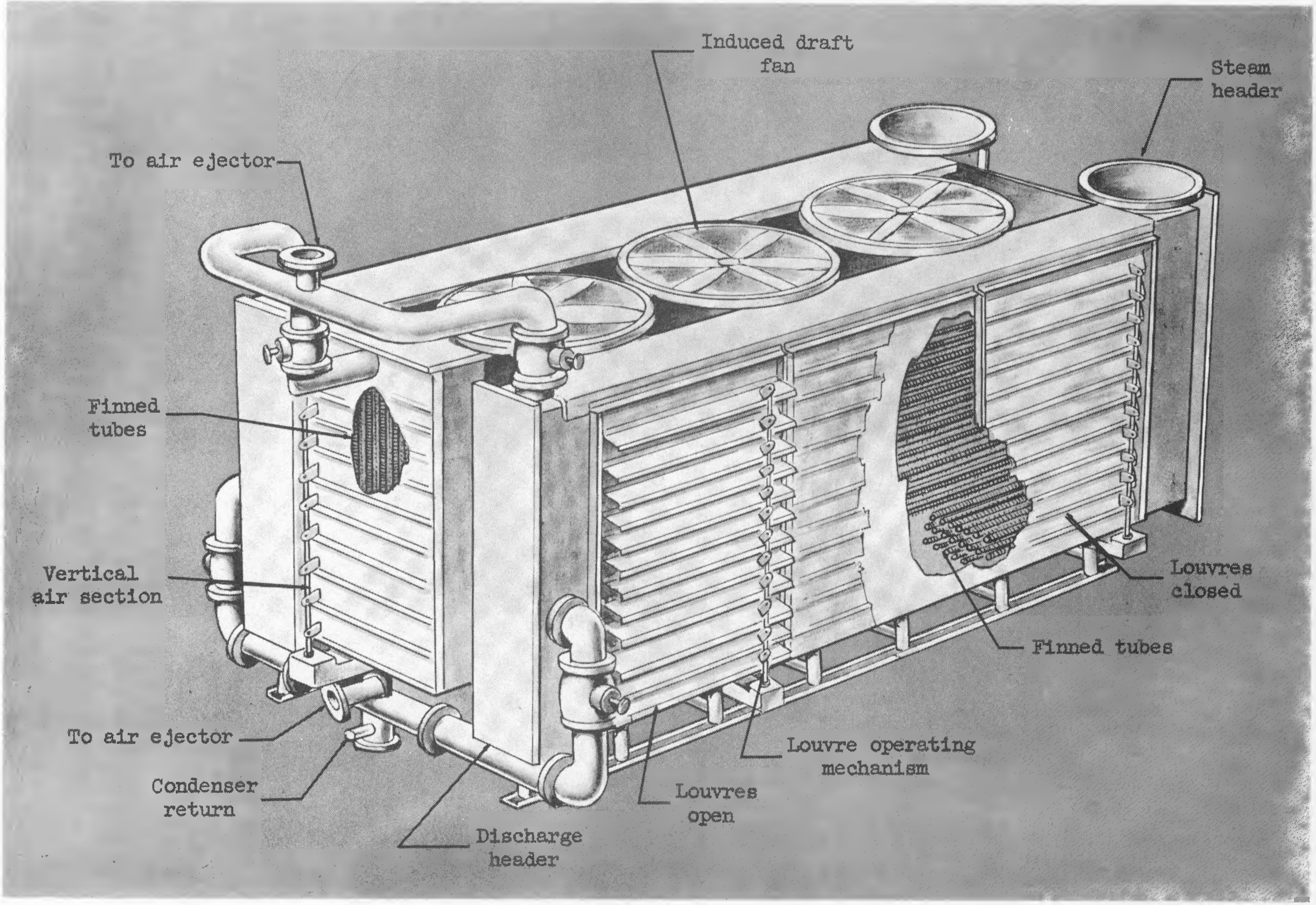

Fig. 1.6. Sketch of Condenser Model

II. TASK 2--PRELIMINARY DESIGN--REACTOR DEVELOPMENT

Project Engineer--Subtasks 2.1, 2.2, 2.3, 2.4: J. O'Brien
Subtask 2.5: R. Akin

The objective of this task is to provide for the performance of the necessary analytical and experimental investigations which are prerequisite to the PM-1 reactor design.

A. SUBTASK 2.1--FLEXIBLE ZERO-POWER TEST

H. B. Rosenthal, E. A. Scicchitano, R. Leavel

The objective of the flexible zero-power test is to provide experimental data to support the final core design of the PM-1 Nuclear Power Plant.

The work planned for this project quarter included:

(1) Completion of design of flexible zero-power test (PMZ-1) components.

(2) Initiation of procurement and fabrication of PMZ-1 components.

(3) Preparation of a detailed experimental program for final review in the PMZ-1 Hazards Summary Report.

(4) Preparation of the PMZ-1 Hazards Summary Report manuscript.

(5) Initiation of analysis on all PMZ-1 experiments requiring preliminary evaluation.

(6) Completion of the excursion analysis.

Actual accomplishments during this quarter were:

(1) The experimental program was detailed.

(2) The Hazards Summary Report was prepared.

(3) Fast flux measurements taken in the PPM-1 Core V were re-evaluated.

(4) Studies to determine the effect of one-, two- and three-group reflector savings on critical mass and full core reactivity were initiated.

(5) The effect of pressure vessel and thermal shield mockups on total core reactivity were examined.

(6) The excursion analysis for the PMZ-1 test was completed.

(7) The suitability of polypropylene for upper and lower grids in PMZ-1 was evaluated and found to be satisfactory.

(8) Design of the following components was completed:

(a) Core support structure

(b) Thermal shields and pressure vessel

(c) Upper and lower grids

(d) Fuel elements

(e) Removable fuel element bundles

(f) CE control rods

(g) Safety rods

(h) Revisions to prototype actuators.

(9) Material procurement and preparation for fabrication of the components were initiated.

During the next quarter, it is anticipated that:

(1) The Hazards Summary Report will be submitted to the AEC Licensing Branch.

(2) Design of all components will be completed.

(3) Fabrication of major components will be completed.

(4) Installation of major components will be about 80% complete.

(5) Studies will be completed to determine specifications for:

(a) Special fuel elements

(b) Special lumped poison rods

(c) Special safety and prototype rods

(d) Void devices.

(6) Pre-experiment analysis on all major experimental cores will be initiated and about 75% completed.

1. Pre-experiment Analysis

An outline of the experimental program was given in the second quarterly progress report (MND-M-1813). The basic program, as outlined, has not been changed. However, two modifications were made as follows:

(1) Determination of the effect of poison particle size on the behavior of poison lumps was eliminated as a result of the decision to use a boron steel alloy.

(2) Relatively large void fractions rather than the predicted local-boiling void distribution will be investigated since design studies indicated that the latter distribution effect was not measurable.

A study to determine the number of stainless steel shields needed in the flexible zero-power test core, PMZ-1, to adequately simulate the PM-1 design was completed. The effect on k_{eff} of successively adding an additional shield, as per the preliminary shield designs (Fig. 2.1), was calculated, using both two- and three-group, one-dimension diffusion theory calculations.

The changes in k_{eff} resulting from the addition of each region are given in Table 2.1.

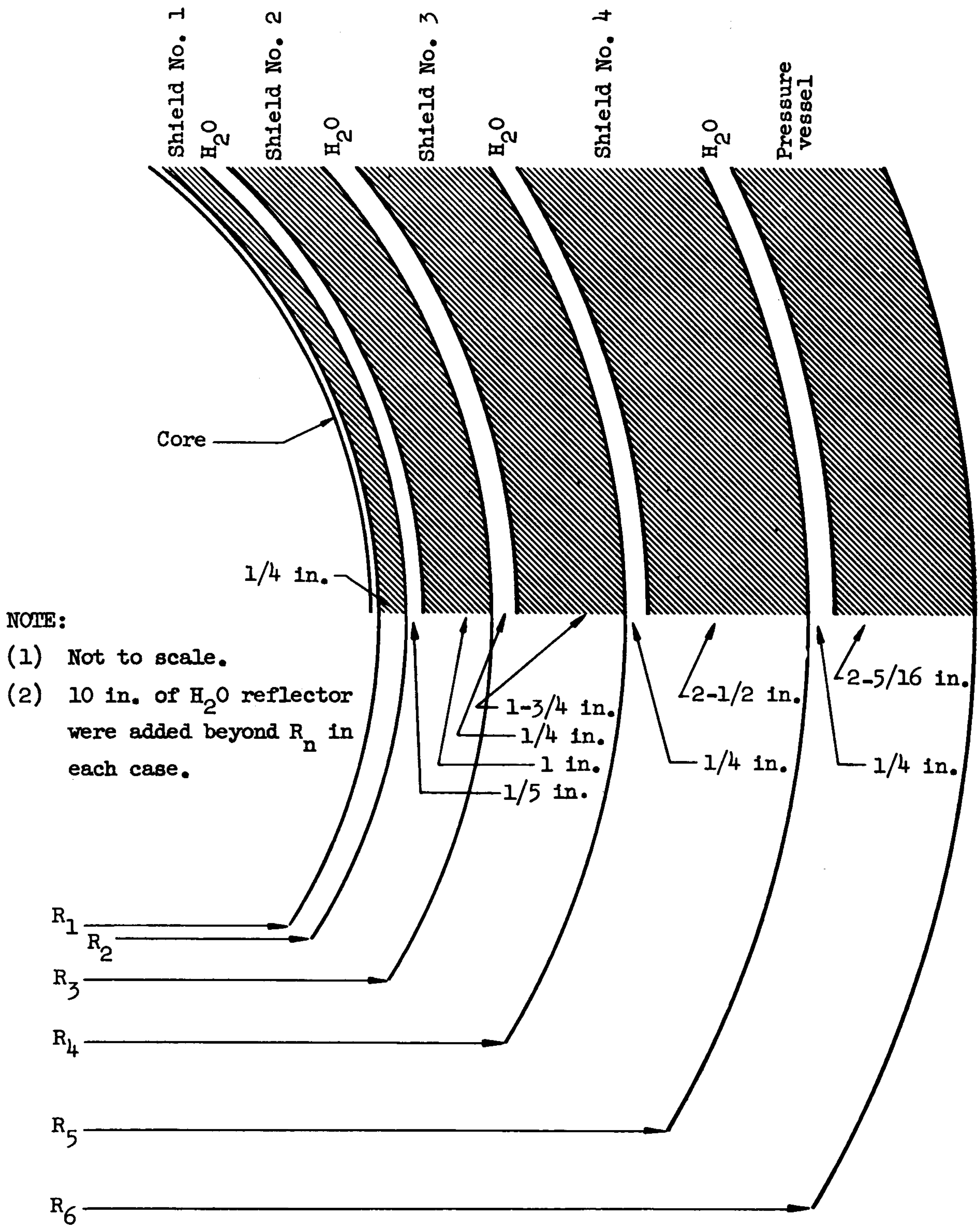

Fig. 2.1. Preliminary Design, Thermal Shield and Pressure Vessel

TABLE 2.1

Core and Shield Configuration (see Fig. 2.1)	Two-Group Calculation		Three-Group Calculation	
	$k_{eff_n} - k_{eff_1}$	$k_{eff_n} - k_{eff_{n-1}}$	$k_{eff_n} - k_{eff_1}$	$k_{eff_n} - k_{eff_{n-1}}$
R_1	0	0	0	0
R_2	-0.0053	-0.0053	-0.0048	-0.0048
R_3	-0.0015	+0.0038	+0.0013	+0.0051
R_4	+0.0050	+0.0035	+0.0090	+0.0078
R_5	+0.0088	+0.0038	+0.0128	+0.0038
R_6	+0.0101	+0.0013	-	-

The studies show a significant change in k_{eff} resulting from the addition of each of the first four shields. The change in k_{eff} resulting from the addition of the pressure vessel of 0.1% is relatively small.

An additional note of interest is the positive contribution in k_{eff} resulting from the shield and pressure vessel design.

The thermal shield design has changed since these studies were performed. Shields 2, 3 and 4 were combined into two shields. However, results of these studies are applicable. Based on the above results and other design considerations, the shroud and thermal shields will be mocked up exactly in the PMZ-1. A 60-degree segment of the pressure vessel will be used in the region where flux measurements will be made.

The effect on reactivity and core power distribution of substituting plexiglass or polypropylene for water in portions of the axial reflector was determined. Results obtained using three-group diffusion theory calculations are summarized below:

Material	Δk_{eff}
H_2O	0
Plexiglass	+0.00040
Polypropylene	-0.00001

These results show that either substitute is satisfactory, with polypropylene slightly better.

The effect of these materials on the core power distribution was found to be negligible.

Polypropylene was chosen because of its good machinability and negligible water absorption.

2. Critical Experiment and Safety Rod Design Studies

A preliminary study for the design of the critical experiment (CE) and safety rods was completed. The design required that each CE rod should be worth ≈ 0.2 to 0.7% in reactivity while each safety rod should be worth ≈ 1.0 to 4.0%. The design considered was a hexagonal bank of "fingers" (small rods), each finger of which fits inside of a fuel element when inserted in the core.

Preliminary nuclear studies indicated that this method would provide satisfactory control. Because of the small diameter (≈ 0.32 inch) of the poison section, the poison will consist of natural boron rather than a boron stainless steel mixture.

The effect on core multiplication of the CE and safety rods in the top axial reflector when fully withdrawn was determined. Results obtained using a "window shade" model technique, in which an equivalent effective quantity of boron is distributed with the water and fuel element "dead ends" in the top axial reflector, showed a negligible decrease of 0.0005 in k_{eff}.

3. Excursion Analysis

The excursion analysis study for the zero-power test has been completed. Results of this study are summarized in the PMZ-1 Hazards Summary Report (MND-M-1854).

In addition to the analysis referred to above, an IBM-709 machine program to solve the kinetic and heat transfer equations for a PM-1 zero-power experiment-type excursion analysis was completed.

4. Maximum Credible Incident

The maximum credible incident could result in a ramp reactivity input of 0.75% $\Delta k/k$ per second. To achieve an incident of this magnitude requires a combination of operator failure and multiple simultaneous system failure. The incident would occur if, with a fully loaded core and all water drained from the reactor tank, the six prototype Y-rods were removed. Water would then be added, due to system failure, to the reactor tank through the fill line at an average rate of 190 gpm from the storage tank. With the water covering only 12.6 inches of the core, which has an active length of approximately 30 inches, the reactor would go critical. At this point, water addition increases reactivity at the rate of 0.75% $\Delta k/k$ per second, the magnitude of the ramp input. If all available water were present in the reactor tank, the reactor would have the full 28% reactivity of the core available. However, since the excursion is over in slightly more than one second after criticality is achieved, less than 1% $\Delta k/k$ of the total available reactivity can ever contribute to such an incident. Table 2.2 summarizes the results of the maximum credible incident.

TABLE 2.2

Results of the Maximum Credible Incident (per cycle)

Maximum period (ms)	317
Peak power (megawatt)	937
Maximum reactivity (k_{ex})	0.0090
Temperature at peak (°C)	72.3*
Energy at $k_{eff} < 1$ (megawatt-second)	29.9
Total energy (megawatt-second)	33.0
Time to $k_{eff} = 1$ (second)	1.276
Temperature $k_{eff} = 1$ (°C)	165.7*

*Temperatures are center-of-fuel-tube-wall values.

As indicated in Table 2.2, the maximum credible incident leads to a total energy release of 33 megawatt-seconds per cycle. If it is assumed that half of the 12.6 inches of water in the actual core is removed during the excursion and the water available for the storage tank continued to flow into the reactor tank, a 33 megawatt-second excursion will occur every 3.5 seconds. However, since only enough water is available from the storage tank to completely fill the reactor tank, the maximum credible incident is one in which a series of 21 energy releases of 33 megawatt-seconds each occur, leading to a total energy release of 693 megawatt-seconds. Since the safety rods would normally be fired in 0.200 second on scram, the maximum credible incident under normal conditions would be limited to only one 33 megawatt-second excursion.

5. PMZ-1 Hazards Analysis

An analysis was made on a hypothetical accident in terms of the potential radiological hazards to the residential population in the off-site area surrounding the Martin Critical Test Facility. The hazards evaluation considered the external direct radiation doses and internal radiation doses from inhalation from an incident cloud during both the stable and average meteorological conditions. The stable meteorological conditions presented the highest dosage that could conceivably occur.

A very pessimistic model was utilized in the analysis to determine actual dosages. It was assumed that 20% of the total fission products would be released from a 154 megawatt-second power excursion based upon a 2% step input of reactivity. Actually, a release of fission products to the environment is not credible because, during the incident postulated, the fuel element cladding will not reach the melting temperature of 1400°F. Therefore, of a total activity of 3.00×10^7 curies, it was assumed that 6.0×10^6 curies would be released to the atmosphere. The analysis assumed that the centerline of the incident cloud will move normal to the point of release and at a distance one meter above the ground level. In actuality, the incident cloud would rise due to its inherent thermal characteristics. Also, a uniform distribution of fission products in a spherical cloud is assumed.

The following meteorological parameters were assumed in the calculations of a power excursion during stable and average meteorological conditions:

Parameter	Average Condition	Stable Condition
Wind velocity	4.69 meters/second	1.8 meters/second
Sutton's diffusion coefficient	0.3 meters	0.05 meters
Stability parameter	0.25	0.5

The external and internal radiation dosages during stable meteorological conditions represent a greater potential hazard than during average meteorological conditions. Under no conditions does the PM-1 Zero-Power Test Core represent a serious hazard to the residential population surrounding the test facility. The nearest property not controlled by The Martin Company is located 600 meters (1970 feet) from the test cell. Table 2.3 tabulates the results of analysis of a postulated accident.

The total direct external gamma radiation to an individual at 600 meters during stable meteorological conditions is 1.8 roentgens. This is well under the permissible dose of 3 roentgens to an individual in any calendar quarter of the year. On Martin-controlled property, the radiation dosages are higher but at no time do they reach the maximum allowable emergency dose of 25 roentgens for an accident in a controlled area.

The external beta dosages from the stable meteorological conditions are higher than those from gamma radiation. However, they present no serious hazard due to the ease of protection against beta radiation. At no time will the residential population be subject to beta dose of 300 roentgens, from which an individual can receive epidermal burns. This analysis assumes the individual will remain on the centerline of the cloud and it will not rise. Therefore, it is highly improbable that an individual could receive the maximum calculated dosages as presented in Table 2.3.

The internal radiation exposures due to inhalation are based on the assumption of uniform distribution of the radionuclides in the incident cloud. The internal radiation doses from radio-strontium, radio-cerium and radio-cesium are almost negligible as the incident cloud reaches 6.00 meters. The internal dosage from radioiodine at 600 meters is 0.45 rem whereas the maximum permissible dose to the thyroid is 30 rem. The internal radiation dosages are conservative in that they do not consider the radioactive decay of short-lived radionuclides as Iodine-132 and Iodine-134.

TABLE 2.3

Summary of Radiological Consequence Postulated Accident During Stable Meteorological Conditions

Distance from Release (d) (meters)	(feet)	Radioactive Cloud Volume (meters^3)	Cloud Radius (meters)	Time for Cloud to Reach Distance "d" (sec)	Dry Deposition $\left(\frac{\text{curies}}{\text{meters}^2}\right)$	Total Curies in Cloud After Dry Deposition (curies)	Concentration in Cloud After Dry Deposition $\left(\frac{\text{microcuries}}{\text{centimeters}^3}\right)$	External Dose on Ground from Airborne Cloud (roentgens)
0	0	524	5	0		6.15×10^6	1.17×10^4	
300	984	1.4×10^3	6.94	167	183	3.94×10^6	2.81×10^3	359
600	1,969	3×10^3	8.95	335	54.3	2.71×10^6	9.03×10^2	249
1,000	3,281	7×10^3	11.87	558	22.2	1.95×10^6	2.61×10^2	187
3,000	9,841	5.2×10^4	22.2	1675	3.24	1.51×10^6	2.9×10^1	103
5,000	16,405	1.6×10^5	33.6	2793	1.33	1.20×10^6	7.50	60
7,000	22,967	3×10^5	41.5	3911	7.37×10^{-1}	9.70×10^5	3.23	41
10,000	32,810	6.5×10^5	53.7	5586	3.95×10^{-1}	8.00×10^5	1.23×10^{-1}	24

TABLE 2.3 (continued)

External Dose on Ground from Airborne Cloud (roentgens)	Time for Cloud to Pass over a Point on the Ground (sec)	I-131, I-132, I-133, I-132, I-135 Thyroid	Internal Exposure of Critical Organs from Various Fission Products		
			Sr-89, Sr-90 Bone	Ce-144-Pr-144 Bone	Cs-137-Ba-137 Muscle
	5.59	1.43	3.14×10^{-2}	1.30×10^{-1}	1.00×10^{-5}
5.31	7.75	7.44×10^{-1}	1.63×10^{-2}	6.79×10^{-2}	5.16×10^{-6}
1.81	10.0	4.48×10^{-1}	9.78×10^{-3}	4.07×10^{-2}	3.11×10^{-6}
7.08×10^{-1}	13.3	2.55×10^{-1}	5.57×10^{-3}	2.31×10^{-2}	1.77×10^{-6}
1.11×10^{-1}	24.8	6.44×10^{-2}	1.41×10^{-3}	5.84×10^{-3}	4.45×10^{-7}
3.98×10^{-2}	37.5	3.15×10^{-2}	6.89×10^{-4}	2.86×10^{-3}	2.18×10^{-7}
2.21×10^{-2}	46.4	2.47×10^{-2}	4.53×10^{-4}	1.89×10^{-3}	1.44×10^{-7}
1.11×10^{-2}	60.0	3.34×10^{-3}	2.72×10^{-4}	1.13×10^{-3}	8.60×10^{-8}

6. PMZ-1 Shielding Analysis

To determine the effectiveness of present shielding of the Martin Critical Experiment Facility Test Cell One, an analysis was performed of the biological dose within the control room as a result of the maximum credible accident of the PMZ-1 core. Total doses along a vertical line on the wall from floor to ceiling in the control room at the nearest point to the core are presented in Table 2.4. A maximum dose of 10 rem occurs along the line at the ceiling. A view of the vertical cross section of the test cell and control room showing position of the core and thermal shields is presented in Fig. 2.2.

TABLE 2.4

Vertical Dose Distribution at Control Room Wall for a Maximum Credible Accident of 693 Megawatt-Seconds

Height Above Floor (feet)	Total Dose (rem)
0	0.37
1	0.68
2	1.0
3	1.4
4	1.7
5	2.0
6	2.6
7	3.3
8	5.0
9	8.2
9.5	10.0

Dose rates at any point within the control room during normal operation will be less than 0.2 millirem per hour per watt of operation power.

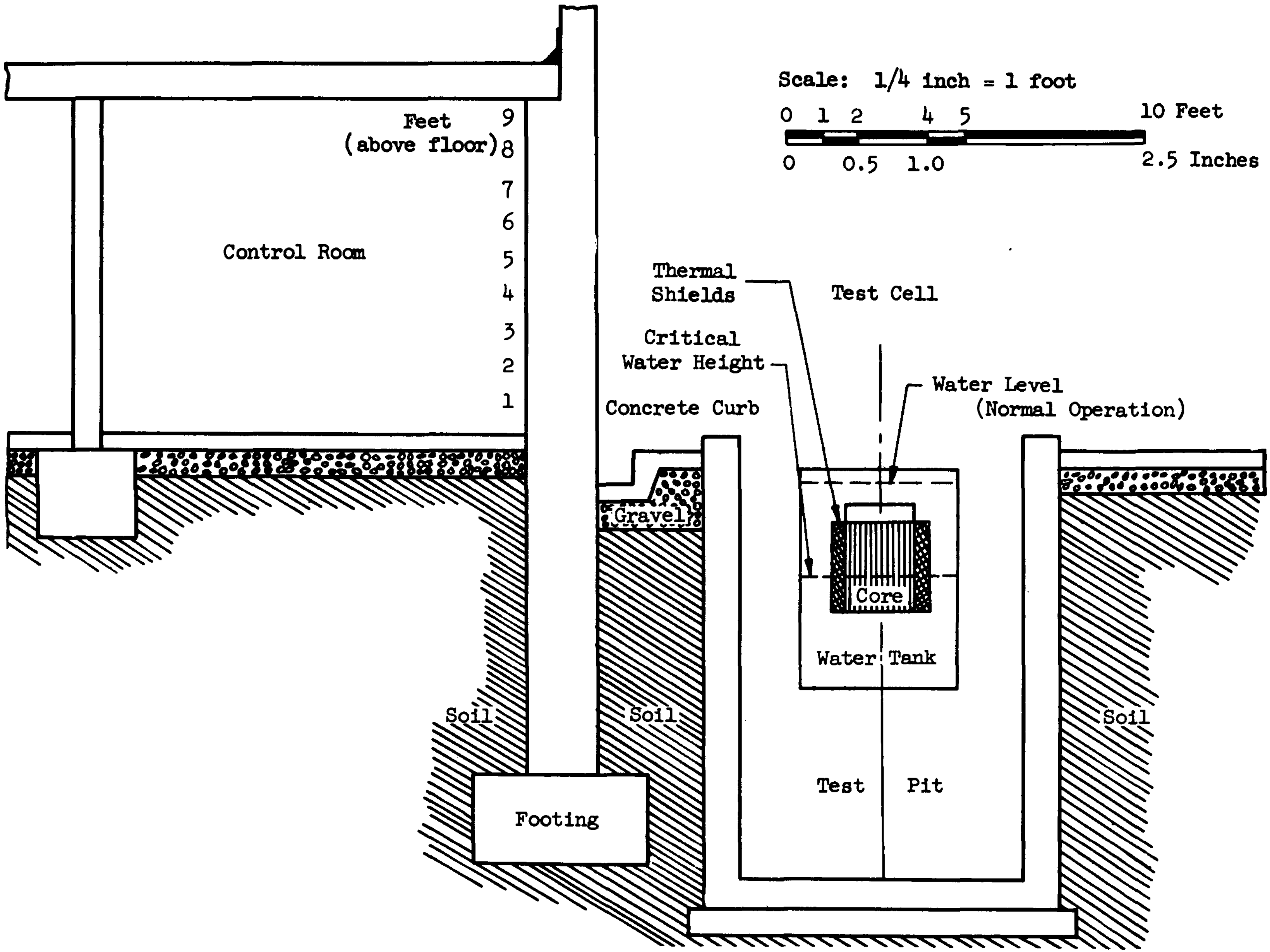

Fig. 2.2. Relation of Core to Control Room

7. Design of Flexible Zero-Power Reactor System

The following description of the flexible zero-power reactor system (PMZ-1) design considers the system as an entity, including those components which have been designed under the current program as well as those parts of the system already in existence at the Martin Critical Experiments Facility:

(1) Test stand

The reactor core and related structures are assembled in an 8-foot by 12-foot deep concrete test pit in the floor of the test cell. A 3-inch drain in the floor of the test pit allows the reactor tank water to be returned to an external storage tank.

The 54-inch diameter aluminum reactor tank is supported by a structural framework 5 feet, 5 inches above the floor of the test pit. The top rim of the 6-1/2-foot high reactor tank is 10 inches below the curb of the test pit. Inside the reactor tank is an annular metal support stand approximately 23-3/4 inches high and 38 inches in diameter. This supports a plastic bottom core grid plate which, in turn, supports the core. The support stand also supports the mockup thermal shields and pressure vessel.

Above the core, reactor tank and test pit is the actuator support structure, a structural steel framework 6 feet high, composed of 8-inch I-beams firmly secured to the curb at each corner of the test pit. This upright support holds a series of 8-1/2-foot steel dollies which are used to support and position the various control, safety and PMZ-1 prototype rod actuators.

(2) Core design

The PMZ-1 reactor is a zero-power test mockup of the PM-1 power reactor. The reactor core is approximately 22-1/2 inches in diameter and 30 inches long. The total reactivity in the core is approximately 12% $\Delta k/k$ for the core in normal cold operating condition with lumped burnable poison. For some of the experiments described herein, studies will be made on the core when it contains no lumped burnable poison. Under these conditions, the reactivity may be as high as 28% $\Delta k/k$. However, throughout the entire experimental program, the reactivity of the core will be poisoned so that at no time will the available reactivity be greater than the 1 to 2% $\Delta k/k$ in the control system.

(a) Fuel elements

The fuel is contained in approximately 725 stainless steel tubular elements. Each fuel element is 36 inches in length with an active length of 30 inches. The outside diameter of the element is 0.500 inch and the inside diameter is 0.416 inch. The fuel is contained in a 0.030-inch thick sintered compact of stainless steel and highly enriched UO_2. The composition of the active centered compact is 27.5% UO_2 and 72.5% stainless steel by weight. The fuel compact is clad inside and outside with 0.006-inch thick layers of stainless steel. At each end of the tube there is a stainless steel annulus sealing off the ends of the fuel element. One dead end is 2 inches long, while the other is 4 inches in length.

(b) Lumped burnable poison

Boron-steel rods are used to simulate the lumped burnable poison rods of the PM-1 power reactor. These are 1/2-inch diameter rods 36 inches long which contain boron in the steel over the same 30 inches as the fuel of the active portion of the fuel elements. These rods have a concentration of approximately 0.04 gram per cubic centimeter of natural boron. Each rod contains approximately 3.48 grams of natural boron.

(c) Grids

To mock up the lower grid of the PM-1 reactor, a 5/8-inch steel plate is located 1 inch below the active portion of the core. The fuel tubes and poison rods pass through this grid and rest on a plastic grid directly below. The plastic grid is made of polypropylene, a hydrocarbon with nuclear characteristics quite similar to water. This plastic grid, in turn, rests on the core support stand. A 1/4-inch thick stainless steel grid is located 1 inch above the active core. Above this grid is a 2-inch-thick polypropylene grid. The function of the upper plastic grid is to guide the fuel tubes and poison rods while they are being inserted into the core. The grids are so designed that individual fuel tubes may be readily removable from the core.

(d) Core layout

The fuel tubes in the PMZ-1 core are positioned on a triangular pitch of 0.665 inch. The core is divided into six equal segments. Along the lines separating adjacent segments, the pitch is increased by 0.100 inch. This mocks up the clearance required between bundles in the PM-1 power reactor. The central 19 tubes are in the form of a removable test bundle which is so designed that the tubes may be removed individually or as a bundle. Surrounding this test bundle there is also the 0.100-inch additional gap. In the three other locations, 19-tube groupings are assembled as bundles; however, the pitch between tubes in the bundle and adjacent tubes is maintained at 0.665 inch.

(e) Y-rod guides

The Y-rod guides serve the dual function of guiding the prototype Y-rods and tying the upper and lower grids together. Their length is such that they just fit axially between the upper and lower grids. They are bolted in place but can be relocated in any other desired location in the core.

(f) Prototype Y-rods

The six prototype Y-rods are located in six positions in the core. The three blades of each Y-rod extend at 120 degrees to each other. Overall blade dimensions are 3.90 inches from the center of the Y to the end of the blade, 5/16 inch thick and 40 inches long. The rod is of picture frame construction which leads to a poison section for each blade 3-1/2 inches by 1/4 inch by 30 inches. The poison is in the form of mixed Eu_2O_3 and stainless steel powders. The prototype Y-rods are driven by Teleflex control drives.

(g) Thermal shields and pressure vessel mockups

The cylindrical inner shroud, thermal shields and pressure vessel of the PM-1 core are mocked up in the PMZ-1 reactor by a series of flat slabs which have the same thickness as the shields they are mocking up but which are each only 10 degrees in width. The inner shroud and the three thermal shields are assembled around 360 degrees and will be in place throughout the entire experimental program of the core. These shields are all included since each shield adds approximately 0.3% $\Delta k/k$ to the reactivity of the core. The pressure vessel, however, is located only in a 60-degree segment since its reactivity contribution is negligible. However, enough of the pressure vessel is included to permit the accurate measurement of neutron and gamma flux through this region.

In addition to its mockup function, the shroud also supports the upper grid. The combination of the shroud and Y-rod guides maintains the accuracy of relative positioning of the core components.

(h) Control rods

The rods which control the PMZ-1 reactor consist of groupings of cylindrical fingers which enter the reactor core through the center of the fuel elements. The hold-down cap assures that those fuel elements which contain control fingers will not be removed as the control rods are withdrawn from the core.

Each finger is a cylindrical tube filled with natural boron or B_4C. The active poison in each finger is 0.319 inch in diameter and 26 inches long. The reactivity worth of any one finger varies from 0.06% $\Delta k/k$ to 0.16% $\Delta k/k$, depending on its location in the core. Enough of these control fingers are grouped together on each control rod to give the individual control rods a worth which can vary between 0.2% and 0.7% $\Delta k/k$, according to experimental requirements. The total reactivity worth of the control system is maintained between 1% and 2% $\Delta k/k$ by the relative positions of the three control rods and the number of fingers in each rod.

(i) Prototype Y-rod actuators

Prototype Y-rods are driven by a Teleflex cable drive whose drive motor is located remotely from the reactor tank. The drive cable passes over an idler pulley which is located above the location of the Y-rod in the reactor core. The actuator has a maximum speed of 6 inches per minute, a 30-inch travel length and reproducible accuracy of ±0.01 inch. The speed of the actuator limits the rate of increase of reactivity of prototype rods to a maximum of 0.06% $\Delta k/k$ per second. A counter weight holds the cable taut on the side of the drive motor opposite the prototype rod. Limit switches actuated by this counter weight stop the drive motor automatically when the rod is fully withdrawn from the core or fully inserted into the core. These limits switches tie into the indicating and interlock circuits. A magnetic brake on the drive motor assures that the position of the rod will be maintained with no slippage and minimal overtravel when no electric current is being supplied to the motor. The idler pulleys are mounted on sliding plates on the actuator support structure. These mounting plates are so designed that the idler may rotate freely about the axis of the drive cable to assure flexibility in positioning.

B. SUBTASK 2.2--IRRADIATION TEST

J. B. Zorn, S. Frank

The objective of the irradiation program is to subject the PM-1 fuel element to burnup in an environment which simulates, as nearly as possible, the conditions of temperature, heat flux, coolant subcooling, coolant temperature rise and heat removal to be experienced during operation of the PM-1 Nuclear Power Plant.

The major objectives during this period were:

(1) To analyze all possible irradiation test programs which could feasibly supplant in-pile loop testing of full length PM-1 fuel tubes.

(2) To select that program which appeared most satisfactory on the basis of economy and reliability of results. Effort was then devoted to the preliminary stages of this alternate program.

(3) To write a detailed statement of work.

(4) To submit new irradiation request forms.

(5) To initiate design work.

During the next quarter, it is anticipated that:

(1) The PM-1 fuel elements will be inserted in the MTR or ETR.

(2) Fabrication of the SM-1 fuel element containing PM-1 components will be completed.

(3) The fabrication of the boron-steel control rod will be completed.

1. Bare Element Irradiation

This analysis has resulted in the design of a three-part irradiation program:

(1) Two PM-1 fuel elements will be irradiated to maximum burnup in the MTR or the ETR (bare element irradiations).

(2) A group of PM-1 fuel elements and burnable poison elements will be enclosed in an SM-1 fuel element configuration and irradiated to maximum burnup in the SM-1 with Core 2.

(3) A boron-stainless steel control rod will be fabricated in the SM-1 configuration and irradiated in the SM-1.

An analysis was undertaken of the various fuel element compositions and sizes being considered for the PM-1 element in order to select those specimen parameters for irradiation testing which appear most promising and which will provide sufficient statistical data to permit extrapolation of results to those types not being tested. During the course of this investigation, total core densities of the specimen elements were determined. They vary from a maximum of 7.60 gm/cm^3 to a minimum of 7.41 gm/cm^3 (90% of theoretical), depending on composition. Meat volumes of the different sizes under consideration were put on a unit length basis and varied from 0.707 cm^3/linear inch to 0.320 cm^3/linear inch.

A survey was made of the various test programs which could be undertaken in lieu of in-pile loop testing. The various costs of each program along with its intrinsic value as a substitute for PM-1 conditions were closely scrutinized. The basic programs covered were:

(1) Capsule irradiations of subsize specimens.

(2) Irradiation of "bare" elements in the SM-1 reactor at pressurized water operating conditions. In this case, PM-1 fuel tubes would be adapted to a standard SM-1 fuel element and incorporated in the reactor as an operating component.

(3) Irradiation of "bare" elements (in contact with coolant water) at low temperatures in the MTR (Materials Testing Reactor) or ETR (Engineering Test Reactor). Subseqent autoclaving at high temperature and pressure will then be performed to simulate PM-1 pressurized water conditions.

Costs of preirradiation inspection, irradiation and postirradiation testing were obtained from Westinghouse (WTR), General Electric (GETR) and Battelle (BMI). In general, the major cost item is the integrated neutron flux required to achieve desired burnup levels. Results of the analysis indicated that the most satisfactory approach would be an irradiation test in the SM-1 reactor which is backed up by a concurrent test on two full-length elements in the MTR or ETR to obtain accelerated burnup. This latter test would not provide the high temperatures desired during irradiation, so it is proposed that a high temperature and pressure autoclave treatment be performed on both specimens subsequent to the irradiation.

2. PM-1 Bundle Irradiations in SM-1

Thermal and hydraulic analyses were performed in support of the design of a simulated PM-1 bundle to be irradiated in the SM-1 reactor.

The configuration of the simulated bundle considered consisted of 14 tubes, 5 plates and 2 burnable poison rods in a bundle the size of an SM-1 fuel bundle, as shown in Fig. 2.3. The active length of the tubes was reduced to 22 inches, but the number of tubes was chosen so that the heat generation of the bundle would be equivalent to that of an SM-1 bundle.

Since the SM-1 core is orificed, the flow to a bundle is a function of its position in the core. For this reason, two possible positions for placement of the PM-1 bundle were analyzed. Since tubes must be supported and held in place by bottom and top grids, the flow resistance is greater across the simulated PM-1 bundle than across an SM-1 bundle, which consists entirely of plates held simply by a comb at either end. Therefore, the PM-1 bundle must necessarily receive less flow in any core position than an SM-1 bundle similarly placed.

The approach was first to design bottom and top grids to provide as much flow area as possible. With the flow resistance (outside the tubes) thereby minimized, a maximum amount of flow through the bundle will be obtained. The second step was to increase flow resistance inside the tubes by swaging the inlets, thus increasing the pressure drop across the inside of the tubes to equal the pressure drop outside the tubes. This results in splitting the flow and the heat generated in the tube equally inside and outside the tubes.

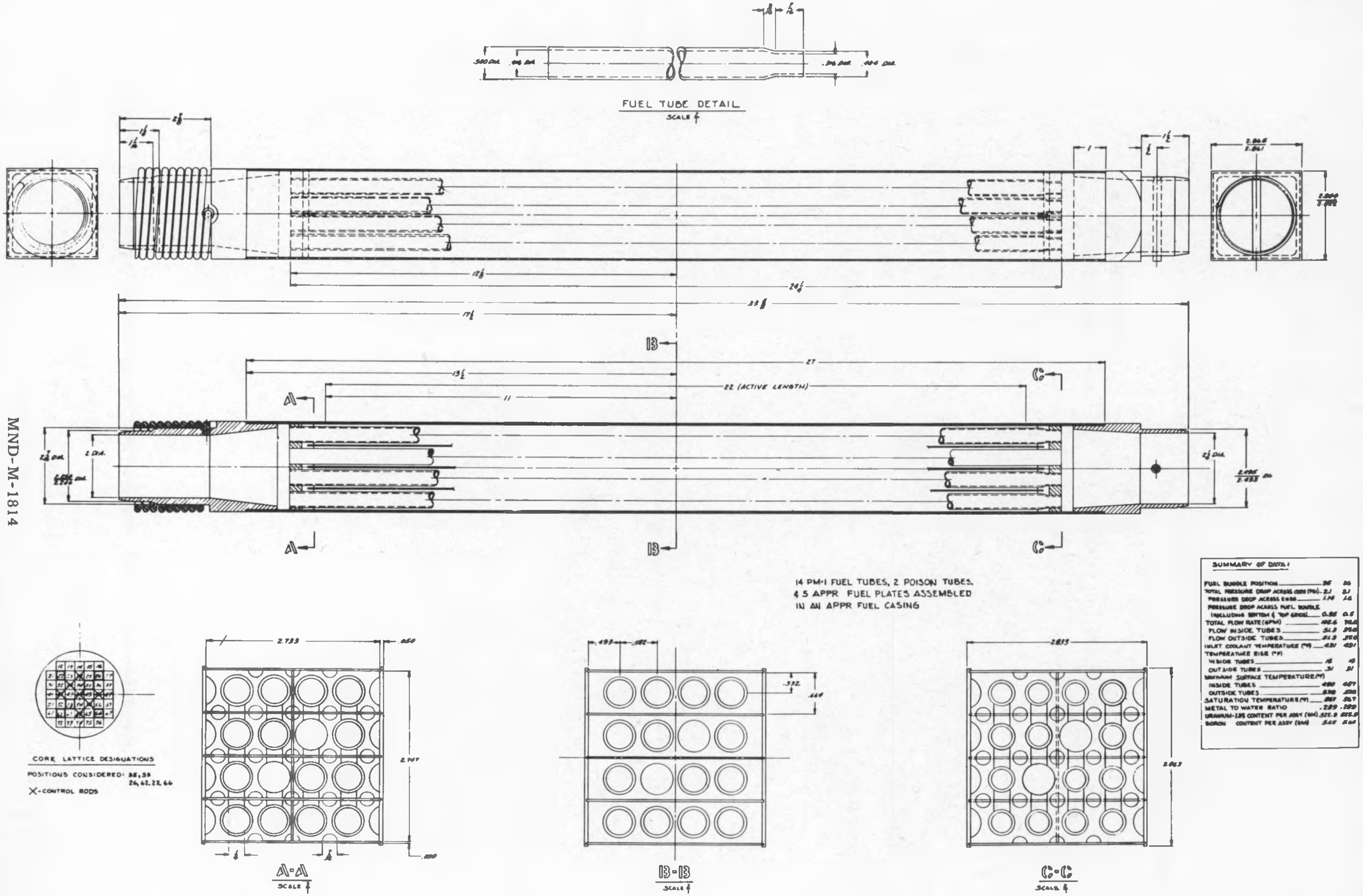

Fig. 2.3. PM-1 Fuel Assembly

The results of the analysis are summarized in the following table for SM-1 core positions 35 (symmetrical with position 53) and 26 (symmetrical with positions 22, 62 and 66):

Fuel Bundle Position	35	26
Total pressure drop across core (psi)	2.1	2.1
Pressure drop across ends	1.14	1.6
Pressure drop across fuel bundle (including bottom and top grids)	0.95	0.5
Total flow rate (gpm)	102.6	74.0
Flow inside tubes	51.3	37.0
Flow outside tubes	51.3	37.0
Inlet coolant temperature (°F)	431	431
Temperature rise (°F)		
Inside tubes	15	15
Outside tubes	31	31
Maximum surface temperature (°F)		
Inside tubes	490	487
Outside tubes	538	532
Saturation temperature (°F)	567	567
Swaged tube inside diameter (in.)	0.316	0.317

C. SUBTASK 2.3--REACTOR FLOW STUDIES

I. Starr, M. P. Norin, W. J. Taylor, J. Sevier

The objective of experimental PM-1 reactor flow studies is to evaluate and optimize the hydraulic design of the reactor. The work is to be conducted through three tests: Two serve to give preliminary information for use in reactor design and in the design of the third test; the third test makes use of a full-scale flow model.

Work planned for the third project quarter included:

(1) Completion of the simplified flow model (1/4-scale) tests.

(2) Completion of the orifice-bundle tests.

(3) Completion of the design of the full-scale reactor flow test.

(4) Initiation of procurement and fabrication of components for the full-scale tests.

Actual accomplishments of this quarter were:

(1) Test of the initial configuration of the simplified 1/4-scale flow model was completed.

(2) Design was completed and fabrication initiated of 1/4-scale model components for the revised upper pressure vessel and water box design.

(3) Design of the orifice-bundle test components was completed. Instrumentation was specified.

(4) Specifications were prepared on the modifications required for the 5000-gpm flow loop so as to accommodate the full-scale reactor test vessel.

(5) A preliminary instrumentation layout for the full-scale vessel was prepared.

(6) The tubing for the orifice-bundle test and the full-scale flow model core was received.

(7) Design of the full-scale flow test pressure vessel was completed.

(8) Loop design modifications necessary to install the pressure vessel were completed.

(9) The feasibility of using carbon steel piping in the full-scale test facility with corrosion inhibitors and pH control was demonstrated.

During the next quarter, it is expected that:

(1) Test of the 1/4-scale model with the revised upper water box will be completed.

(2) Fabrication of the orifice-bundle test components will be completed.

(3) The 200-gpm flow loop will be modified to accommodate the orifice-bundle test rig.

(4) An experimental program will be designed for the orifice-bundle test.

(5) Modification of the 5000-gpm flow loop will be initiated.

(6) Fabrication of the gross flow test pressure vessel will be completed.

(7) Design of the full-scale gross flow test will be completed.

(8) Instrumentation layout for the full-scale flow studies will be completed.

1. One-Fourth-Scale Flow Model Test

An experimental study of the initial configuration of the prototype reactor was completed using a simplified 1/4-scale flow model. The objective of the work was to determine, for design purposes, the gross coolant flow pattern of the prototype reactor as influenced by the inlet water box, the inlet water box orifice plate and the outlet configuration. The water box configuration and the inlet and outlet nozzle positions of the prototype were revised after the 1/4-scale model was fabricated. The test data are still useful since the basic water box configuration remains essentially the same. The values of measured pressure drops and velocities will apply only approximately to the present PM-1 design and will show the effect of altering the shape of the water box when compared with results obtained in future tests. The experimental work also established a basis for predicting flow distribution in future designs and comparing previously predicted head losses with experimental values.

The results of the tests are summarized below:

(1) Flow distribution in the inlet water box was found to be independent of velocity and Reynolds number in the range tested which included the prototype design velocity.

(2) A pressure recovery from the kinetic energy of the inlet flow was observed. This caused a minimum flow from the water box at the inlet side of the vessel and a maximum flow at the opposite side. (The flow variation was about 25%.)

(3) The flow variation resulting from the water box was reduced considerably by the characteristics of the flow annulus formed by the thermal shields. (Variation about 11%.)

(4) The overall pressure drop measured from inlet to outlet was 23 feet of head for a prototype flow rate of 1900 gpm as compared to the predicted value of 21 feet.

(5) The pressure drop across the orifice plate below the inlet water box was about 20% higher than anticipated.

The internal geometry of the water box of the PM-1 was duplicated in the model in 1/4 scale. All other flow channel dimensions were approximately 1/4 size. The flow channels between the thermal shields were approximated by a single annulus to allow sufficient space for instrumentation sized according to good design practice. That is, the instrumentation was small with respect to the dimensions of the annulus. For simplicity, an orifice plate simulated the reactor core. The orifices were sized to duplicate the core pressure drop at prototype velocity. The upper shroud was duplicated and contained discharge orifices equivalent to PM-1 design. A dual outlet was provided. One outlet simulated that of the prototype. The other outlet was located at the top of the model and was symmetrical about the vertical centerline of the vessel. Valving was provided so that either outlet could be used during testing. When the outlet through the top was used, the exit flow restriction did not disturb the flow distribution upstream. Thus, with this configuration, nonuniform distributions may be traced directly to the inlet configuration. The side outlet permits determination of any nonuniform distributions traced to the PM-1 exit configuration. Figure 2.4 shows a sectional view of the model. The upper and lower outside sections and the upper shroud are made of plexiglas to allow visual observation during testing. Figure 2.5 gives the configuration and dimensions of the water box. The model components are shown in Fig. 2.6. Figure 2.7 depicts the assembled model. The model as installed in the loop is shown in Fig. 2.8.

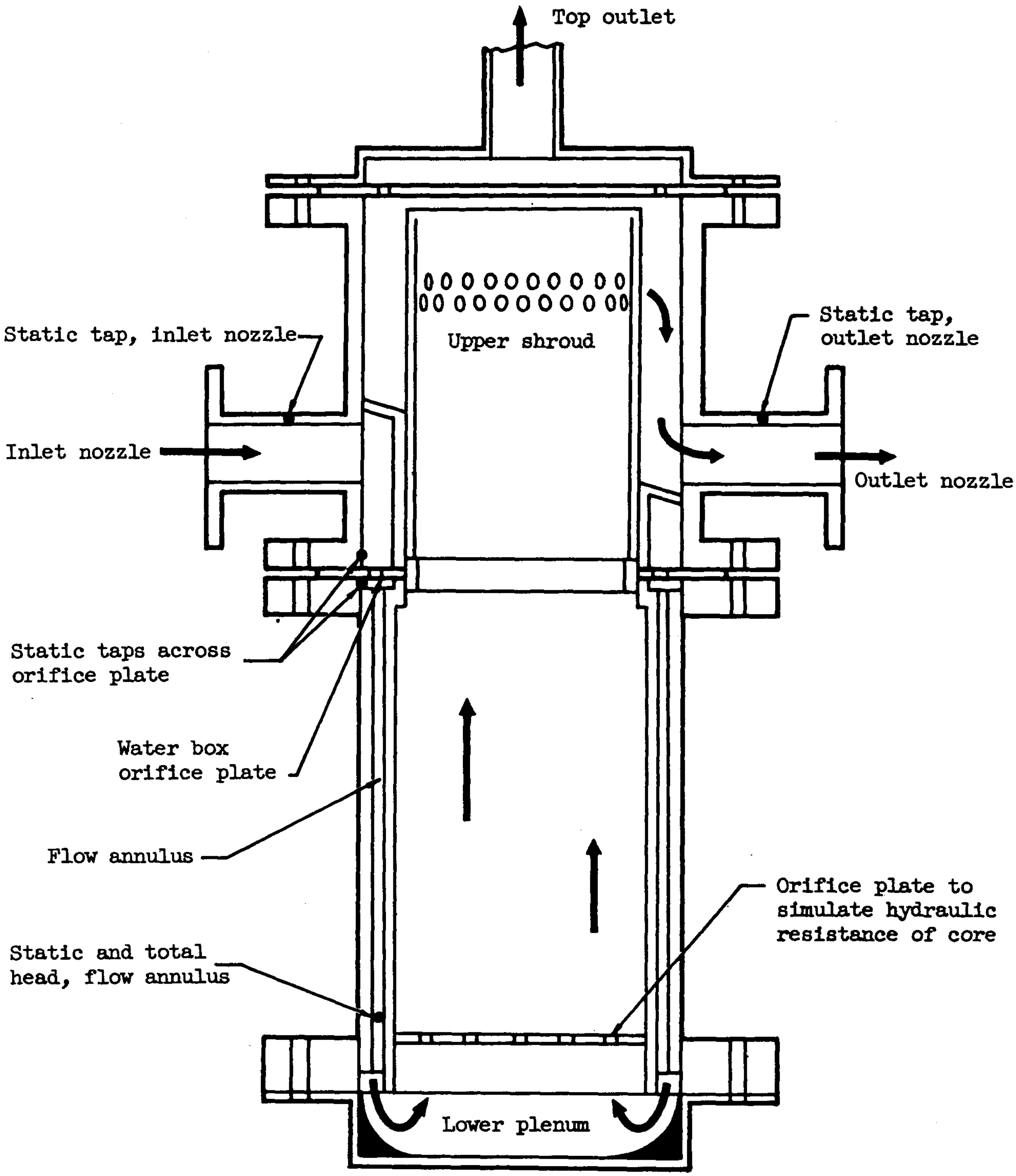

Fig. 2.4. Quarter Scale Flow Model (initial configuration)

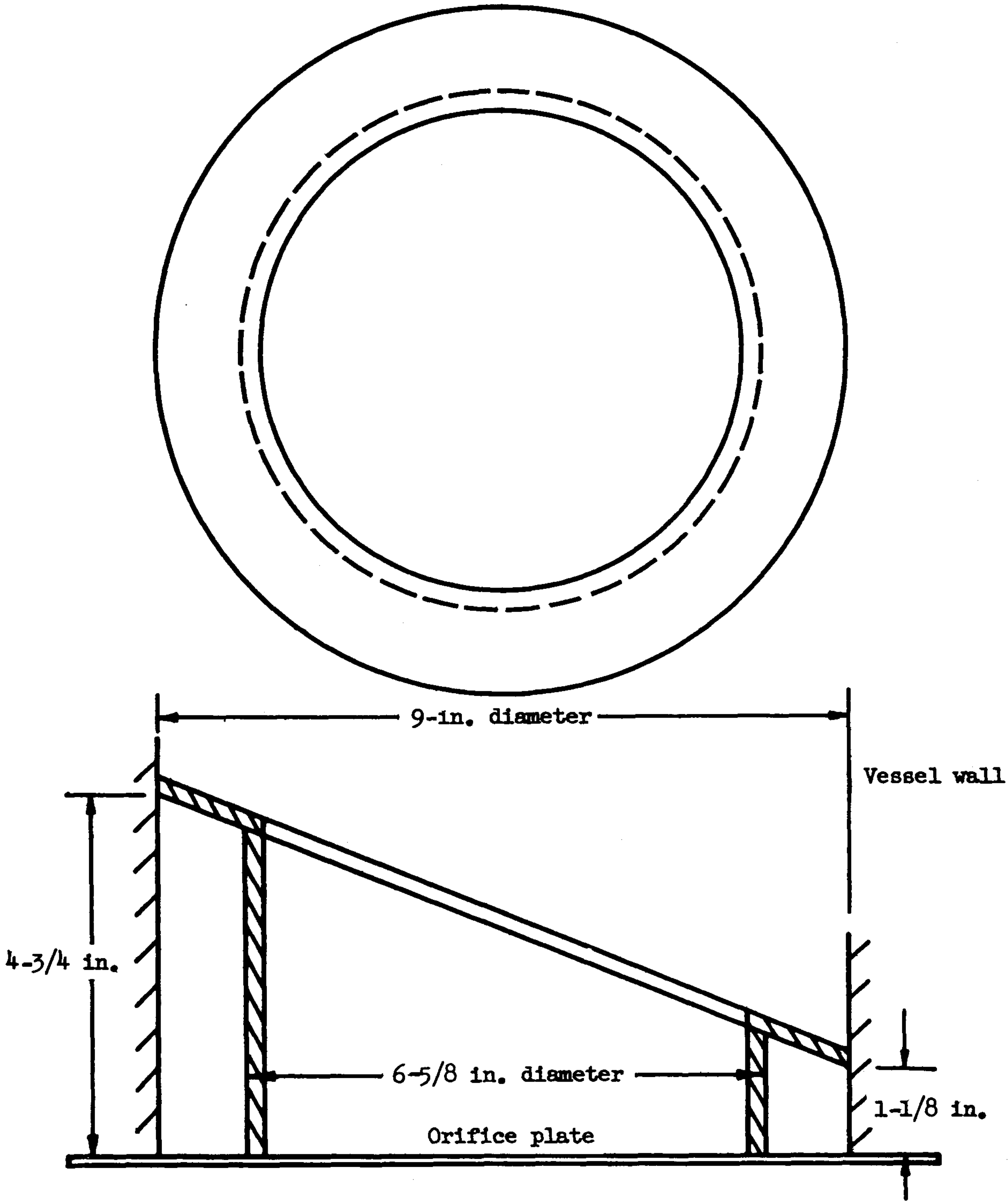

Fig. 2.5. Model Water Box Configuration (inlet nozzle not shown)

Fig. 2.6. Model Components

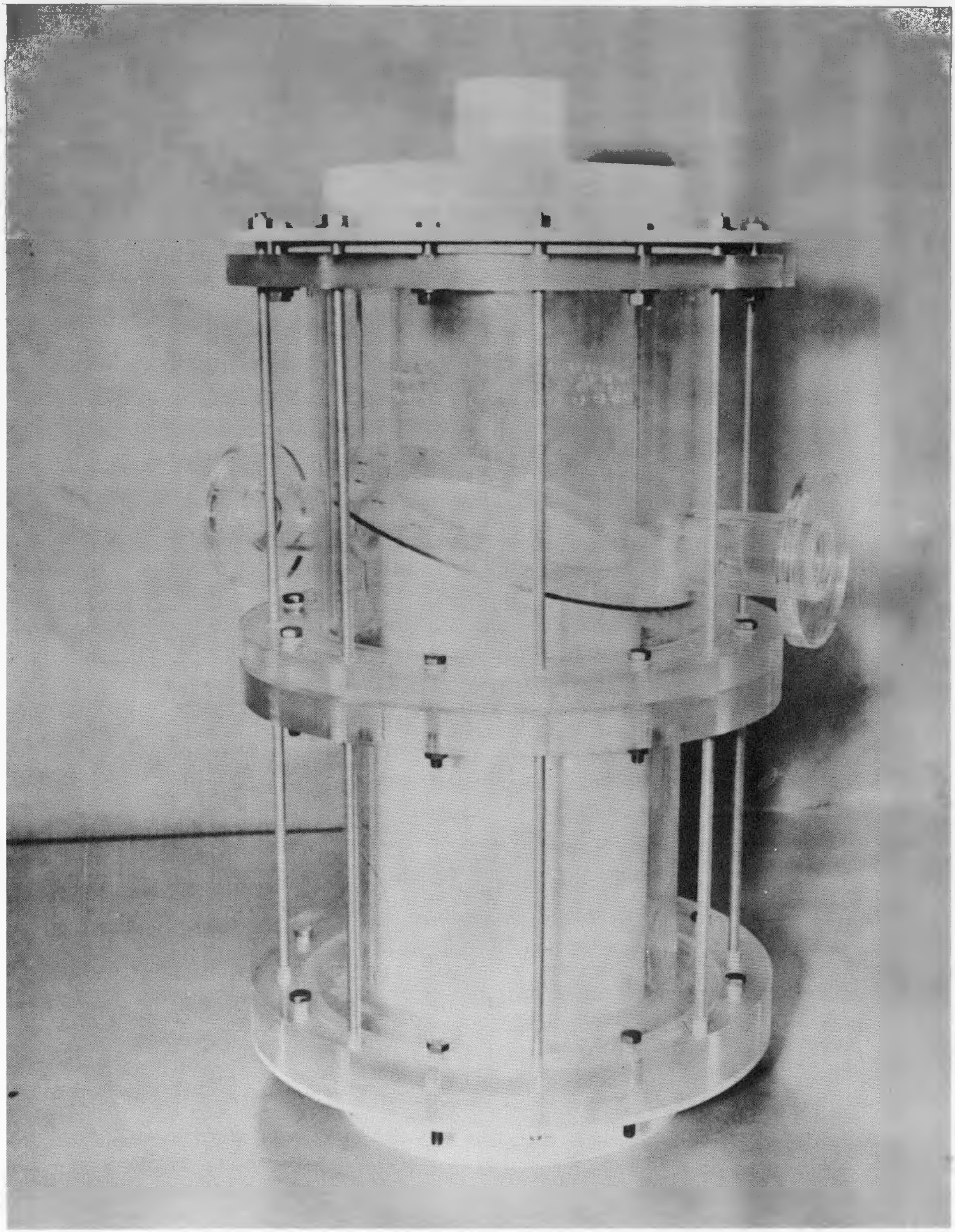

Fig. 2.7. Quarter Scale Model Assembly

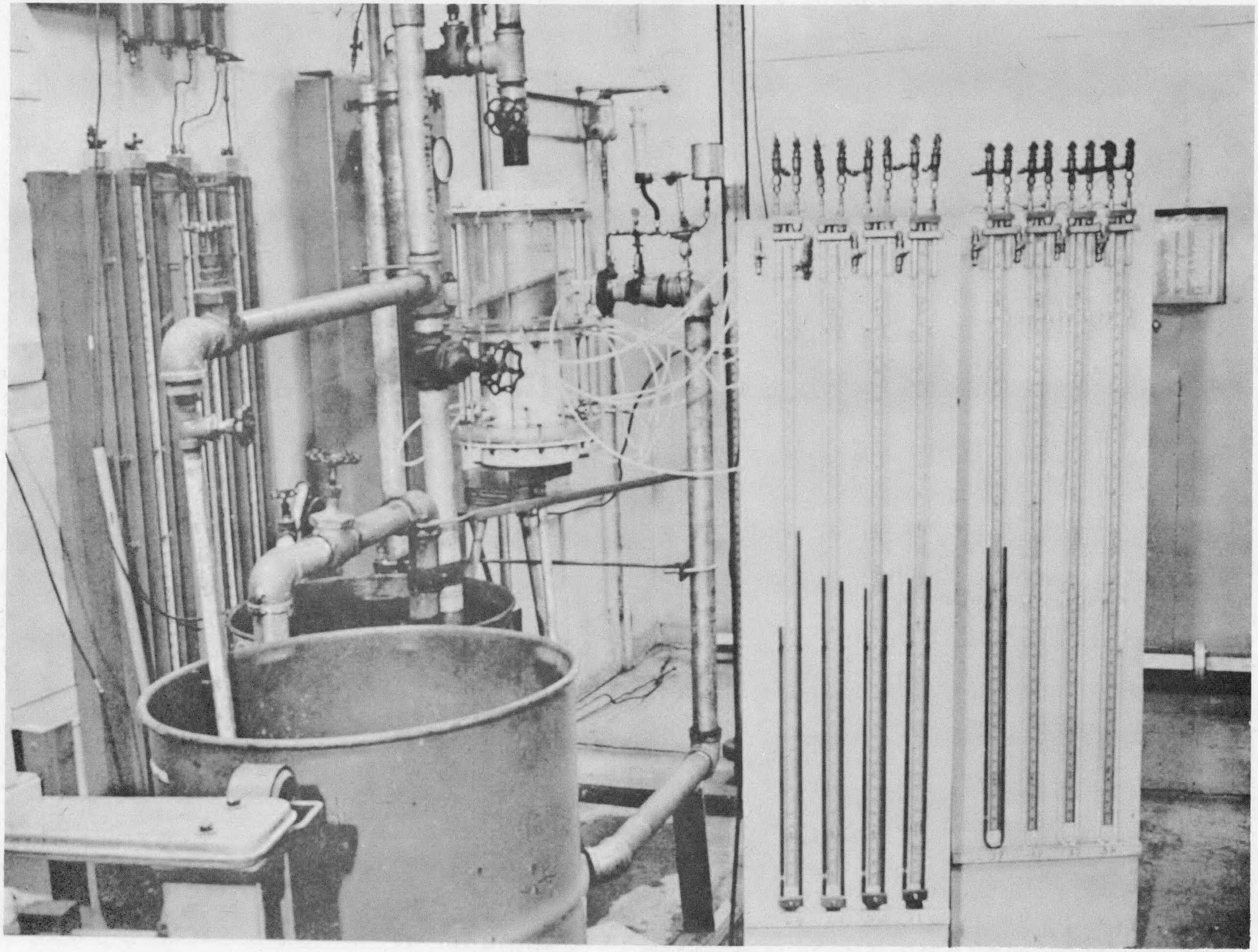

Fig. 2.8. Quarter Scale Model Installed in Loop

Instrumentation used in the 1/4-scale model included flange-type static taps across the water box orifice plate located at nine positions around the vessel, velocity head probes which read total and static pressures in the lower portion of the flow annulus at eight positions around the vessel, and static pressure taps in the inlet and outlet nozzles which indicated the overall vessel head loss. Figure 2.9 shows the pressure tap configuration for the measurements of pressure drop across the water box orifice plate.

Figure 2.10 shows the normalized distribution of differential head across the water box orifice plate for three flow rates. This was obtained by calculating the ratio of Δh to the mean differential head $\Delta \bar{h}$. This graph indicates that the distribution is not a function of velocity or Reynolds number in the range tested and remains essentially constant. The effect of the inlet configuration is seen to be experienced through approximately 60 degrees on each side of the inlet nozzle centerline. The distributions of Fig. 2.10 were essentially constant for exit flow through either the top or side outlet. Sample curves of the head across the orifice plate versus flow rate for some vessel locations are given in Fig. 2.11. The curves show that Δh varied very nearly with the square of the flow rate. Taking the flow as proportional to the square root of the head, the distributions of Fig. 2.10 give a maximum flow variation of about 25%.

The difference in static head between that at various locations and that below the inlet nozzle is shown in Fig. 2.12. This is on a plane parallel to the nozzle centerline and upstream of the water box orifice plate. The measurements are for a model flow rate of 119 gpm which gives the same velocities as the prototype when operating at the preliminary design flow rate of 1900 gpm. Figure 2.12 shows the static pressure recovery as the coolant passes around the water box.

Coolant velocity was measured in the flow annulus near the entrance to the lower plenum. This is shown in Fig. 2.13 for various flow rates. The maximum variation in velocity was about 11%. Static differential heads were also measured around the outer periphery of the flow annulus of the plane of the velocity measurements. The maximum differential was 0.013 foot of water showing that there is little tendency for cross flow, a condition which, if it existed, would invalidate velocity head measurements.

The overall head loss across the model is shown in Fig. 2.14. At the preliminary design flow rate (1900 gpm), the head loss is 23 feet of water for the prototype. (This corresponds to the head loss at 119 gpm in the model.) The experimental head loss compares favorably with the predicted loss of 21 feet.

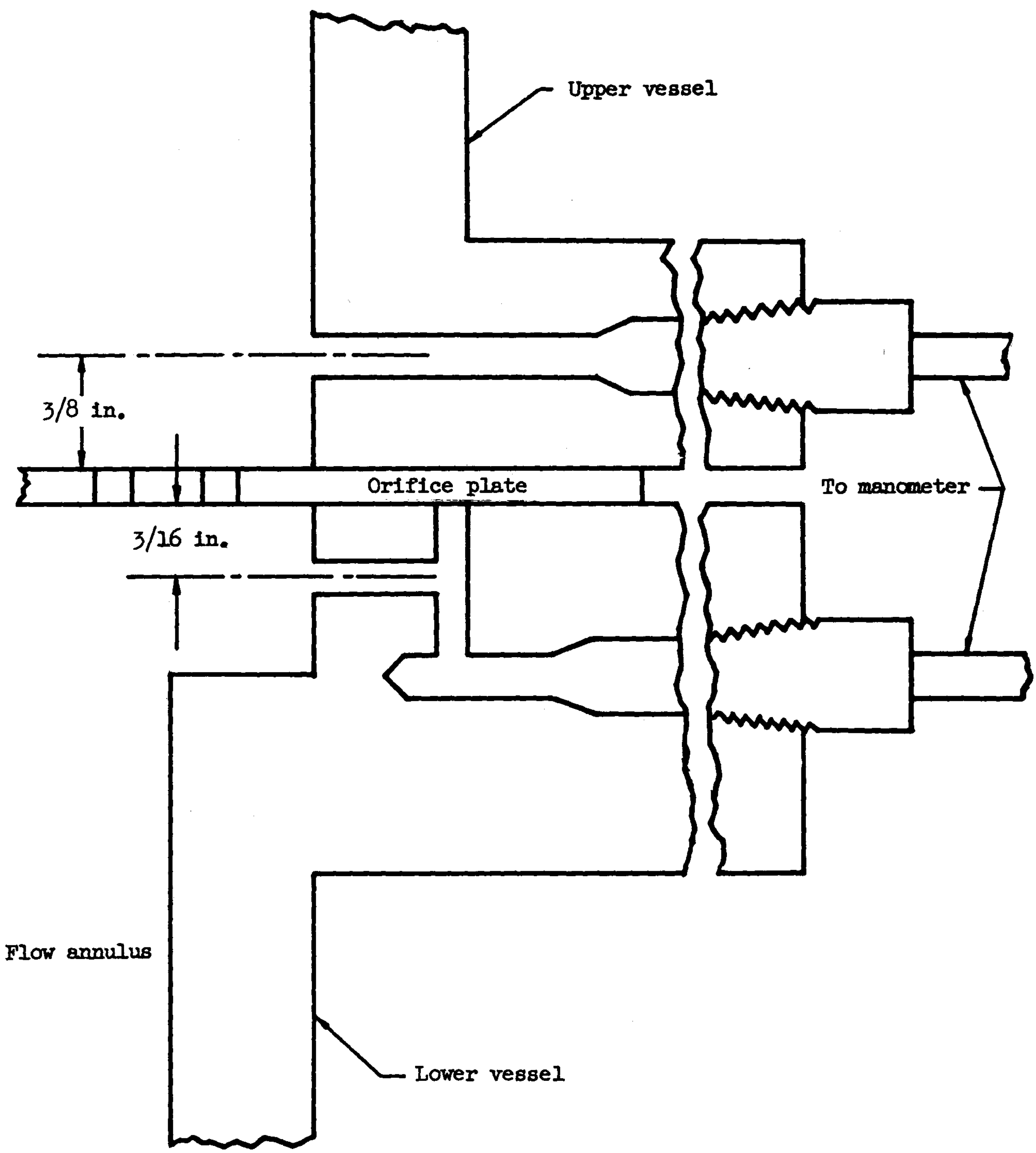

Fig. 2.9. Water Box Orifice Plate Flange Taps

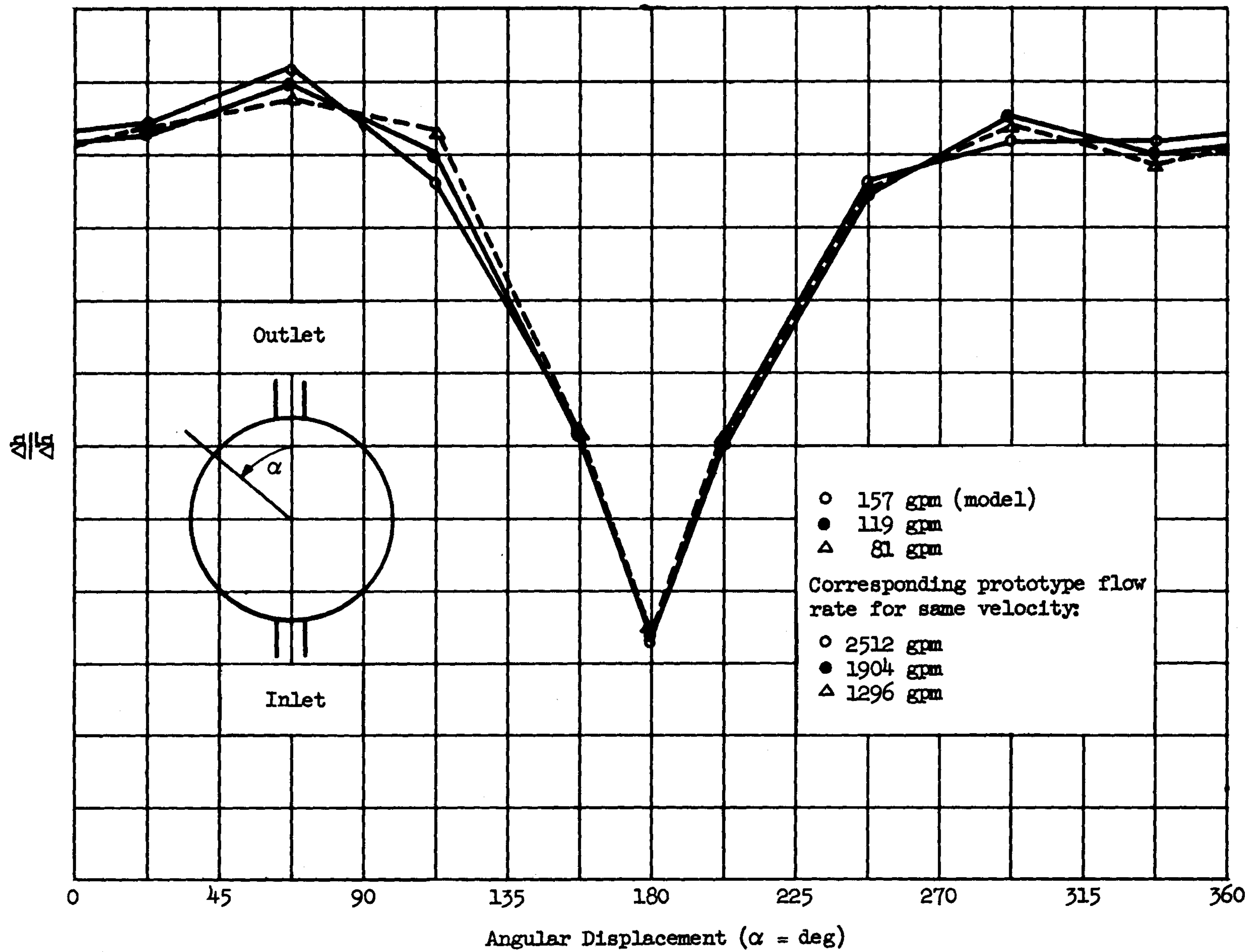

Fig. 2.10. Ratio of Head Across Water Box Orifice Plate to Mean Head Across Orifice Plate Versus Angular Displacement

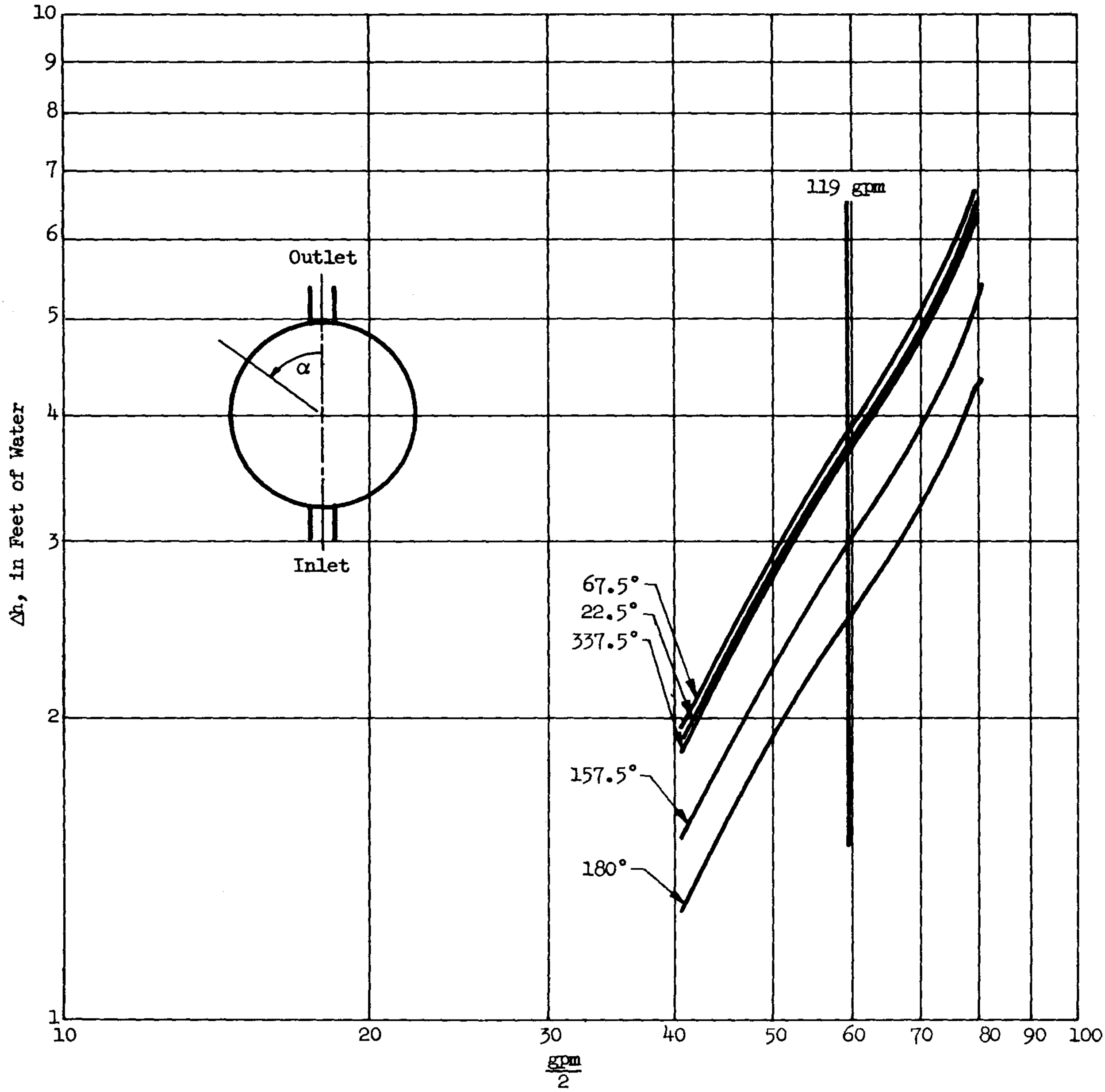

Fig. 2.11. Head Across Water Box Versus Total Flow for Various Locations

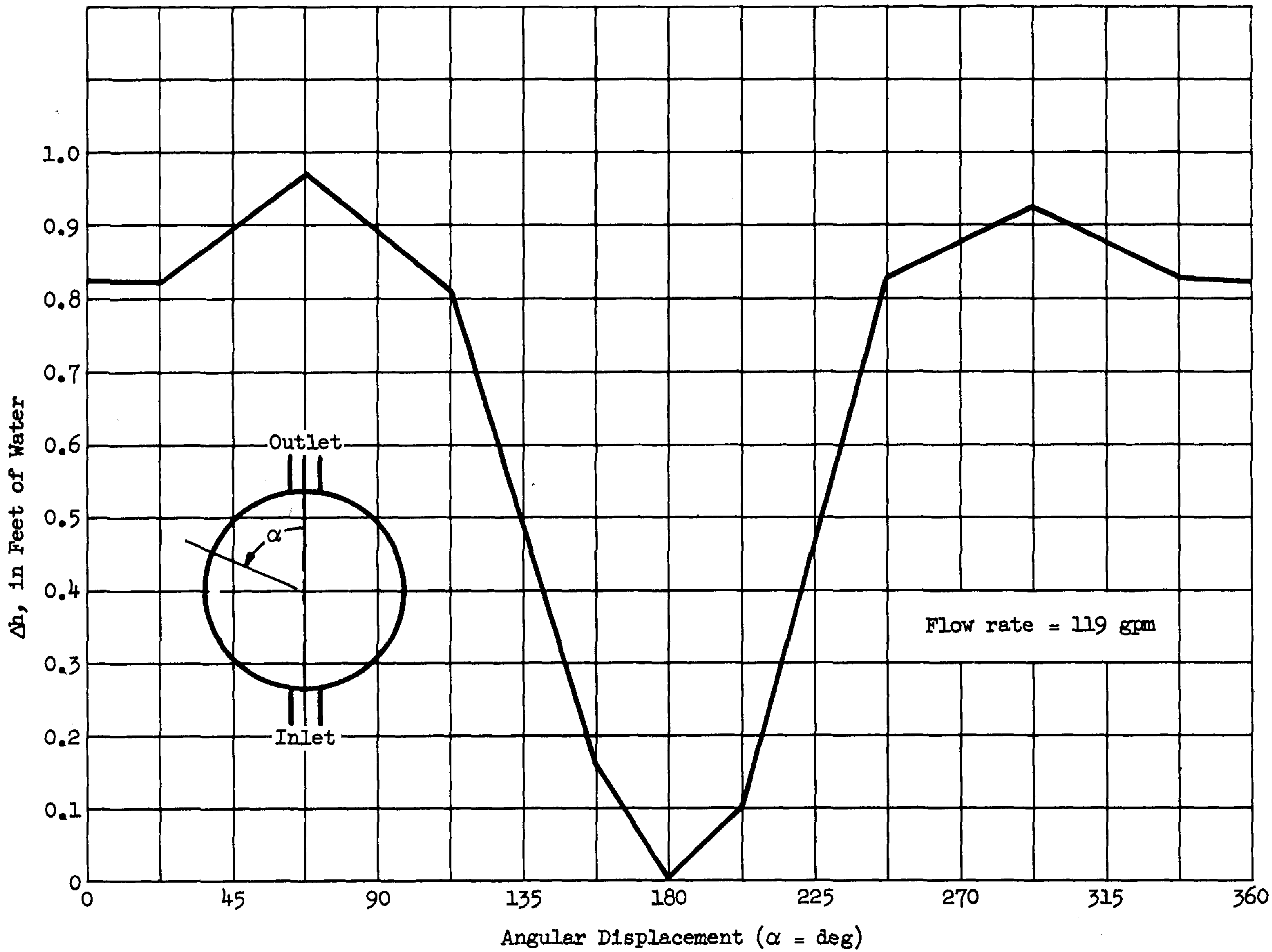

Fig. 2.12. Δh Measured Relative to Static Head at 180° at Various Vessel Positions Above Water Box Orifice Plate

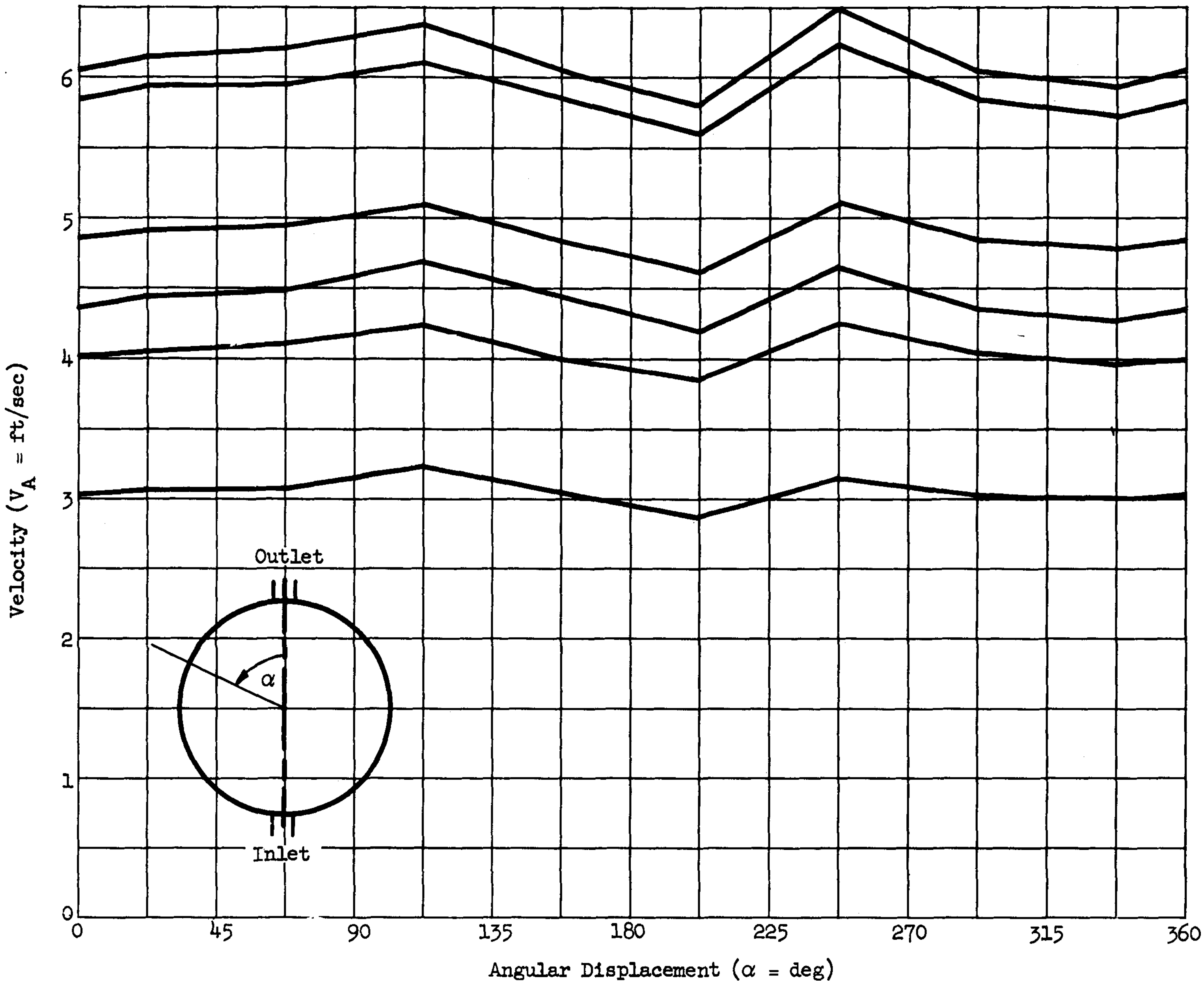

Fig. 2.13. Velocity Distribution Near Exit of Flow Annulus

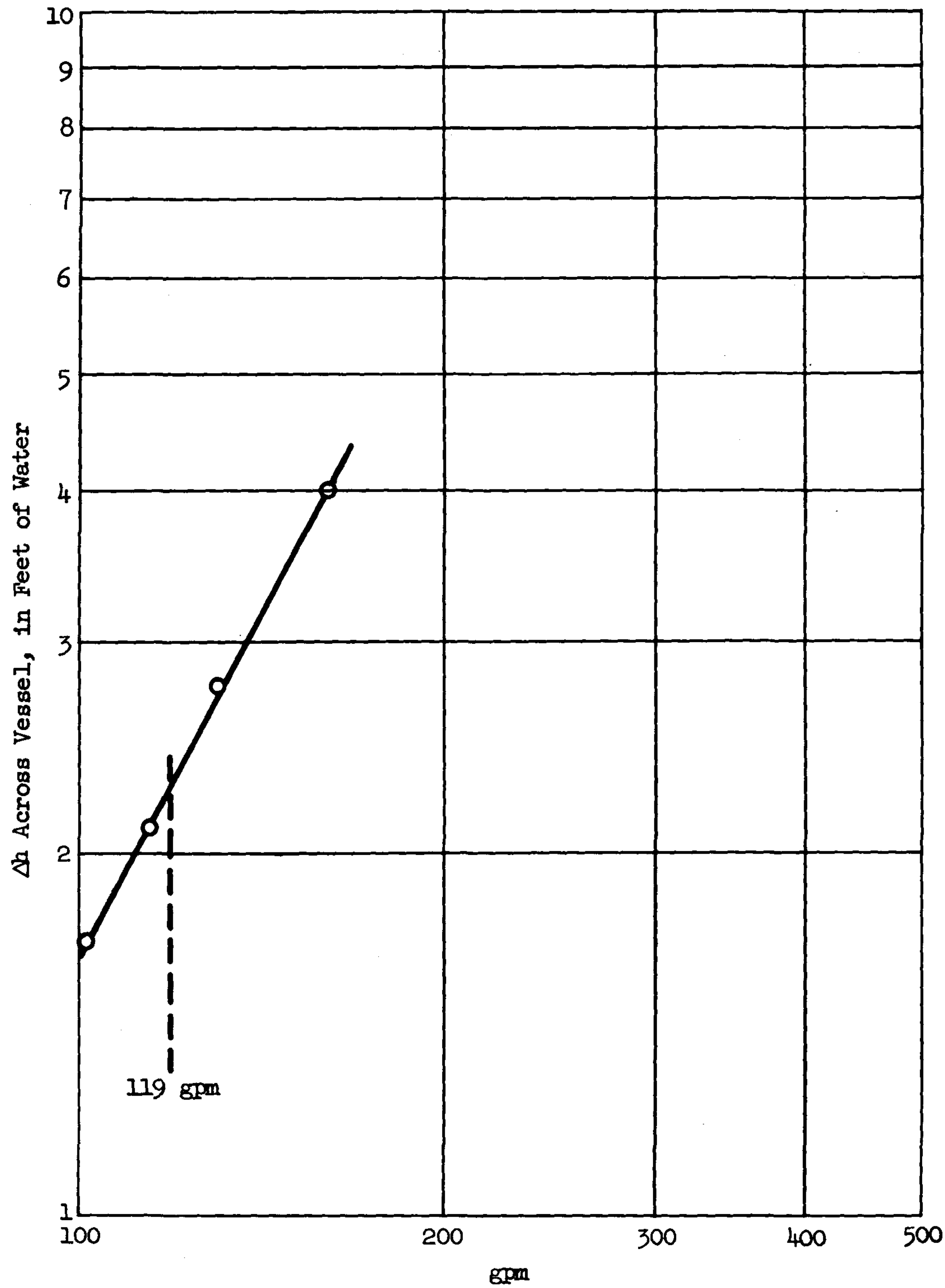

Fig. 2.14. Overall Head Loss Versus Flow Rate

Fabrication of model components for the revised upper vessel configuration is nearly complete. The new configuration will be tested during the next quarter. Means for the injection of dye in the inlet nozzle was included in the model and checked out. Dye studies will be included as part of the test on the revised configuration.

2. Orifice-Bundle Test

The orifice-bundle test components have been completely designed. The upper grid configuration features a header plate into which the fuel tube ends are fitted with sufficient clearance to allow axial motion. The ends of these tubes are swaged to a reduced diameter. Orifices are provided in the plate for the exit flow from the channels formed by the outer surfaces of the tubes. This configuration is being analyzed for hydraulic adequacy. Fabrication will start early in the next quarter.

Upon completion of the 1/4-scale model tests of the revised configuration, the 200-gpm loop will be modified to receive the orifice-bundle test rig.

Instrumentation used in the bundle flow test will consist primarily of static pressure taps along the length of selected tubes. These will be calibrated to measure flow rate through the tubes. A total flow rate through the tubes will be determined from this measurement. The total loop flow measurement will supply the additional information necessary to determine inside-to-outside flow ratio. The inlet tube orifices will be varied to obtain a desired inside-to-outside flow ratio.

3. Full-Scale Reactor Flow Model

Modification of the 5000-gpm loop for the full-scale test is in the design stage. Instrumentation layouts are being prepared for the model.

The feasibility of using the carbon steel piping of the 5000-gpm facility with corrosion inhibitors and pH control was demonstrated. The 5000-gpm flow loop containing the MPR 2-pass core was cleaned with oxalic acid to remove rust accumulation. After adequate acid flushing, a 500-ppm sodium chromate solution was maintained. Sodium hydroxide was added to maintain the pH above 10. The loop was operated during a two-week period over temperature and flow ranges corresponding to actual test operation. Pressure differentials were measured periodically in an instrumented core tube for each of the two passes. The data obtained are shown in Fig. 2.15. Two important results were obtained from this testing effort:

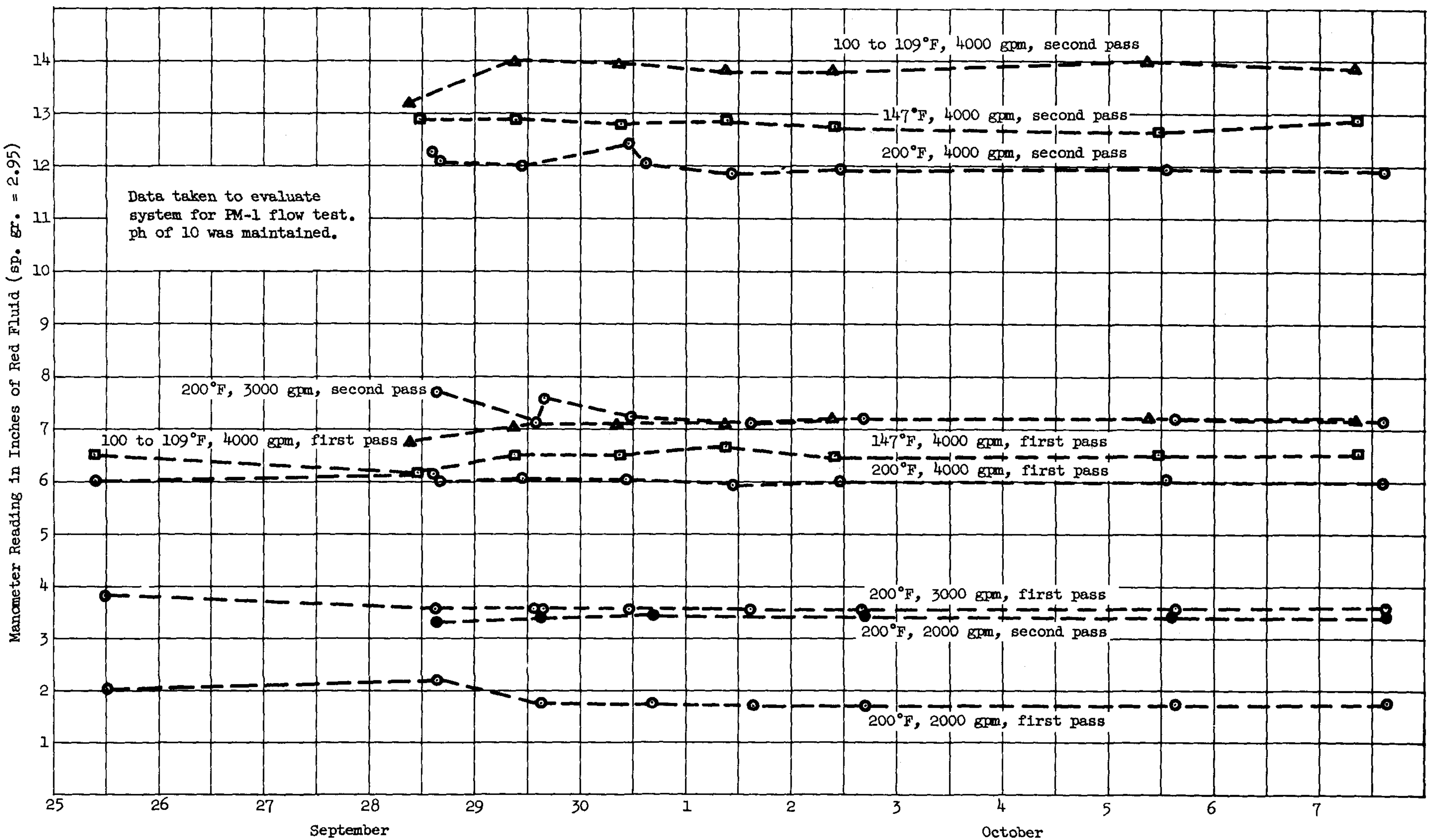

Fig. 2.15. 5000-gpm Flow Loop Studies--Effect of 500-ppm Sodium Chromate upon Pressure Drop Measurements Made in MPR Two-Pass Core

(1) There was no noticeable increase in pressure drop across either pass after an initial break-in period.

(2) Water samples removed from the loop after the two-week operation could not be visually distinguished from laboratory standards prepared prior to testing.

This testing effort indicates that no adverse effects will influence PM-1 full-scale flow test data by using a carbon steel loop with the existing pump and corrosion inhibitors added to the system.

D. SUBTASK 2.4--HEAT TRANSFER TESTS

J. J. Jicha, E. Jules, M. P. Norin, N. Webb, C. Eicheldinger

The overall objectives of this subtask are to obtain experimental data to support refined thermal and hydraulic design of the PM-1 core and to determine those quantities, such as burnout heat flux, which are difficult to calculate. The remaining planned PM-1 program is designed around three test sections, as described below.

(1) STTS-3, single-tube test section. A single-tube design with flow inside the tube only. This test section is instrumented to obtain local boiling pressure drop and heat transfer data inside tubes.

(2) STTS-4, single-tube test section. A single-tube contained within a housing so as to provide coolant flow both inside and outside of the tube. This unit will be used for burnout measurements.

(3) SETCH-2, seven-tube test section. This unit will have coolant flow outside the tubes only and will be instrumented to obtain pressure drop and heat transfer data outside of the tubes.

In addition to the above test sections, which were designed expressly for the geometry of PM-1, two test sections have been used in the program. These are STTS-2, a single-tube test section similar to STTS-4 and SETCH-1, a seven-tube test section similar to SETCH-2, but with flow both inside and outside the tubes. STTS-2 and SETCH-1 were fabricated during a company-sponsored program. The tube dimensions were not identical to those of PM-1. However, the test sections were operated at PM-1 conditions in order to obtain some preliminary data for tubes, to gain experience with heat transfer loop operation under PM-1 conditions and to evaluate the designs of STTS-2 and SETCH-1 so as to obtain improved designs for the PM-1 test sections noted above.

Actual accomplishments of this quarter were:

(1) Analysis of SETCH-1 testing was completed.

(2) The STTS-2 test program was completed.

(3) The design of STTS-3 was completed and the test procedure completed.

(4) The design of STTS-4 was completed and test procedure initiated.

(5) The design of SETCH-2 was completed.

The anticipated accomplishments for the next quarter are:

(1) Test procedure for STTS-4 will be completed.

(2) Test procedure for SETCH-2 will be completed.

(3) Fabrication of STTS-3 will be completed.

(4) Fabrication of STTS-4 and SETCH-2 will be initiated.

(5) Testing of STTS-3 will be completed.

1. Test Section Design Parameters

The following table summarizes the dimensions of the three PM-1 test sections:

		STTS-3	SETCH-2	STTS-4
Heated length	(in.)	30	30	15
Outside diameter	(in.)	0.500	0.500	0.457
Inside diameter	(in.)	0.416	0.457	0.416
Wall thickness	(in.)	0.042	0.0215	0.0205
Inside shell diameter	(in.)	--	2.1	0.668
Number of tubes		1	7	1
Tube material		347SS	347SS	347SS
Power, maximum	(kw)	266	285	296
Voltage, maximum	(v)	71	38	79
Current, maximum	(amp)	3750	7500	3750

All test sections were sized to simulate the PM-1 geometry as closely as possible. It was possible to make the dimensions of the single-tube test section (STTS-3) the same as the PM-1 tube and still have a sufficient amount of power available in the test loop.* Local boiling will occur at the outlet end of the STTS-3 with a power on the order of 13 kw for design flow and inlet coolant temperature.

In order to obtain a high power for the seven-tube test section (SETCH-2), the resistance of each tube must be seven times the total resistance of 38/7500 ohm. This necessitates a thinner tube wall than that of the PM-1 tube. Since flow is outside the tubes, the outside diameter was kept the same and the inside diameter was increased. The shell diameter was sized to provide the same equivalent diameter outside the tubes that exists in the PM-1 core. A power of approximately 200 kw will produce local boiling at the outlet for design values of flow rate and inlet coolant temperature.**

Since it is desirable to end the heated section without disturbing the flow, copper rod extensions were added to each of the seven steel tubes. These rods carry the current from the tubes over about a 3-1/2-inch length to the outlet header, but produce negligible heating because of their low resistivity and large (compared to the tube walls) cross-sectional area. To improve the corrosion resistance of these rods, they are nickel plated.

In the burnout test section (STTS-4), it was especially necessary to reduce the wall thickness so that the maximum power available might be utilized. Matching a resistance of 38/7500 ohm would give a wall thickness greater than that of the PM-1 design, while matching 79/3750 ohm yields a thinner wall. The latter was chosen since, if there is an effect of heat capacity of the tube wall on burnout, the thinner wall would give a lower (conservative) burnout heat flux than will exist in the PM-1. The inside diameter was held the same and the diameter of the shell was sized to give velocities in the test section corresponding to those in the PM-1 design.

---

*The maximum power presently available in the test loop is 300 kw. There are two voltage hookups. The maximum direct current on the 40-volt hookup is 7500 amperes and on the 80-volt hookup is 3750 amperes. These current values cannot be exceeded without damage to the equipment. The loop resistance external to the test section is estimated to be 2.6667×10^{-4} ohm.

**Based on the Jens and Lottes and Dittus-Boelter correlations.

It was also necessary to decrease the length of the tube; the longer length at the design flow rate and at high values of subcooling would require a prohibitively low coolant temperature at the test section inlet.* By halving the length, reasonable values of coolant inlet temperatures are obtained at design flow and high amounts of subcooling. There is some controversy as to whether the length has any effect at all on local boiling burnout. Most correlations do not include it. The only correlation which does include it is the Westinghouse correlation which shows that a 50% decrease in length increases the burnout heat flux by only 4-1/2%.**

In the burnout test section, it is also desirable to stop the heated portion of the tube without disturbing the flow in the vicinity of the outlet ends. However, since flow occurs inside as well as outside, a tubular extension rather than a rod must be used. Also, since it is impractical to nickel plate a copper tube, the 4-inch length required will be made completely of nickel. Despite a resistance which is four times that of copper, the heat generated is only 2-1/2% of the total. This is not restrictive.

All test section tubes have their heated length made of Type 347 stainless steel. This steel was chosen over 304 and 316 because of its higher yield strength at high temperatures.

The tolerances which will be held on the test section tubing will be +0.002, -0.000 inch on the outer diameter and ±5% on the tube wall.

An analysis was made to establish the equations to be used in computing the temperature drop across the tube wall. This information is necessary for reducing data in both the STTS-3 and SETCH-2 tests, where it is desired to know the surface temperature on the coolant side (in order to calculate the film coefficient), but where the temperature measurement is made on the insulated side.

The steady-state diffusion equation for heat conduction in one dimension, with a thermal conductivity which varies linearly with temperature and a constant heat generation term, was set up and solved for the temperature distribution throughout the entire wall thickness. The wall was then divided into regions and the diffusion equation resolved

---

*Based on the Jens and Lottes local boiling burnout correlation.

**WAPD-188

for each region, with a representative thermal conductivity and source term based on the first calculation of the temperature distribution. Starting with the region which has the insulated boundary (since both the gradient and the temperature, having been measured, will be known at this boundary), the solution for this and successive regions may be obtained using boundary conditions from the previous region. A second and more accurate solution for the temperature distribution and, with it, the temperature drop across the wall may thereby be found, the accuracy increasing with increasing number of sample solutions.

Hand calculations for both two and four regions for a typical case resulted in accuracy improvements of less than one degree. An iterative procedure is therefore not required. The main reason for this result is that heat fluxes in these tests are low and the temperature drops across the tube wall are less than 50° F. The variation in resistivity (source term) across the wall is therefore insignificant.

A study was also made to investigate the effect of the nickel extension on the location of burnout in the burnout test section.

The PM-1 burnout test section (STTS-4) has a short length of nickel tubing brazed to the end of the stainless steel tube to prevent flow disturbance near the burnout point. The heat generation rate in the nickel is quite low relative to that in the stainless steel. The location of the burnout point is quite important, since most correlations of burnout heat flux are very dependent on the amount of local subcooling, and this will vary as much as 20° F per inch in the PM-1 burnout test.

In order to analyze the problem completely, it would be necessary to solve a three-region, two-dimensional heat conduction problem with volumetric heat generation. The three regions are:

(1) The portion of the stainless steel tube having local boiling along its surfaces.

(2) The portion of the stainless steel tube cooled sufficiently by the nickel extension to have no boiling along its surfaces.

(3) The nickel tube.

Furthermore, an iterative procedure would be required to determine the location of the division between regions (1) and (2).

To avoid such a complicated problem, a number of simplifying assumptions were made. These were:

(1) The problem was analyzed in a rectangular coordinate system. This will introduce little error, since the ratio of wall thickness to radius of the burnout test section is only 10%.

(2) The nickel tube was assumed to cause a temperature equal to the bulk coolant temperature at the stainless steel-nickel interface. This assumption is conservative.

(3) Only a single region was analyzed. Two separate computations were made: one using a boiling film coefficient, the other using a nonboiling film coefficient.

Thus, the problem was reduced to determining the two-dimensional temperature distribution in a rectangular plate having volumetric heat generation. The necessary equation was derived and numerical computations made.

It was concluded that the temperature distribution of the stainless steel tube will not be affected at a distance greater than 0.10 inch from the stainless steel-nickel interface. Therefore, unless there is some local flow disturbance elsewhere along the test section, burnout should occur within this distance from the outlet end of the stainless steel tube. This is based on the maximum amount of subcooling at the outlet of the test section (i.e., 100° F).

2. Results of SETCH-1 Tests

The results of testing SETCH-1 are given below.

a. Description of test section

SETCH-1 is a seven-tube test section in which the tubes are subjected to a uniform heat flux obtained through direct current resistance heating. The unit is shown in Fig. 2.16. The tube dimensions in inches are: 0.375 outside diameter, 0.030 wall, 0.315 inside diameter, with a 22-inch heated length. The active lengths of the tubes are made of stainless steel. At either end, the tubes are fitted with copper tubes. The ends of the copper tubes are brazed into copper headers so as to make up a bundle of one central tube and six peripheral tubes. The header configuration is shown in Fig. 2.17. Those surfaces of the copper tube in contact with the coolant are nickel plated.

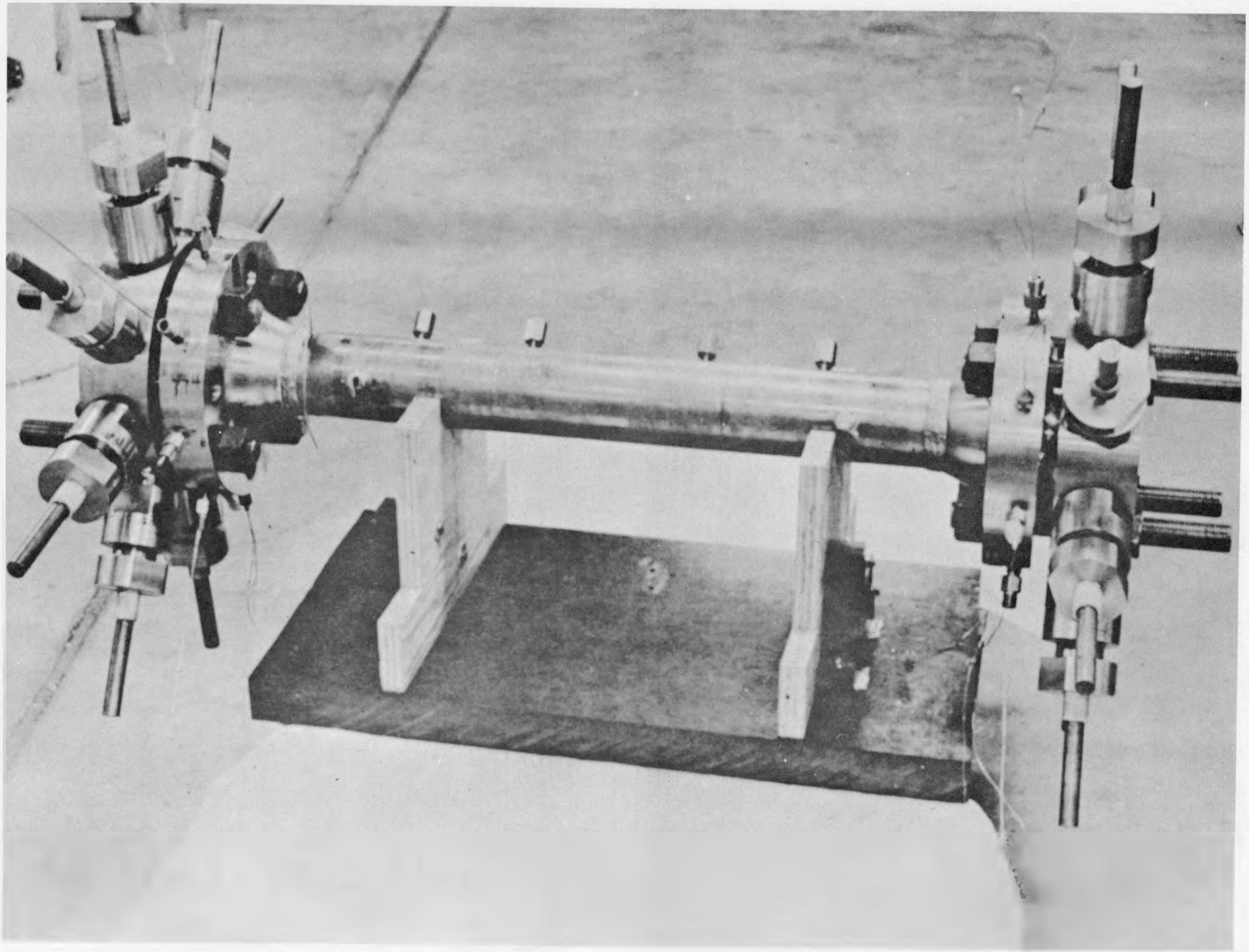

Fig. 2.16. Seven-Tube Test Section (SETCH-1)

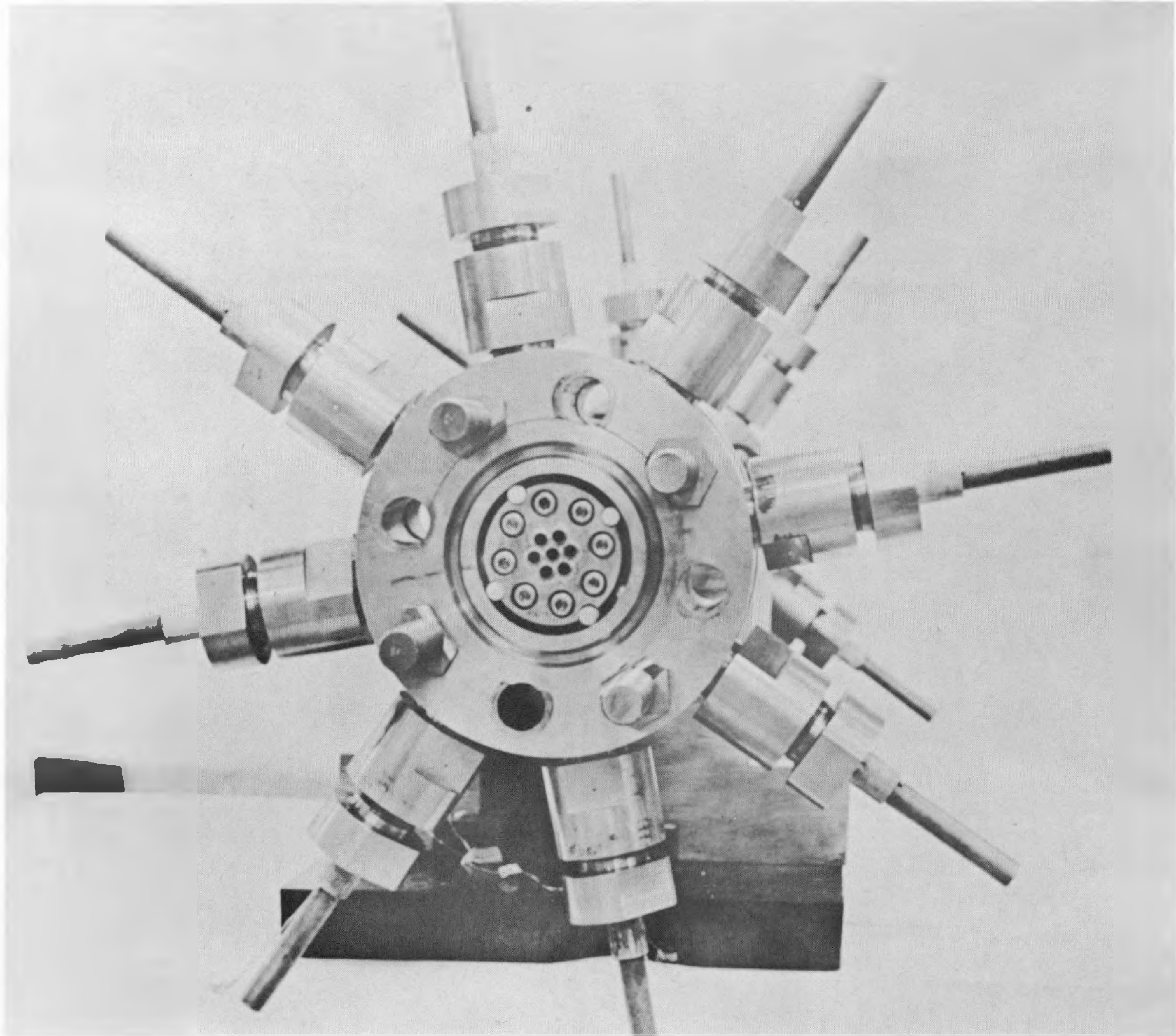

Fig. 2.17. End View of SETCH-1 Showing Header and Electrode Configuration

As shown in Fig. 2.17, the headers are electrically insulated from and spaced in the plate containing the electrodes by four ceramic cylinders. It is seen that the fluid to the outside flow path of the tubes entered the test section through an annulus formed by the periphery of the header and the inner surface of the plate. The fluid then passed through a converging channel (transition piece) to the straight cylindrical section which composed the active region of the test section. The straight section was bounded by a ceramic cylinder of a diameter selected to give a coolant velocity outside the tubes identical to that within the tubes. The ceramic cylinder is provided with several small holes through its wall, thus giving nearly equal pressures on either side of the wall. The differential pressure across this wall is due only to the head loss in the test section.

The ceramic cylinder is surrounded by a steel cylinder welded at the ends to flanged transition pieces to form a housing for the unit. Electrical power is supplied to the test section through electrodes connected to the headers. Eight electrodes, equally spaced around the periphery of each header, are made of round copper bars, the ends of which are connected to copper cables. The loop power lines are clamped to the bars and the cables are fitted into sockets in the headers and held by set screws. The cables are the only restraints imposed on the tube-header assembly. Thus, a degree of flexibility allows the tubes some freedom in longitudinal variations under temperature changes.

A detailed study of the test section may be gained by reference to The Martin Company drawings listed in Table 2.5 below.

TABLE 2.5

Major Components--SETCH-1

Drawing No.	Title
335-0515075	MPR Fuel Element Test Section
335-0515080	Housing Assembly
335-0515081	Header
335-0515082	Plate
335-0515090	Electrode Assembly
335-0515092	Tubing Assembly

b. Instrumentation

Static pressure taps were provided for the measurement of pressure drop within the central tube, within one peripheral tube, and in the outside flow path formed by the outer surfaces of the tubes and the inner surface of the ceramic cylinder. One set of taps, spaced at 20 inches apart, was provided for each of the above. The pressure taps were connected to differential pressure cells; these were diaphragm-type devices which transmit a low pressure pneumatic signal to chart recorders.

Ten pairs of thermocouples were placed along the length of the central tube. One thermocouple of each pair was located on the outside surface of the tube and the other placed in the flow stream adjacent to the tube. The thermocouples were connected through a selector switch to a manually operated galvanometer-type potentiometer. Thermocouples were also provided at the loop elbows upstream and downstream of the test section for the measurement of coolant inlet and outlet temperatures.

Electrical connections were made at the test section electrodes for the measurement of voltage drop across the test section. An indicating and a recording voltmeter were used in conjunction with a recording ammeter in order to monitor and measure the power (heat flux) supplied to the test section.

The total flow rate to the test section was measured with a Pottermeter. The Pottermeter sensing element signal was transmitted to an integrating instrument which gave a record of the flow rate. For fine measurements, the signal was read out on a scaler equipped with a timer.

c. Flow calibration of tubes

Flow calibration tests were performed for the central tube and outer tube of SETCH-1. This was required so that, in the nonboiling or forced convection regime, the flow rate outside the tubes could be calculated. That is, the flow through the tubes would be determined by the measured head loss of the instrumented tubes through the calibration. Subtraction of this flow from the measured total flow to the test section gave the flow outside the tubes.

The calibrations were performed out of the loop using the setup of Fig. 2.18. The ranges in variables were:

Velocity: 1.5 to 15 feet per second

Temperature: 55 to 200° F

Reynolds No.: 3×10^3 to 8×10^4.

In the experimental program, the ranges in these parameters were (with local boiling runs included):

Velocity: 0.75 to 1.8 feet per second

Temperature: 441 to 560° F

Reynolds No.: 1.2×10^4 to 3.4×10^4.

Near the end of the calibration tests, a leak was observed at the downstream pressure tap of the central tube. This leak was not repaired, since the tap was inaccessible without major rework of the test section. Therefore, only the test results for the outer tube are given here. These are shown in Fig. 2.19 as friction factor versus Reynolds number. A curve computed from smooth tube data is included for comparison. Over the Reynolds number range of the experimental program:

$$f = 1.01\,(Re)^{-0.36}$$

$$1.1 \times 10^4 \leq Re \leq 3.4 \times 10^4$$

where

$$f = \frac{h}{\frac{L}{D} \times \frac{V^2}{2g}}$$

h = head loss

L = length of tube

D = inside diameter of tube

$\frac{V^2}{2g}$ = velocity head.

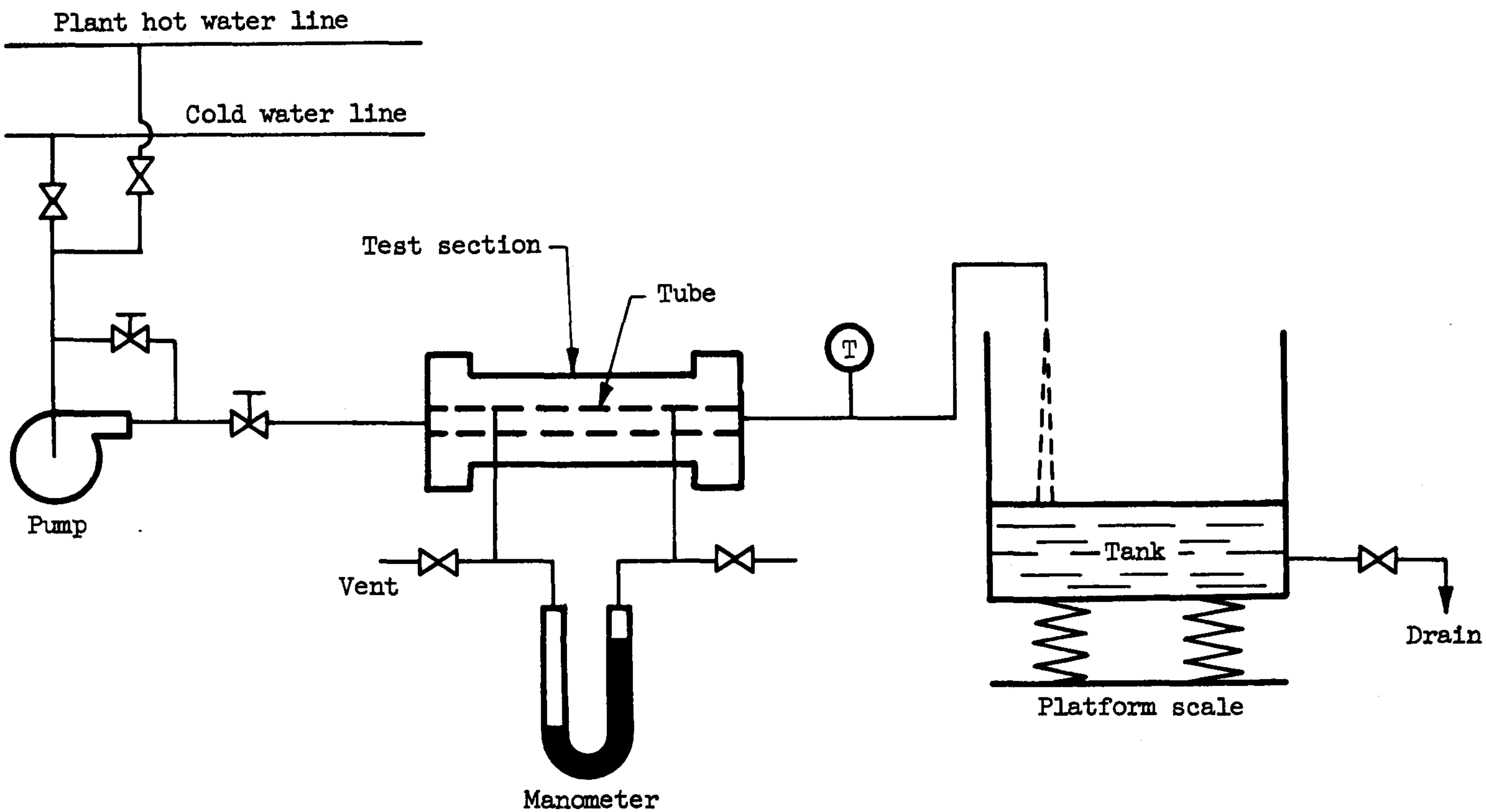

Fig. 2.18. Test Setup, Flow Calibration of SETCH-1 Tubes

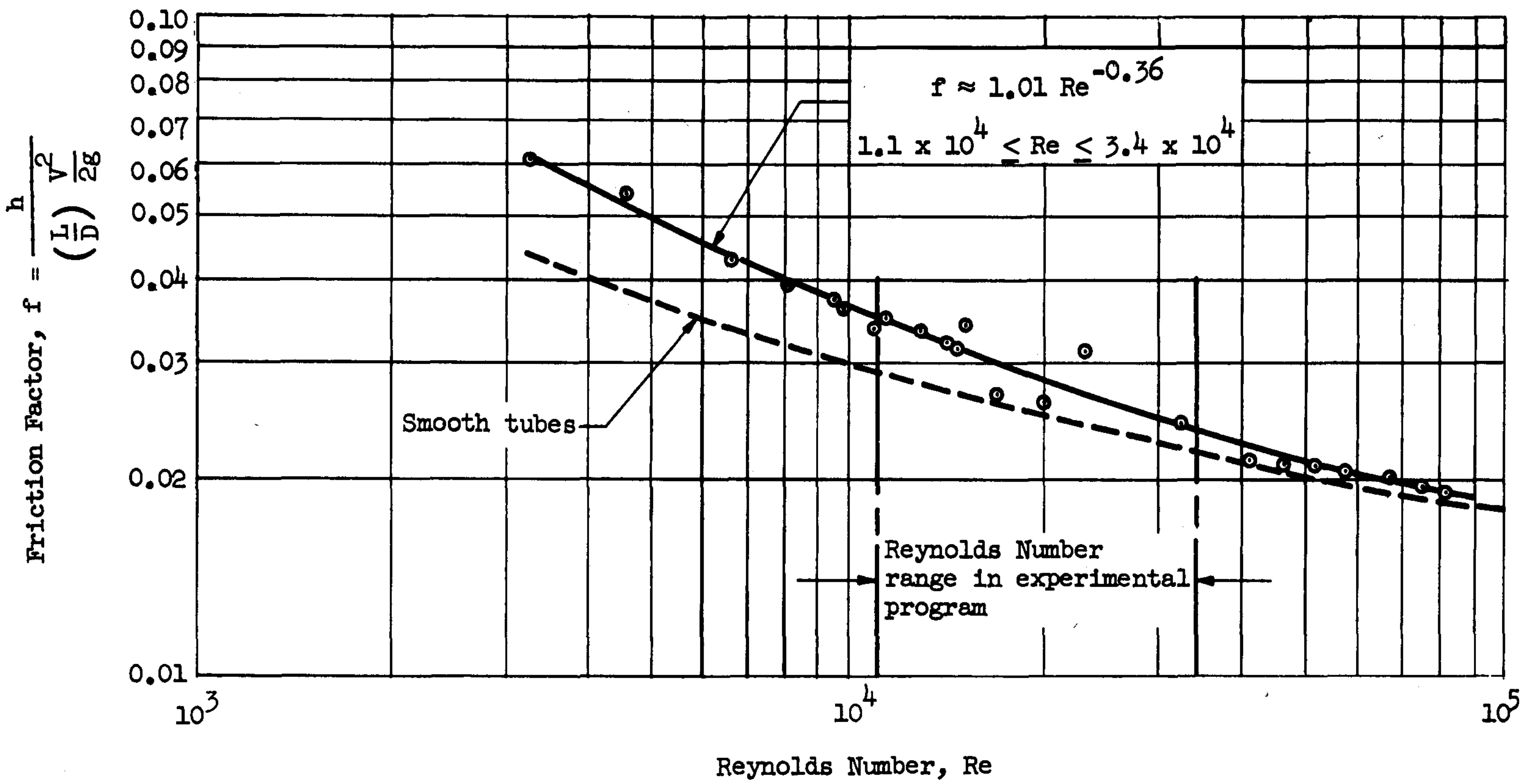

Fig. 2.19. Friction Factor Versus Reynolds Number, SETCH-1 Outer Tube

d. Installation of test section and preliminary operation

The unit was installed in the loop vertically as shown in Fig. 2.20. Instrument connections were then made and the test section subjected to hydrostatic tests. Considerable difficulty was experienced because of leaks at the electrode fittings. Some modifications to the design were required in order to accomplish leak-free operation.

After shakedown operation and checks of the electrical connections, the test section was thermally insulated. The complete installation is shown in Fig. 2.21.

e. Experimental program

The program was based on the operating conditions anticipated for PM-1. The range of variables is shown in Table 2.6. Heat flux was limited by bulk coolant saturation at the outlet. Experiments to determine heat losses across the test section were also included in the program.

TABLE 2.6

Operating Conditions

Pressure (psia)	Inlet Temperature (°F)	Velocity (fps)	Heat Flux (Btu/hr-ft^2 x 10^{-3})			
1300	441	0.75	44	59	74	81
		1.5	118	132	147	162
		1.8	162	176	184	199
1300	460	0.75	37	44	59	66
		1.5	110	116	132	140
		1.8	140	147	162	169

f. Results and discussion

As previously stated, instrumentation difficulties arising from design features of SETCH-1 were encountered during preliminary testing. All 10 of the thermocouples placed on the central tube wall and most of the thermocouples at adjacent bulk coolant locations failed. Therefore, only a reduced test program to obtain local boiling pressure drop data

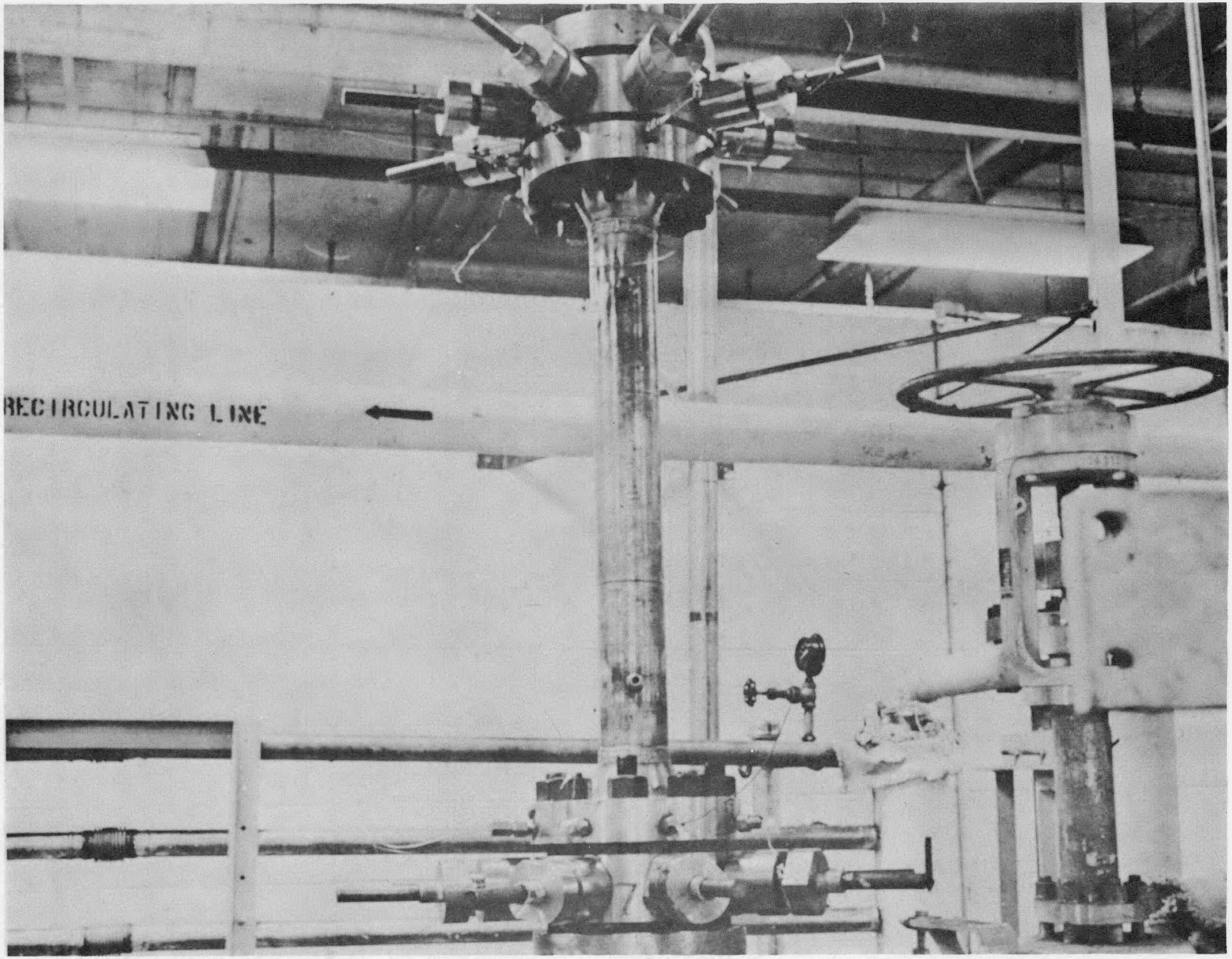

Fig. 2.20. SETCH-1 Installed in Loop

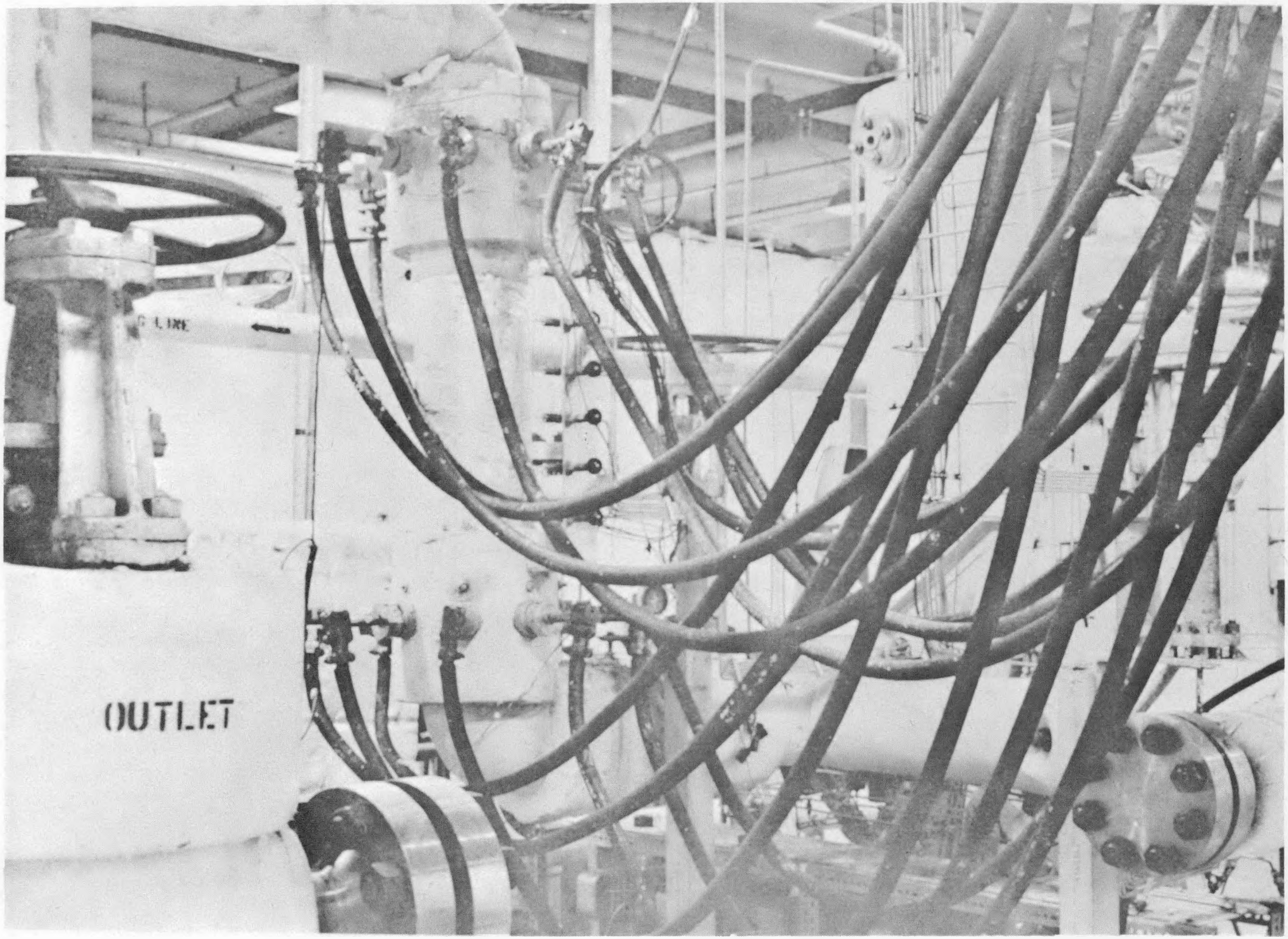

Fig. 2.21. SETCH-1 Complete Installation

inside and outside the tubes was initiated. The failure of the thermocouples could have been due to failure of the braze material holding the central steel tube in the copper extension tubing. When the central tube was disengaged, the fragile thermocouples were broken. This failure was not discovered until after the test when the test section was removed from its housing. The central tube could have worked loose during the differential thermal expansion encountered at the hot steel-cold copper junction.

The original objectives of the test, local boiling pressure drop and heat transfer studies were, therefore, completely compromised. Despite this, the reduced program was carried to completion. The primary objective was to complete the evaluation of the SETCH-1 design and to gain operating experience with the loop under PM-1 local boiling conditions. Considerable down-time was experienced due to gasket leaks at the top and bottom sets of electrodes. "Durabla" gasket material, which was originally employed, was abandoned in fabor of "Garlock 900" and copper gaskets. These difficulties ranged from slight leaks at the inner and outer electrode gaskets and cracks at the silver solder joint to gasket blowouts. It became evident during the course of the program that this type of electrode design should be avoided in future test section design.

The data obtained enabled a heat loss determination to be made which attested to the adequacy of the thermal insulation. This heat loss, as shown in Table 2.7 for a few typical runs, was well within the accuracy of the thermocouple, ammeter and voltmeter calibrations.

It should be noted that, at the low flow rates of interest in the PM-1 program, test section inlet temperature was extremely difficult to obtain due to the available controls for the pre-heaters and the heat exchanger. The flow control valve of the heat exchanger secondary system was too large for the coolant flow rates required. Thus, too much sensible heat was removed in the heat exchangers and the limited line heaters failed to meet inlet temperatures. When flow to the heat exchanger was completely cut off, the on-off control of the line heaters resulted in inlet temperatures higher than desired. A solution to this problem would be realized with a smaller flow control valve in the secondary system of the heat exchanger and proportional-type control of the line heaters. A flow control valve capable of controlling secondary flow at extremely low rates has already been installed. Proportional control for the line heaters will be provided by means of three 6.7-kva Wheelco saturable reactors. These are presently being installed.

TABLE 2.7

Test Section Heat Loss Measurements

Flow Rate (gpm)	Pressure (psi)	Inlet Coolant Temperature (°F)	Outlet Coolant Temperature (°F)	Heat Loss (kw)
3.10	1300	442.8	440.9	0.760
3.06	1300	487.0	487.5	--
3.05	1305	303.0	303.3	--
3.05	1305	410.7	410.7	0
3.14	1300	417.0	417.0	0
3.14	1300	447.0	447.0	0
3.16	1300	447.5	447.6	--
3.16	1290	501.7	501.8	--
3.16	1290	507.0	507.0	0

Upon completion of the 24-run reduced program, the test section was removed from the housing. Subsequent examination revealed, as previously stated, that the central tube was disengaged from the copper extension tube at the flow inlet end. Visual indications showed that this condition was probably present throughout the test since only the six peripheral tubes had a significant amount of boiler scale on the "hot" end, i.e., the outlet end, of the tube. Figure 2.22 is a photograph of the tube bundle and headers showing the boiler scale. Emission spectroscopy showed iron, magnesium, silicon and aluminum as the major constituents of this deposit while chromium, nickel and copper were present to a lesser extent. This sample presented a mixture of molecular structures, the dominant pattern being $MgO \cdot 2\ SiO_2 \cdot H_2O$. The inlet ends of the tubes and, in particular, the inlet header, were generously coated with what emission spectroscopy revealed to be hydrated nickel oxide $NiO \cdot H_2O$. In addition to the nickel, aluminum also appeared as a major constituent, with copper, silicon and cobalt as minor constituents. The origin of this nickel oxide was the nickel-plated copper extension tubing and nickel-plated copper header. During the test program, daily checks

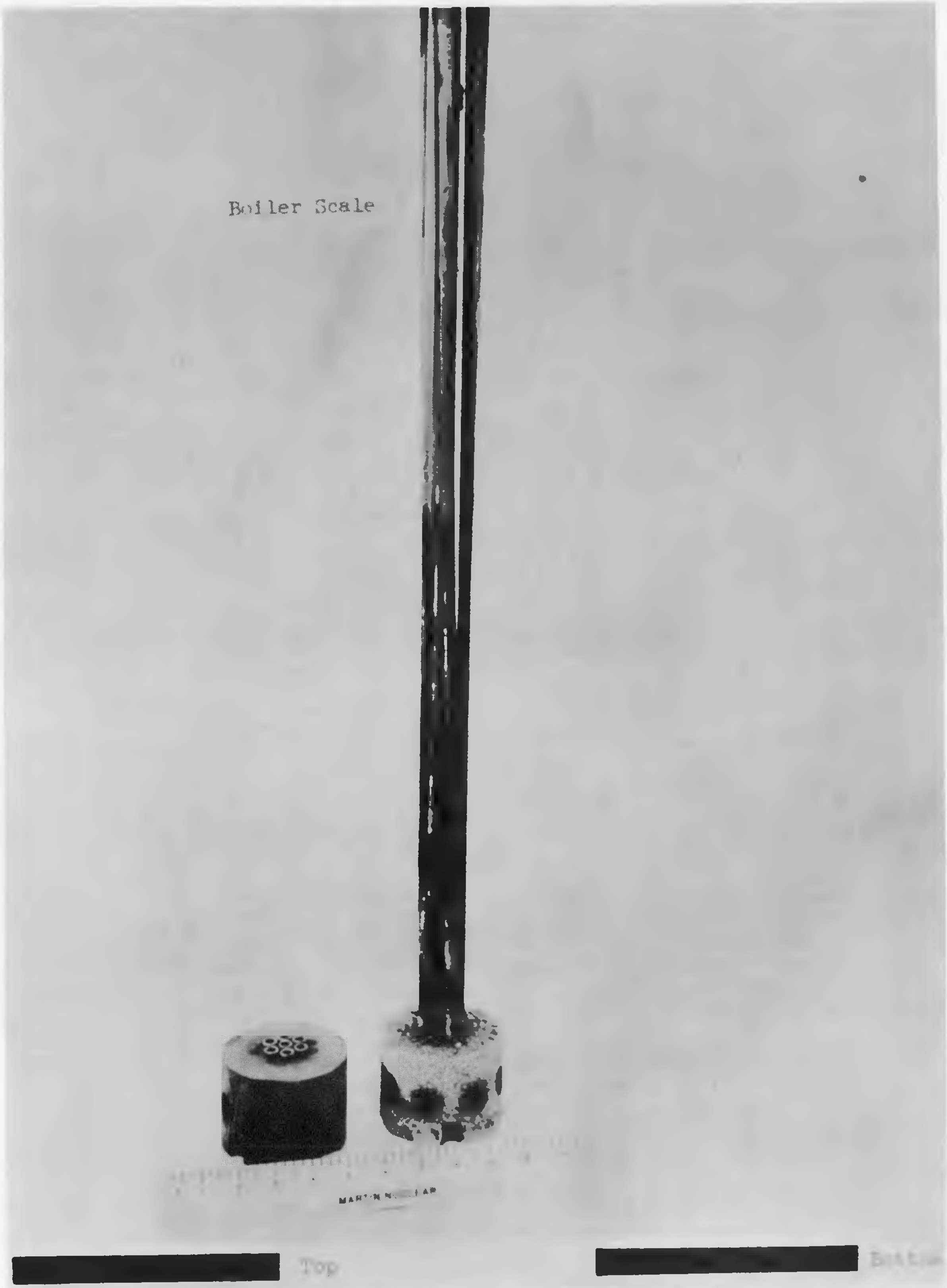

Fig. 2.22. SETCH-1 After Testing

of the water purity were made. Resistivities over the test period averaged 750,000 ohm-cm which is the equivalent of less than 0.5 ppm of ionizable impurities. Demineralized and deaerated water was employed to charge the loop but no samples were tested for solids content once the loop was operated. Thus, the solids content could have been appreciable despite the continuous operation of the loop demineralizer. It is widely reported in the literature that such solids are preferentially deposited on a boiling heat transfer surface.

The results of two research groups*, ** engaged in determining the effects of scaling during local boiling heat transfer operation lead to the conclusion that scaling on the heat transfer test surfaces can be minimized by treating the water, thereby maintaining the pH between 9.5 and 10.5. This can be accomplished by employing 75 ppm of 67% disodium phosphate--33% trisodium phosphate. Water so treated would be required to bypass the system demineralizer during normal test operation. Thus, the loop water resistivity would have to be brought to a purity level desired (1×10^6 ohm-cm) and the demineralizer then isolated from the loop. Water treatment would follow with periodic sampling to maintain the desired pH.

g. Recommendations

The efforts of the evaluation program of SETCH-1 has resulted in the following recommendations which are presently being incorporated in the design of PM-1 test sections.

(1) A new approach to electrode installation should be considered to reduce down-time due to leaks.

(2) Thermocouples employed to measure wall temperature should be placed along an isotherm, with from 3/4 to 1 inch of the couple mechanically bound to the surface.

(3) Pressure taps should be installed such that the density corrections to the indicated pressure drop are small, positive and capable of accurate determination.

---

*Jens, W. H., and Lottes, P. A., "Analysis of Heat Transfer, Burnout Pressure Drop, and Density Data for High Pressure Water," ANL-4627, 1951.

**Howells, E., and Fergurson, K. M., "CS-2 Nucleate Boiling Tests," Babcock and Wilcox Company, Report No. 5432, 1957.

(4) Two test sections, one of the seven-tube-type and one single-tube design, should be fabricated to accomplish the objectives proposed for the SETCH-1 program.

The experience gained at the low power inputs and low flow rates of the PM-1 design pointed out a need for several modifications to the heat transfer loop control systems. These modifications are:

(1) Finer control of the primary flow rate.

(2) Finer control of the heat exchanger secondary flow rate.

(3) Proportional control of the loop line heaters, i.e., better control of test section inlet temperature.

3. Results of STTS-2 Testing

An experimental program to obtain local boiling pressure drop and heat transfer data at PM-1 design conditions was conducted with a 3/8-inch diameter stainless steel tube. This program reached the 40% completion point when an electrical short caused a test section failure. However, reasonable local boiling pressure drop data were realized.

The heat transfer data were not of sufficient accuracy because of the degree of error in the measurement of wall temperatures. This situation will be alleviated in future test work by incorporating additional auxiliary runs to establish accurate heat transfer surface temperatures.

a. Description of test section

STTS-2 is a single-tube test section equipped with backup plates to ensure structural integrity during high pressure/high temperature tests. This unit was installed in the loop as shown in Fig. 2.23. Pertinent tube dimensions, in inches, are: 0.375 outside diameter, 0.030 wall thickness, 0.315 inside diameter, with a 23-inch heated length. The entire length of the stainless steel (Type 316) test section is activated by direct current resistance heating which produces a uniform heat flux. A stainless steel collar is fitted to each end of the tube and the collar, in turn, is welded to the transition section.

A flange assembly is employed to make the connection between the three-inch stainless steel loop pipe and the transition piece. The coolant flow plenum in the flange assembly and the transition section is tapered to present a smooth flow transition from the large loop pipe to the smaller test section tube.

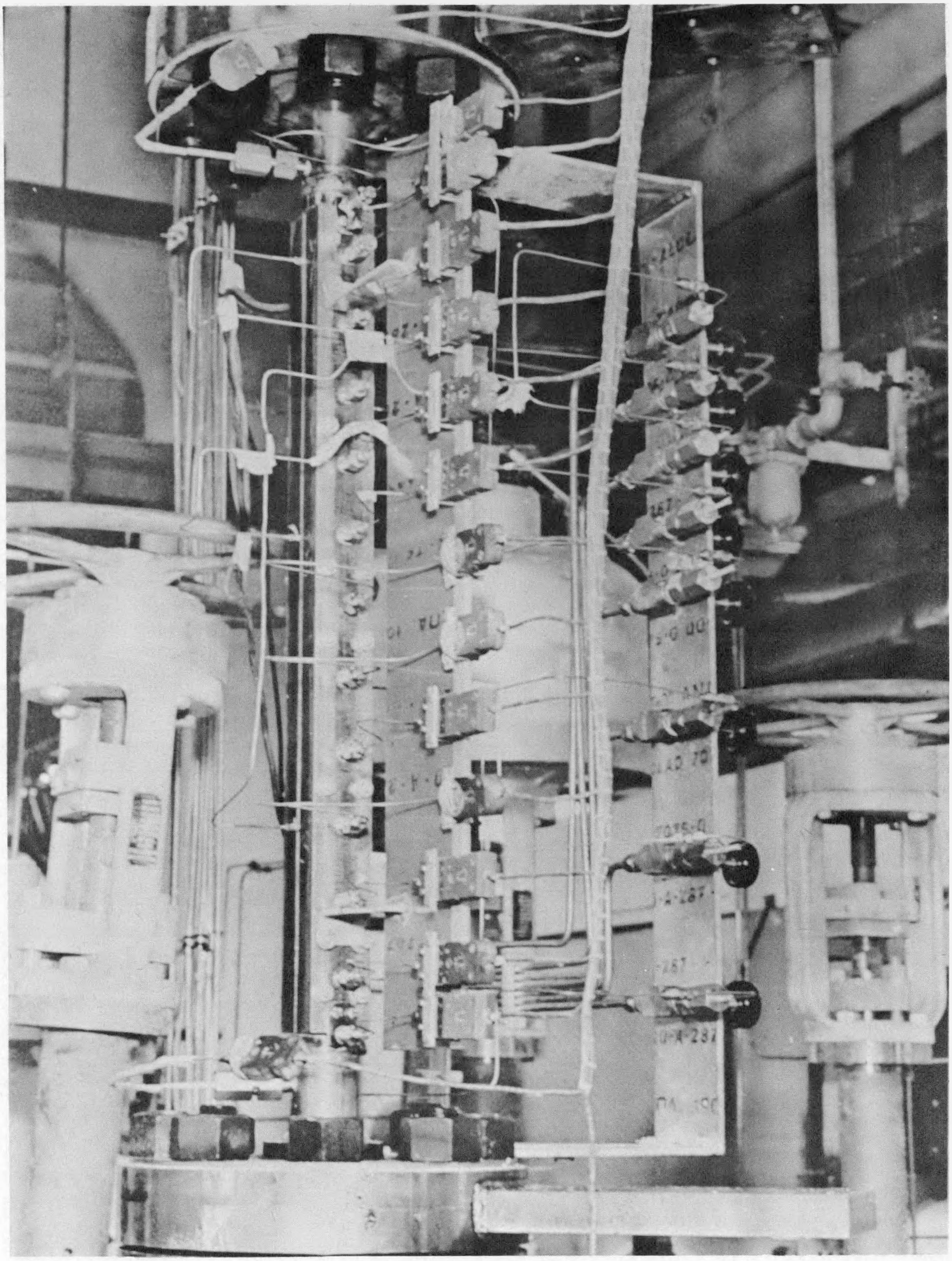

Fig. 2.23. STTS-2 Installed in Loop dP Manifold and Thermocouple Assemblies Attached

The test section assembly is completed by placing the two rectangular backup plates around the stainless steel tubing as shown in Fig. 2.24. (Figure 2.24 shows the test section and backup plates after testing.) Electrical power is supplied to the test section by eight power lines bolted to both the inlet and outlet flange assemblies. The lines are supported by a steel cradle suspended from the ceiling, thereby reducing the side loading on the test assembly.

A detailed study of the test section may be gained by reference to The Martin Company Drawing No. 372-05150000, Single Tube Test Section, STTS-2, PM-1.

b. Instrumentation

Static pressure taps were provided at eight points to obtain incremental pressure drop measurements during local boiling. Six taps were placed on the stainless steel tube at 4-inch intervals, with the first and last tap 1.5 inches from the transition piece. One tap was placed in each transition piece to give the overall pressure drop. These taps were 1.5 inches from the test section as shown in Fig. 2.25. Thus, there were five 4-inch pressure drop intervals and two 3-inch intervals. The low flow rates of interest in the PM-1 program give rise to extremely low pressure drops. It was necessary, therefore, to increase the interval of measurement from the 3 and 4 inches originally provided to 7- and 8-inch intervals. This was accomplished, as shown in Fig. 2.25, with the No. 5 tap not being used. Differential pressure cells capable of measuring up to 200 inches of water were recalibrated to give differential pressures in the range of 0 to 20 inches of water. This range represents the minimum range capability of the 200-inch differential pressure cells. Six Minneapolis-Honeywell differential pressure diaphragm-type cells were employed with a manifolding system to give six incremental readings and one overall reading. During normal operation, only five incremental readings were recorded. The increment between taps Nos. 3 and 7 was employed as a check on the data obtained during normal operation.

Thermocouples were placed at 13 positions along the tube wall as shown in Fig. 2.25. The stainless steel tube was first coated with approximately 10 mils of ceramic electrical insulation (Al_2O_3). The thermocouple wire, 10 mils in diameter, was wrapped around the ceramic coated tube along an isothermal and bonded to the tube with copper cement. Copper cement was employed because of its good thermal conductivity and poor electrical conductivity. Three of the wire thermocouples were broken during installation of the backup plates. It was necessary to replace these couples with sheathed bayonet-type thermocouples at positions 6, 8 and 9.

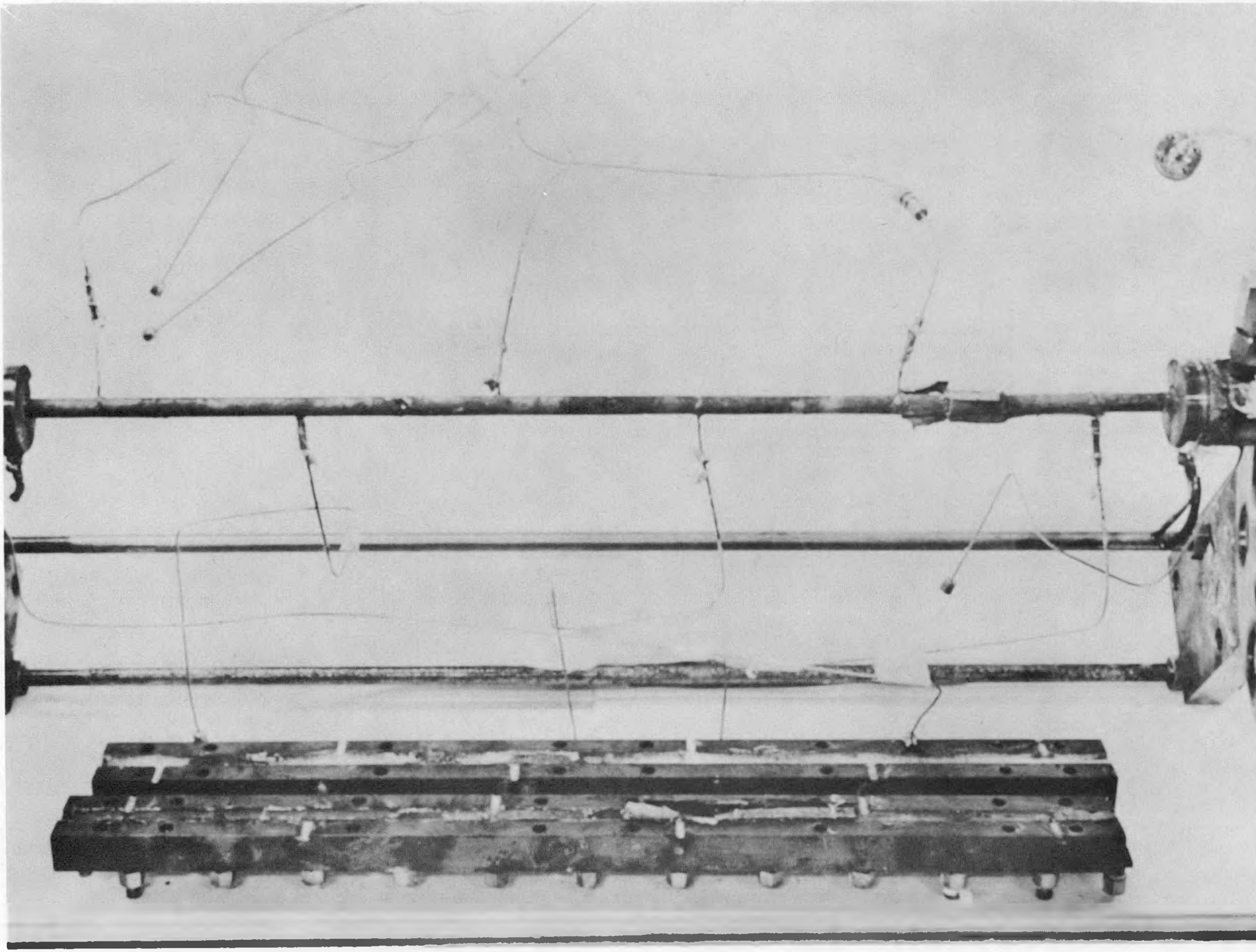

Fig. 2.24. Test Section and Backup Plates after Testing

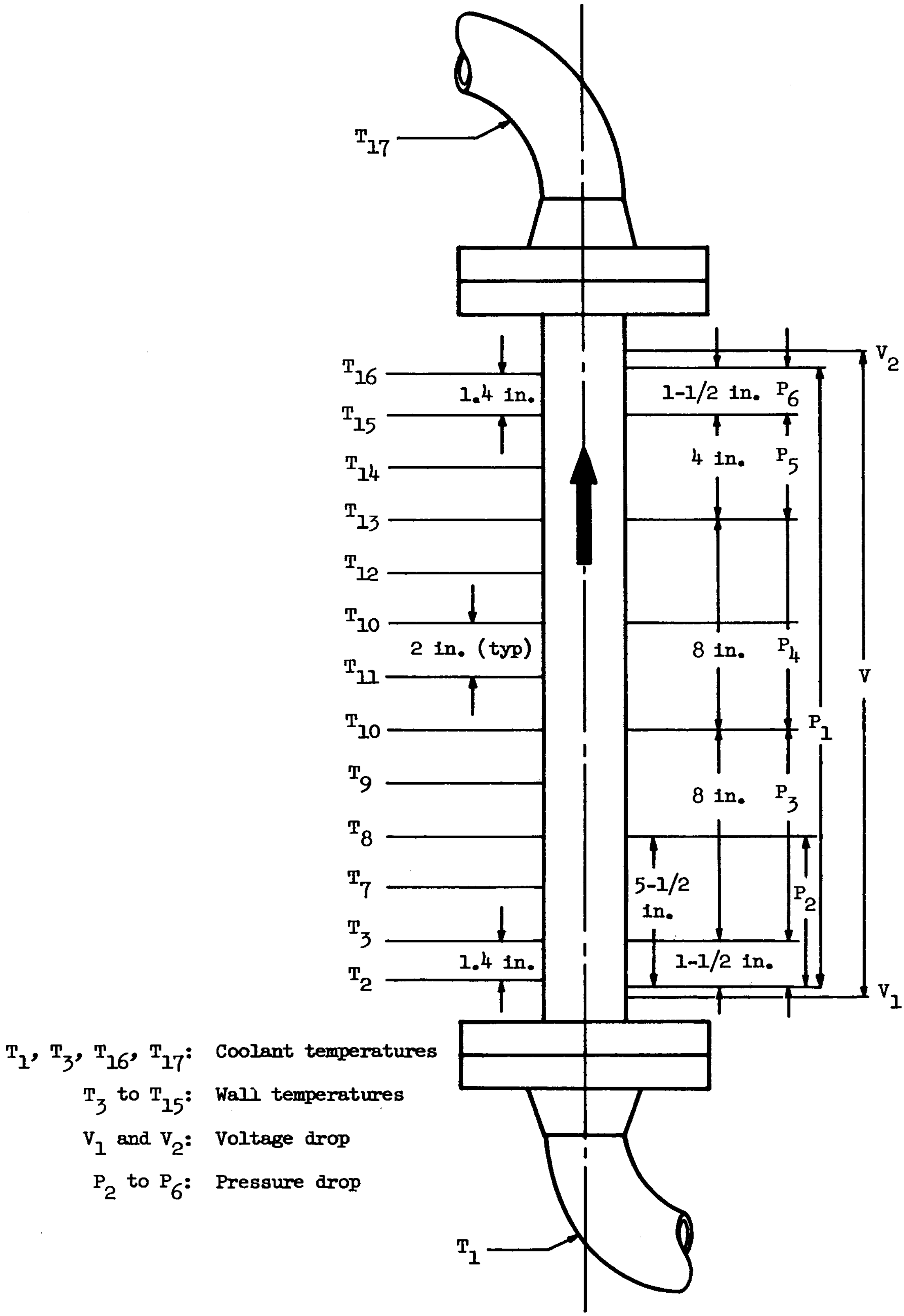

Fig. 2.25. Location of STTS-2 Instrumentation

In addition to the wall temperature measurements, bulk coolant temperatures were obtained at four points. Thermocouples were located in the inlet elbow, outlet elbow, inlet transition section and outlet transition section. Thermocouples were connected through a 24-point selector switch to a manually operated Rubicon galvanometer-type potentiometer.

In order to measure the low flow rates encountered, a low flow Pottermeter, range 0.9 to 9 gpm, was installed and used in conjunction with a 2.7- to 27-gpm Pottermeter. The output signal was recorded on an integrating-type instrument and indicated on a scaler equipped with a timer.

Power measurements were obtained by the measurement of voltage and current. Voltage probes were connected across the inlet and outlet transition sections. Voltage measurements were taken on both a recording and an indicating voltmeter. Current was measured with a recording instrument.

A diagram of the heat transfer loop is given in Fig. 2.26. A photograph of that portion of the loop in which the test section is mounted is shown in Fig. 2.27.

c. In-loop calibration

In-loop flow calibrations were performed which enabled nonboiling isothermal pressure drop data to be obtained at temperatures and flow rates close to those at test conditions. This gave the opportunity of carrying out the calibration with the differential pressure cells, flow metering instrumentation and end conditions employed during the test; therefore, a number of variables were accounted for that are normally neglected. In-loop calibration also allowed heat loss data to be taken along with the isothermal pressure drop data, thus affecting a considerable saving in test time.

A total of 19 runs was conducted to accomplish the above calibrations. Pressure drop data, however, were realized in only 10 runs. The ranges of variables over which pressure drop data were obtained are:

Velocity:	4.45 to 10.7 fps
Flow rates:	1.08 to 2.6 gpm
Reynolds No.:	6.6×10^4 to 1.55×10^5
Temperatures:	235 to 470° F

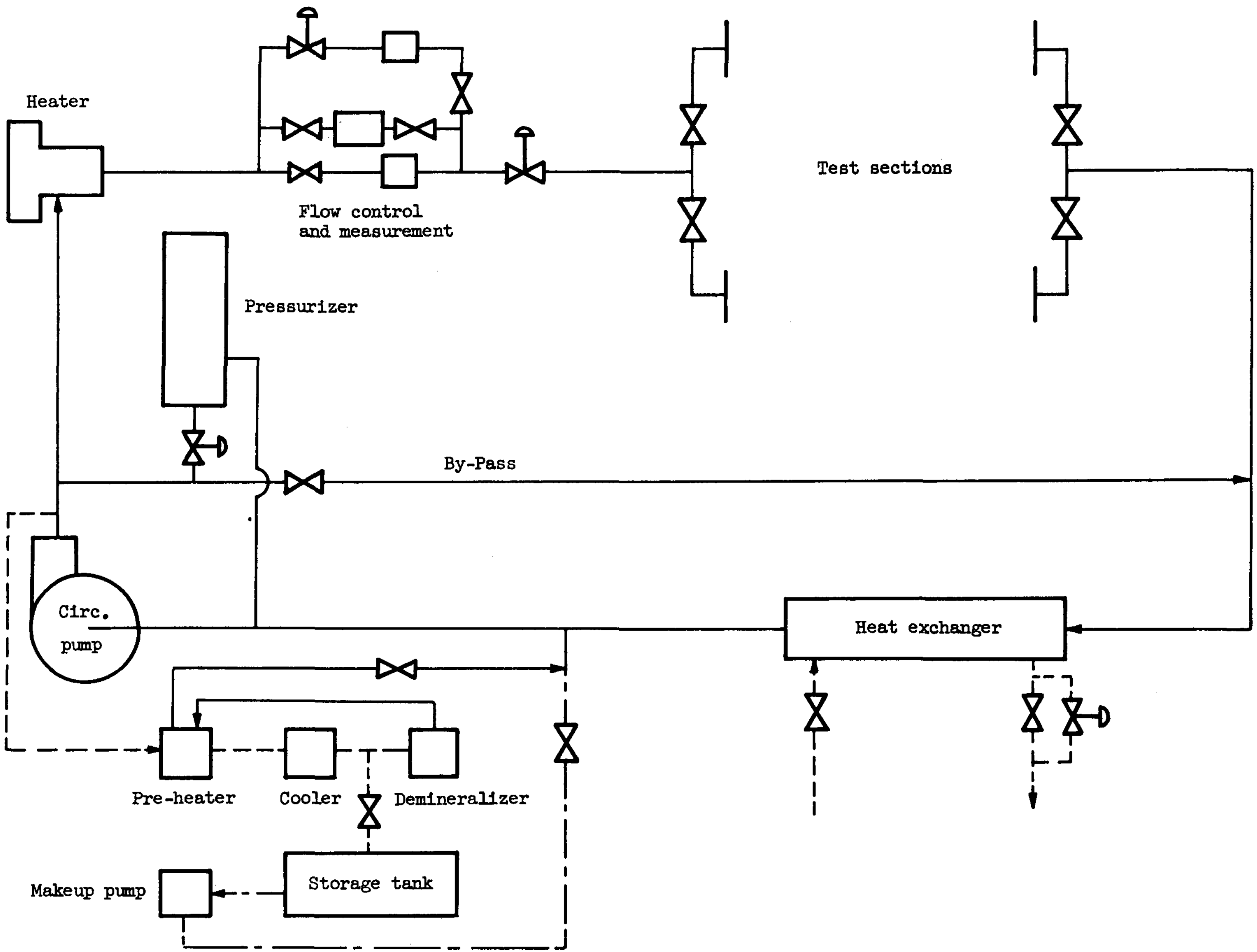

Fig. 2.26. Heat Transfer Loop Schematic

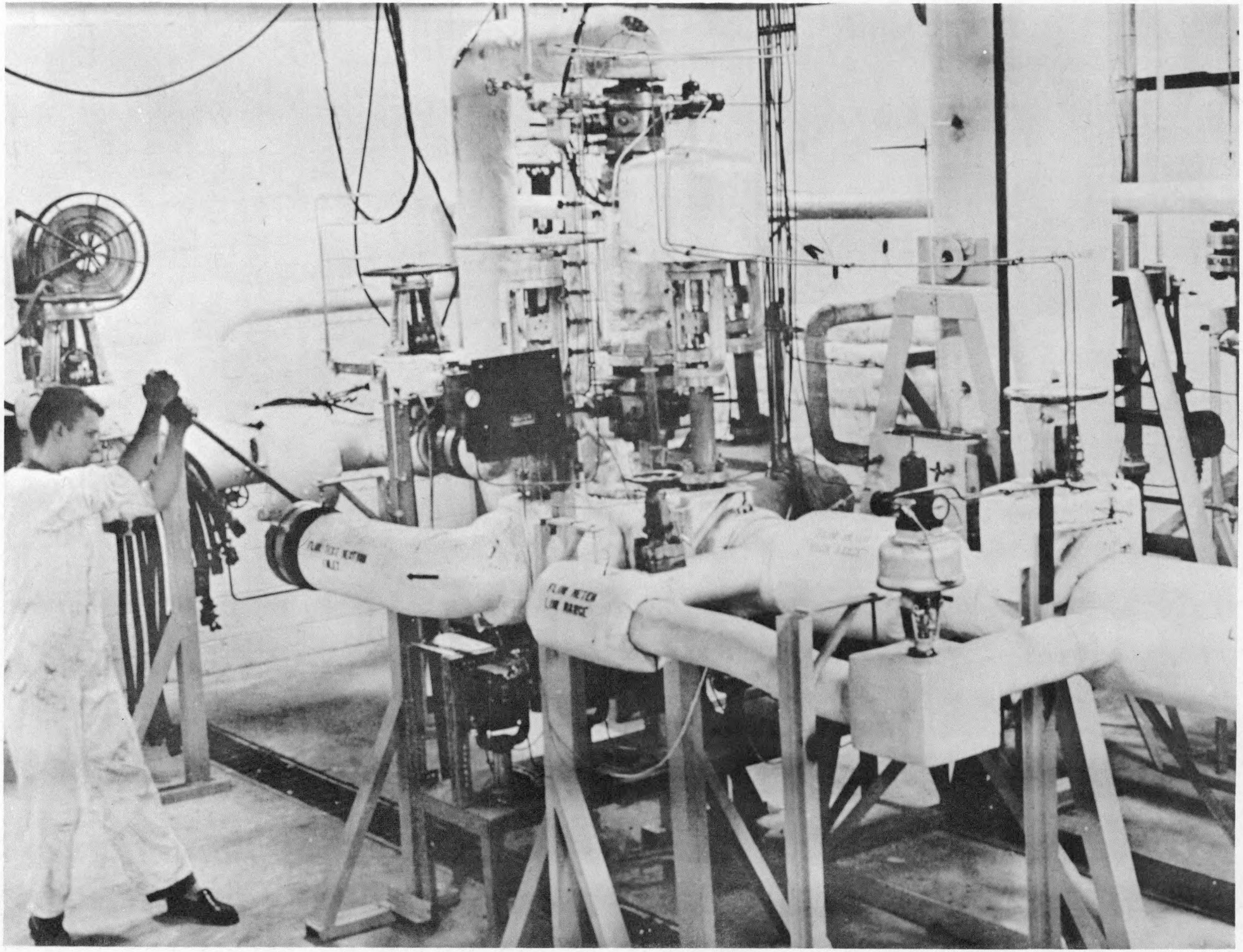

Fig. 2.27. Heat Transfer Loop

The isothermal pressure drop data obtained are shown in Fig. 2.28 along with the isothermal data obtained during out-of-loop calibration of one tube of the SETCH-1 test section. SETCH-1 had tubes of dimensions identical to those of STTS-2. A comparison to smooth tube friction factor data is also given. The Fanning friction factor employed is defined:

$$f = \frac{\Delta p^2 \, 2g_c \, D}{4G^2 \, v_m \, L}$$

D = diameter

L = length

G = mass velocity

v_m = *specific volume*

Δp = frictional pressure drop

g_c = gravitational constant.

The best equation fitting the experimental friction factor data is given by:

$$f = 0.058 \, Re^{-0.212}$$

$$3 \times 10^4 \leq Re \leq 1.75 \times 10^5$$

d. Installation of test section and preliminary operation

The unit was installed in the loop vertically. Instrument connections were then made, the test section assembly was subjected to hydrostatic tests and the design proved leak free. After shakedown operation and checks of the electrical connections, the test section was thermally insulated.

e. Experimental program

The program was based on the operating conditions anticipated for PM-1. The complete range of variables proposed is listed in Table 2.8 below. Experimental runs to determine the test section heat loss were also conducted along with isothermal pressure drop determinations.

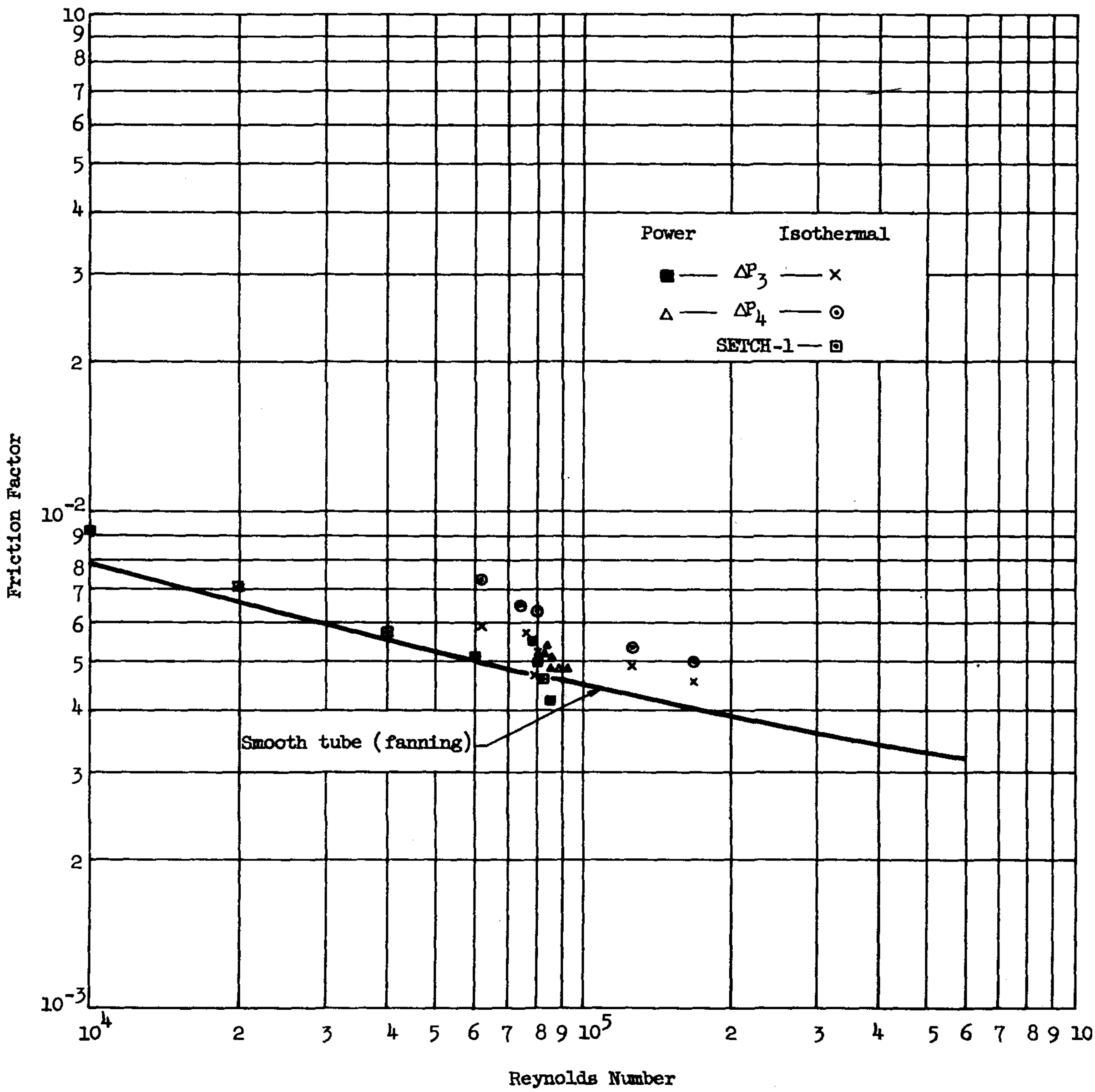

Fig. 2.28. Reynolds Number Versus Friction Factor for Nonboiling STTS-2

TABLE 2.8

Proposed Test Variables*

Pressure (psi)	Inlet Temperature (°F)	Flow Rate (gpm)	Power (kw)			Heat Flux (Btu/hr-ft^2 x 10^6)		
1300	445	1.09	12	15	18	0.259	0.324	0.389
		1.75	16	25	30	0.346	0.540	0.648
		2.50	20	30	43	0.432	0.648	0.929
	425	1.09	12	16	20	0.259	0.346	0.432
		1.75	17	25	35	0.367	0.540	0.756
		2.50	25	37	50	0.540	0.713	1.08
1100	445	1.09	8	12	16	0.173	0.259	0.346
		1.75	14	20	25	0.303	0.432	0.540
		2.50	18	25	36	0.389	0.540	0.778
	425	1.09	10	15	19	0.216	0.324	0.411
		1.75	14	22	30	0.303	0.476	0.696
		2.50	20	32	43	0.562	0.692	0.924

* The above program was only partially completed due to test section failure. It should be noted that the proposed inlet temperatures and flow rates were not, in general, accurately achieved due to inadequate control on the preheaters and flow control valve. The parameters investigated covered the following ranges:

Power:	5.5 to 40.6 kw
	0.119 x 10^6 to 0.878 x 10^6 Btu/hr-ft^2
Inlet temperatures:	418 to 450° F
Pressure:	1300 to 1325 psia
Flow rates:	1.20 to 2.5 gpm.

f. Discussion and results

Data analysis established trends with respect to the effect of each variable investigated.

Data reduction was divided into two areas: local boiling heat transfer and local boiling pressure drop. Emphasis was placed on the latter due to its present significance in the PM-1 analytical studies.

(1) Pressure drop

The local boiling pressure drop data realized in this program was obtained over a 20-inch length of the 23-inch test section. Local boiling pressure drop data are usually correlated as a ratio of either the local boiling pressure gradient to the isothermal pressure gradient or local boiling friction factor to isothermal friction factor. The latter ratio was employed and compared with a WAPD correlation* as shown in Fig. 2.29. Most of the experimental points fall above the WAPD correlation* which is presented as a function of coolant subcooling (ΔT_{sub}).

$$f/f_{iso} = \frac{1 + T_B - T_{sat} + 76}{C_4} = 2.17 - \frac{\Delta T_{sub}}{65} \text{ for } \Delta T_{sub} \leq 76° F$$

$$f/f_{iso} = 1 \text{ for } \Delta T_{sub} \geq 76° F$$

T_B = bulk coolant temperature, °F

T_{sat} = saturation temperature at system pressure, °F

C_4 = pressure dependent constant = 65.0 at 1300 psi.

It should be noted that WAPD believes that this relationship should give conservative results at low pressure, i.e., 1300 psi. However, WAPD does not present the confidence limits of this correlation. Since the length of test section that is undergoing local boiling and the vigor with which local boiling takes place are functions of heat flux, it would appear that any correlation that is not a function of heat flux would be limited in application. The data, therefore, were also compared to Rohde's correlation* of the data of Buchberg, etc.,** which ranged as shown below:

*Wilson, E. E., "A Basis for Rational Design of Heat Transfer Apparatus," Trans. ASME, 37, 1915.

**Jens, W. H., and Lottes, P. A., "Analysis of Heat Transfer, Burnout, Pressure Drop and Density Data for High Pressure Water," ANL-4627, May 1951.

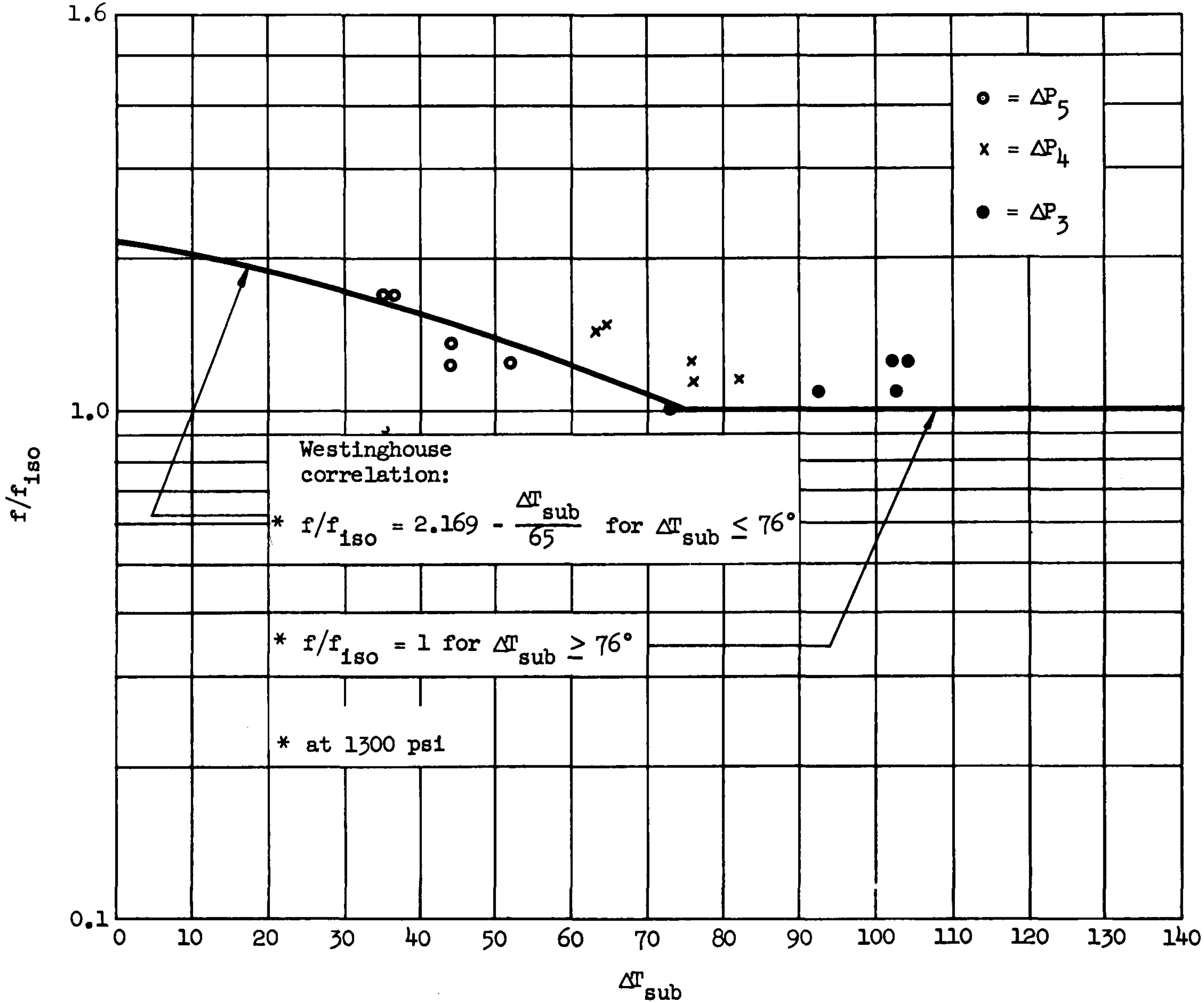

Fig. 2.29. ΔT_{sub} Versus f/f_{iso} for Local Boiling STTS-2

Pressure:	100 to 2000 psia
Velocity:	5 to 30 fps
Heat flux:	Up to 2×10^6 Btu/hr-ft^2
Tube diameter:	0.226 inches
Tube length:	24.6 inches.

$$\frac{\left(\frac{dp}{dL}\right)_{LB}}{\left(\frac{dp}{L}\right)_0} = e^{\frac{384}{p}\left(\frac{q''_{LB}}{q''_0} - 1\right)}$$

where

p = pressure, psia

$\left(\frac{dp}{dL}\right)_0$ = pressure gradient, liquid flow

$\left(\frac{dp}{dL}\right)_{LB}$ = pressure gradient with local boiling

q''_{LB} = heat flux during local boiling, Btu/hr-ft^2

q''_0 = maximum heat flux prior to local boiling.

Figure 2.30 represents a plot of the experimentally determined local boiling pressure gradient versus the local boiling pressure gradient calculated by means of Rohde's equation. Most of the experimental data fall within ± 20% of the Rohde relationship.

(2) Heat transfer data

Neither sufficient quality nor quantity of heat transfer data were realized to adequately compare the results to those presented in the literature. Some of the data, however, are shown in Fig. 2.31 with the Jens and Lottes relationship. The experimental superheat values shown

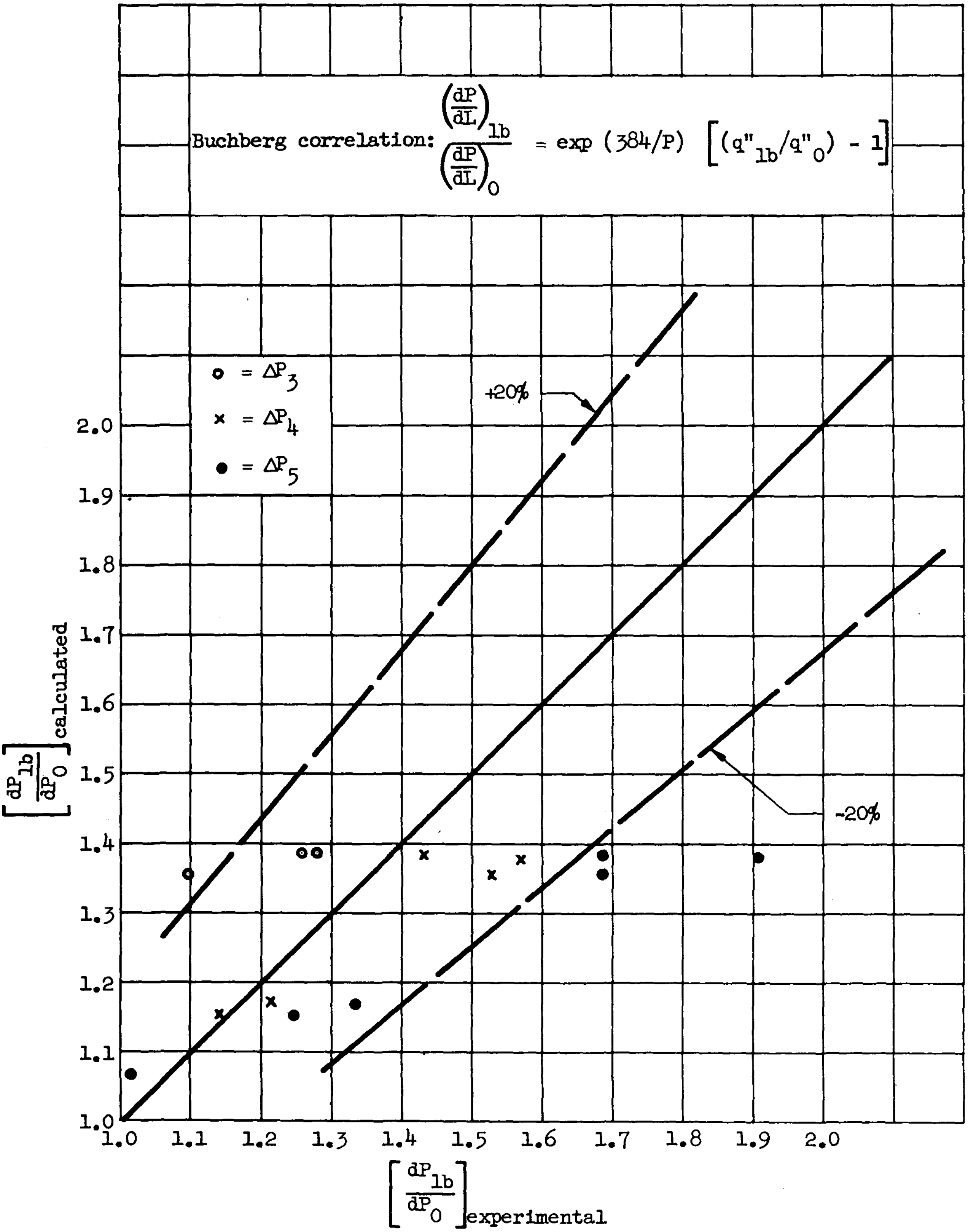

Fig. 2.30. Experimental Versus Calculated Local Boiling Pressure, Local Boiling STTS-2

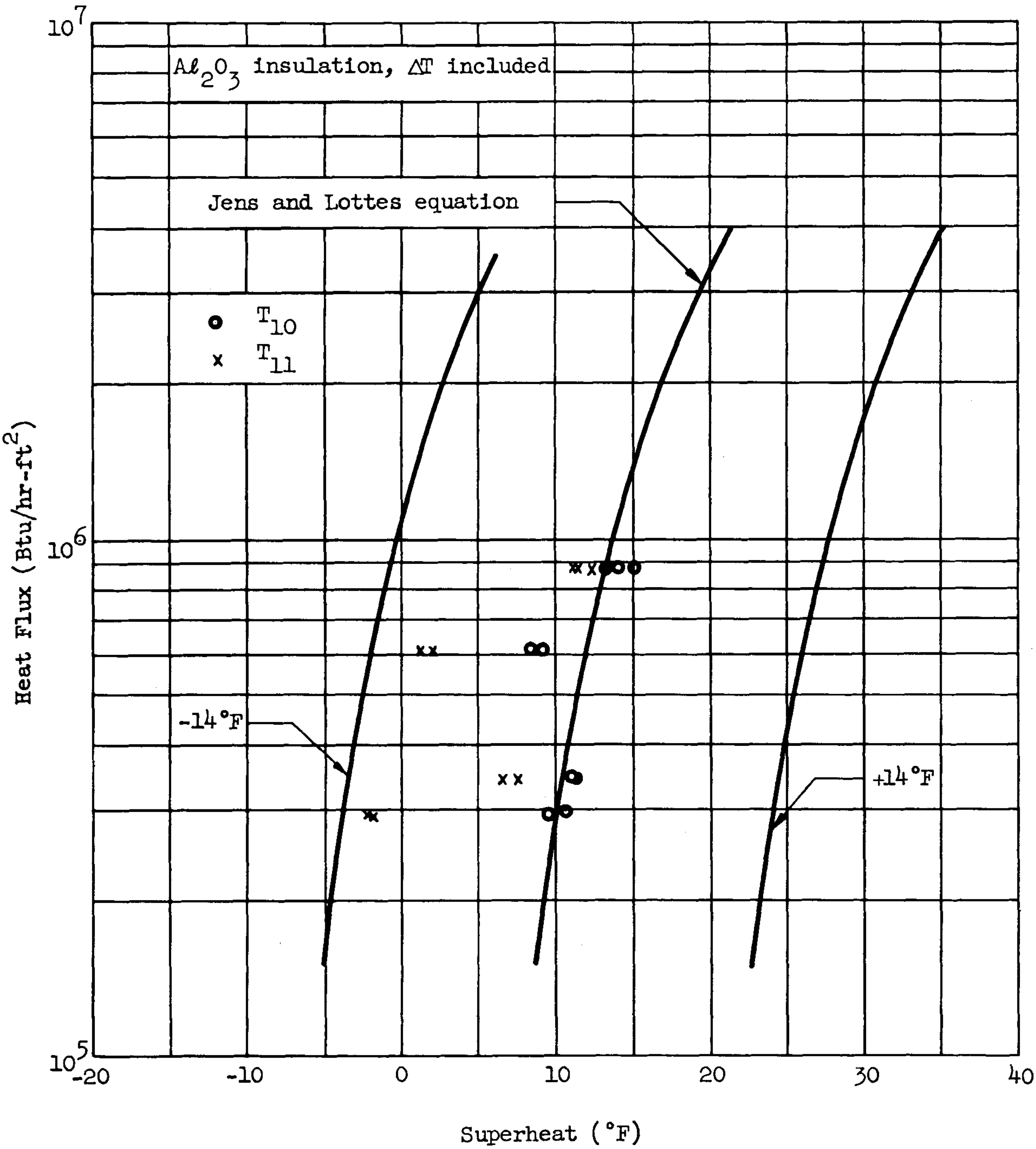

Fig. 2.31. Local Boiling Heat Transfer

were determined by computing the individual temperature gradient through the test section stainless steel wall and Al_2O_3 electrical insulation. These calculations encompassed certain assumptions that introduce some uncertainty in the superheat values, but the results are well within the ±14° F confidence limits of the Jens and Lottes equation*.

In general, the data pointed out the need of employing the Wilson method** for determining the overall thermal resistance between the point of temperature measurement and the desired test section surface temperature. This method has been incorporated into the STTS-3 test procedure.

E. SUBTASK 2.5--ACTUATOR PROGRAM

J. Sieg, R. Manoll

During the third quarter, the major efforts planned and accomplished in the actuator program consisted of monitoring and controlling the performance of the actuator subcontractor (the TAPCO Group of Thompson Ramo-Wooldridge). This same type of effort will be pursued during the fourth quarter.

The principal subcontractor efforts of the quarter were devoted to:

(1) Design of the mechanical portion of the actuator including the position indicator transmitter and coil stack assembly.

(2) Development and testing of a switching signal generator.

(3) Performance of tests in support of lift, hold and grip coil design and specification.

(4) Performance of tests in support of the design and specification of the actuator scram spring.

---

*Jens, W. H., and Lottes, P. A., "Analysis of Heat Transfer, Burnout, Pressure Drop and Density Data for High Pressure Water," ANA-4627, May 1951.

**Wilson, E. E., "A Basis for Rational Design of Heat Transfer Apparatus," Trans. ASME, 37, 1915.

1. Design

Shop drawings of the mechanical portion of the actuator contained within the pressure shell were submitted on schedule. The drawings were generally acceptable with the exception of the latch utilized to attach the control rod to the actuator. The latch is being redesigned.

The shop drawings of the position indicator and coil stack assembly were submitted on schedule and were, in general, acceptable. The weights of some components were believed to be excessive, and the assembly was not suitable from a maintenance viewpoint. Redesign is in process to eliminate these objectionable features.

Design drawings for the position indicator transmitter were completed and are ready for review by The Martin Company.

The preliminary design of the relay and selector switch circuit was completed.

Preliminary design of the relay and servo power supplies was in process.

2. Testing

A breadboard model of the prototype switching signal generator, the output of which provides the signals necessary for programming the activation and deactivation of the hold, lift and grip coils, was completed. Tests were performed on this unit by operating it continuously for more than 600 hours--equivalent to approximately 100 years of anticipated reactor operation. Results reported indicate the generator to be extremely reliable and stable. Pulse time durations (300 to 500 milliseconds, depending on application) did not vary from cycle to cycle by more than a fraction of a millisecond. This breadboard model satisfactorily passed a thermal cycling test.

From this breadboard circuit, four carded assemblies were prepared, packaged and final tests were initiated. Results were not available by the end of the quarter.

Tests were initiated on mockup versions of the hold, grip and lift coils during the quarter. The objectives of the tests were to determine the relationships between the current flow in the coils and either the horizontal force applied to the individual bundle rods (hold and grip coils) or the vertical force applied to the movable armature (lift coil). Although data has not been reduced as yet, it appears that initial design calculations were conservative.

Figure 2.32 shows the typical variation of bundle rod deflecting force with coil current for an initial bundle-to-pole gap of 0.005 inch. Inasmuch as there are 10 coils and 4 bundle rods involved in either gripping or holding, the total horizontal force developed would be 40 times that read on the ordinate for a given current. The solid curve represents the force acting on the rods prior to deflection; the broken curve represents the force acting on the bundle rod when it is in contact with the actuator pole face. It may be noted that, assuming a friction coefficient of 0.3 and current flow of 9 amperes, a force of more than 250 pounds would be required to move the bundle rod assembly.

During the quarter, tests were initiated using a core segment and dummy control rod supplied by The Martin Company to determine the hydraulic resistance of the control rod during scrams as a prerequisite to sizing of the scram spring. Although the data resulting from these tests have not been completely reduced, it appears that no great difficulty will be encountered in meeting the specification requirements concerning scram time and that high initial spring preloads need not be imposed on the actuator.

The test installation, as shown in Fig. 2.33, indicates the pressure vessel containing the dummy rod and core segment, the pump drive engine for providing various flow rates of water over the core segment and rod, and the scram spring housing.

3. Fabrication

Approximately 80% of the shop drawings relating to the mechanical portion of the actuator drawings were released to TAPCO manufacturing for fabrication. Fabrication of parts to be used in the position indicator and coil stack assembly should begin during the next quarter.

A magnetic jack obtained from ANL as government furnished equipment was shipped to TAPCO for inspection and testing.

During the next quarter, design and design tests should be completed and approved, and a report should be submitted to The Martin Company. Fabrication should be substantially completed and tests should be underway.

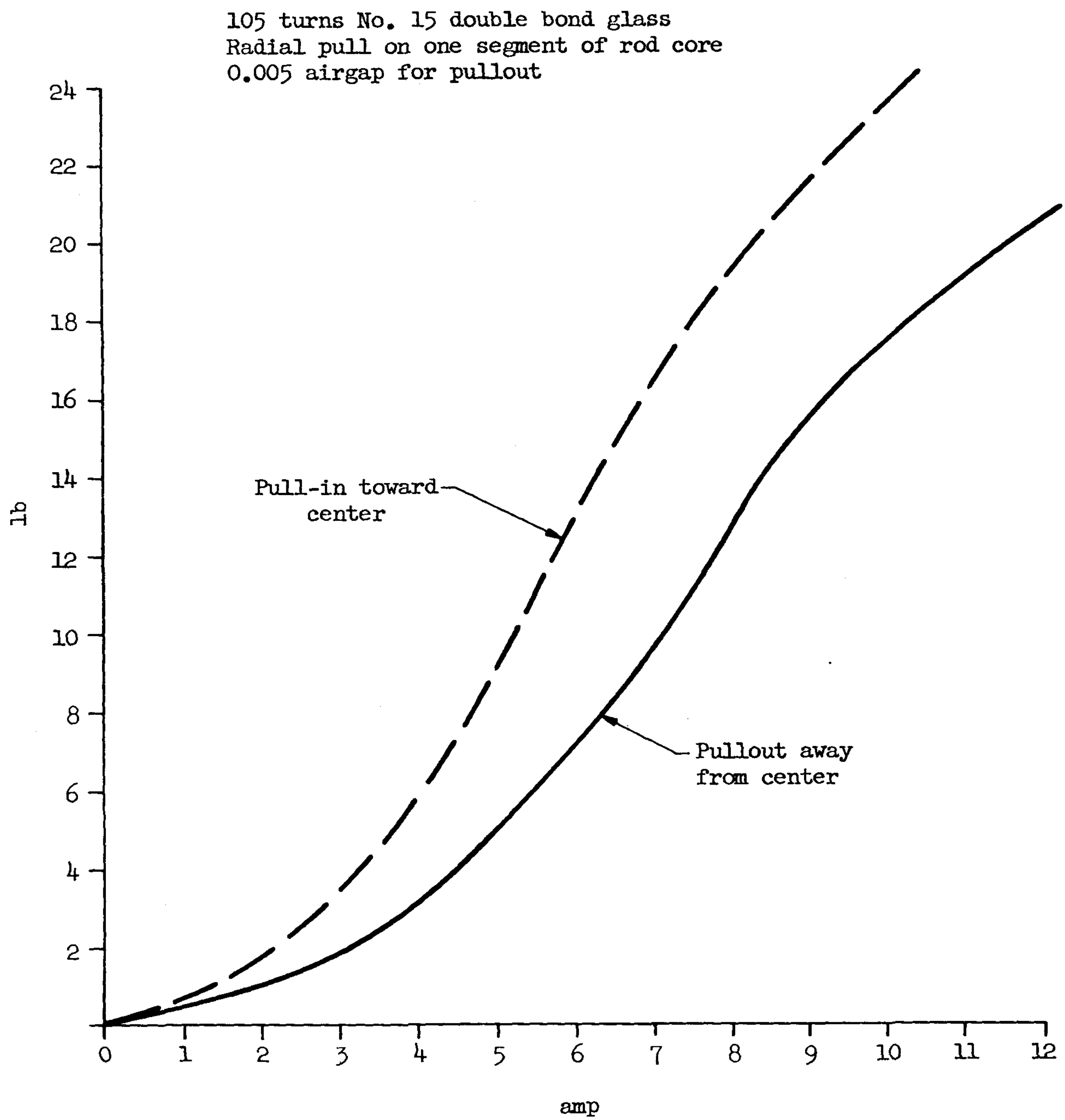

Fig. 2.32. Hold Coil Results

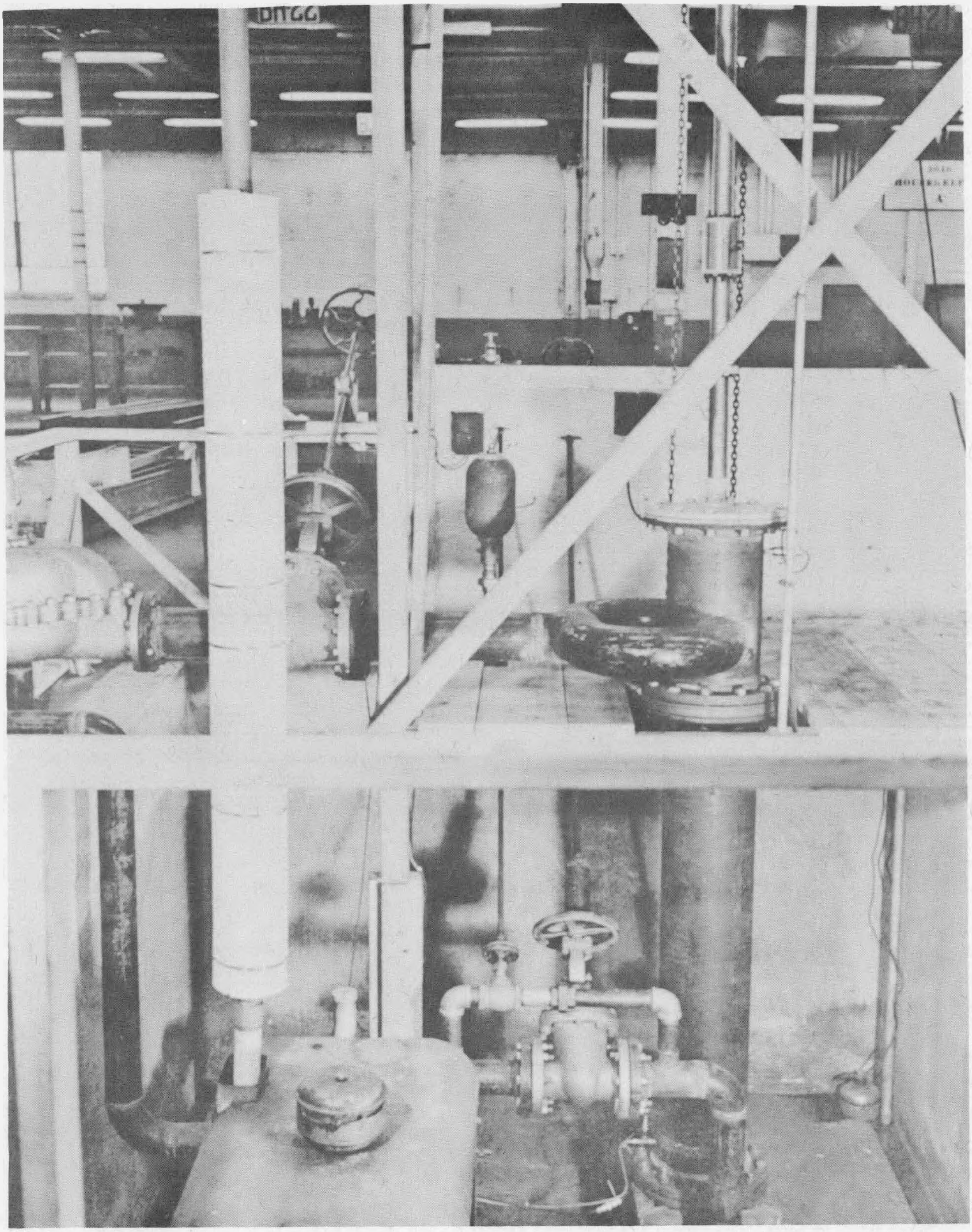

Fig. 2.33. Scram Spring Test Installation

III. TASK 4--FINAL DESIGN

Project Engineer--R. Akin, C. Fox, G. Zindler

The objectives of this task are to prepare and analyze the final design of the PM-1 Nuclear Power Plant. This was the major effort during the third project quarter and will continue to be so during the fourth quarter. The task is scheduled to be completed in March 1960.

It should be noted that subcontractor efforts contributing to the final design are reported under other tasks mainly for administrative reasons:

Westinghouse Electric Corporation--Secondary System Development, Subtask 1.6

Gibbs and Hill, Inc.--Consulting, Task 16.

According to the program plan, Task 4 is divided into three subtasks:

4.1--Design Analysis

4.2--Detail Construction, Shop Drawing and Specifications

4.3--Spare Parts.

During the quarter, a plan was devised to transmit completed portions of the work to the AEC in a series of 37 subsystem submittals at various dates during the fourth project quarter. In general, subsystems including components which have long-lead procurement items come first. A list of the subsystems agreed upon with the AEC follows:

List of Subsystems

Subsystem Number		Responsible Project Engineer
1	Plant Instrumentation and Control Part A: Primary System Part B: Secondary System Part C: Fluid Sampling System Primary Secondary Part D: Communication System Part E: Control Console and Annunciator	G.F. Zindler

List of Subsystems (continued)

Subsystem Number		Responsible Project Engineer
2	Nuclear Instrumentation System	G.F. Zindler
3	Reactor Rod Control System	R.J. Akin
4	Reactor Safety System	G.F. Zindler
5.	Radiation Monitoring System	G.F. Zindler
6	Reactor Coolant System	R.J. Akin
7	Pressurizer and Pressure Relief System	R. J. Akin
8	Coolant Charging System	R. J. Akin
9	Coolant Discharge and Vent System	R.J. Akin
10	Coolant Purification System	R.J. Akin
11	Coolant Chemical Addition System	R.J. Akin
12	Decay Heat Removal System	R.J. Akin
13	Reactor Component Cooling Water System	R.J. Akin
14	Reactor Plant Heating and Cooling System	R.J. Akin
15	Core Cask Cooling System	R.J. Akin
16	Radioactive Waste Disposal System	R.J. Akin
17	Reactor Plant Container	R.J. Akin
18	Main and Auxiliary Steam System	C.H. Fox
19	Main Turbine and Generator Unit	C.H. Fox
20	Main Condenser and Condensate System	C.H. Fox
21	Feedwater System	C.H. Fox
22	Extraction Steam and Heater Drain System	C.H. Fox

List of Subsystems (continued)

Subsystem Number		Responsible Project Engineer
23	Cooling Water System	C.H. Fox
24	Main Transformer and Distribution System	C.H. Fox
25	Station Service	C.H. Fox
26	Lighting and D-C Emergency Lighting	C.H. Fox
27	Plant D-C System	C.H. Fox
28	Emergency Power Systems	C.H. Fox
29	Water Treating Systems Part A: Water Treating System Part B: Treated Water System Part C: Soft Water System Part D: Chlorinated Water System	C.H.Fox
30	Condensate Make-Up System	C.H. Fox
31	Fire Protection System	C.H. Fox
32	Service Steam System	C.H. Fox
33	Secondary Building Heating, Air-Conditioning and Ventilating Systems	C.H. Fox
34	Primary Loop Building, Air-Conditioning and Ventilating System	C.H. Fox
35	Secondary System Building	C.H. Fox
36	Decontamination Equipment Decontamination Building	C.H.Fox
37	Maintenance Equipment Shipping Package for Plant (open-truss type) Interconnecting Walkways Plant Layout	C.H. Fox

In order to keep progress reporting in accordance with the other work of the task, this section will be organized on a subsystem basis instead of on the usual subtask basis. The discussions which follow cover the subsystems in numerical order.

A discussion of nuclear analysis studies, shielding studies, Secondary System studies and miscellaneous studies, which do not fit conveniently into any single subsystem, are included at the end of the section.

In general, the primary loop embraces Subsystems 3 and 6 through 17. The Secondary System and supporting equipment are in Subsystems 18 though 37. Controls and instrumentation are covered in Subsystems 1, 2, 4 and 5 and in the control aspects of various other subsystems.

SUBSYSTEM 1--PLANT INSTRUMENTATION AND CONTOL

During this report period, all designs, specifications and drawings were completed and issued for plant instrumentation and controls in the following areas (bound together in MN-7601):

Part A--Primary System

Part B--Secondary System

Part C--Fluid Sampling System.

During the next period, the following systems will be completed:

Part D--Communication System

Part E--Control Console and Annunciator System.

Procurement action will be taken on all PM-1 controls and instrumentation so that the entire system will be on order, with delivery scheduled to be completed in December 1960.

1. Stability Analysis

R. Wilder, R. Caw

The primary loop of the PM-1 was analyzed for stability with a linearized transfer function representation used for primary loop components. The analysis consisted of:

(1) Open-loop analysis with no external control.

(2) Open-loop analysis utilizing an average temperature, on-off, deadband operating, automatic rod control system.

The purpose of (1) was to investigate the inherent stability of the primary loop over the 0 to 200% full-power range. In (2), the system was expanded to investigate the characteristics of a rod controller needed to ensure stable operation under automatic control.

The stability investigations were made by applying a sinusoidal change in reactivity to the analog model. The frequency of the reactivity variation was adjusted over a broad range, and the gain-phase shift characteristics of the primary loop were determined.

The study revealed that the PM-1 primary loop can be expected to remain stable at least to 200% of design full power. At very low power, the primary loop response to a change in reactivity will be "sloppy" (i.e., show slower response times of an underdamped nature). At the high power levels of routine plant operation, this sloppy condition does not exist. According to this study the PM-1 primary system will be stable without an automatic rod control system.

A second investigation was made to determine the characteristics of an automatic rod control system which would completely eliminate manual rod positioning when the reactor was operating in the power range. The results of this study indicate an on-off controller with the following characteristics:

(1) Actuator excitation at ± 5° F changes in T_{avg}.

(2) Actuation de-energized at ± 3.6° F after (1).

(3) Reactivity insertion rate with rod at 3.33×10^{-5} δ k/sec.

Satisfactory operation was obtained using a deadband of ±5° F about T_{avg}. The study showed that this is probably the minimum deadband that can be used with good stability. A larger deadband would give larger stability margins.

It appears that a deadband requirement of less than ±5° F could only be obtained by a proportional decrease in rod speed.

This study indicates that automatic control can be achieved relatively easily and would perform satisfactorily. However, it would only relieve the operator of the long-term rod position correction resulting from fuel burnup and poison buildups. Based upon these results and the inherent stability of the primary system without automatic control, it was decided not to adopt the automatic control scheme for the PM-1.

2. Secondary System

It was planned, during the quarter, to complete the basic design and/ or selection of all major secondary system controls requirements and types of equipment. This was accomplished under Subsystem 1. Pertinent data were submitted to the AEC for approval. During the next quarter, we plan to complete all specifications and detailed procurement data, select vendors, complete console arrangement and start on final wiring diagrams.

The following controls were studied closely during the quarter with the results noted.

a. Turbine control

The control of turbine speed in the PM-1 plant has been emphasized because of the transient frequency limitations outlined in the power plant quality objectives. Several turbine speed control systems and methods of control were reported in previous reports. The control systems under consideration were the electric and the mechanical-hydraulic types. The methods of control are proportional loop, proportional plus reset loops and proportional plus reset plus load sensing or rate loops.

Based on the Westinghouse data and their recommendations, the electric control system was eliminated from consideration because it is heavy, costly and unproven.

The mechanical-hydraulic-type controller was selected, and its method of control must be determined. Westinghouse states that all three control methods will very nearly meet the frequency quality objectives. These objectives are ±2% fluctuation with recovery to ±0.25% within 1.5 seconds after an instantaneous load change of 30% of rated capacity (300 kw). Examination of their data indicated that after a 30% load change, the proportional loop (Curve A of Fig. 4.1) causes a permanent change in frequency that is greater than ± 0.25%. Thus, this method of control did not meet the frequency quality objectives even during steady state and is unsatisfactory. The above loop, with the addition of a reset loop, will control the frequency (speed) more satisfactorily but still does not fully satisfy the frequency quality objective, since the time for the frequency to return to ±0.25% of its original value is 0.3 second over the allotted time. It was decided that the small time discrepancy should not disqualify this control method.

The third method utilizes the proportional and reset loop plus an external load sensing device or rate loop. With the addition of the rate loop, the frequency recovery takes place within the allotted time of 1.5 seconds.

It should be noted that the power quality is an objective and not a contractual requirement. For it to be a requirement, the other objectives of low weight, low cost and reliability would have to be seriously compromised. The selection of the turbine control system must be founded on that system satisfying, or nearly satisfying, all the objectives of the plant. On this basis, the proportional plus reset method of control has been selected for the PM-1 plant. The gain of 0.3 second in response time does not offset the increase in weight, cost and complexity of the control method utilizing an external load sensing device.

The above selection was established based upon Westinghouse data. Communications with Westinghouse turbine engineering personnel indicated that the data submitted were the result of their experience and "feel" for turbine speed response. They stated that analytical confirmation would be undertaken when the turbine design was completed.

To obtain analytical substantiation for the above recommendation, a turbine-generator model was developed at Martin and programmed on the analog computer containing the PM-1 power plant model. A proportional plus reset control model was also programmed. The equations for the turbine-generator and controller used on the computer were:

Turbine-generator--

$$J\frac{dN}{dt} = T_{in} - T_{out}$$

$$T_{in} = f\,(W_g)$$

$$T_{out} = f\,(ekw)$$

Controller--

$$\Omega = K_1\,(N - N_o) + K_2 \int (N - N_o)\,dt$$

Turbine throttle valve--

$$W_g = C\,\Omega P_s$$

where

C = valve constant

J = rotational moment of inertia, pound (gravity)-feet squared

K = adjustable gains

N = measured speed, rpm

N_o = reference speed, rpm

P_s = steam pressure, psia

T = torque, ft-lb

W_g = steam flow, lb/sec

Ω = turbine throttle opening, %

The values for moment of inertia and speed, as obtained from Westinghouse, were:

$J_{turbine}$ $= \frac{168}{g}$ lb-ft^2 referred to the turbine shaft

$J_{gear + generator}$ $= \frac{6320}{g}$ lb-ft^2 referred to the generator shaft

$N_{turbine}$ = 7500 rpm

$N_{generator}$ = 1200 rpm

The gains K_1 and K_2 were adjusted to obtain the best frequency control. Using this model, a 300-ekw instantaneous load change was made. The turbine speed (frequency) response is shown in Fig. 4.1 as Curve A. Westinghouse data are plotted as Curve B in Fig. 4.1 for comparison purposes.

The degree of agreement of the two curves is quite remarkable, considering that the approach differed in the determination of each one. With the agreement of data, the choice to use the proportional plus reset control method is substantiated.

Finally, the selection of this control method does not preclude the use of the external load sensing device. During operation, should the gain available in the proportional plus reset controller prove inadequate in regard to meeting the frequency quality objectives, the external load sensing device can be added to the speed controller in the field to improve its response.

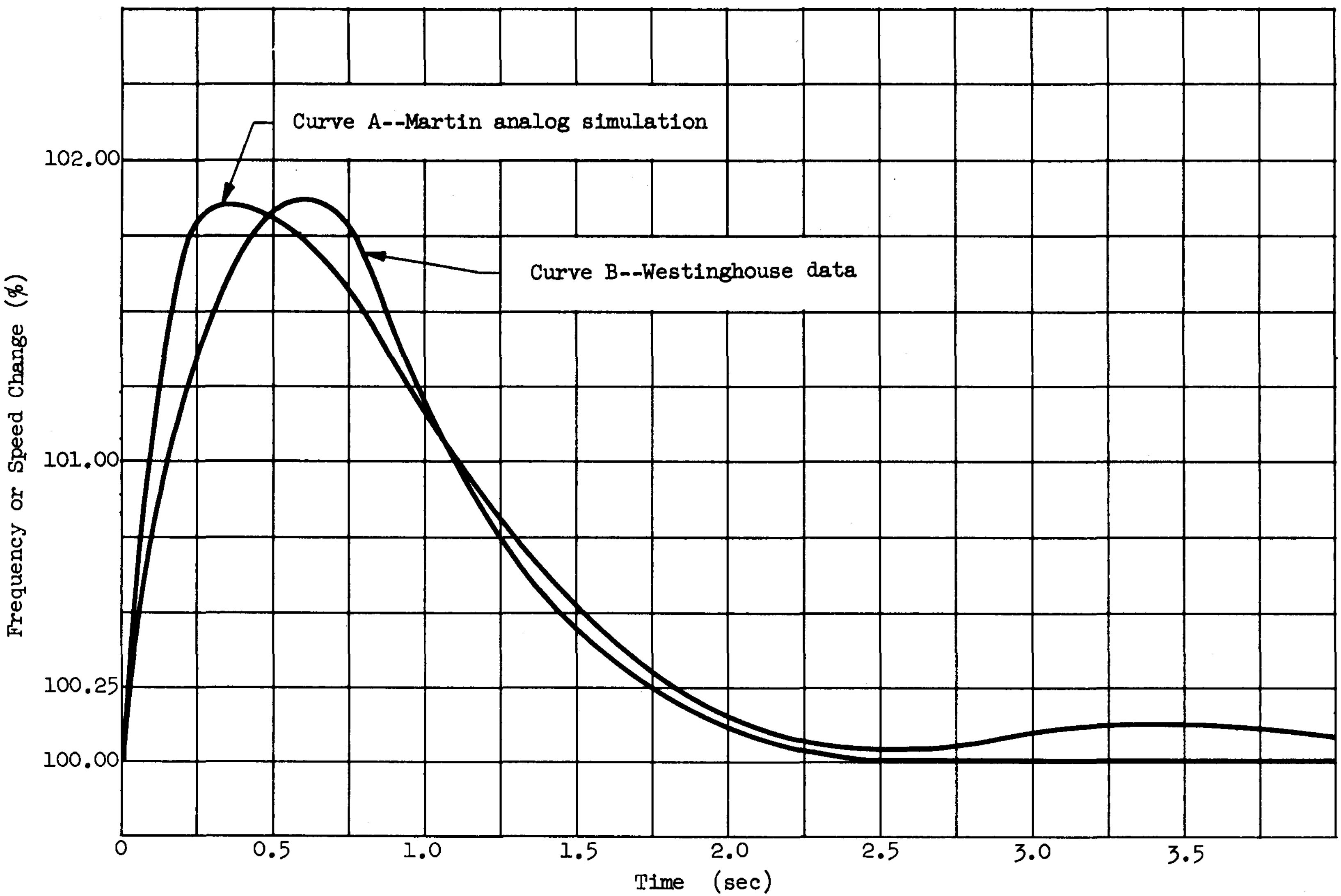

Fig. 4.1. PM-1 Mechanical-Hydraulic Turbine Speed Controller Response Using Proportional plus Reset Loop Method of Control After a 30% Load Change

b. Feedwater Control

The PM-1 feedwater control system is an all-electric, three-element type, the elements being steam flow, feedwater flow and steam generator water level. The steam flow and water level signals require density compensation since steam generator pressure varies with load; thus, an additional signal, steam pressure, is necessary.

With three signals available, there are several methods for combining them to produce a control signal. To determine the best method of control, the transient requirements of the steam generator and of the Secondary System are examined and established.

Steam generator requirements. The density of the steam-water mixture in the boiler varies with load in such a manner that the least amount of mass exists at the highest load (lowest pressure) and, conversely, the greatest mass exists at no load. For an increasing load maneuver, mass must leave the steam generator; therefore, feed flow must be less than steam flow until the new mass requirement (measured as water level) can be met. For a decreasing load maneuver, mass must enter the boiler, and the feed flow must be transiently greater than the steam flow. Thus, in both maneuvers, the feed flow must transiently lag the steam flow.

During an increasing load maneuver, the steam generator water level rises or surges. This surge must be limited so that the separating equipment is not drowned and carryover is prevented. The surge associated with a change in steam flow is usually not sufficient to accomplish separator drowning. However, during this surge, feed water flow should lag the steam flow so that it cannot reinforce the increase in level and cause separator malfunction. The same response is desirable during a decreasing load maneuver when the level drops or shrinks. Too great a shrink in level can result in the loss of circulation in the steam generator. This results in a "once-through" boiler with an accompanying steam blanketing of tubes or, effectively, a loss in heat transfer area. With lagging feed flow, the level is held up because more water is entering the boiler then there is steam leaving it. From an internal performance standpoint, lagging feed flow minimizes level transients.

When an increasing load maneuver is executed, the additional steam is initially supplied from the stored energy in the mass on both the primary and secondary sides of the boiler. This stored energy is utilized for approximately one loop time (13.5 seconds) until the reactor comes up to its new power level. It is desirable, during this time, for the stored energy to be used only to supply the heat of vaporization for the additional steam. Feed flow should remain close to its original value during the early stages of the transient so that the additional load of feed water heating will not be imposed on the boiler. During the decreasing load maneuver, if the feed flow is maintained at its initial high value, it can be thought of as "quenching" the heat in the steam temperature overshoots. By eliminating the feedwater heating load during the transient, reactor power surges can be kept to a minimum. So, again, a lagging feed flow is desirable.

Secondary System requirements. While the transient on the steam side of the Secondary System (boiler through turbine) is rapid, the water side (condenser through deaerator) is quite slow because of the volumes of the condenser, its hotwell and the deaerator. Because of its storage capacity, the deaerator effectively disconnects the feed system from the condensate system. Thus, only the effect of the feed system on the deaerator will be examined. The majority of the water entering the deaerator is condensate. This flow will approximate the turbine steam flow delayed by an appropriate amount of time to account for the length of the path between the turbine inlet and condensate pump discharge. With a slow response feed system, the flow out of the deaerator will be similar to that into it, and water level variations will be kept to a minimum. If a fast response feed system is employed immediately after an increasing maneuver is executed, the deaerator outflow will be increased; for approximately 1/2 to 1 minute, the deaerator mass decreases as the load increases and this mass must be stored in the Secondary System, the majority of it going to the deaerator. If mass is to be stored in the deaerator, its level should be increasing, not decreasing. A fast response feed control system works against the natural response of the deaerator. While this will not seriously affect the performance of the deaerator (with the possible exception of setting off the low-level alarm, causing the operator to add make-up when it is not really needed), it is preferable to have a control system that will allow the desired response of an attached component. This, in effect, will uncouple the deaerator control from the feed flow; that is, the feedwater controller cannot induce a transient in the deaerator that will cause the deaerator control or the operator to take action. A slow response control system is preferred, then, when considering the secondary loop requirements.

With the steam generator and Secondary System requirements established and the desirable characteristics of transient lag and slow response or recovery time determined, an integral controller is selected as best meeting these characteristics. The control equation can be written:

$$W_{fw} = K_F (W_g - W_{fw}) - K_L \int (L - K_p W_g - \beta)\, dt$$

where

W_{fw} = feed flow

W_g = steam flow

L = steam generator water level

ß = a constant representing a reference steam generator water level

K_F = adjustable flow gain

K_L = adjustable level gain

$K_p W_g$ = programmed water level (if used).

The gains K_L and K_F can be adjusted to obtain the characteristics desired--the so-called proper setting. The ratio K_L/K_F will determine the initial response (lag) of the system, and the absolute values of K_L and K_F will determine the overall response time.

To exhibit the ability of this control system to meet the desired characteristics, a controller model was placed on an analog computer in conjunction with a steam generator model and a turbine throttle valve controller model. The reference maneuver of a 30% step change in net electrical load was performed, and the effect of the values K_L and K_F was investigated.

A review of these results indicates that an integral controller with sufficient gain adjustment is capable of obtaining the proper system setting.

SUBSYSTEM 2--NUCLEAR INSTRUMENTATION SYSTEM

R. Caw

The Nuclear Instrumentation Subsystem includes the reactor flux monitoring equipment used for reactor control.

Block diagrams of the various instrument channels are presented in Figs. 4.2, 4.3 and 4.4. The three channels of neutron flux coverage are:

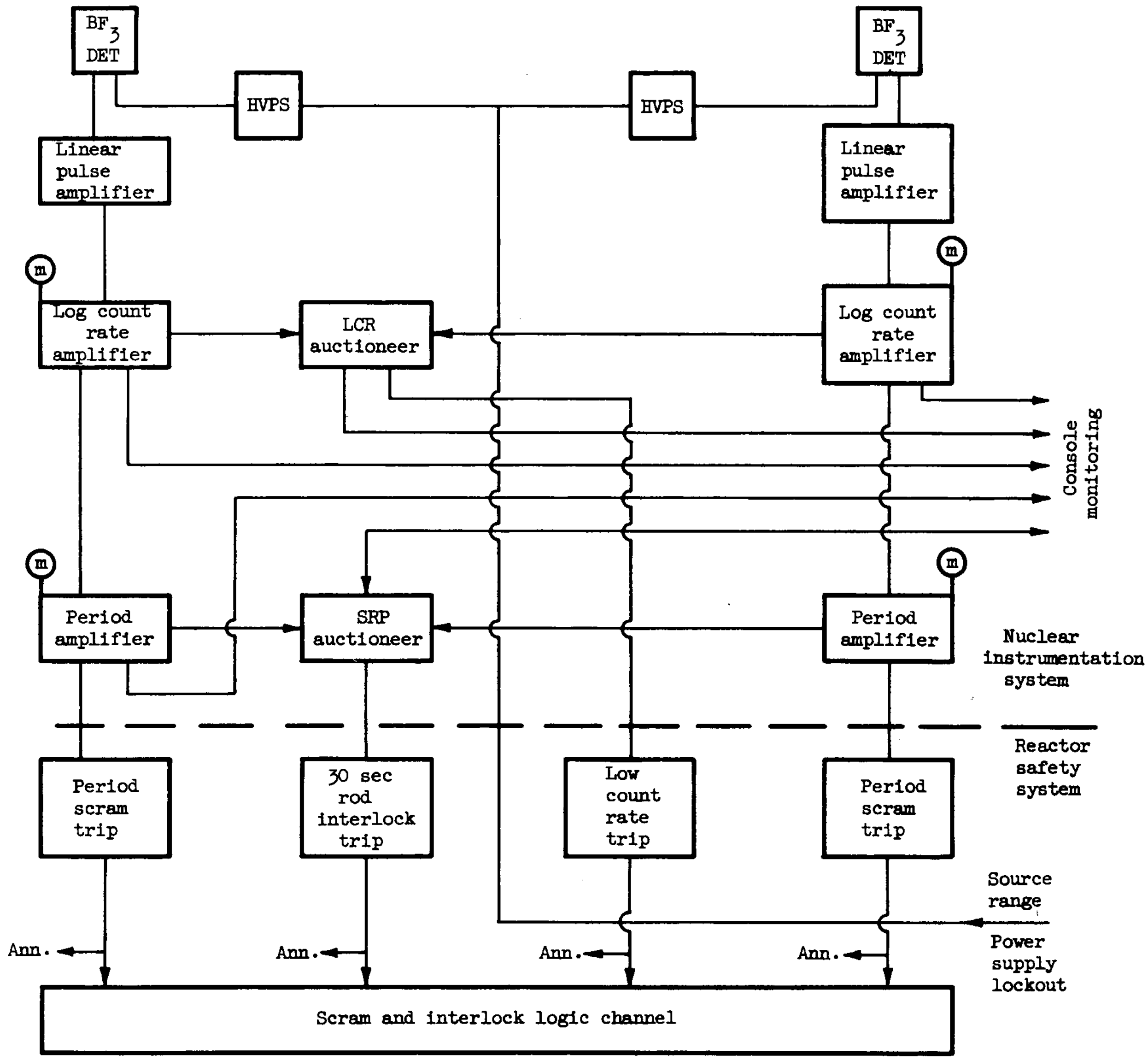

Fig. 4.2. Startup Instrumentation

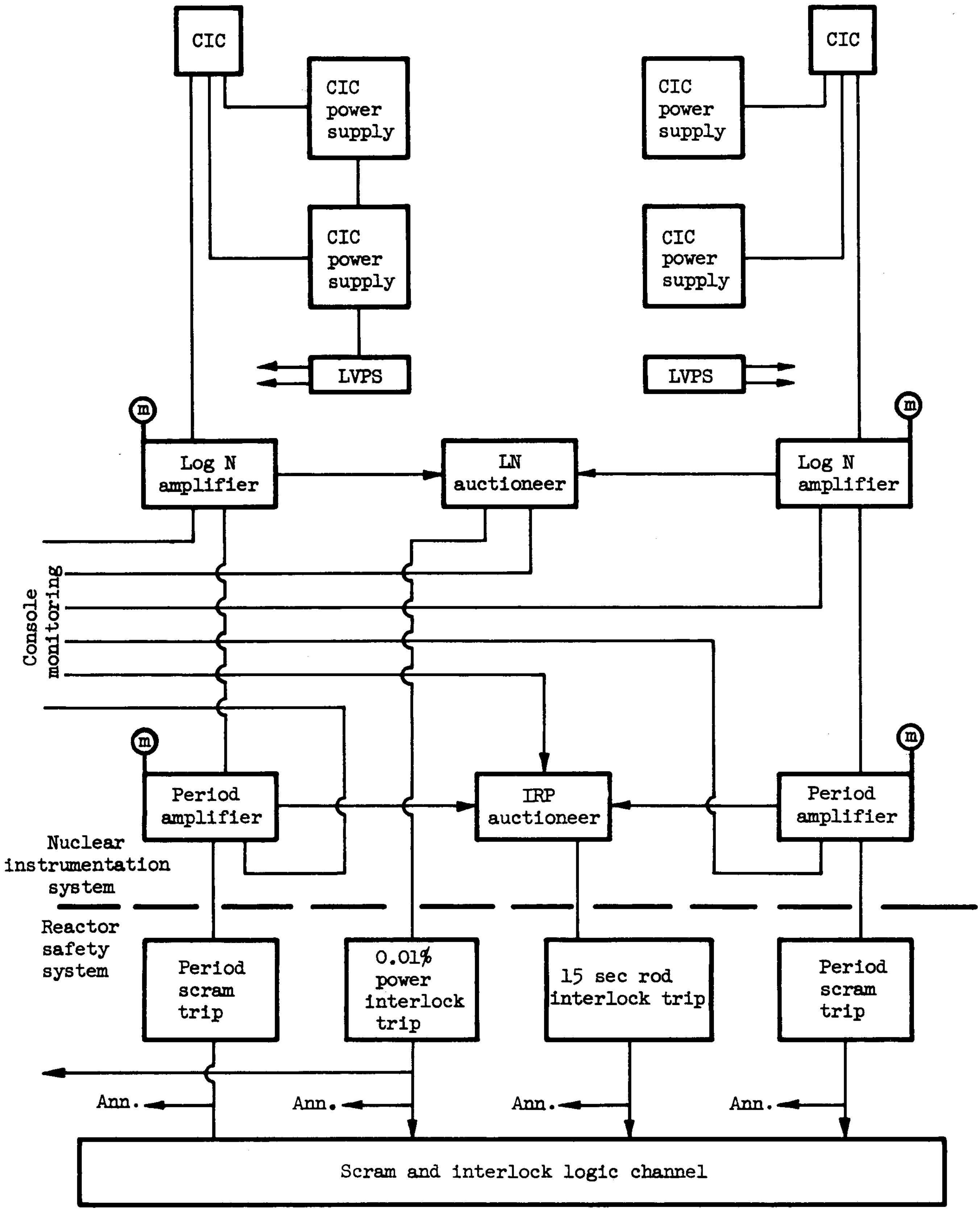

Fig. 4.3 Intermediate Range -- Instrumentation

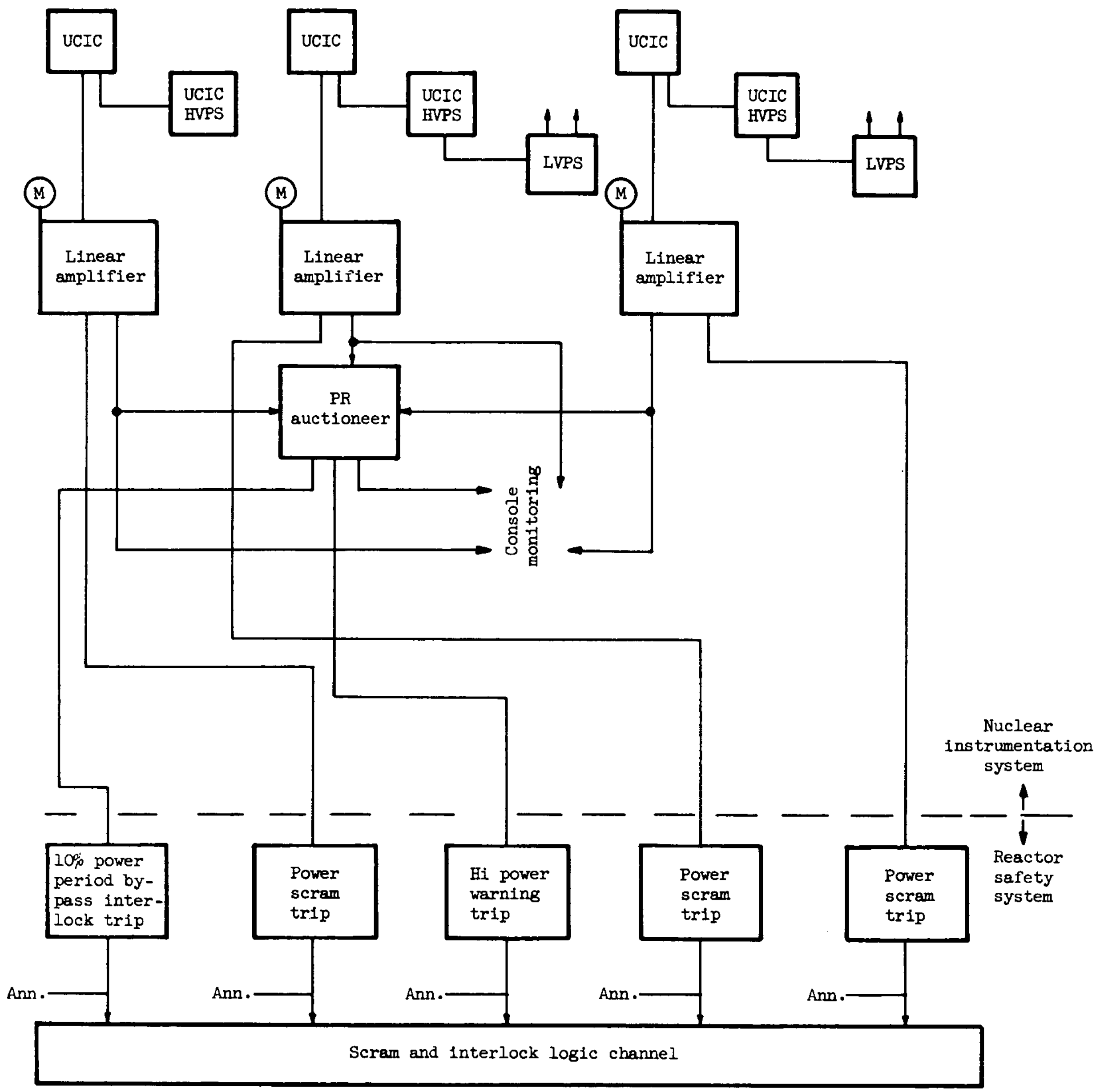

Fig. 4.4 Power Range -- Instrumentation

(1) Startup

(2) Intermediate

(3) Power.

The channels provide a minimum of one decade of overlap of range between each other. The use of duplicate and triplicate channels is specified from reliability and plant safety requirements.

Each of the nuclear instrumentation channels interconnects with the Reactor Safety System to provide reactor "scram" protection. These interconnections are shown also in Figs. 4.2, 4.3 and 4.4.

SUBSYSTEM 3--REACTOR ROD CONTROL SUBSYSTEM

J. Sieg, R. Manoll

The design, fabrication and testing associated with this subsystem have been subcontracted to the TAPCO Group of the Thompson Ramo-Wooldridge, Inc. The Martin Company efforts during this quarter and the next quarter are limited to monitoring the design of the prototype actuator system described under Subtask 2.5.

This system contains all the components (electrical and mechanical) needed to activate, control and monitor control rod motion. Means are provided for rod motion to be initiated by either plant process instrumentation or by the operator. The system is designed such that any "rods in" signal overrides any "rods out" signal. Rods are operated in the manual-electric mode from the console.

The major components of the subsystem will be as follows:

(1) Six actuators.

(2) Six position indicator transmitter and coilstack assemblies.

(3) Six position indicator receivers and indicators.

(4) A system power source and signal generator.

(5) System operating controls.

(6) Interconnecting cabling.

(7) Special tools and support equipment.

SUBSYSTEM 4--REACTOR SAFETY SYSTEM

R. Wilder, R. Caw

During this report period all designs, drawings and specifications for this subsystem were completed and issued. A brief description of the subsystem follows.

This system acts as the summing point for all-nuclear and non-nuclear instrumentation. It consists of the most reliable circuit elements so as to provide minimum failure which would initiate scram. The elements are arranged and circuit design set up so that the functions performed have flexibility in such a fashion that trip points may be coincidence protected, made adjustable over discrete ranges or functions bypassed according to specifications (see Fig. 4.5).

SUBSYSTEM 5--RADIATION MONITORING SYSTEM

R. Wilder, R. Caw

During this report period, preliminary designs, specifications and drawings for this subsystem were completed. Final specifications and drawings will be completed for issue during the next report period.

SUBSYSTEM 6--REACTOR COOLANT SYSTEM

The reactor coolant subsystem, sketched in Fig. 4.6, includes the reactor pressure vessel, the steam generator, the primary coolant pump and associated piping. Subsystem objectives accomplished during the third project quarter were:

(1) Completion of design, drawings and specifications for the reactor coolant system.

(2) Completion of design of components, including analysis of the reactor pressure vessel for combined transient and steady-state stresses.

(3) Invitations to vendors to bid on the components.

In addition, the core reference design was reviewed and modifications were introduced to eliminate objectionable features. The overall reactor pressure vessel design also underwent review and analysis.

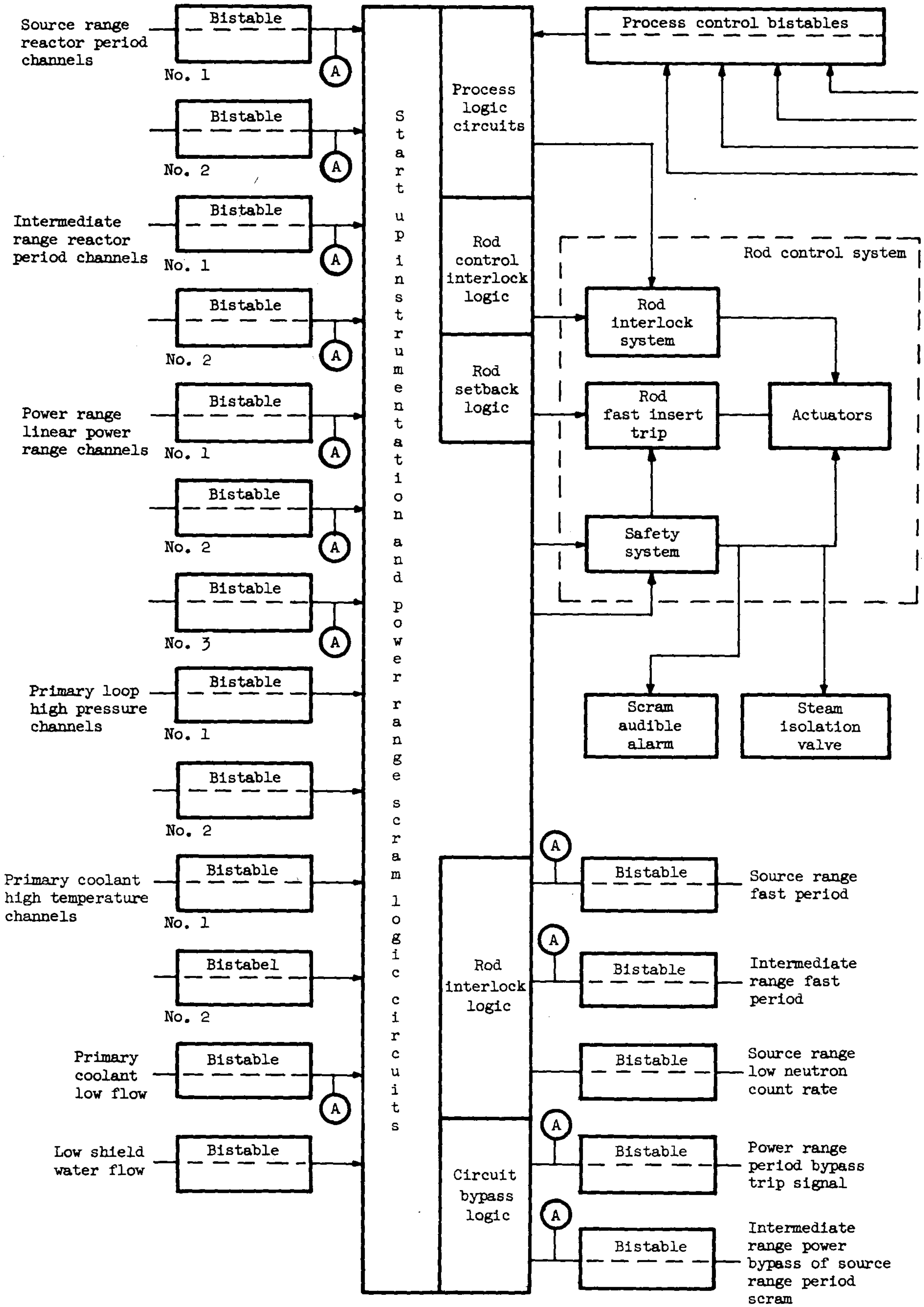

Fig. 4.5. Reactor Safety System

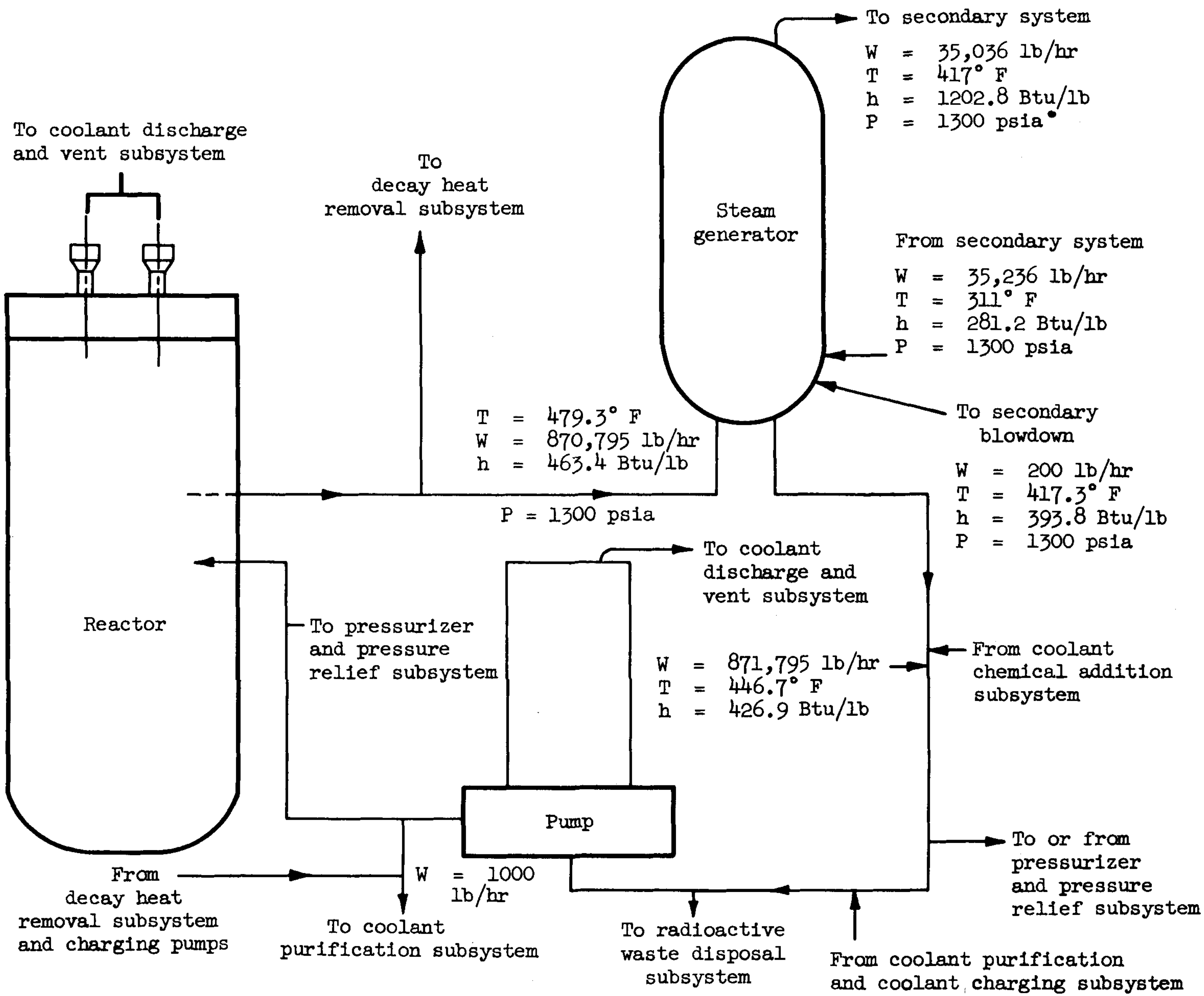

Fig. 4.6. Reactor Coolant Subsystem--PM-1 Power Plant

The following will be accomplished during the next project quarter:

(1) Core design, drawings and specifications will be completed.

(2) Vendor's proposals will be evaluated.

(3) Subcontracts will be let for reactor coolant system components (i.e., pressure vessel, primary circulating pump and steam generator).

(4) The stress analysis for the pressure vessel will be completed.

A. THERMAL AND HYDRAULIC SUPPORTING ANALYSIS STUDIES

A. Carnesale, R. Baer, J. Kudrick, S. Frank, J. Goeller

The supporting analysis studies performed during the third project quarter were concerned with four main areas:

(1) Determination of reactor coolant flow rate.

(2) Rewriting of BUBBLES-1 for the IBM 709.

(3) Thermal and hydraulic analysis of the pressure vessel thermal shields.

(4) Reactor head loss calculations.

1. Reactor Coolant Flow Rate

Work previously reported has shown that the fundamental criteria are that no bulk boiling of the primary coolant occurs and that burnout heat flux is not exceeded.* The preliminary design study indicated that the former was the limiting criterion. The analysis involved determination of the following:

(1) Maximum allowable coolant temperature.

(2) The fuel element channel in which the maximum coolant temperature exists.

(3) Hot channel factors.

---

*See Second Quarterly Progress Report, PM-1 Nuclear Power Plant Program, MND-M-1813, pages III-34 ff.

(4) Flow rate per fuel element.

(5) Total primary loop flow rate.

Maximum allowable coolant temperature. In order to preclude the existence of bulk boiling, the highest exit coolant temperature from a fuel element channel must not exceed the saturation temperature corresponding to the pressure in that region. The pressurizer is designed to limit the minimum operating pressure to 1200 psia. Since the saturation temperature of 1200-psia water is 567.2° F, the maximum coolant temperature under all expected operating conditions may not exceed 567.2° F.

Evaluation of the fuel element channel in which the maximum coolant temperature exists. Normally it would be expected that the maximum coolant temperature in the core would occur at the exit of the channel associated with the fuel element producing the most power. It was found that this element produces 2.1 times the power produced in a hypothetical average element. This condition is expected to exist in the element immediately adjacent to the control rod channel when the rod is fully extracted (Element "A" in Fig. 4.7). However, in the absence of the control rod blade, additional coolant flows in the vacant channel, thereby increasing the coolant flow rate associated with the "hottest element." Therefore, the maximum coolant outlet temperature may not be associated with this element.

Among the fuel elements not adjacent to control rod blades, that producing the most power was found to produce 1.9 times as much power as the average tube (Element "B" in Fig. 4.7). This occurs at the beginning of core life when the control rods are inserted deepest into the core.

When the control rods are fully extracted, the increased flow through the rod channels results in a decrease in flow along the elements away from these channels, i.e., those in the "infinite" array. The hottest element in this region (Element "C" in Fig. 4.7), produces 1.43 times the power produced in an average channel when the rods are extracted. A gross flow test of a configuration, similar to the PM-1 core, indicated that the coolant velocity in the vacant control rod channels was approximately 10% higher than the average coolant velocity outside the tubes. An investigation of this flow loss indicates that this results in a general flow decrease of 18% outside each element in the "infinite" array. This element, however, generates 25% less power than the hot element in the infinite array when the rods are inserted; thus, when the flow is reduced outside the element by 18%, the power is decreased by 25%.

Fig. 4.7. Schematic Diagram of the Core Configuration

Table 4.1 lists the flow required in the average channel to prevent bulk boiling in the channels for the above three cases. The coolant flow that will be provided to the average element is greater than the required amount in all cases.

Hot channel factors. In the determination of the maximum coolant temperature in the core, consideration must be given to uncertainties in the power generation and flow rate due to manufacturing tolerances and uncertainties in analytical techniques. The effects of these uncertainties are incorporated through the use of the hot channel factors, F_q and F_b, which are applied as follows:

$$Q = F_q Q'$$

$$W_i = \frac{W_i'}{F_{b_i}}$$

$$W_o = \frac{W_o'}{F_{b_o}}$$

where

Q = maximum possible power produced in element, kw

W_i = minimum possible flow rate inside element, gpm

W_o = minimum possible flow rate outside element, gpm

$'$ = denotes expected value of parameter without the hot channel factors

F_q = hot channel factor to account for uncertainties in fuel element power production

F_{b_i} = hot channel factor to account for uncertainities in flow rate inside element

F_{b_o} = hot channel factor to account for uncertainties in flow rate outside element.

The uncertainties contributing to the above hot channel factors are shown below. In order to consider the worst case, all of these uncertainties are assumed to be acting in a detrimental fashion simultaneously, i.e., the contributing factors are multiplied together to determine the resultant hot channel factor.

TABLE 4.1

Summary of Hot Element Parameters

Element Location (refer to Fig. 4.7)	Ratio of Power Produced in This Element to Power Produced in Average Element	Time in Core Life	Flow Rate per Average Element Required to Prevent Bulk Boiling in this Element (gpm)
A	2.1	End of life	2.130
B	1.9	Beginning of life	2.185
C	1.43	End of life	1.639

Hot Channel Factors	F_q	F_{b_i}	F_{b_o}
Uncertainty in neutron flux distribution calculations	1.10	---	---
Uncertainty in reactor power level	*1.01	---	---
Variation in meat thickness	1.03	---	---
Variation in fuel concentration	1.02	---	---
Plenum chamber flow variations	---	1.07	1.07
Flow variation due to uncertainties in channel and orifice dimensions	---	1.01	*1.03
Resultant hot channel factor	*1.17	*1.08	*1.10

*Factor differs in magnitude from value given in last quarterly report.

Since the Second Quarterly Report, MND-M-1813, certain factors in this table have been assigned to different hot channel factors and the numerical values have changed. In this present tabulation all factors influenced or determined by the fuel element or reactor power were placed under the factor, F_q. All factors influenced or determined by mechanical or hydraulic considerations were placed under the factors, F_{b_i} and F_{b_o}.

The value of the factor for uncertainty in reactor power level was changed since the control mode for the trim of the reactor was modified. Since the automatic reactor trim has been eliminated, the value of 1.12, previously used to account for possible instrument errors and their effect upon the resultant power level, has been re-evaluated at 1.10.

The uncertainty in reactor power level is due to variation in primary loop mean temperature. The thermal efficiency of the entire system decreases slightly if this temperature is slightly less than the nominal operating value. A heat balance on the secondary loop indicates that the power supplied to the steam generator must be 9.37 megawatts. The heat balance in the secondary system is conservative and as a result no hot channel factor has been assigned. The preliminary design study indicated that the heat introduced by the primary coolant pump is approximately equal to the loop heat loss. Thus, the reactor power level is 9.37 megawatts.

The variations in flow rate due to channel and orifice dimension uncertainties were based upon the following manufacturing tolerances: fuel element inside and outside diameters, ±0.001 inch; fuel element pitch, ±0.006 inch; inlet grid plate orifice diameters, ±0.002 inch. With all tolerances acting in a fashion most deterimental to coolant flow, it was found that the flow rates inside and outside of the elements would be decreased by no more than 1% and 3%, respectively.

Flow rate per fuel element. The limiting criterion in the selection of the primary loop flow is that the primary coolant temperature is not to exceed 567.2° F at the exit of any channel. The channel is assumed to be producing 120% of its normal power, since studies performed on an analog computer indicated that the maximum positive power transient expected in the core is 20%. All uncertainties are applied in the form of hot channel factors. All fuel element thermal and hydraulic analyses were performed with BUBBLES-1. The analytical techniques employed were described briefly in the PM-1 Preliminary Design report.

The method of analysis in the determination of the required flow rate per fuel element was as follows:

(1) Determination of the maximum expected power production in the hot element excluding the transient consideration.

(2) Determination of the minimum expected flow rates inside and outside of the hot element corresponding to selected flows inside and outside of an "average" element.

(3) Using BUBBLES-1, the axial distributions of coolant temperature, surface temperature, heat flux, pressure, velocity, film coefficient and enthalpy were calculated, as well as radial temperature distributions within the fuel cell.

(4) The 20% transient condition was assumed to result in a 20% increase in the coolant temperature rise along the fuel element. The minimum flow rate required to prevent bulk boiling was that which resulted in an exit coolant temperature of 567.2° F.

The maximum expected power production in each of the hot elements was determined by multiplying the power production of an average element, Q

$$Q = \frac{9370 \text{ kw}}{725 \text{ elements}} = 12.92 \text{ kw per element}$$

by the hot spot factor accounting for uncertainties in power production, F_q = 1.17, and maximum peak-to-average power production ratios; 2.1 and 1.9 for the elements adjacent or not adjacent to a control rod channel, respectively. This results in maximum power productions (excluding the transient condition) in these elements of 31.7 and 28.7 kw.

Based on the results of the preliminary design investigation, it was known that the flow rate required per fuel element would be in the range between 2.00 and 2.45 gpm. Average element flow rates of 2.00, 2.15, 2.30 and 2.45 gpm were considered and the minimum expected flow rates in the hot channels corresponding to these "average" values were obtained. It was known also that a flow ratio of 0.48 (flow inside the element to total flow associated with the element) resulted in very nearly equal exit coolant temperatures inside and outside the channel (the inlet orifices then were sized to yield this distribution in the average element). The flow rates inside the hot elements were determined by:

$$W_i = \frac{0.48 \times W}{F_{b_i}} = 0.444$$

where

W = the total flow rate corresponding to an average element.

The flow rate outside of a hot element adjacent to a control rod channel was found to be at least 1.49 times that outside of an average element, based upon the existence of equal pressure drops per unit length along this channel and an average channel. Using the hot channel factor to account for uncertainties in the flow rate outside an element F_{b_o}, the equivalent flow rate for the hot element adjacent to a control rod channel is found to be:

$$W_o = \frac{1.49\ (1.00 - 0.48)}{F_{b_o}}\ W = 0.704\ W$$

The flow rate outside the hot element not adjacent to a control rod channel is given by:

$$W_o = \frac{(1.00 - 0.48)}{F_{b_o}} W = 0.473 W$$

Analysis of each of these cases was performed using BUBBLES-1. There were twelve cases in all since the average element, hot element adjacent to a control rod channel, and the hot element away from the channel were each analyzed at flow rates corresponding to 2.00, 2.15, 2.30 and 2.45 gpm in the average element.

The 20% transient condition was assumed to result in a 20% increase in the coolant temperature rise across each element. A plot of maximum expected coolant temperature versus flow in the average channel for each of the hot elements is shown in Fig. 4.8. It can be seen that the hot element in the infinite array at the beginning of core life requires a higher flow rate to prevent bulk boiling than does the hot element adjacent to a control rod channel at the end of core life. The average flow rate per element required to exclude the possibility of the occurrence of bulk boiling in the core under any expected operating conditions, from Fig. 4.8, is 2.185 gpm.

The average heat flux in the core is 73,000 Btu/hr-ft^2. The maximum heat flux in the core will occur at the beginning of core life. The peaking in the axial direction which is caused by the insertion of the control rods results in a maximum heat flux of 290,000 Btu/hr-ft^2. The burnout heat flux is 1,300,000 Btu/hr-ft^2 based upon the Jens and Lottes correlation. The maximum per cent of burnout heat flux existing in the core under normal operating conditions then is 22%. Since this is well within the limits of safe design, the limiting criterion in the determination of the required flow rate per fuel element was properly selected as the exclusion of bulk boiling.

Total primary loop flow rate. The core is composed of 725 active fuel elements, 18 dummy elements (stainless steel tubes) and a maximum of 77 burnable poison rods. The dummy elements are of the same dimensions as the active elements and the diameter of the burnable poison rods is equal to the outside diameter of a fuel element.

The elements in the core are not in an infinite array. Therefore, allowance must be made for deviation from this array, particularly in areas adjacent to control rods, control rod guides and spaces between the fuel element bundles. Since the flow rate inside the elements is strongly controlled by the orifice at the inlet of each of these well-defined channels, only the flow deviations outside of the elements need be considered.

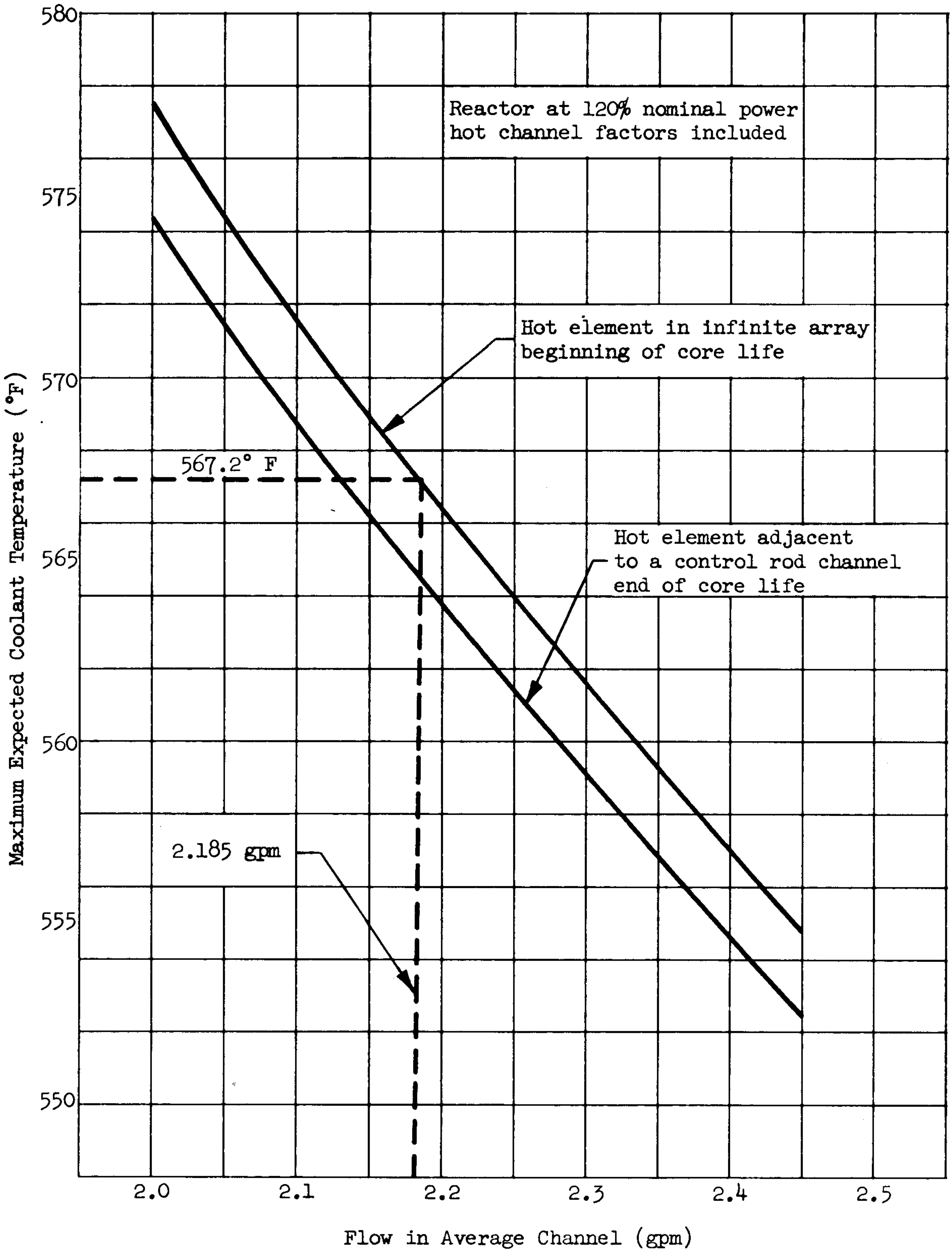

Fig. 4.8. Maximum Expected Coolant Temperature Versus Flow in an Average Channel for the "Hot" Fuel Elements

The areas mentioned above have flow areas and hydraulic diameters which differ significantly from the elements in the infinite array; therefore, it would be expected that the flow rates outside of these elements also would differ. These flows were determined on the basis of equal frictional pressure drops per unit length of channel.

If the friction factor outside of the elements is assumed proportional to the -0.2 power of Reynolds number (which is the case for smooth tubes), then it may be shown that

$$\frac{V}{V_\infty} = \left(\frac{D}{D_\infty}\right)^{2/3}$$

where

V coolant velocity

D = the hydraulic diameter.

The nonsubscripted variables refer to the channel under consideration; the subscript ∞ refers to a channel in the infinite array. The hydraulic diameter is computed as four times the channel flow area divided by its wetted perimeter. The ratio of the flow rates is given by:

$$\frac{W}{W_\infty} = \frac{A}{A_\infty} \frac{V}{V_\infty} = \frac{A}{A_\infty} \left(\frac{D}{D_\infty}\right)^{2/3}$$

where

W = the flow rate

A = the flow area.

Analysis was performed to determine the flow losses associated with all fuel elements, dummy elements and burnable poison rods which were not in the infinite array. These areas were considered in nine sections; the hydraulic parameters of each section are presented in Table 4.2.

The total number of fuel elements, dummy elements and burnable poison rods in the core is 820. It can be seen from Table 4.2 that 248 of these were considered in the nine special sections. The flow required outside of these elements is 503 gpm. The remaining 572 elements are essentially in the infinite array, hence the outside flow rate of each is 52% of 2.185 gpm, or a total of 650 gpm. The flow rates inside the 743 active and dummy elements are 48% of 2.185 gpm, or a total of 779 gpm. The required primary loop flow rate is:

TABLE 4.2

Flow Outside of the Elements

Section	Flow Area ($in.^2$)	Hydraulic Diameter (in.)	Ratio of Weight Flow Rate to Weight Flow Rate Outside an Element in the Infinite Array	Number of Places in the Core	Flow Rate (gpm)	Number of Elements Cooled
1	0.181	0.499	0.987	144	162	72
2	0.235	0.295	0.905	18	19	0
3	0.0688	0.368	0.307	18	6	3
4	0.0819	0.338	0.345	36	14	9
5	0.5111	0.366	0.567	12	31	24
6	0.932	0.359	0.585	6	28	21
7	1.186	0.458	0.873	6	41	21
8	0.252	0.642	0.818	69	129	69
9	1.330	0.846	1.103	12	73	29
					503	248
Infinite array	0.188	0.480	1.0	572	650	572

$$W_T = 503 + 650 + 779 = 1932 \text{ gpm}$$

This flow rate determination is applicable at the beginning of core life when the control rods are inserted. Table 4.2 indicates that 201 gpm (Sections 1, 2, 3 and 4) flows through the control rod channels under these conditions. Since the pressure drop through the orifices in the lower grid plate is approximately five times the frictional drop through the rest of the core, the total core flow rate is relatively insensitive to control rod positions. However, extracting the control rods does result in increased flow in the vacant channels. As stated before, gross flow tests indicated that the velocity in these vacant channels was 10% higher than the average velocity outside of the elements. Based upon this distribution, a total flow rate of 374 gpm would be expected in the vacant control rod channels. This represents 173 gpm more flow than is expected when the rods are inserted. The total flow rate outside of the elements not adjacent to the control rods is 952 gpm when the rods are inserted. Extraction of the control rod, therefore, results in an 18% decrease in the flow rate outside of the active fuel elements not adjacent to the control rod channels.

This analysis resulted in a required primary loop flow rate of 1932 gpm. Applying a 10% safety factor to account for uncertainties not previously considered, and to supply a reasonable margin of safety, results in a required primary loop flow rate of 2125 gpm.

2. BUBBLES-1

A FORTRAN-709 version of BUBBLES-1, the thermal and hydraulic analysis code, has been written and compiled for the IBM-709. This version includes all modifications which were made to the original IBM-704 version, as well as several other improvements.

The basic analysis has not been altered. A brief description appeared in the PM-1 Preliminary Design Technical Report. Of particular note is the incorporation of small subprograms for the performance of the various code functions. In this manner, the correlations employed for the determination of heat transfer film coefficients, pressure drops, burnout heat flux, etc., may undergo major revision with recompilation of only a small part of the code. The correlation presently employed for the determination of the local boiling friction factor is:

$$f_{lb} = f_{iso} \left[1 + \frac{\theta + 76 - \theta_{sat}}{\phi} \right]$$

where

f_{lb} = local boiling friction factor

f_{iso} = isothermal friction factor

θ = bulk coolant temperature, °F

θ_{sat} = saturation temperature, °F

ϕ = a function of pressure, °F (see Table 4.3).

The correlation presently employed for the determination of burnout heat flux is:

$$q_{bo} = \frac{2.8 \times 10^5}{\left(\frac{H}{1000}\right)^{2.5}} \left[1 + \frac{G}{10^7}\right] e^{-0.0012\ L/D}$$

TABLE 4.3

Local Boiling Friction Factor Correlation Parameter as a Function of Pressure

Pressure (psia)	Parameter, ϕ (°F)
1100	50.9
1200	57.6
1300	65.0
1400	71.0
1500	77.5
1600	86.4
1700	96.2
1850	105.7
2000	126.3

where

$$\frac{f}{f_{iso}} = 1 + \left[\frac{\theta + 76 - \theta_{sat}}{\phi} \right]$$

where

q_{bo} = burnout heat flux, Btu/hr-ft^2

H = bulk coolant enthalpy, Btu/lb

G = mass flux, lb/hr-ft^2

L = fuel element length, ft

D = equivalent hydraulic diameter, ft

3. Thermal Shield Heat Transfer Analysis

The objective of this analysis was to ensure that no local boiling will occur in the annuli surrounding the thermal shields. Since the coolant flow is downward in these annuli, local boiling would lead to flow instability and should be avoided. The approach was to determine the surface temperature for a particular shield configuration, modify the configuration as required, then recalculate the surface temperature for the new configuration.

In the absence of actual test results, it was necessary to make some assumption concerning the flow distribution in the shield region in order to perform the analysis. Accordingly, it was assumed that the distribution going into the annuli (that leaving the inlet water box) is uniform. Since the annuli have the same equivalent diameter, this assumption results in equal average velocities.

Since the surface temperature of the shields is a function of coolant temperature and heat generation within the shields, and since the axial variation of coolant temperature along the shield is extremely small, the maximum surface temperature was assumed to occur at the elevation associated with the greatest heat generation within the shield.

The steady-state diffusion equation for heat conduction in the radial direction only, and considering the internal heat generation to be dependent on position, is:

$$\frac{d^2T}{dr} + \frac{1}{r}\frac{dT}{dr} = -\frac{S(r)}{k} \tag{1}$$

where the thermal conductivity (k) is assumed to be constant. The convection boundary conditions are:

$$\frac{dT(R_i)}{dr} = \frac{h_i}{k}\left[T(R_i) - \theta_i\right] \tag{2}$$

and

$$\frac{dT(R_o)}{dr} = \frac{-h_o}{k}\left[T(R_o) - \theta_o\right] \tag{3}$$

The solutions for the inside and outside surface temperature are:

$$T(R_i) = \frac{1}{1 + R_i h_i\left[\dfrac{1}{R_o h_o} + \dfrac{1}{k}\ln\dfrac{R_o}{R_i}\right]}\left\{\frac{G(R_o) - G(R_i)}{k} + R_i h_i \theta_i \left[\frac{1}{R_o h_o} + \frac{1}{k}\ln\frac{R_o}{R_i}\right] + \frac{F(R_o) - F(R_i)}{R_o h_o} - \frac{1}{k}F(R_i)\ln\frac{R_o}{R_i} + \theta_o\right\} \tag{4}$$

$$T(R_o) = \frac{F(R_o) - F(R_i)}{R_o h_o} - \frac{R_i h_i}{R_o h_o}\left[T(R_i) - \theta_i\right] + \theta_o \tag{5}$$

where

$$F(r) = \int r\,S(r)\,dr \tag{6}$$

and

$$G(r) = \int \frac{1}{r}F(r)\,dr \tag{7}$$

where the following terminology is used:

h	=	film coefficient of heat transfer	Btu/ft^2-hr-F
k	=	thermal conductivity	Btu/ft-hr-F
r	=	radius from core center	ft
F	=	function, defined where used	Btu/ft-hr
G	=	function, defined where used	Btu/ft-hr
R	=	constant value of radius	ft
S	=	volumetric heat generation	Btu/ft^3-hr
T	=	temperature of metal	°F
θ	=	temperature of coolant	°F

Subscripts

i	=	inner boundary of metal
o	=	outer boundary of metal

These equations are applicable to the core shroud and thermal shields since all are cylindrical shells with two convection boundaries. However, the pressure vessel wall is insulated at its outer boundary; therefore, its solution is somewhat different, although simpler:

The **same** differential equation and inner boundary conditions hold; (Eqs (1) and (2))

but the other boundary condition is:

$$\frac{dT(R_o)}{dr} = 0 \tag{8}$$

The inside surface temperature of the pressure vessel is then:

$$T(R_i) = \frac{1}{R_i h_i} \left[F(R_o) - F(R_i) \right] + \theta_i \tag{9}$$

where the function $F(r)$ is as defined in Eq (6).

The first configuration analyzed had three thermal shields. The highest surface temperature was 450° F. Considering that the saturation temperature at thermal design pressure (1200 psia) is 567° F, it is seen that this situation is far removed from local boiling. Thus, it was realized that design of the thermal shields is not heat transfer limited in this case. Since it is desirable to reduce the number of shields, the configuration was changed to two thermal shields.

The limiting consideration then became thermal stresses. After a series of trials, a two-shield configuration which resulted in a stress of approximately 20,000 psi in both shields was obtained. This value is within the limits specified by Navy and ASME codes. The configuration which yielded this stress has a 1.6-inch inner thermal shield, a 3.4-inch outer thermal shield, and all annuli are 0.338 inch. The surface temperatures for this configuration are shown in the following sketch (not to scale):

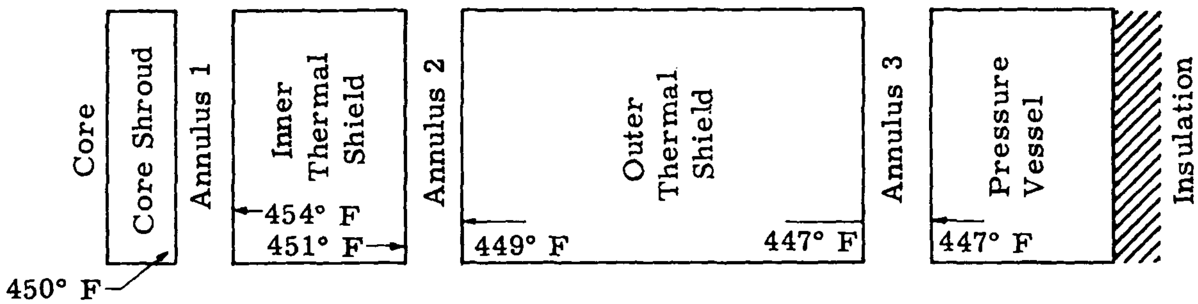

The maximum surface temperature was recalculated and found to be 454° F, again far removed from the local boiling condition. This configuration was chosen for design.

Once the size and number of the thermal shields were established, the number and nominal dimensions of the flow passages adjacent to the thermal shields were fixed since the outside diameter of the core shroud and the inside diameter of the pressure vessel were previously established. The only remaining question is the determination of the permissible manufacturing tolerances. There are two aspects to this problem: first, the effect on pressure drop, and second, the effect on maximum surface temperature.

In order to determine the maximum effect of tolerances on pressure drop, the head loss was calculated for a number of values of the width of the flow passages adjacent to the thermal shields. The head loss was calculated as an abrupt contraction, a friction loss, and an abrupt enlargement. The head loss increased rather rapidly from 1.6 feet for the nominal passage width of 0.3375 inch to 3.4 feet for a spacing of 0.255 inch. The rate of increase of head loss with reduced passage width became even more rapid as width decreased. Tolerances which would permit a minimum passage of 0.255 inch were initially suggested as a compromise between high head loss and ease of manufacturing.

In order to investigate the effect of tolerances on the maximum surface temperature, the width of the flow passage along which the maximum surface temperature occurs was assumed to be at the minimum value, and the width of the other passages at their nominal value. The head loss in the three flow passages was then equated and the resultant velocities in the passages calculated. It was found that the velocity in the passage with the minimum width was decreased by less than 10%. This results in an increase of surface temperature of less than 1° F. Therefore, the tolerances do not increase appreciably the possibility of local boiling.

4. Reactor Head Loss Calculations

The head loss of the reactor from inlet to outlet was calculated by summing the individual losses. (Each loss was conservatively calculated.) Table 4.4 gives a summary of the individual losses.

TABLE 4.4

Head Losses

(ft H_2O)

	1932 (gpm)	2125 (gpm)
Reactor inlet pipe	8.8	10.1
Inlet water box	0.2	0.2
Water box orifice	3.0	3.6
Thermal shield	2.9	3.5
Entrance to bottom plenum	Negligible	Negligible
Core (including upper and lower grids)	0.7	0.8
Orifice of outlet of upper plenum	3.0	3.6
Outlet water box	0.1	0.1
Reactor outlet pipe	4.7	5.7
Total	23.4	27.6

B. SUPPORTING SYSTEM ANALYSIS STUDIES

C. Smith, J. Beam, L. Hassell, R. Baer, S. Zwickler

The system studies performed during the past quarter concerning the reactor coolant subsystem were divided into the following four principal subsystem areas:

(1) Head loss

(2) Heat balance

(3) Startup

(4) Decontamination.

1. Head Loss

Subsystem head loss was computed for flow rates of 1932 gpm and 2125 gpm.

The reactor head loss was previously shown to be 23.4 and 27.6 feet of water for flow rates of 1932 and 2125 gpm, respectively.

The head loss in the piping and fittings connecting the reactor, steam generator and primary coolant pump was calculated by summing individual losses as follows:

Item		Pressure Loss ($ft\ H_2O$) 1932 (gpm)	Pressure Loss ($ft\ H_2O$) 2125 (gpm)
6-inch piping	(20.92 feet in length)	4.03	4.92
8-inch piping	(14 inches in length)	0.06	0.07
6-inch-90°-long radius elbows	(3 each)	4.75	5.75
6-inch-45°-long radius elbows	(2 each)	3.01	3.62
6-inch-60°-long radius elbows	(1 each)	1.54	1.86
6-inch-30°-long radius elbows	(2 each)	1.70	2.04
Total		15.09	18.26

All calculations and constants are in accordance with the Hydraulic Institute Pipe Friction Manual and generally are conservative.

The steam generator head loss was stated by the Westinghouse Company to vary with the square of the flow. Westinghouse calculations are tabulated below:

Flow (gpm)	Head Loss ($ft\ H_2O$)
1932	33.6
2125	40.6

The total head loss to be overcome by the pump is the summation of the reactor, steam generator and piping and fitting head losses.

Flow (gpm)	Total System Head Loss (ft H_2O)
1932	72.1
2125	86.5

2. Heat Balance

In order to meet the power plant requirements of 7.0 million Btu/hr of heat and a net of 1000 kw of electrical energy, the secondary heat balance shows that the steam generator must produce 9.37 megawatts of heat in the form of 300 psia steam, dry and saturated.

The heat balance shown in the tabulation below assumes, as discussed previously in MND-M-1813, that the energy added by the primary coolant pump is about equal to that lost through reactor vessel, piping and steam generator insulation, and that lost to the shield water from the purification system.

	1932 (gpm)	2125 (gpm)
Reactor thermal power, mwt	9.37	9.37
*Reactor flow, lb/hr	782,230	870,795
*Primary pump flow, lb/hr	783,230	871,795
**Blowdown flow, lb/hr	1000	1000
Mean loop temperature, °F	463	463
Reactor temperature rise, °F	36.33	32.64
Hot leg temperature, °F	481.2	479.3
Cold leg temperature, °F	444.8	446.7
Enthalpy hot leg, Btu/lb	466.2	463.4
Enthalpy cold leg, Btu/lb	425.3	426.9

*Reactor and primary pump flow evaluated at 1300 psia and 463° F.

**Blowdown flow evaluated at 1300 psia and high pressure demineralizer influent temperature of 120° F.

3. Startup

Various methods of reactor coolant subsystem cold startup were analyzed. The only variation in the methods analyzed is the procedure used to bring the pressurizer up to normal temperature and pressure. The various schemes considered for pressurizer cold startup are discussed in the section on the Pressurizer and Pressure Relief Subsystem.

The basic rules used to establish the cold startup procedure are as follows:

(1) The primary coolant pump is specified to operate with a 60-foot minimum net positive suction head. An allowance for instrument accuracy in addition to the 60-foot head is used to give a minimum system pressure of 81 feet (35 psig) prior to placing the pump in operation.

(2) The heatup rate is 100° F per hour.

(3) The pressurizer temperature always exceeds the system temperature by a minimum value of 100° F to ensure that steam is produced in the pressurizer only upon a decrease in subsystem pressure.

The cold startup procedure then selected for the reactor coolant subsystem is described below.

Step 1. Fill loop and purification subsystem with vents open on both subsystems; stop after solid water appears at vents; close vents.

Step 2. Operate charging pumps to bring the reactor coolant subsystem pressure up to 35 psig.

Step 3. Put pressurizer heaters in operation to raise pressurizer temperature to approximately 280° F at a rate of 100° F per hour; operate remotely operated discharge valve (from control room) to prevent subsystem pressure from exceeding 35 psig during this step.

Step 4. When pressurizer reaches 280° F, continue to remove fluid from the subsystem to maintain a pressure of 35 psig (steam will form in pressurizer); continue operating discharge valve until level in pressurizer reaches normal level.

Step 5. Put the reactor coolant pump in operation.

Step 6. Place the charging subsystem in operation (to maintain pressurizer level).

Step 7. Place low flow scram in operation.

Step 8. Bypass low pressure scram and bring the reactor critical; raise the reactor power to a predetermined kilowatt level and heat the subsystem at a rate not exceeding 100° F per hour.

Step 9. When the subsystem temperature has reached 180° F, place the pressurizer heaters into operation to raise the pressurizer temperature at rate of 100° F per hour.

NOTE: During subsystem warmup and increase in pressure, the pressurizer heaters are operated to maintain the pressurizer temperature 100° F above the reactor coolant subsystem temperature at all times.

Step 10. When the subsystem pressure reaches 1230 psia, put the low pressure scram into normal operation.

Step 11. Continue heating subsystem. When pressurizer temperature reaches normal operating temperature put the required number of heaters on automatic fine control and the remaining heaters on automatic coarse controls.

4. Decontamination

The investigation was completed of promising decontamination processes, commercially available and currently used for pressurized water reactors was completed.

Study of reports on decontamination processes show that although electrolytic, ultrasonic and chemical methods have been given serious consideration, the chemical method is the only practical means of decontaminating full-scale nuclear power reactors.

The chemical processes which showed the most promise and the reports in which they are discussed are listed below:

(1) ALCO Products. The caustic permanganate-rinse decontamination treatment as discussed in APAE No. 43, Vol. 2, dated February 1959.

(2) Westinghouse Atomic Power Department. The basic permanganate and citrate solution treatment as discussed in YAEC 90, dated November 1958.

(3) Westinghouse Electric Corporation (Bettis Plant). The sulfamic acid treatment as discussed in WAPD-PWR-CP-2719, dated 1957.

(4) TURCO Products. The TURCO Decontamination 4501 Process as discussed in HW-57635 dated December 1958 and BAW-99, dated June 1959.

(5) TURCO Products. The TURCO Two-Step Decontamination Process as discussed in HW-60767, dated 1959.

The criteria for comparison of these five processes and for selection of the reference design process is:

(1) Ease with which the decontamination treatment may be applied, i.e., simplicity, brevity and economy in applying the process.

(2) Capability of achieving maximum removal of activity.

(3) Provisions required in the radioactive waste disposal subsystem to accommodate the volumes of contaminated liquids evolved during treatment.

(4) Effect of the chemicals upon the materials of construction used in the reactor coolant subsystem.

(5) Ease with which the chemicals used may be stored. Weight and volume of chemicals stored per cycle and ability to store over a temperature range from - 40° F to 85° F are important considerations.

On the basis of the preceding comparison, the TURCO Two-Step Decontamination Process was chosen as the reference design process. The steps involved are:

Step 1. Immerse in TURCO Decon 4502 for 30 to 60 minutes at 210° F.

Step 2. Water rinse at ambient (20 to 30°C) for 5 minutes.

Step 3. Immerse in TURCO Decon 55-14A for 45 minutes at 30°C.

Step 4. Water rinse at ambient for 5 minutes.

Step 5. Circulate Step 4 water rinse through an ion exchanger.

The mode of operation planned for the PM-1 is to decontaminate the entire reactor coolant, pressurizer and high pressure purification subsystems simultaneously rather than individual components separately. Circulation of the solutions through the pressurizer can be accomplished allowing flow through the spray line. To effectively decontaminate the high pressure purification loop, the resin will be dumped to permit flow through the high pressure demineralizer. Also, the cooling supply to the demineralizer cooler will be shut off and the shell will be drained to prevent heat removal and boiling of cooling water in the cooler.

Both powders will be mixed in a 285-gallon mixing tank located in the decontamination package. A portable pump is used to pump the solutions from the tank into the reactor coolant subsystem. The reactor coolant pump may be used to circulate the solutions.

Steam will be introduced into the secondary side of the steam generator to heat the solutions after being pumped into the subsystem. Approximately 100 kw are available from the auxiliary steam boiler (located in secondary system) to both heat the solutions and to evaporate them in the waste disposal evaporator.

As a result of using the TURCO process, five loop volumes (including initial loop drain) or an estimated 2700 gallons of solutions will be produced per decontamination cycle.

This solution will be treated and reduced in volume in the waste disposal system.

C. DESIGN STUDIES

Component design studies were made of each of the major components of the reactor coolant subsystem.

1. Reactor Pressure Vessel

The general design of the reactor pressure vessel, with the exception of the areas (head to shoulder closure and seal, center bundle closure and seal, top head insulation, and remote handling equipment) to be assigned to the pressure vessel fabrication subcontractor, was essentially completed during this quarter. Effort was concentrated on fatigue analysis of the vessel, changes to the mounting scheme and water box, and preparation of the procurement data and vendor briefings.

Fatigue analysis. The preliminary analysis of critical areas in the vessel was performed, based upon a coolant temperature change of 100° F per hour during startup and shutdown. Fatigue analysis was based on 750 startup-shutdown cycles. The analyses were made in accordance with the method set up in "Tentative Structural Design Basis for Reactor Pressure Vessels (Pressurized Water Cooled Systems)," published by BuShips, December 1958 (hereafter referred to as the Navy Code).

The results indicate that no fatigue failures will occur at startups and shutdowns at the rate of 100° F per hour. Further work is in progress to determine the maximum tolerable rate. The results will be published later in a technical memorandum.

Mounting scheme changes. The reactor vessel external mount was redesigned. The trunnion mounts mentioned in previous reports were replaced with a fixed skirt at the bottom of the vessel. Expansion of the primary loop piping will now be accommodated by allowing the steam generator to move. The outlet and inlet nozzle were relocated to facilitate this new arrangement. To obtain expansion forces as near "straight-line" as possible, the nozzles are located at 60 degrees to each other on that side of the reactor vessel nearest to the steam generator. A location closer than 60 degrees is not feasible because ligament stresses between the nozzles would increase sharply.

Water loop changes. In order to maintain uniform flow of inlet water to the thermal shields, allowance must be made for a 60-degree minimum angle between inlet and outlet nozzles, and the overall height of the reactor vessel must be maintained. A redesign of the water box was required as shown in Fig. 4.9.

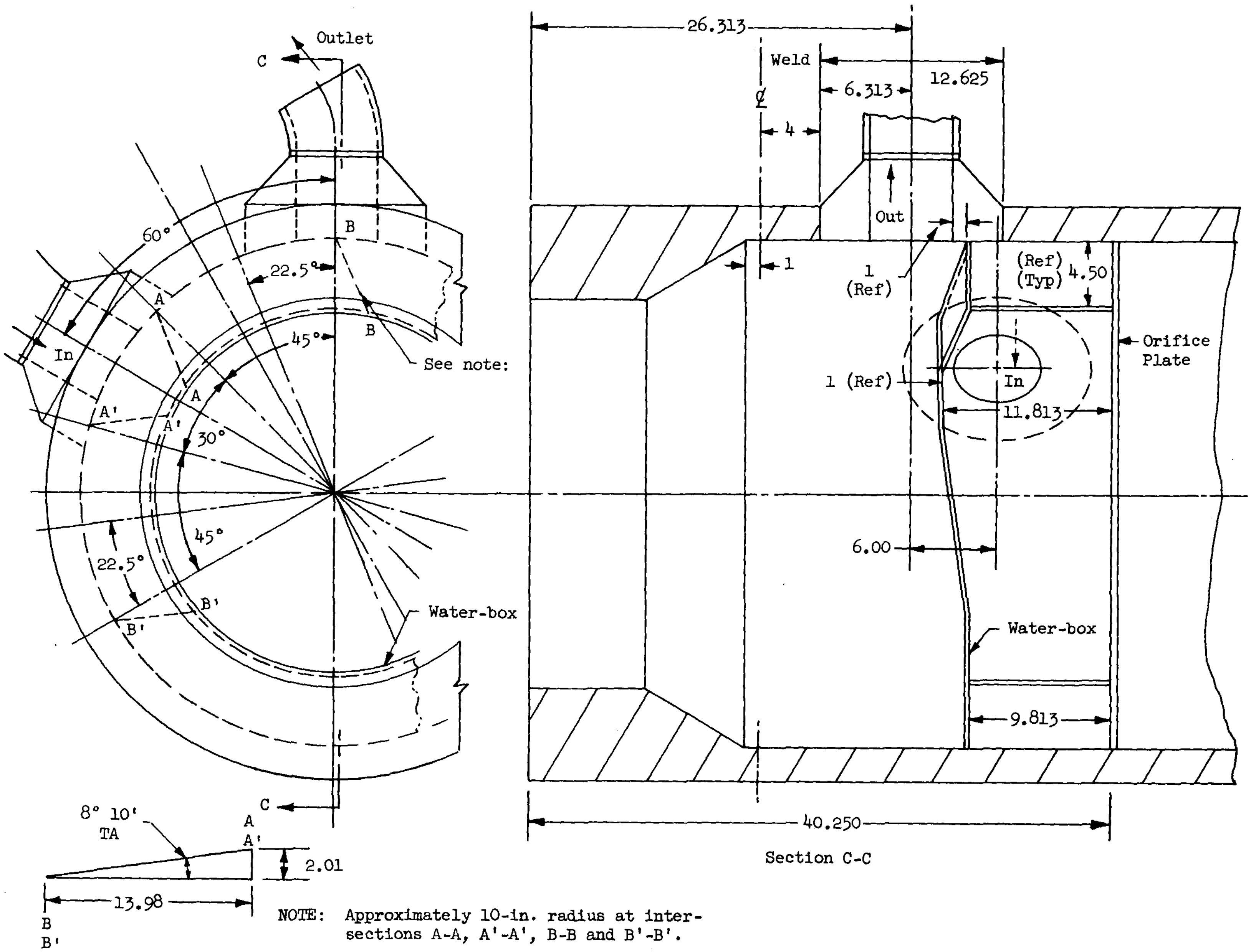

NOTE: Approximately 10-in. radius at intersections A-A, A'-A', B-B and B'-B'.

Fig. 4.9. PM-1 Reactor Vessel Nozzle Location and Water-Box Configuration

Procurement data and vendor briefings. The concepts developed during preliminary design and modified during the quarter were prepared as drawings and a specification and were submitted to 12 vendors.

Technical proposals accompanied by fixed price bids for the detailed design, fabrication and testing of the reactor pressure vessel and associated equipment are expected to be received early in December.

After evaluation of the proposals, the final drawings and specification will be modified and a subcontract will be awarded.

2. Steam Generator

The steam generator specification was received from Westinghouse Electric Corporation and was reviewed and revised with corrections and comments added. It will be submitted for approval with an outline drawing during the next quarter.

3. Primary Coolant Pump

A preliminary specification for the primary coolant pump was prepared and submitted for bids to ten pump manufacturers. The specification was broad enough to stimulate replies from the manufacturers of mechanical seal, controlled leakage and canned motor pumps which could be evaluated to determine the optimum type of pump for our application.

An evaluation was made in which comparisons were based on reliability, weight, volume and cost. It was recommended that the canned motor-type pump be used. The recommendation was based on the high reliability shown by this pump, lower weight and smaller volume despite its somewhat higher cost.

The specification was revised and corrected to stipulate a canned motor pump and invitations to rebid were extended. Fixed price bids are expected early in December; a contract will be let shortly thereafter.

4. Associated Piping

The design of the main loop piping, i.e., only two flange connections required to complete the main piping loop, enables the primary system to be installed with a minimum of effort. During site installation, the steam generator floating support carriage must be positioned within the container tank to make the flange connections. This design allows for correction of any misalignment problems during erection and thermal expansion of the pipe during operation.

Additional flanges near the steam generator nozzles provide a means of disconnecting, removing and replacing the steam generator in the main loop piping without field welding of the pipe.

The need for maintenance on the steam generator or main pump demands depressurization and removal of heat from the system. The design of the main loop makes provision for heat removal through the use of the auxiliary coolant pump and cooler. With the system depressurized, the heat is removed by opening the coolant system shutoff valve which allows the auxiliary coolant pump to circulate the main loop water through the cooler and back to the system. The loop between the steam generator and primary pump is drained to the sump. The design of the main loop piping provides a positive head condition at the suction outlet which prevents auxiliary coolant pump cavitation and the loss of the coolant supply.

Stress analysis of piping from steam generator to pump showed thermal and pressure stresses low enough to permit the steam generator and pump to be mounted in a common base. The analysis was made two ways: by the tube turns flexibility analysis and by the strain energy method. Basic agreement between the two methods was achieved.

A preliminary evaluation of loads in the primary piping from reactor to steam generator was made. With the temperature of one pipe at 481.5° F and the other at 444.5° F (ΔT = 37° F), reaction loads were found to be less than 11,000 pounds. It is felt that the actual loads are considerably less than 11,000 pounds because of additional flexibilities which have not been included. Further load analysis will be performed during the next quarter.

5. Reactor Core

During the third quarter, the reactor core bundles were redesigned to reduce their overall length and to eliminate the requirement for an upper alignment spider.

Length reduction. The original length of the core bundles was so great that the shipping weight of the spent-core shipping cask would have been excessive. Therefore, it would have been necessary to supply either a mechanical disconnect joint on the control rod guides or to provide equipment for cutting them. Since either would be a remote operation, it would have been expensive and time-consuming during core reloading. In addition, reuse or disposal of the support structure would be difficult from both design and general facility considerations.

An outline drawing of the new reference core design, eliminating this problem area, is presented in Fig. 4.10. The basic method of flow baffling, fuel tube support, control rod configuration and general alignment is essentially unchanged. Fundamental modifications were made both to the method of guiding the control rods and of supporting the core.

The full-length control rod guides were eliminated through the use of a slotted guide tube which is used to position the control rod centerline through its top guide ring. Three control rod guides, similar to those of the previous design, provide for both angular and radial positioning at the bottom of the control rod. The rod guides extend well above the core, thereby providing the necessary angular alignment over the full stroke of the rod.

A hold-down force is also applied to each individual fuel bundle by means of the slotted guide tubes. These forces, as well as the upper skirt hold-down force, are supplied through the use of a multiple unit spring compressed by the pressure vessel head. Differential thermal expansions and manufacturing tolerances are taken up by this spring which will be fabricated from a single sheet of Inconel X with contours to provide a dual cantilevered spring arm to each hold-down guide tube. Positioning of the pressure vessel head loads both the guide tubes and the skirt simultaneously.

Normally, the spring is effectively enclosed by the upper skirt assembly and the pressure vessel head to prevent it from falling into the vicinity of the core if it should break. When the head is removed during refueling, the spring, although still retained, is readily available for inspection or replacement. Cooling flow passes to the head through the guide tubes and returns to the reactor vessel around the periphery of the upper skirt assembly.

Each bundle rests on a lower alignment spider which is a permanent part of the core shroud. The core weight plus the hold-down force on each bundle is taken out through the spider and core shroud to the inlet orifice plate.

The second major core design improvement is the elimination of the separate upper alignment spider. Alignment of the top of each individual fuel bundle is achieved directly by extending the control rod guide structure to alignment pins located on the core shroud flange. The control rod guide structure is used to position the rod guides relative to each other and to accept the hold-down load from the slotted guide tubes. Exclusion of this alignment spider eliminates the potentially cumbersome task of fitting it simultaneously to each fuel bundle during the refueling operation.

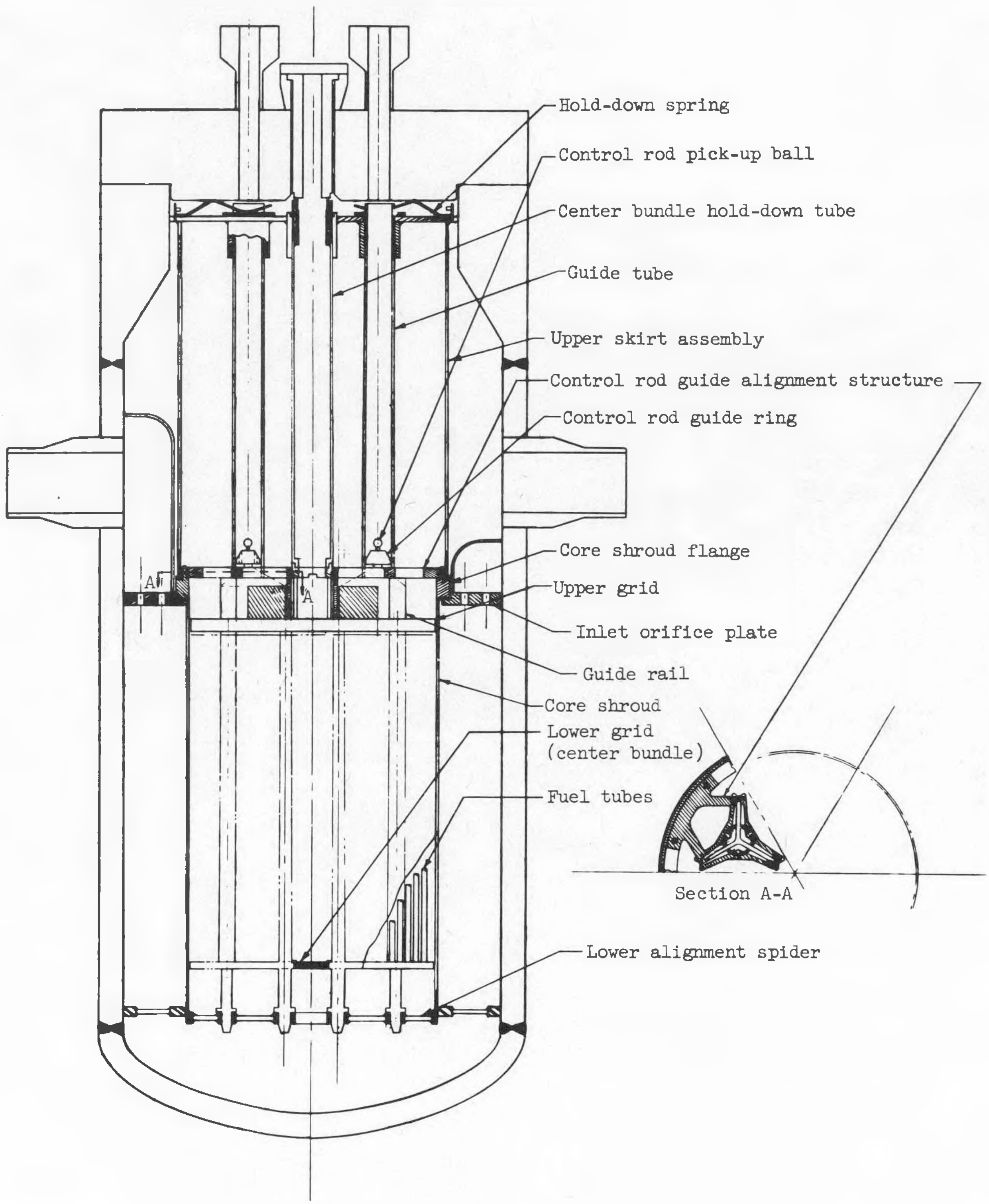

Fig. 4.10. Revised Core Support Structure

The center bundle has been designed with considerable versatility in order to facilitate its replacement by two different methods:

(1) Through the pressure vessel head, for ease of substituting an instrumented fuel or test bundle.

(2) During the standard core refueling operation without any increase in time over the standard refueling schedule.

In the initial noninstrumented core loading, the center port in the upper head will be plugged. The center bundle will be spring loaded against this plug; the fuel region will be held down with a compression tube in a manner similar to the peripheral bundles.

For a conventional refueling operation, the upper skirt, springs, guide tubes and the center bundle hold-down tube are taken out as a complete assembly. These components are reusable. After the upper skirt assembly is removed, the core may be replaced either as a single package or by individual bundles. During a package core reload operation, the core shroud containing the fuel bundles is removed and replaced as a single component. The shroud remains for positioning purposes with the core in the spent fuel shipping container. Replacement of an individual bundle requires removal of the upper skirt assembly and the center bundle.

In replacing the center bundle through the head, it is necessary to:

(1) Remove the closure from the center part flange.

(2) Insert a tie bar for locking the center bundle fuel region, hold-down tube, spring and head plug into a complete unit.

(3) Withdraw this assembly from the reactor.

An additional change was made in the control rod guide width to provide a larger wear area for the control rod weak pads. Although the total steel contained in the rod guide was held constant by contouring, the number of fuel tubes displaced by each rod guide was necessarily increased from three to five. However, aside from the nuclear disadvantage of losing potential fuel space, several design and nuclear advantages were realized:

(1) The effective poison width in each leg of the control rod was increased by 1/4 inch.

(2) The minimum wear pad contact area was increased significantly.

(3) The minimum moment of inertia of the rod guide (now being loaded in compression) was considerably increased, thereby improving its rigidity.

(4) Complexity of the upper tube grid design was decreased by the elimination of several tubes which would have proven to be difficult to position.

A preliminary overall alignment study has been completed for the new reference design utilizing the latest values available in the core design plus tolerances assigned within the control drive mechanism and reactor pressure vessel areas. Utilizing this information, it was found that the control rod slide plate formerly utilized to make up for misalignments was not necessary. This device will be eliminated from the design.

D. REACTOR COOLANT SYSTEM CONTROLS (FIG. 4.11)

R. Wilder, R. Caw

This control system provides the necessary equipment and instrumentation for control and protection of the reactor coolant system. Of the components making up the reactor coolant system, only the coolant pump involves active process control. The pump control is manual-electric, on-off exercised at the console. Pump startup interlock is so devised that pump cooling water must be circulating before the pump can be started. This interlock is such that once the coolant pump is in operation, loss of cooling water will not interrupt its operation. Pump protection is provided by measuring the outlet temperature of the pump cooling water, the pump bearing temperature and the stator winding temperature. Visual alarms are provided when the above temperatures exceed their set points.

Additional instrumentation is provided to measure plant parameters and to indicate when plant operating conditions are incorrect. This instrumentation measures the temperature of the reactor coolant at the reactor outlet and inlet (reactor coolant average temperature is computed from these two temperatures) and the reactor coolant flow. A scram is initiated by high reactor outlet temperature and low reactor coolant flow.

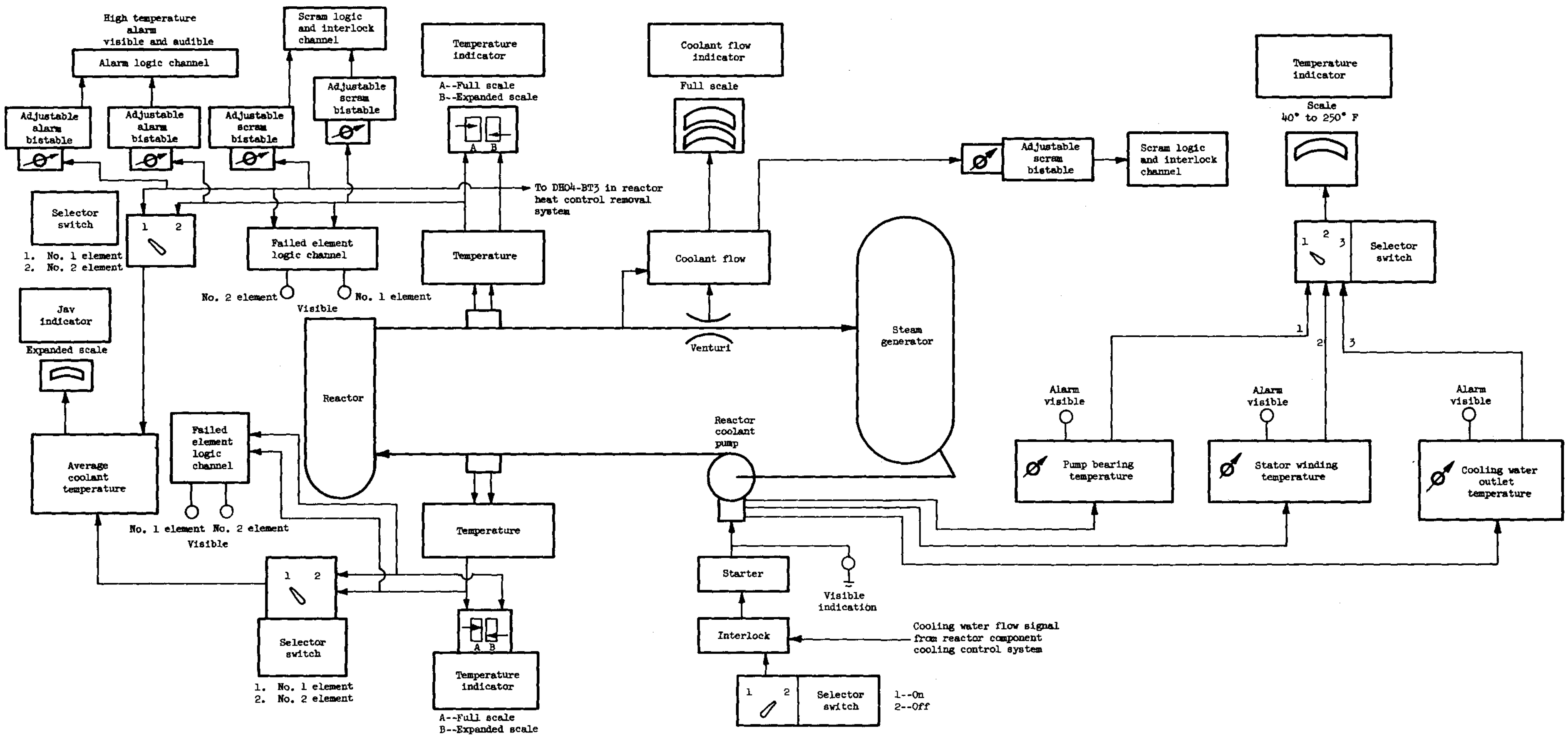

Fig. 4.11. Reactor Coolant Control System

SUBSYSTEM 7--PRESSURIZER AND PRESSURE RELIEF SUBSYSTEM (FIG. 4.12)

The pressurizer and pressure relief subsystem includes the pressurizer, safety valves, recirculating spray system, pressurizer heaters, and all piping, controls and instrumentation required for satisfactory operation of this equipment.

The pressurizer serves the dual purpose of maintaining the base operating pressure of the system at 1300 psia and also providing a flexible member to nullify the effects of variation in fluid volume. During operation, two-thirds of the volume of the pressurizer is composed of steam in contact with water at about 577° F. This temperature is attained and maintained by heaters submerged in the pressurizer water. These heaters are energized by pressure-sensing transducers which sense a drop in pressure incurred by normal pressurizer heat loss or fluid outflow caused by contraction of primary system fluid.

Upon fluid flow into the pressurizer, as a result of reactor coolant subsystem fluid expansion, a pressure operated valve opens the recirculating spray line and a water spray dissipates the steam head in the pressurizer and thus prevents a rise in pressure.

In the event of excessive pressure, however, a pair of relief valves open at 1500 and 1550 psia, respectively, and exhaust pressurizer steam into the expansion tank.

A water level sensing device in the pressurizer maintains the proper quantity of fluid in the reactor coolant subsystem and shuts off the pressurizer heaters in the event of low pressurizer water level.

A. COOLANT PRESSURIZING AND PRESSURE RELIEF CONTROL SYSTEM (FIG. 4.13)

R. Wilder, R. Caw

This system provides the necessary equipment to maintain the coolant pressure automatically within a specified band and to protect the reactor coolant system automatically from pressures exceeding the design pressure. The pressure is controlled within the specified band by an automatic-electric control which activates either the pressurizer spray valve or the pressurizer heaters. A high-pressure signal opens the spray valve and a low-pressure signal energizes the heaters.

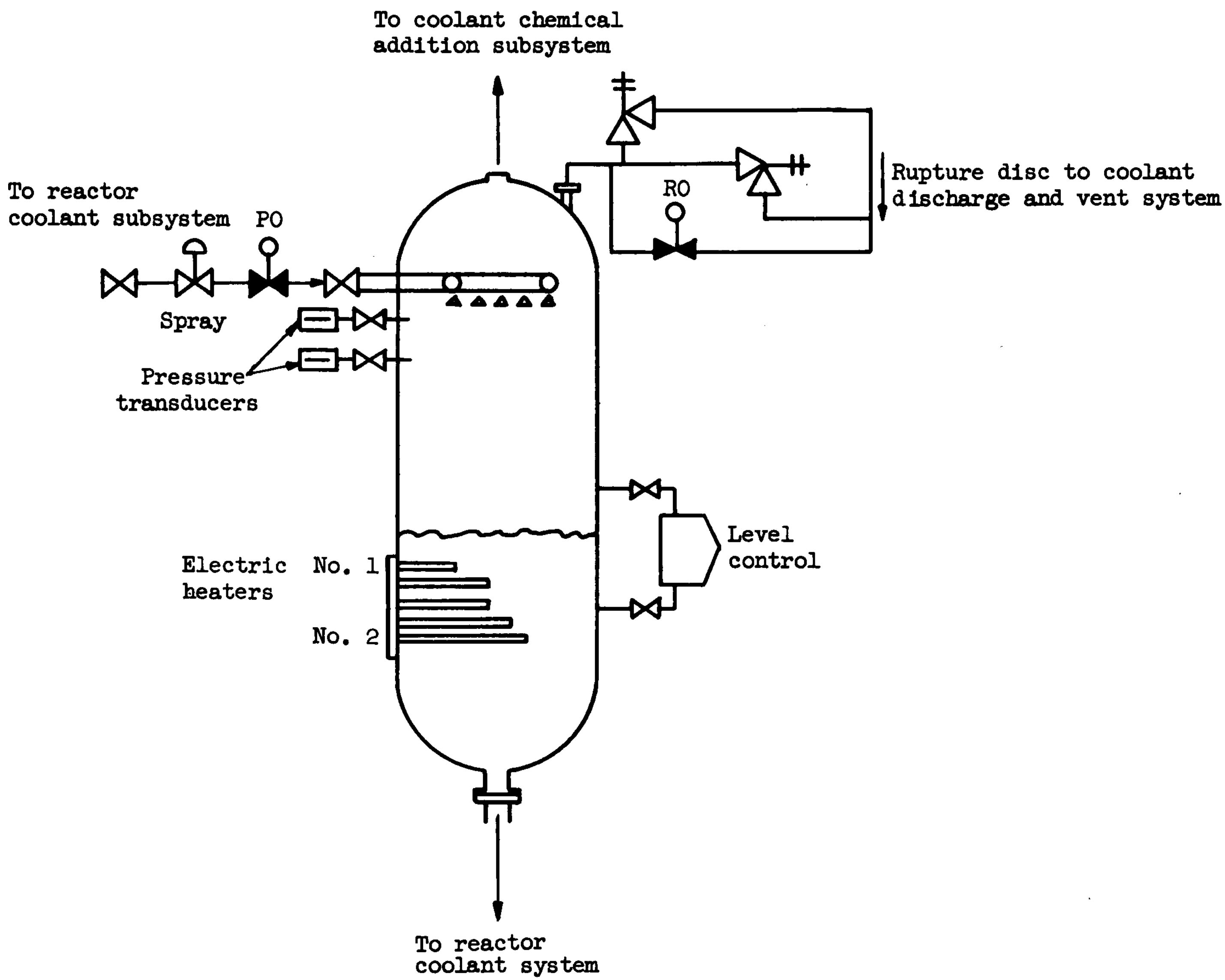

Fig. 4.12. Pressurizer and Pressure Relief Subsystem Schematic Diagram

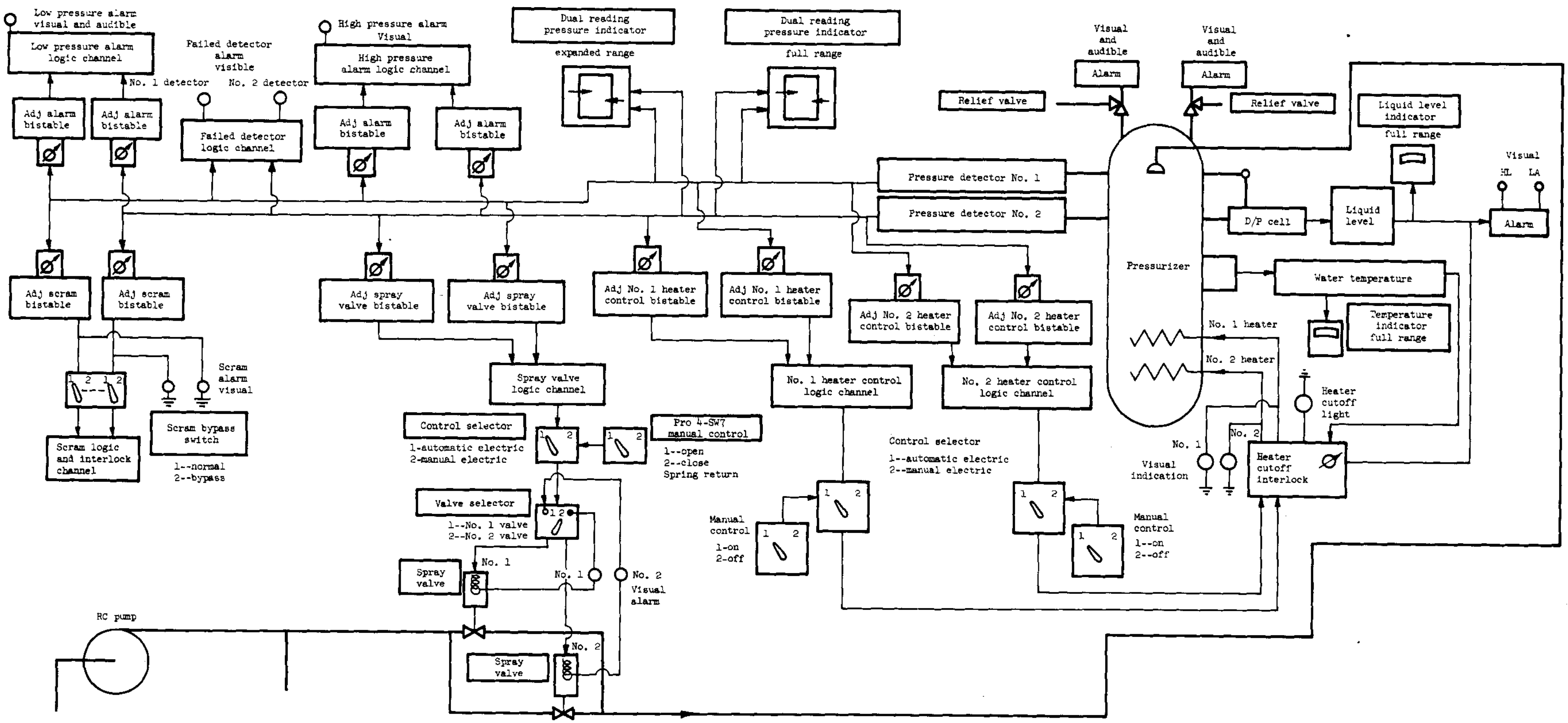

Fig. 4.13. Coolant Pressurizing and Pressure Relief Control System

Alarms are provided to warn the operator if a dangerous condition exists due to malfunction of the pressurizing control system. Manual-electric control of the spray valve and both heaters is also provided. The plant is scrammed at low pressure to protect the core. This scram signal is manually bypassed during startup until system pressure is above the scram pressure. This system also provides the necessary equipment to allow manual-electric control of the pressurizer water level. Alarms are provided for high- and low-water levels. The pressurizer heaters are interlocked with the water level so that the heaters cannot be energized when the level is below a certain minimum. Control of the water level is exercised through the use of the equipment provided for the control of the coolant charging system and the coolant discharge and vent system. The reactor coolant system is automatically protected from excessive pressure by two pop-type spring-operated, pressure actuated relief valves. Indication is provided to show that the pressure relief system has functioned.

B. SUPPORTING SYSTEM ANALYSIS STUDIES

J. Beam, L. Hassell

The system analysis effort during the past quarter was concerned with three major areas, namely:

(1) Pressurizer size

(2) Startup

(3) Relief valves.

1. Pressurizer Size

The pressurizer developed from the studies performed during preliminary design was quite large. During the past quarter efforts were made to reduce both the required water and steam volume.

The pressurizer water volume is the summation of the allowances for normal level control range, maximum negative surge, heaters, heater exposure and the hemispherical bottom head. A decrease in water volume has been effected by using bayonet-type heaters in preference to the direct immersion type which require more space due to connecting flange requirements. Present pressurizer layouts with bayonet heaters show that 2.5 ft^3 of water is needed for heater allowance and that the total water volume is approximately 5.33 ft^3. The heater allowance is based upon installation of 33 heaters, each having a 1-kw capacity. If the required heater capacity for startup is greater, strip heaters will be added to the outside of the pressurizer shell or the water volume will be increased slightly to allow for the installation of additional bayonet heaters.

The pressurizer steam volume resulting from studies performed during preliminary design was based on insurge and outsurge volumes obtained as a result of runs made on the Martin nuclear analog computer. These runs used what is now believed to be a very conservative (by a factor of approximately 2) negative temperature coefficient. No runs have been made based on the present reactor coolant system arrangement and a realistic negative temperature coefficient because of recent changes in reactor coolant subsystem piping arrangement and flow rate. Estimates to be confirmed by additional analog runs were, however, made of the insurge and outsurge volumes anticipated using a more realistic temperature coefficient and final piping arrangements and flow rates. Based on these estimates, a steam volume of approximately 10 ft^3 appears adequate to maintain the system pressure within the desired limits. Therefore, a total pressurizer volume of 15 to 16 ft^3 appears to be required as opposed to the 26 ft^3 previously considered necessary.

2. Startup

In conjunction with the studies made on the reactor coolant subsystem cold startup, two methods of pressurizer cold startup were investigated. The methods, classified as normal startup and solid startup, are described in detail in the following paragraphs. In both studies, the pressurizer initially is filled completely with water at 50 psig.

For purposes of comparing the two schemes, a pressurizer with a 16 ft^3 total volume and a 2-to-1 steam to water volume ratio was chosen. A pressurizer vessel with a 20-inch ID cylindrical midsection and hemispherical ends was taken to fix the overall dimensions and the vessel weight. The calculated value used for the vessel metal weight is 2800 pounds based upon 304 stainless steel material. To calculate heat loss through the insulation, a 2-inch insulation thickness and a still ambient air temperature of 80° F were assumed.

Normal startup is accomplished in the three steps outlined below. For the purpose of this study, the formation of the steam bubble occurs when the water in the pressurizer is a saturated liquid at 50 psig.

(1) Raise pressurizer water and vessel from ambient to 300° F.

(2) Form steam bubble by dumping water until pressurizer water level reaches normal.

(3) Elevate pressurizer water, steam and vessel temperature to normal operating conditions (1300 psia and 577° F).

NOTE: The heat source for all three steps is the pressurizer heaters.

Calculations were made to determine heatup rates and times required to perform the steps above as a function of total installed heater capacity. Results of this study can be seen in Fig. 4.14 and the following tabulation.

	Step 1		Step 2	Step 3		
Total Heater Capacity (kw)	Heatup Rate (°F/hr)	Time (hr)	Time (min)	Heatup Rate (°F/hr)	Time (hr)	Total Time (hr)
15	38	6.1	1.7	60	4.6	10.7
20	51	4.5	1.3	81	3.4	7.9
30	77	3	0.9	123	2.2	5.2
39	100	2.3	0.7	162	1.7	4.0

Analysis of these results shows that to bring the reactor coolant subsystem and the pressurizer up to normal operating conditions at the prescribed rate of 100° F per hour, a 39-kw heater capacity is required.

In an attempt to reduce the heater capacity and time required for startup, a startup procedure using a solid-water pressurizer was investigated. This procedure is as follows:

(1) Heat up reactor coolant subsystem at the rate of 100° F per hour and simultaneously circulate through the pressurizer using the spray equipment.

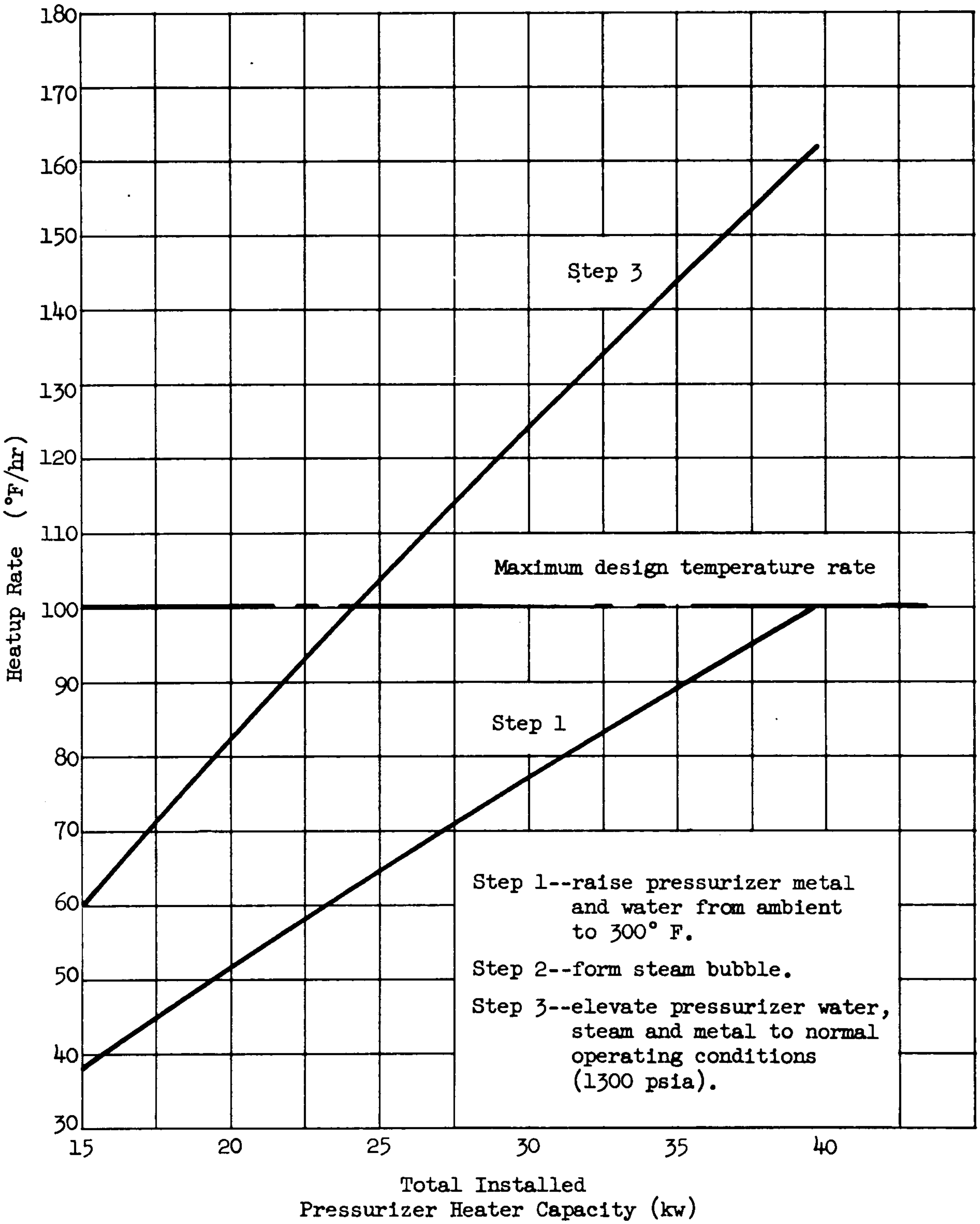

Fig. 4.14. Pressurizer Heatup Rate Versus Installed Heater Capacity (cold startup)

(2) At some reactor coolant subsystem mean temperature equal to or less than the normal operating temperature, stop the circulation through the pressurizer and cease the increase of temperature in the reactor coolant subsystem.

(3) Heat the pressurizer to 100° F above the reactor coolant subsystem temperature by use of the pressurizer heaters.

(4) Form steam bubble.

The analysis was performed by writing a differential equation describing a transient heat balance of the pressurizer. This equation was solved in terms of the average temperature of the pressurizer, the flow rate through the spray equipment, the rate of increase of temperature in the reactor coolant subsystem, and the pressurizer heater capacity. The result for the case of no pressurizer heaters is shown in Fig. 4.15 for various flow rates through the pressurizer. This figure shows that for a moderate flow rate of 4 gpm, the temperature in the pressurizer lags the temperature of the reactor coolant subsystem by only 1/2 hour.

It should be pointed out that the full advantage of this method is only realized when the temperature increase of the reactor coolant subsystem is severely limited by the heater capacity of the pressurizer. This is not the case in the PM-1 power plant since the 100° F per hour rate of temperature increase is also established by thermal stress considerations. The time saved in bringing the subsystem to normal operating temperature using a solid rather than normal pressurizer startup procedure is only one hour for the PM-1 power plant.

The use of a solid-water pressurizer has the very serious drawback of rapid rate of increase of system pressure. If the reactor coolant subsystem is heated at a rate of 100° F per hour, the system pressure increases at a rate of 1.1 psia/sec, if no liquid is discharged from the system. However, discharge of only 0.36 ft^3 of water at 1500 psia reduces the system pressure to atmospheric. Therefore, pressure control of such a system would be quite difficult.

Considering the control difficulties involved with the solid startup procedure, and the fact that only a time saving of one hour would result from this method, it has been decided to use the normal startup procedure described above.

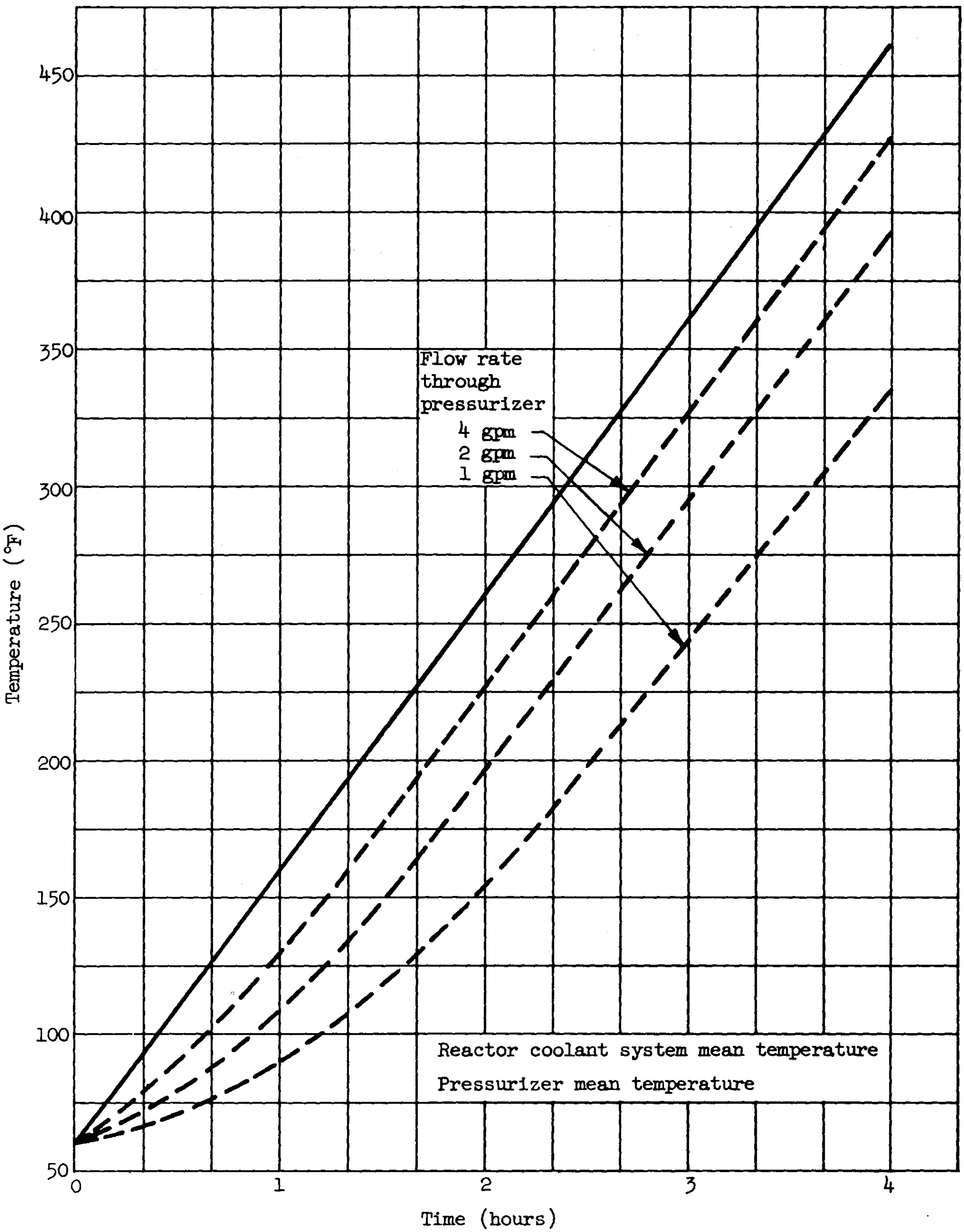

Fig. 4.15. Solid Water Pressurizer Startup--Pressurizer Heater Capacity = 0 kw

3. Relief Valves

Under the subsystem breakdown used in the final design phase, only the pressurizer safety valve assemblies and their associated piping are included in the pressure relief subsystem. Equipment downstream of the safety valve assemblies is included in the coolant discharge and vent subsystem.

During the past quarter, the reactor coolant subsystem was simulated on the analog computer and various transient maneuvers were executed to determine the most severe primary loop expansion. This was found to be a step function closing of the steam generator steam valve with initial reactor power of 100% (9.37 megawatts), no control rod movement, primary pump off instantaneously with steam valve closing (primary coolant flow of 3% resulting from natural convection is assumed). The value of the reactor negative temperature coefficient is taken as $-1.3 \times 10^{-4} \delta$ k/°F. The analog traces are reproduced in Fig. 4.16.

The energy input to the pressurizer is that of the primary coolant insurge and the pressurizer electrical heaters. The probability of the heaters being on during the transient is remote but the possibility must not be overlooked. The energy received by the pressurizer as a function of time is shown in Fig. 4.17.

During the first ten seconds of the transient, the energy flow rate is at a maximum with magnitude of approximately 1660 Btu/sec.

At the initiation of the transient, the steam in the pressurizer steam dome is saturated at 1300 psia; it is conservatively assumed that steam is isentropically compressed to the safety valve set point of 1500 psia, at which time the valve opens and relieves the pressure. The valve is sized to relieve at the maximum rate of heat supply, the theoretical nozzle area is approximately 0.08 in.^{2}.

The ASME Code for Unfired Pressure Vessels, Section VIII, Special Ruling No. 1271N for pressurized water nuclear reactors requires a minimum of two safety valves on the pressure system; these will be provided.

C. DESIGN STUDIES

During the third quarter, completion of the preliminary design of the pressurizer vessel and determination of heater and relief valve requirements was scheduled. During the next quarter, completion of design and preparation of the specifications and drawings prior to submittal for AEC approval is anticipated, and bids will be solicited.

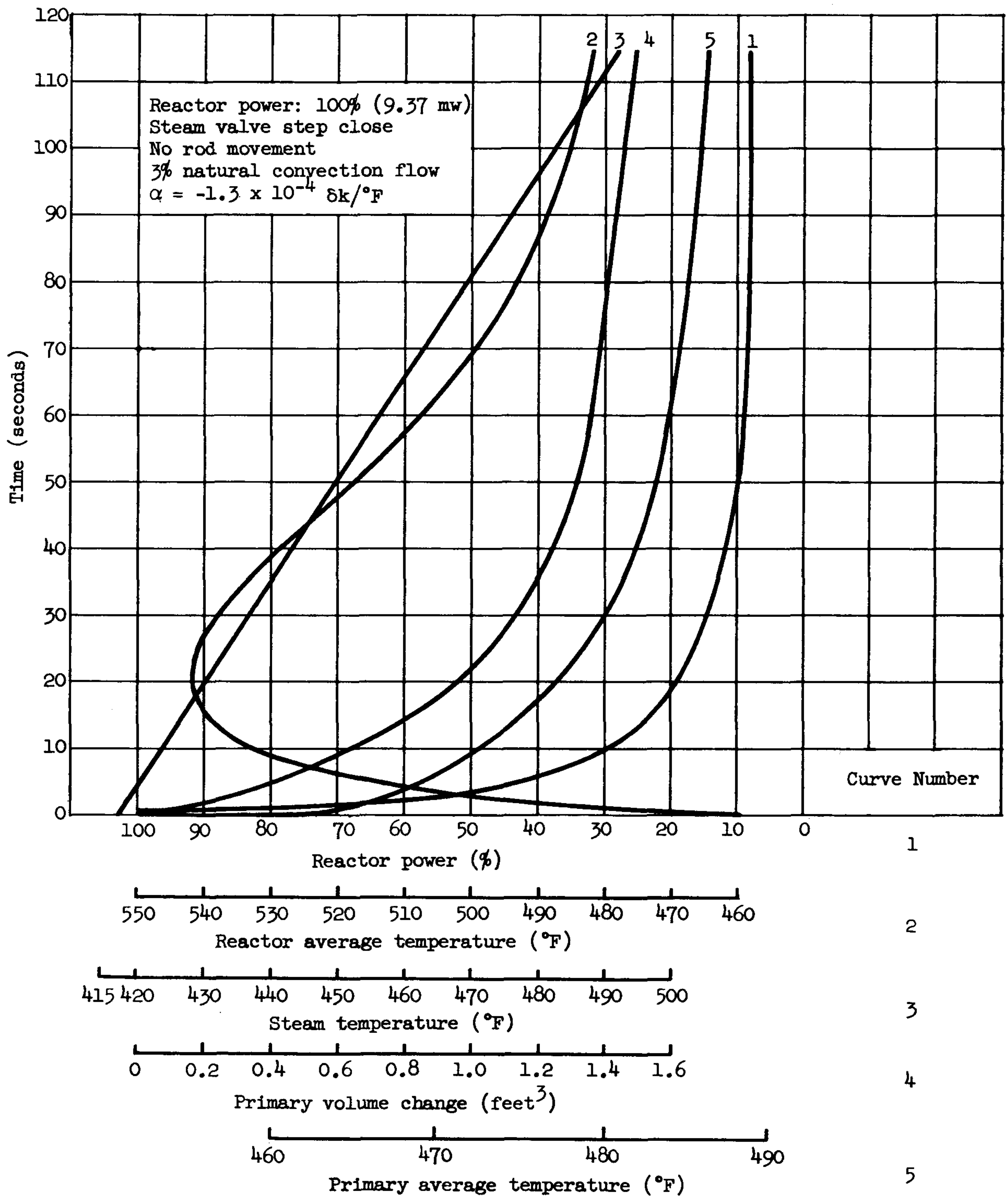

Fig. 4.16. PM-1 Primary Loop--Transient Maneuver

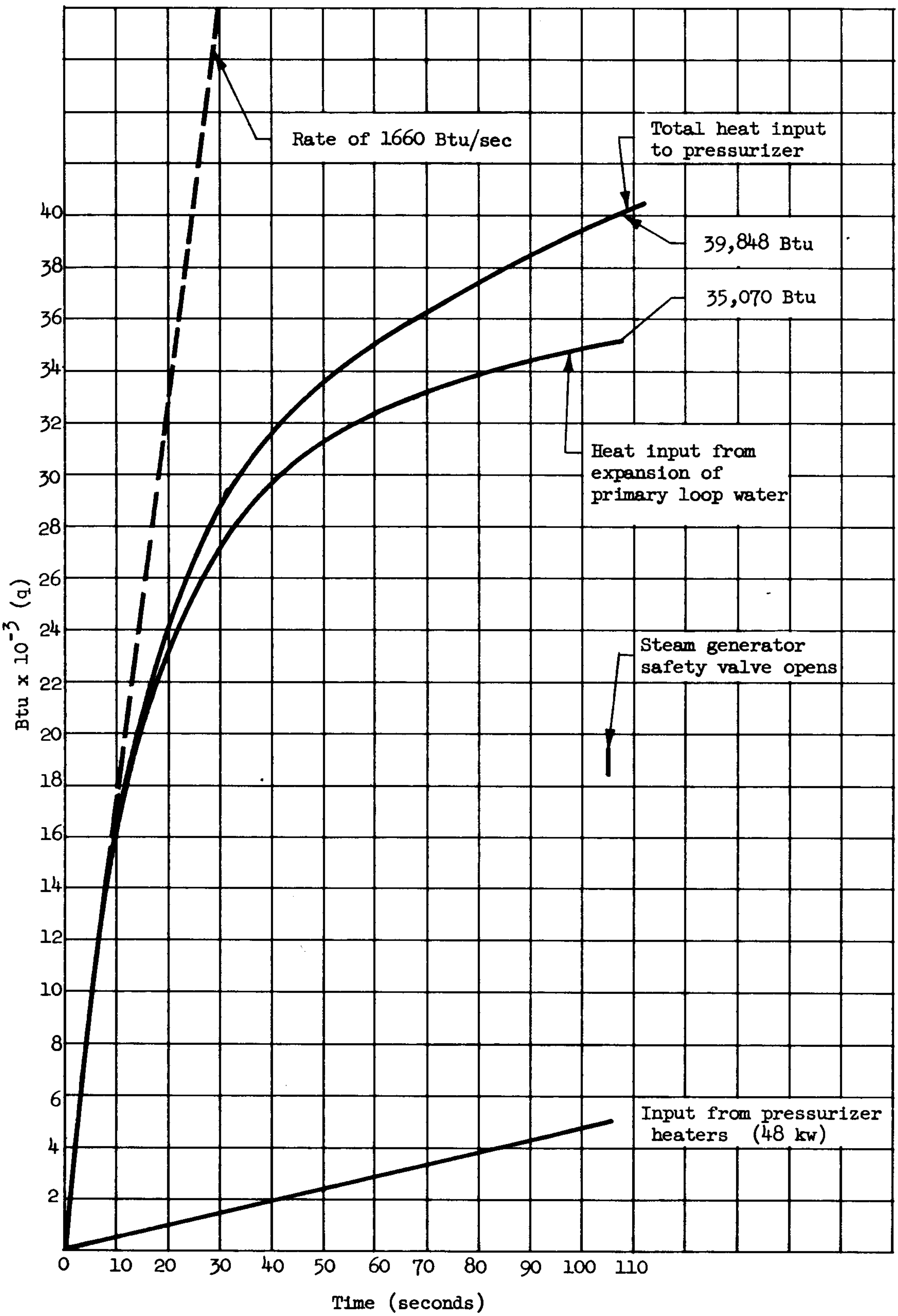

Fig. 4.17. Energy Received by Pressurizer as a Function of Time

Preliminary design of the pressurizer vessel has been completed. Configuration, material, wall thickness, weight, and insulation requirements of the vessel have been determined. Handling and installation provisions for the vessel have been established and the preliminary assembly drawing was completed.

As was mentioned previously, bayonet-type heaters are being considered for use in the pressurizer since, in addition to space considerations, maintenance is simplified and the possibility of plating out of the heater refractory material on the core is greatly reduced in that a double wall failure would have to occur.

Heater layout studies have been made to obtain the configuration which will give the best heat transfer characteristics and allow easiest heater maintenance.

SUBSYSTEM 8--COOLANT CHARGING SUBSYSTEM

R. Baer

The coolant charging system includes both the equipment necessary for high pressure charging into the reactor coolant subsystem and low pressure filling of either the reactor coolant or shield water subsystems.

High pressure charging. In the preliminary design, the charging pump suction was at the shield water pump discharge. Since the shield water will be saturated with dissolved oxygen at 125° F, it was decided to use water with the lowest possible oxygen content as the makeup supply for the reactor coolant subsystem. The boiler feed pump discharge at the steam generator was selected as the main supply of makeup water. Since the oxygen content of the secondary water is chemically controlled, it will not exceed 0.005 cc/liter. The charging pumps discharge to the coolant purification subsystem where the primary circulating pump forces the makeup flow through the economizer, demineralizer cooler, the high pressure demineralizer and the economizer before it enters the reactor coolant subsystem. At the high pressure demineralizer, chemicals added to the secondary water are removed, thus ensuring a water quality of 0.5 ppm total dissolved solids and 0.005 cc/liter of dissolved oxygen. In the event that the boiler feed pump is off the line or the coolant purification subsystem is shut down, the charging pumps will take a suction at the shield water pump discharge.

The charging pumps charge at a rate of 1 gpm (each) at a maximum head of 1500 psi. The maximum makeup water requirement is 425 lb/hr during the initial start of the reactor coolant system cool down at a rate of 100° F per hour. This is equivalent to 1.11 gpm at 460° F.

No design effort was scheduled on this subsystem during the past quarter. During the fourth quarter the subsystem design will be accomplished, a specification will be prepared and submitted for approval and bids will be solicited on components.

A. COOLANT CHARGING CONTROL SYSTEM (FIG. 4.18)

R. Wilder

This system provides the necessary equipment and instrumentation for the control and protection of the coolant charging system. The coolant charging system is composed of two positive-displacement, high-head, low-flow charging pumps, pressure instrumentation, control and relief valves and connecting piping. Each charging pump has in its discharge line a normally closed automatic-electric controlled on-off valve, a pressure instrument set and a pressure relief valve. The discharge valve is automatically opened when the charging pump is energized. The pressure instrument set is used for indication purposes only. The pressure relief valve provides protection for the system in the event that the discharge valve fails to open when the pump is started.

The pumps take suction from a common inlet header which contains an automatic, electrically controlled, two-way valve. The two-way valve is normally positioned such that the pump suction is taken from the boiler feed pump discharge line. The two-way valve control is interlocked with the coolant purification system inlet isolation valve such that when the isolation valve is closed, the two-way valve changes the charging pump suction to the shield water pump discharge header. Manual-electric control of the two-way valve is also provided. The valve position is visibly indicated when the charging pump suction is taken from the shield water pump discharge header. Visible indication of charging system operation is provided.

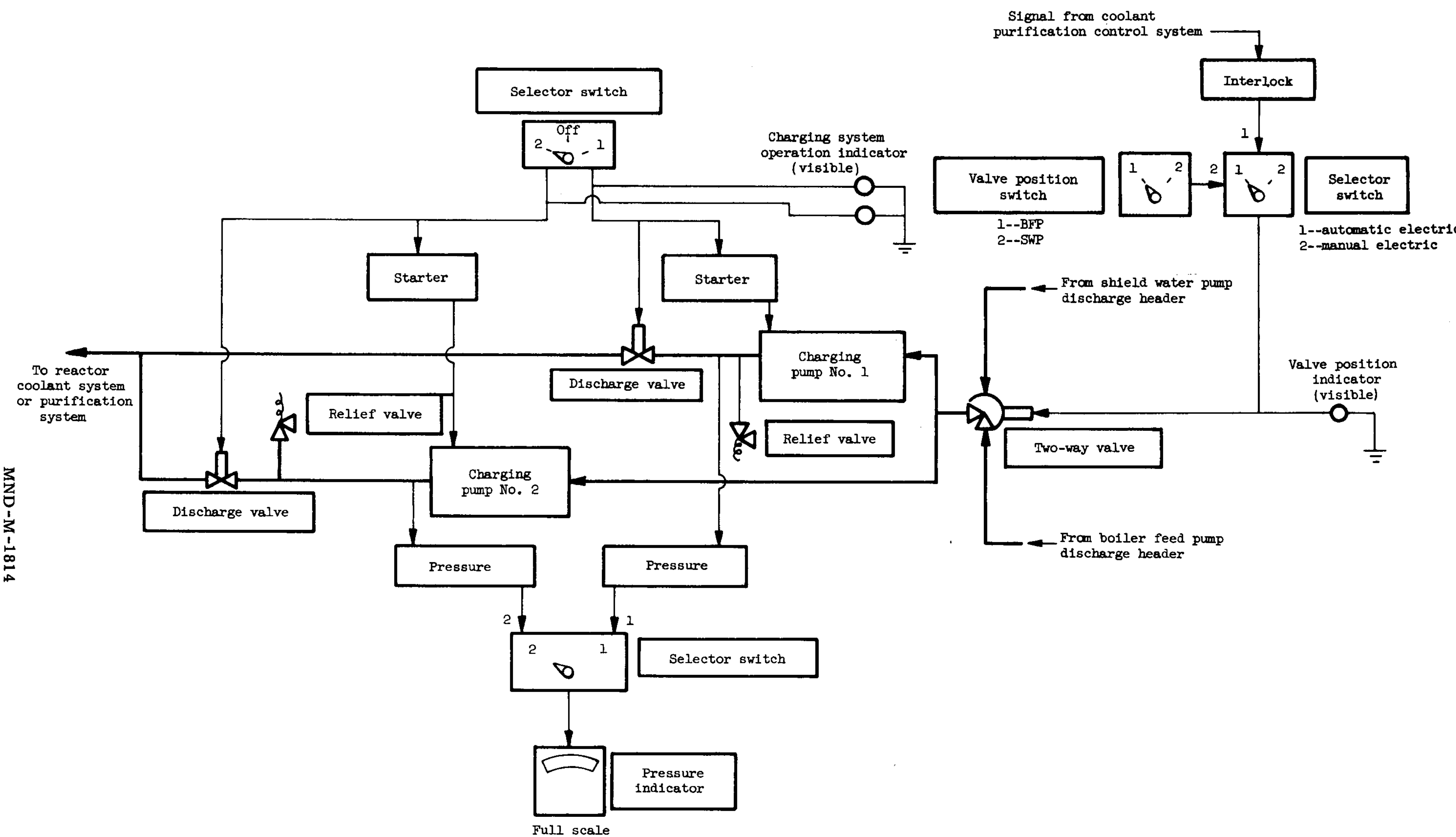

Fig. 4.18. Coolant Charging Control System

SUBSYSTEM 9--COOLANT DISCHARGE AND VENT SUBSYSTEM

R. Moore

This subsystem includes the components between the pressurizer relief valves and the radioactive waste disposal subsystem; also included are the pressurizer gas removal equipment, the expansion tank gas charging equipment, the liquid line from the pressurizer leg to the expansion tank, the primary coolant drain line, and vents from the reactor coolant and waste disposal subsystem. The subsystem is shown schematically in Fig. 4.19.

Effort during the past quarter was centered on the handling of radioactive gases and a more definite appraisal of the subsystem requirements than was made in the preliminary design phase. A detailed study of the components and their operation was initiated.

During the next quarter the subsystem design will be completed, specifications will be prepared and submitted for approval and bids will be solicited.

Radioactive gases. The analyses performed concerning radioactive gases were made on the basis of a maximum release of 0.1% of the total radioactive gases in a period of 24 hours. This is felt to be a conservative estimate of the maximum possible rate of fuel element disintegration. To avoid the use of the very low maximum permissible concentration imposed by the presence of iodine, the gases are first passed through iodine removal equipment, consisting of a heater to condition the gases followed by a 2-inch diameter by 10-inch long silver nitrate reactor. The reactor is packed with 1/4-inch Berl saddles impregnated with silver nitrate. Passage through the iodine removal system results in a decontamination factor of better than 10^3 and permits direct controlled venting of the off-gas system through the air blast coolers. Calculations were made which indicate that the remaining fission gases can be released to the air discharge side of the air blast coolers under the following conditions:

(1) The gases are released over a period of not less than 24 hours.

(2) Gases are released at a minimum height of 10 meters into a 15-mph wind.

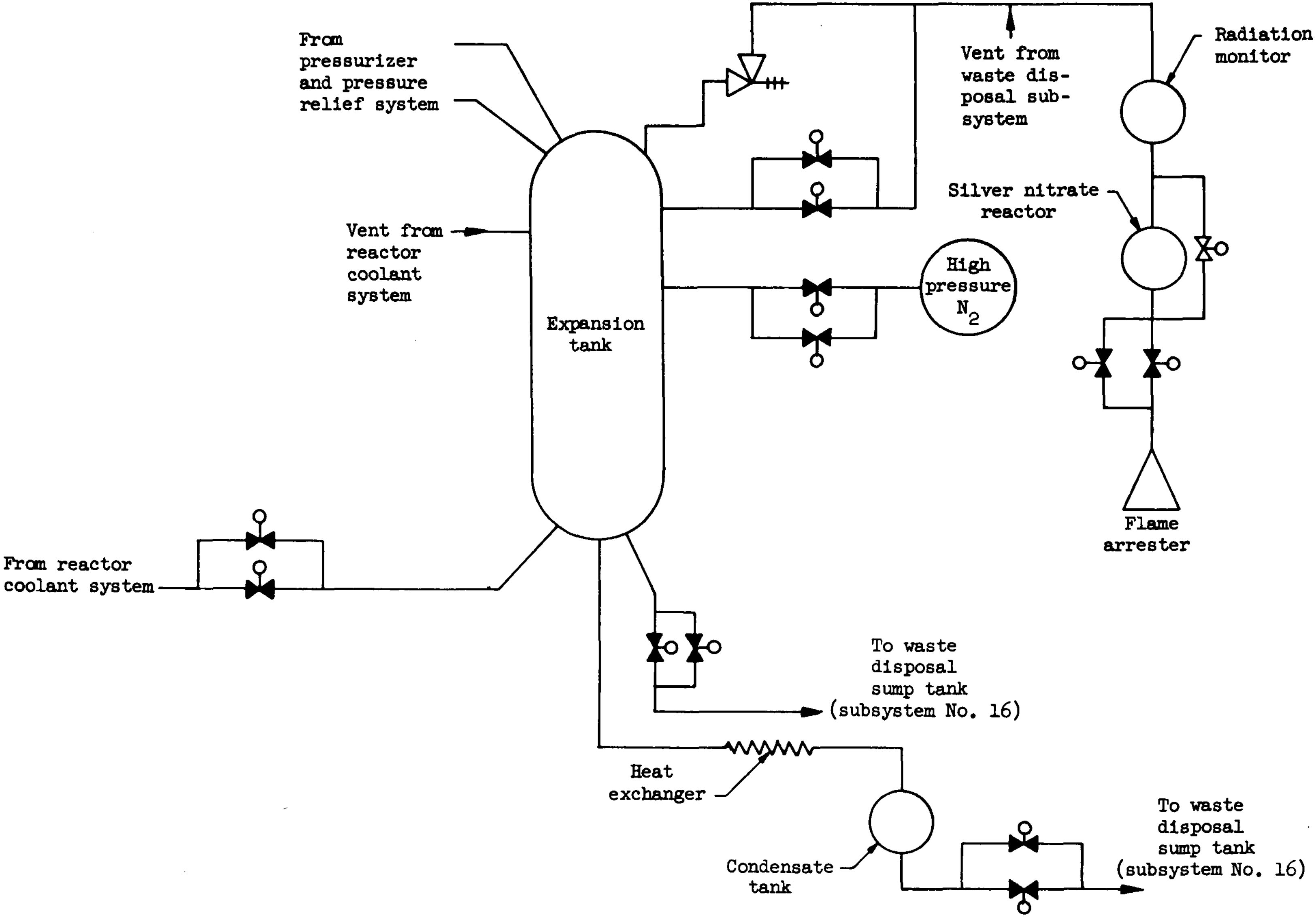

Fig. 4.19. Coolant Discharge and Vent System

Components and operation. The pressurizer is equipped with a pilot operated valve which may be used to transfer gases (hydrogen or radioactive gases resulting from a fuel tube rupture) to the expansion tank where a low pressure (approximately 5 psig) nitrogen environment is maintained. Upon receiving the gas in the expansion tank, the plant operator may open the expansion tank gas vent line which passes the gases to the gas disposal system where they are monitored. If the gases are radioactive, they are passed through the silver nitrate reactor where the iodine is removed and then they are diffused through a flame arrester into the discharge air stream from the air blast shield water coolers. If the gases are not radioactive, they are diffused through a flame arrester into the discharge air stream from the air blast shield water coolers. The expansion tank is purged by allowing continuous nitrogen flow during the venting process.

Between the pressurizer liquid leg and the expansion tank there is a line containing a remotely operated valve which is opened to bleed water from the primary loop (required when the loop is brougnt from ambient to operating temperature).

The expansion tank also receives the steam discharged from the pressurizer safety valves in the event of an overpressure in that system. The expansion tank will be adequately sized to expand the discharge from the pressurizer from its initial state of 1500 psia to 500 psia. Once in the expansion tank, the steam will flow to the heat exchanger which is a vertical tubular surface exchanger submerged in the shield water. The temperature of the steam at 500 psia is 467° F, while the shield water, which is at atmospheric pressure, is at 125° F. From these boundary conditions, the heat exchanger will condense the steam on the inside of the tubes and boil the shield water on the outside surface; these processes yield a rapid transfer of heat. The condensate is drained by gravity from the tubes to a small collecting header and when the pressure has decayed to approximately 5 psig, the operator may open the drain valves on both the collecting header and expansion tank which drains the condensate to the waste disposal sump tank. The size of the expansion tank and heat exchanger are dependent upon the size of the pressurizer and, since efforts are underway to reduce the size of that vessel, the size of the expansion tank and heat exchanger is subject to change. The maximum size of the tank is predicted to be 6-1/2 ft^3; the heat exchanger will furnish approximately 10 ft^2 of transfer area.

SUBSYSTEM 10--COOLANT PURIFICATION SUBSYSTEM

R. M. Wolfe

The coolant purification subsystem includes the demineralizers, heat exchangers, valves, fittings, piping, control and instrumentation required to maintain the purity of the coolant in the reactor coolant subsystem at the levels specified in the preliminary design.

The principal efforts of the past quarter concerned the establishment of the flow diagram, determination of demineralizer type, establishment of a sampling arrangement and liaison with vendors.

During the next quarter, a subsystem description will be prepared, the floor diagram will be reviewed, specifications will be prepared for the components and submitted for approval, and bids will be solicited.

Flow diagram (Fig. 4.20). Water from the reactor coolant subsystem is recirculated at a rate of 1000 lb/hr to the coolant purification subsystem. The recirculated coolant leaves the reactor coolant subsystem at 446.7° F from the primary circulating pump discharge and re-enters the subsystem at 370.3° F at the primary circulating pump suction. The pumping head of the primary circulating pump is utilized to pump the recirculation flow through the coolant purification subsystem. Leaving the reactor coolant subsystem, the recirculated flow passes through the economizer and demineralizer cooler which reduces the temperature to 120° F before entering the high pressure demineralizer. On leaving the high pressure demineralizer, the recirculated flow passes through the shell side of the economizer where the temperature is increased to 370.3° F before re-entering the reactor coolant subsystem.

A calibrated flow valve ahead of the high pressure demineralizer is set to allow a flow rate of 1000 lb/hr (2 gpm at 120° F). A temperature alarm after the demineralizer cooler is set for 135° F is provided to ensure protection of the demineralizer resin from high temperature water. In the event of loss of shield water flow (coolant for the demineralizer cooler) the coolant purification subsystem is automatically isolated by the closing of the solenoid valve ahead of the high pressure demineralizer.

Demineralizers. During the past quarter it became evident that the use of a cartridge-type demineralizer involved more complex handling equipment and larger shipping casks than was anticipated. Accordingly, the tentative decision reached during preliminary design to use a cartridge-type demineralizer was re-evaluated.

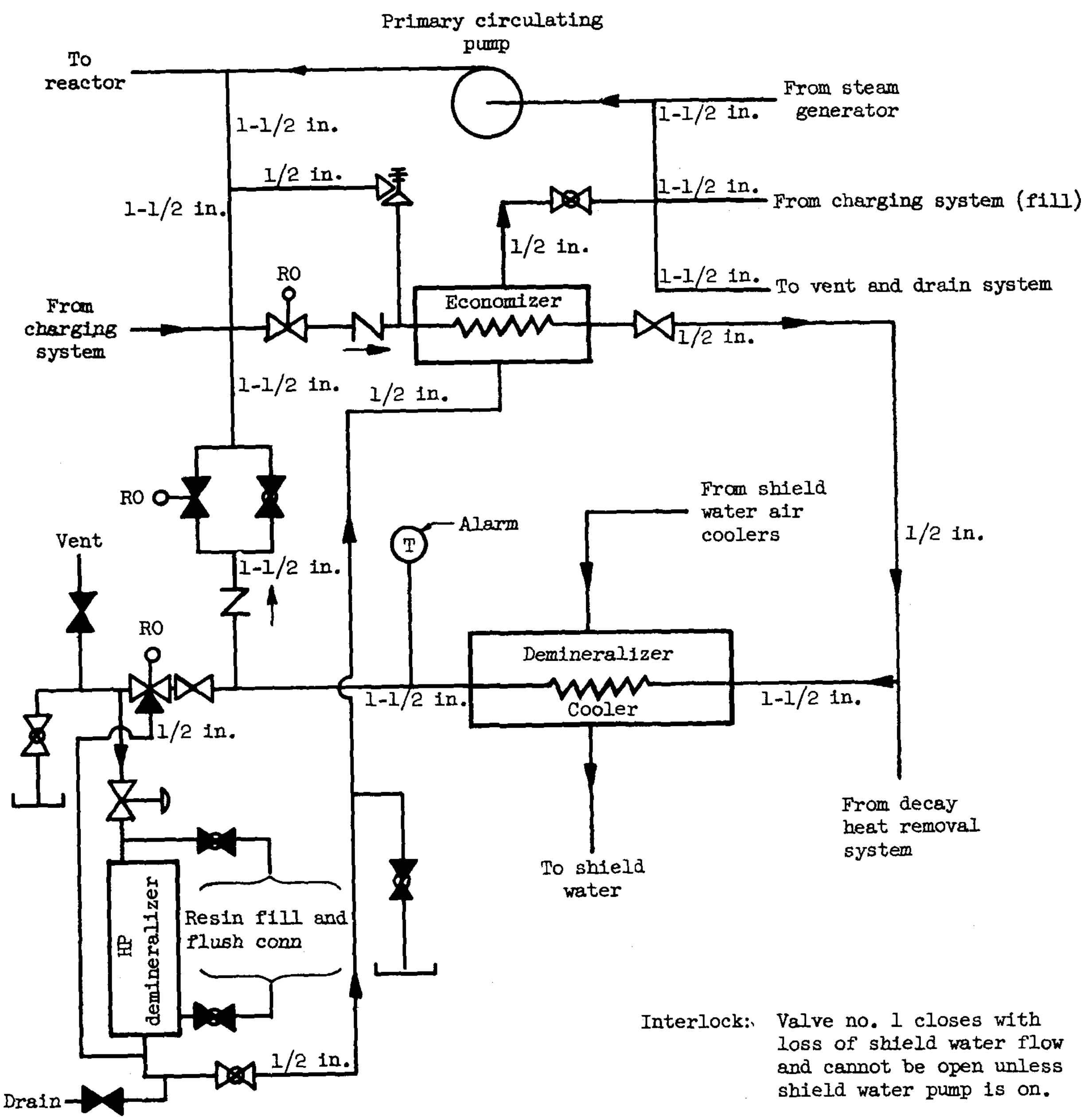

Fig. 4.20. Coolant Purification System

The use of a regenerative-type demineralizer was reconsidered and again found impractical for the reasons stated in the Preliminary Design Technical Report. The throw-away type also was reconsidered and found to offer only marginal improvement at a considerable additional cost.

Three demineralizer vendors were contacted and the problem presented to them. Representatives of all three companies agreed that, considering the small amount of resin involved and the difficulties of handling either spent cartridges or the throw-away type of demineralizer, a flush-type demineralizer was best suited for the plant. In this type of demineralizer two additional connections are provided: one to permit a back flow to loosen the resin bed, and the other to permit flushing the resin bed out of the demineralizer.

The demineralizer can be refilled with a fresh charge without separation of the cation and anion resins by using an additional small tank to mix the resins and a gravity feed. The resin is mixed in the tank and enough water is added first to fluidize the resin. Then either of two methods may be used. The first requires draining the water from the demineralizer and associated piping. A valve under the mixing tank is opened, and the resin flows by gravity into the demineralizer. In the second method, the demineralizer and piping is not drained. The valves at the outlet of the demineralizer and at the bottom of the mixing tank are opened simultaneously. As the resin flows by gravity to the demineralizer, additional water is added to the mixing tank to prevent separation of the resins.

The flush-type demineralizer will be used both for the low and high pressure systems.

Coolant sampling. In order to monitor the condition of the water in the shield water and reactor coolant subsystems and to check on the effectiveness of the demineralizers, water sampling points are provided. Sample locations are as follows:

(1) High pressure demineralizer influent. Provides means for checking condition of reactor water and also assists in determining demineralizer performance.

(2) High pressure demineralizer effluent. Provides a check on demineralizer performance.

(3) Low pressure demineralizer influent. Provides means for checking condition of shield water and assists in determining demineralizer performance.

(4) Low pressure demineralizer effluent. Provides a check on demineralizer performance.

(5) Reactor coolant subsystem hot leg. Provides a check on reactor water condition. The principal purpose of this location is to check conditions during reactor coolant subsystem cold startup after addition of fill water.

Samples extracted at locations (1), (2), (3) and (4) are at 120° F and require no further cooling. A sample extracted at location (5) may be at a temperature of 480° F and must be cooled. Samples will be extracted periodically and will be checked by chemical analysis for pH, hydrogen and oxygen. To measure the dissolved solids in the water, continuous reading conductivity cells are provided at locations (1), (2), (3) and (4). To minimize the amount of sample water not returned to the reactor coolant subsystem, in-line cells are planned at all four locations.

SUBSYSTEM 11--COOLANT CHEMICAL ADDITION SUBSYSTEM (Fig. 4.21)

R. M. Wolfe

The coolant chemical addition subsystem consists of pumps, tanks, valves, fittings, controls and instrumentation required for the injection into the reactor coolant subsystem of chemicals for either startup control, operational control or shutdown control of the coolant. Emergency injection equipment for the injection of poison into the reactor in case of malfunction of the reactor rod control subsystem is also provided.

During the third quarter, review of subsystem requirements was initiated and a preliminary flow diagram was prepared.

During the next quarter, a study of the coolant chemical addition subsystem will be made, a final flow diagram will be prepared, a subsystem description will be prepared, specifications for the components will be written and submitted for approval, vendor contacts will be made and bids will be solicited.

SUBSYSTEM 12--DECAY HEAT REMOVAL SUBSYSTEM

T. J. Vild

The decay heat removal system consists of an auxiliary cooling pump, air auxiliary cooler (the same cooler used to cool the primary water entering the high pressure demineralizer) and the piping and valving necessary for component interconnection.

The effort during the past quarter was concerned with two major areas, namely, the method of cooling the reactor coolant subsystem after shutdown and the equipment required to maintain a sufficiently low temperature so as to permit maintenance of the subsystem.

Cool-down. The reactor coolant subsystem will be cooled to a temperature of 170° F prior to drainage for maintenance and/or repair. Normally, the reactor coolant subsystem will be cooled by generating steam in the steam generator and condensing this steam in the steam-to-air condenser. Since the time required for cool-down is important, a maximum cool-down rate of 100° F per hour will be employed--the limit presently imposed by thermal stress considerations. This high cooling rate, coupled with the pumping power and core afterheat, results in a heat load which is beyond the capacity of the shield water air coolers. When the loop mean temperature is 170° F, the total heat load is 415 kilowatts.

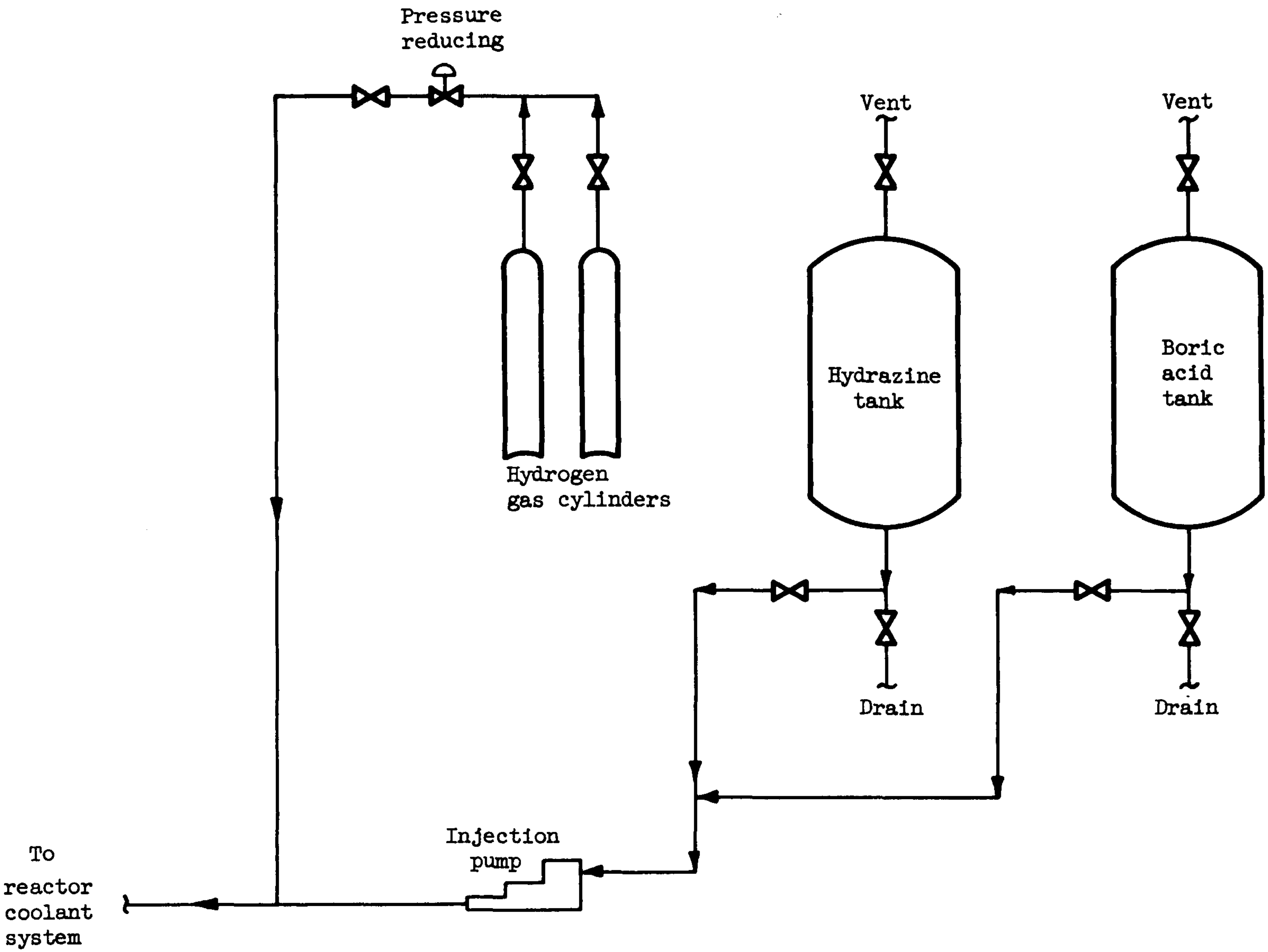

Fig. 4.21. Coolant Chemical Addition System

The cool-down procedure will be:

(1) The primary circulating pump will remain on so that a uniform temperature in the primary loop and a high heat transfer coefficient on the primary side of the steam generator may be obtained.

(2) The primary coolant will be cooled at a maximum rate of 100° F per hour.

(3) The steam flows from the steam generator to the steam-to-air condenser through the 6-inch main steam header.

(4) Air is continuously removed from the condenser such that the partial air pressure does not interfere with the condensing coefficient or create a back pressure which will prevent the necessary steam flow.

(5) One fan is used in the steam-to-air condenser.

In the event of an electrical fault, the primary circulating pump and electrically driven boiler feed pump cannot be employed. Mass transport from the reactor core to the steam generator will be accomplished by natural convection (since sufficient level difference has been provided), and the steam generator makeup water will be pumped by the steam-driven boiler feed pump. The loop mean temperature can be maintained by this method.

In the event of a rupture of the main steam line downstream of the main stop valve, steam from the steam generator cannot be sent to the steam-to-air condenser and condensed. The steam is vented to the atmosphere to remove afterheat. This water will be replaced by use of the electrically-driven boiler feed pump.

Equipment. The decay heat removal system is designed to remove 85 kilowatts (reactor core afterheat three hours after shutdown) with the reactor coolant system at a mean temperature of 170° F. This system employs a canned rotor centrifugal pump which takes suction from the reactor outlet in the steam generator package and discharges the coolant at a rate of 20 gpm through the tube side of the demineralizer cooler back into the reactor coolant system at the reactor inlet in the steam generator package. This system is not intended to cool down the reactor coolant system. However, as the amount of core afterheat decreases, the reactor coolant mean temperature will decrease below 170° F. Also, this system can reduce the mean temperature of the reactor coolant system three hours after shutdown from 240° F to 195° F in two hours or to 182° F in three hours. The earliest that this system can be turned on to aid in the cool-down of the reactor coolant system (should this prove desirable) is presently under study. The inherent problem of nucleate boiling on the shell side prevents the use of a high coolant temperature in the tubes of the cooler.

Normally, the decay heat removal system is employed to hold the reactor coolant mean temperature below 170° F while the loop can be opened for repair or maintenance work on the steam generator and/or primary circulating pump. This maintenance work requires that the reactor coolant system be partially drained; therefore, the reactor coolant piping is designed to ensure a flooded line at the pump suction and discharge after the loop has been drained from a point between the pump and the steam generator. Also, since the loop will be at atmospheric pressure after draining, the decay heat removal pump is designed for a low NPSH (approximately 13 feet).

<u>Decay heat removal control system (Fig. 4.22)--R. Wilder.</u> This system provides the necessary equipment and instrumentation for efficient and reliable control of the decay heat removal system. The system consists of a high pressure, centrifugal, canned rotor pump, valves and piping. The pump has in its discharge line two, normally closed, manual-electric solenoid valves which are energized simultaneously with the pump through the pump and valve control switch. This ensures that the line is open when the pump is running. Energizing of the valves is interlocked in such a fashion that both the purification system inlet and outlet isolation valves are closed and the primary loop temperature is below 250° F before they can be activated. This ensures that:

(1) The coolant does not circulate through the demineralizer.

(2) High temperature coolant does not cause boiling in the demineralizer cooler.

SUBSYSTEM 13--SHIELD WATER SUBSYSTEM (FIG. 4.23)

T. J. Vild

The shield water subsystem consists of two shield water pumps, four parallel air blast coolers, a low pressure demineralizer and interconnecting piping and valves.

During the past quarter, the analyses performed in support of preliminary design were refined (with all parameters being established), the demineralizer previously specified was discarded and another se-

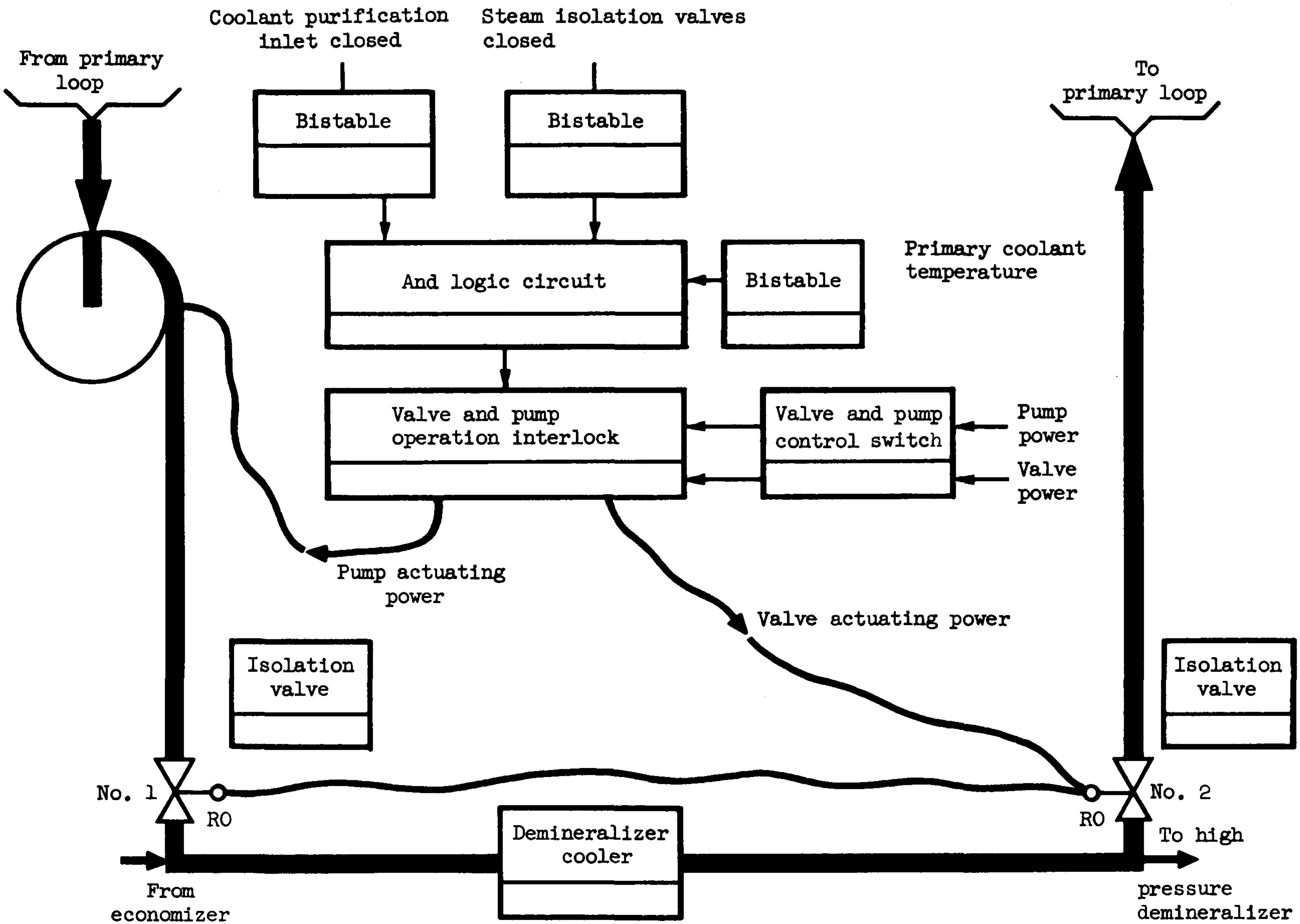

Fig. 4.22. Decay Heat Removal Control System

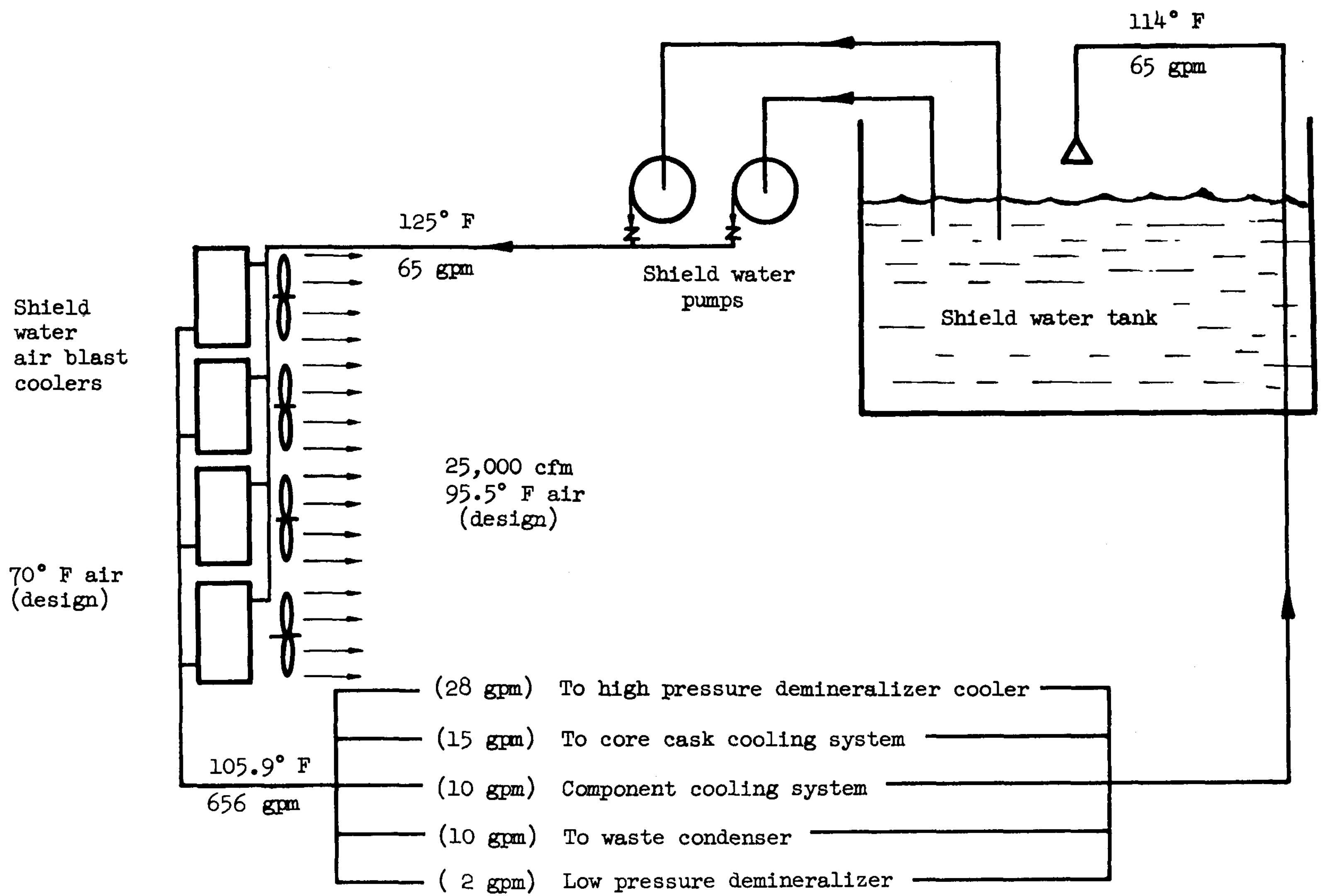

Fig. 4.23. Shield Water Subsystem

lected (see the section concerning the coolant purification subsystem), subsystem design was completed and draft specifications and a flow diagram were prepared. Specifications will be submitted for approval during the next quarter and bids will be solicited.

The preliminary design contemplated the presence of 170° F shield water and 100° F cooling air. Since 170° F water would make it necessary to insulate the demineralizers and to assure continuous flow to cool them, it was decided that the design temperature of the water should be limited to 140° F with a normal operating temperature of 125° F. The danger of melting the demineralizer resin is greatly reduced thereby. It was found that the maximum anticipated air temperature will be 85° F.

A study based on the following parameters revealed that design should be based on a 17° F to 20° F water ΔT, a maximum number of water tubes and minimum air flow velocity:

(1) Heat load . . . . 325 kwt (75 kwt above preliminary design load primarily due to waste condenser requirements)

(2) Air inlet . . . . 85° F

(3) Water inlet . . . . 125° F

Further analysis refinement lead to lowering the design heat load from 325 kwt to 180 kwt. The reduction stemmed from re-evaluation of the gamma heating of the shield water (76 kwt rather than 170 kwt) and the decision to perform waste disposal operations either during plant shutdown or when the ambient air temperature is low.

The following design parameters were evolved:

(1) Maximum shield water temperature for continued plant operation . . . . 140° F

(2) Maximum water exit temperature . . . . . . 120° F

(3) Maximum expected air temperature . . . . 85° F

(4) Maximum time that air temperature exceeds 80° F . . . . 6 hours

(5) Maximum time that air temperature exceeds 70° F . . . . 12 hours

Based upon these parameters and heat generation of 180 kwt, the water flow requirement becomes 65 gpm and shield water temperature does not exceed 125° F with design air temperature 70° F or less.

Four identical parallel air blast coolers will be mounted with a total heat capacity of 615,000 Btu/hr. Fans will draw 25,000 cfm of air through ducts and control dampers over cooling coils and will exhaust it to the outside of the primary building.

The subsystem is capable of operating with three units if the outside air temperature does not exceed 70° F.

If the outside air temperature drops below 70° F, dampers in the air stream close partially, thereby preventing too much heat from being dissipated.

If the outside temperature should rise to 85° F for an extended period of time, the shield water temperature would rise to 140° F from the normal 125° F.

Consideration was given to recirculating the air in the primary building in order to use the rejected heat for space heating--the high air velocities that would be created in the building made this scheme unfeasible.

Two 65-gpm centrifugal, vertical, deep well pumps will be provided. The pumps will operate at atmospheric pressure against a head of 100 feet. Although the pumps will be parallel, only one will operate at a time. The backup pump will add to the reliability of the system.

SUBSYSTEM 14--REACTOR PLANT HEATING AND COOLING SYSTEM

J. Todd

The reactor plant heating and cooling system consists of all equipment necessary to maintain the temperature of the refueling reactor and steam generator packages at design values regardless of internal or external environmental conditions. The equipment required may include heating coils, ventilating fans, duct work, etc., and is independent of the heating and cooling system equipment for the Primary Building.

The objectives for this subsystem concerned only the steam generator package during the third quarter. The reactor package and refueling package shield water heating system will be covered in the next quarter. During this time, if it is established that there is a requirement for heaters within the shield water, heater loads and sizing of the equipment will be determined. Specifications for all heating and ventilating equipment in the two packages will also be formulated during the next quarter. Vendor contacts will be established.

The steam generator package ventilating system has been tentatively selected and is shown in Fig. 4.24. The system is composed of an axial blower fan rated at approximately 650 cfm. By means of proper ducting, the fan intake receives air from the open area under the floor of the Primary Building. The fan moves air down a circular duct to approximately two feet above the package floor; at this point, the flow divides and goes into two rectangular outlets, located 180 degrees apart, around the steam generator package wall. The chosen flow rate of inlet air at 85° max. will maintain the package temperature at approximately 125° F during operation. Preliminary calculations to determine ambient temperature are based on the maximum release of heat from equipment during plant operation (i.e., 26,062 Btu/hr to the tank environment), and assumes no heat loss through the package wall to the 47° F backfill around the package.

Upon shutdown, this ventilating system will be used to make maintenance possible in the steam generator package.

SUBSYSTEM 15--FUEL CASK FUEL COOLING SYSTEM

R. Manoll

The fuel cask fuel cooling system consists of casks required to store and transport a spent core, the equipment necessary to handle and store these casks for various periods of time and the necessary cooling system.

The objectives during this quarter were to establish outline dimensions and weight limitations on the cask due to heat removal limitations and to establish surface radiation levels for various lead thicknesses at several time increments.

The outline dimensions of the cask established during the quarter are shown in Fig. 4.25 and the aircraft loadings during shipping in Fig. 4.26. The plot of required lead thickness versus surface dose rates and cask weights for various storage times is shown in Fig. 4.27

During the next quarter, final dimensional requirements will be established and specifications and drawings prepared for the subsystem components.

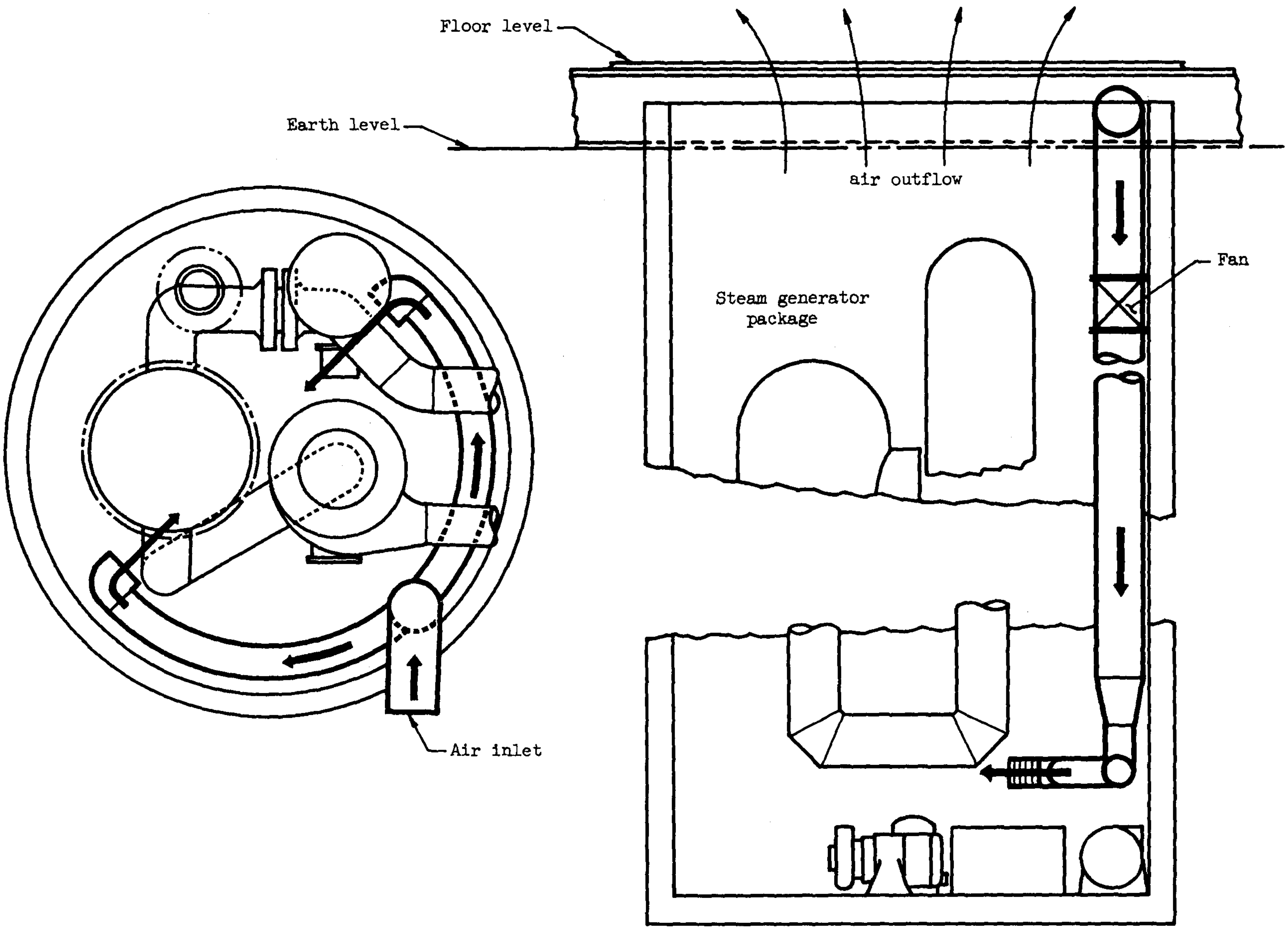

Fig. 4.24. Steam Generator Package Ventilation System

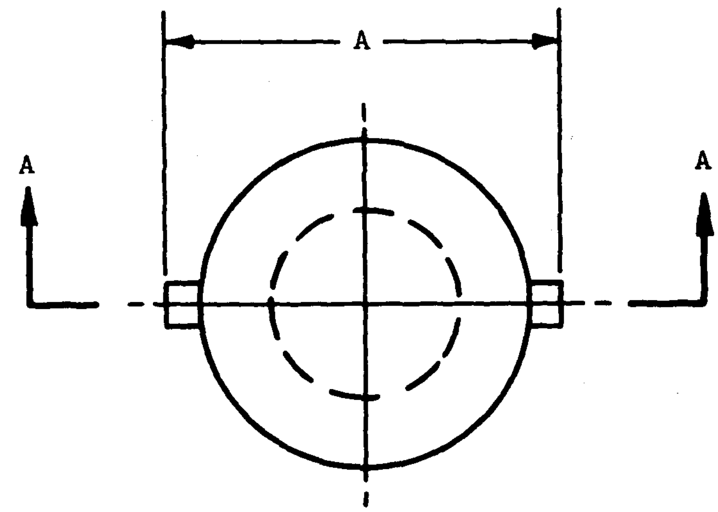

A = 50 inches maximum
B = 26 inches minimum
C = 45 inches minimum

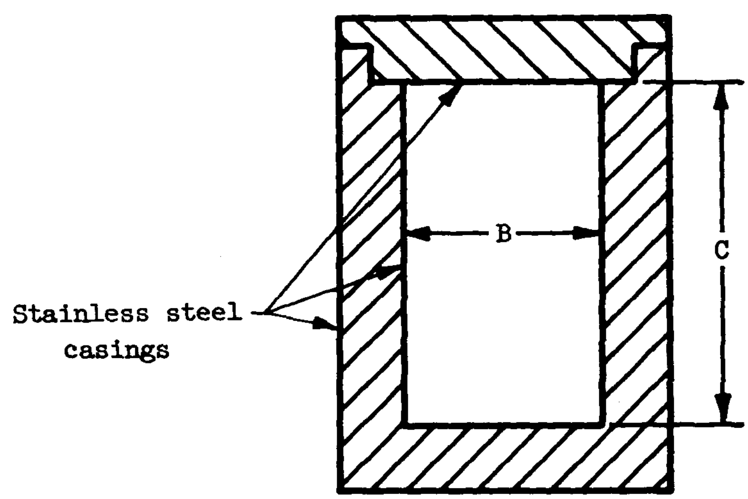

Section A-A

Fig. 4.25. Spent Core Cask

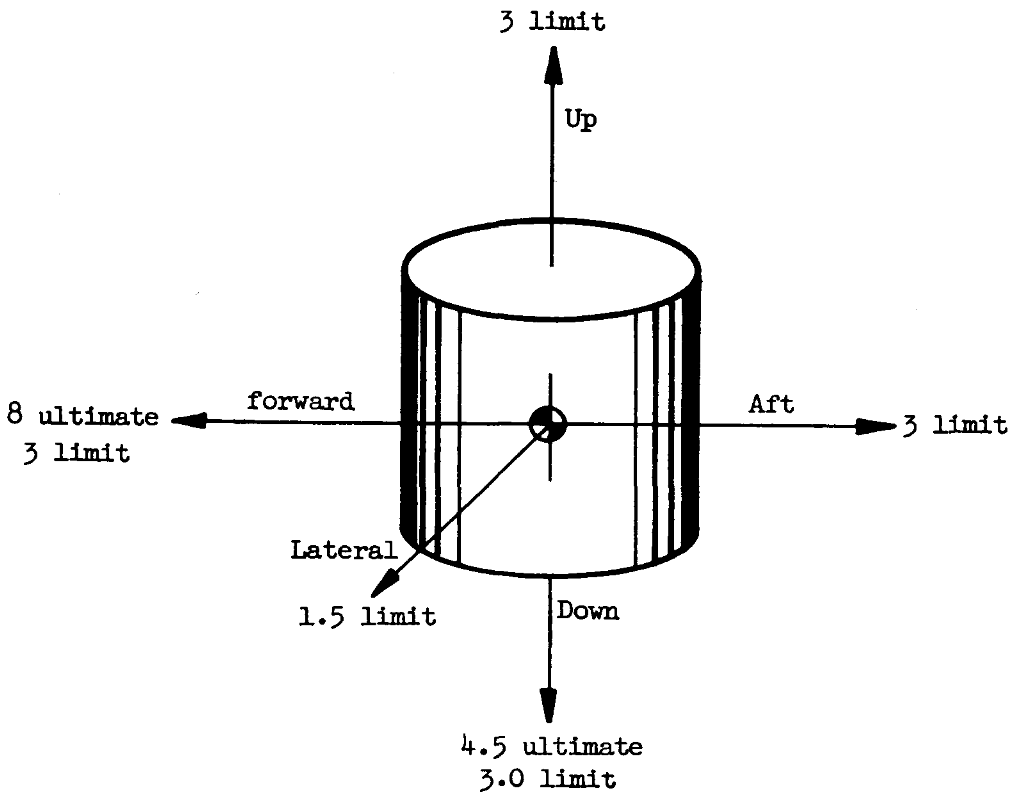

Fig. 4.26. Cask "G" Loads

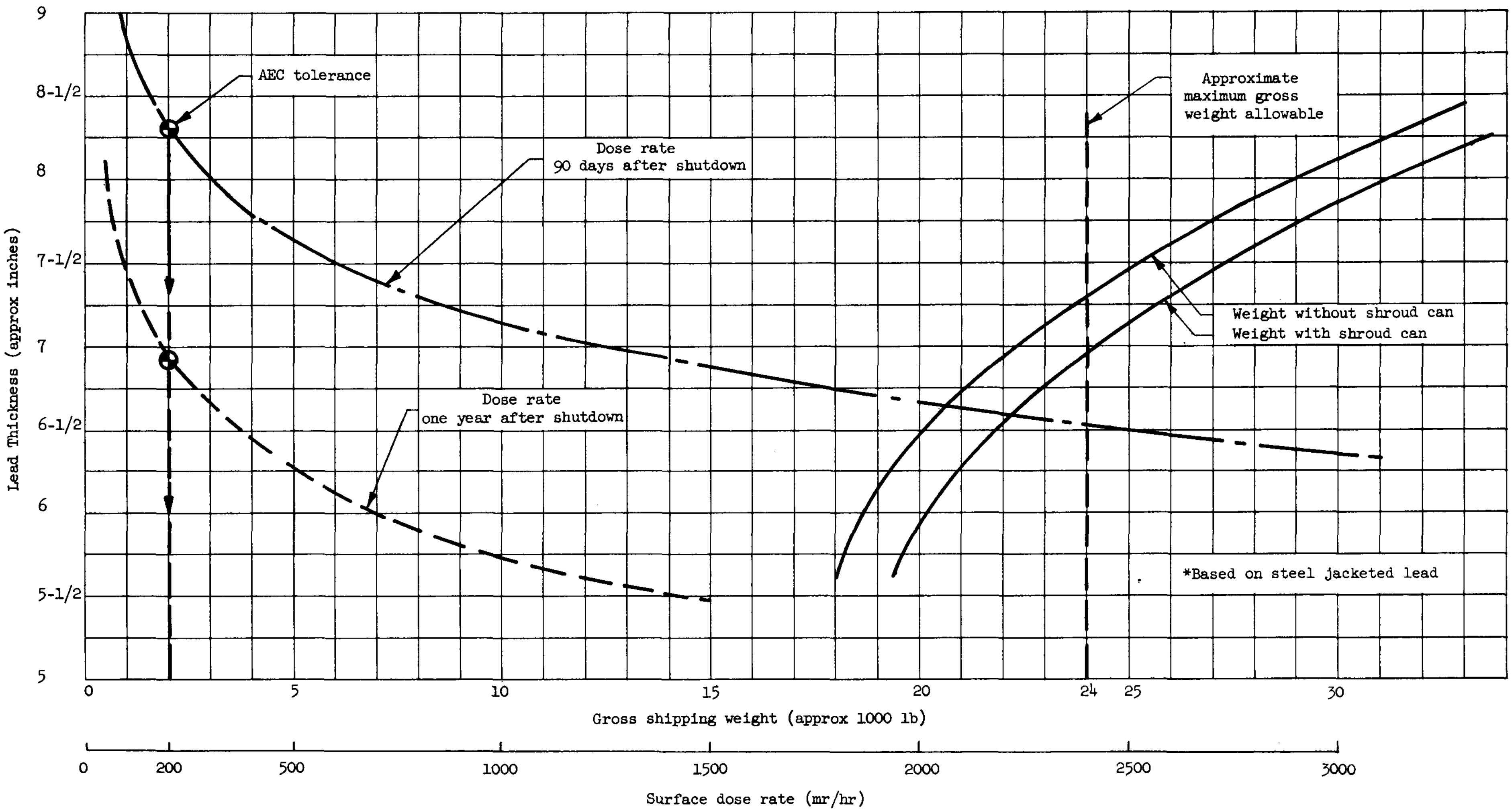

Fig. 4.27. Gross Shipping Weight of Spent Core Cask (critical geometry) and Estimated Cask Surface Dose Rate* Versus Lead Thickness

The following data were determined:

(1) Spent core thermal output

(a) 8 hours after shutdown . . . . 60 kw

(b) 14 hours after shutdown . . . . 50 kw

(c) 24 hours after shutdown . . . . 42.3 kw

(d) 90 days after shutdown . . . . 7.3 kw

(e) 94 days after shutdown . . . . 7.2 kw

(f) 1 year after shutdown . . . . 2.0 kw

(2) Cask shipping weights

	With Shroud Can (lb)	Without Shroud Can (lb)	ΔWt (lb)
(a) 6 inches lead	20,180	18,660	1520
(b) 6-1/2 inches lead	21,750	20,050	1700
(c) 7 inches lead	24,150	22,310	1840
(d) 8 inches lead	31,230	29,100	2130

(3) Cask surface dose rates versus wall thickness

(a) After 90-day storage period:

(i) 6 inches of lead . . . . 5,000 mr/hr
(ii) 6-1/2 inches of lead . . . . 2,500 mr/hr
(iii) 7 inches of lead . . . . 1,250 mr/hr
(iv) 8 inches of lead . . . . 320 mr/hr

(b) After 1-year storage period:

(i) 6 inches lead . . . . 700 mr/hr
(ii) 6-1/2 inches lead . . . . 360 mr/hr
(iii) 7 inches lead . . . . 180 mr/hr
(iv) 8 inches lead . . . . 45 mr/hr

(4) Spent core thermal output

(a) After 90-day storage period . . . . 7.3 kwt

(b) After 1-year storage period . . . . 2.0 kwt

Recommendations. From Paragraph (1) above, it is evident that, in order to ship a cask containing the entire spent core, the lead thickness must be reduced to between 6-1/2 and 7 inches.

The shipping weight of the cask must be in the range of 23,000 pounds to 24,000 pounds in order to allow for the skid chassis required in a C-130 aircraft. The following estimates are based on a core redesign. This new design would facilitate reduction in the original cask height by approximately five inches.

(1) Storage period--90 days

	Basic Cask Weight (lb)
(a) At 200 mr/hr surface dose rate	30,500 *
(b) At 500 mr/hr surface dose rate	24,000

(2) Storage period--one year

(a) At 200 mr/hr surface dose rate	22,000
(b) At 130 mr/hr surface dose rate	24,000

*Nonair transportable

An estimated storage period of 10 months would make it possible to ship an entire spent core by air (i.e., for cask weight = 24,000 pounds) without exceeding 200 mr/hr surface dose rate. This would require approximately 7-1/4 inches of lead thickness.

The Knapp-Mills Company, Wilmington, Delaware was contacted to gather preliminary cost information on shipping casks. The following figures were established:

(1) A cask designed for removal of 60 kw of decay heat and using auxiliary cooling equipment would cost about $45,000, less pumps, piping, etc.

(2) A cask designed for removal of 7.3 kw of decay heat would cost approximately $35,000. This design is marginal as far as heat removal without an auxiliary cooling system is concerned.

(3) A cask designed for removal of 2.0 kw of decay heat would cost approximately $25,000. This cask design would be the least complicated of those considered.

SUBSYSTEM 16--RADIOACTIVE WASTE DISPOSAL SYSTEM

M. Rosenberg

The radioactive waste disposal system includes:

(1) Evaporator.

(2) Condenser.

(3) Sump tank.

(4) Waste holdup tank.

(5) Sump pump.

(6) Piping and valves.

(7) Decontamination holdup tank(s) (located in decontamination package).

(8) Decontamination mixing tanks(s) (located in decontamination package).

(9) Miscellaneous pumps.

(10) Supports for equipment.

A schematic flow diagram of the waste disposal subsystem is shown in Fig. 4.28.

The objectives established for the past quarter were to outline the equipment required, derive approximate sizes and determine the shipping and installed configurations for the subsystem.

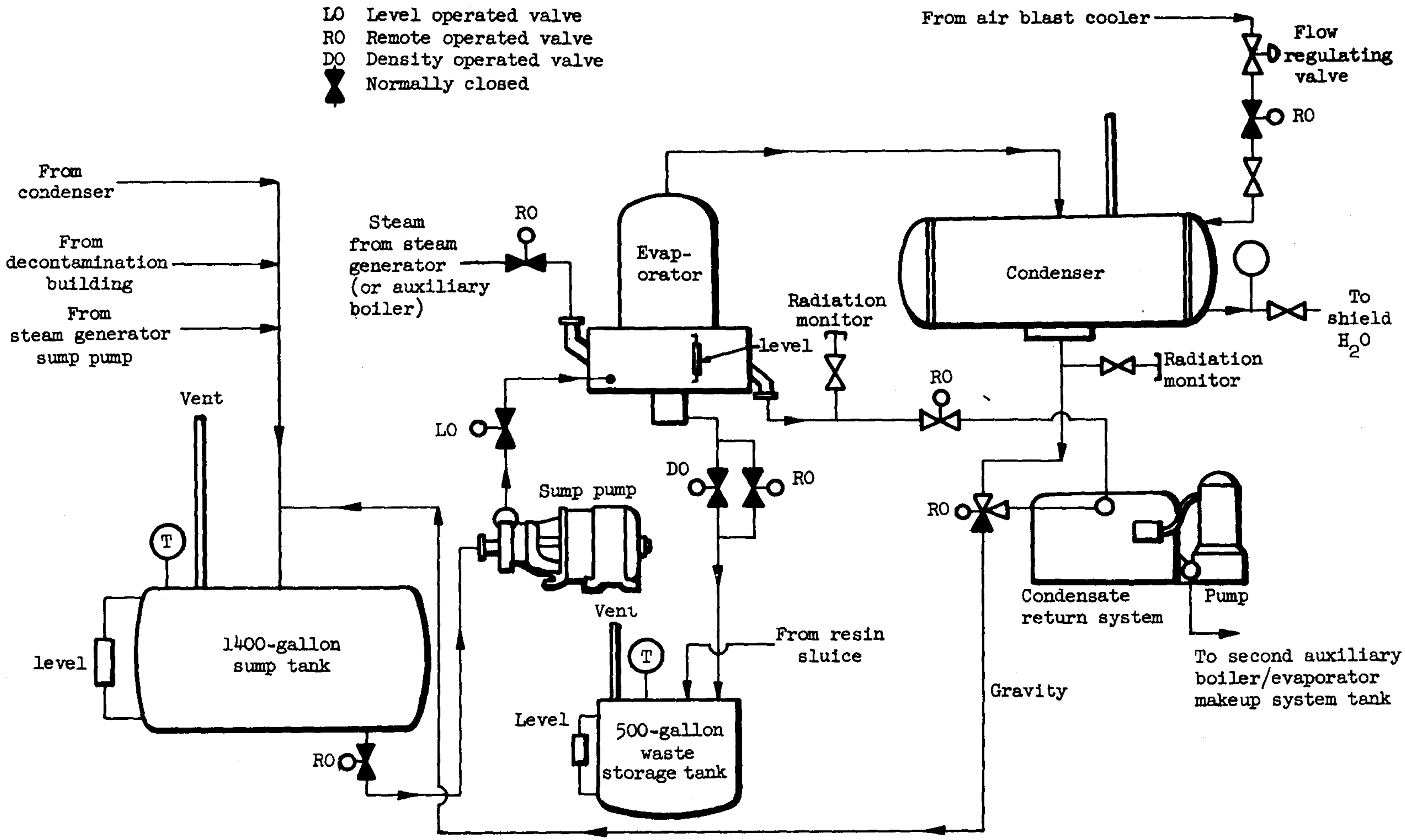

Fig. 4.28. Waste Disposal Subsystem

During the next quarter, final configuration drawings will be prepared, drawings and/or specifications for the components prepared and vendor contact established.

The volume of the waste disposal system was tentatively sized to be capable of containing both the primary and secondary loop operating volumes. A 500-gallon concentrated waste holdup tank was selected and provisions made to add extra holdup tanks in the future.

The design shown indicates a common skid for the relocatable equipment and supports for the storage equipment in the installed position.

During the past quarter, further analyses were made of the procedures necessary to dispose of liquid wastes generated during the operation of PM-1 power plant.

Under normal operation, the bulk of the liquid wastes will be generated during routine maintenance shutdowns. This waste will consist of the volume of the primary loop and the wash and rinse waters from the TURCO cleaning process. In the TURCO process, the loop will be treated with two wash and two rinse solutions with the total waste volume being approximately 2700 gallons.

All contaminated liquids will be drained to the sump tank from where the liquid wastes will be pumped into an evaporator which will evaporate the water and concentrate the solutions to approximately 65% to 70% solids. The bottoms from the waste evaporator will be drained into a concentrated waste storage tank. In addition to the above solution, the final waste tank also will receive directly the spent resin from the demineralizers.

The vapor effluent from the evaporator will be condensed, monitored and pumped back to the secondary system storage tank or sent to the sewer system. The evaporator will be required to deliver a decontamination factor of 10^6, which will be sufficient to reduce the activity in the condensate below 10^{-7} μcuries/cc, the maximum permissible concentration (MPC) value for water activity. Should the condensate fail to meet the above standard, it will be pumped back into the sump tank for re-evaporation.

The evaporator will be sized to provide an evaporation rate of 40 to 50 gallons per hour. This rate will be sufficient to handle the wastes during a shutdown period.

SUBSYSTEM 17--PLANT CONTAINER

R. Manoll

The plant container subsystem (uncontained version) includes:

(1) The container tank housing the reactor pressure vessel, the low pressure demineralizer and the shield water pumps.

(2) The container tank housing the steam generator, the primary system pump, the pressurizer, the high pressure demineralizer, the changing pumps, etc.

(3) The spent core storage tank.

(4) The spent core transfer dolly (traverses between Items (1) and (3), above).

(5) Interconnections between the above mentioned tanks.

(6) Supports for the equipment mounted within the tanks and for piping, wiring, light fixtures, etc., within the tanks.

(7) The common support base upon which the tanks (Items (1), (2) and (3)) are mounted.

(8) The superstructure supporting the primary system building and the gantry crane.

(9) The gantry crane including a 15-ton main hoist and a 1-ton auxiliary hoist.

(10) The primary system flooring.

(11) The vapor barrier for Item (1) above.

The plant container subsystem arrangement, shown in Fig. 4.29, represents the noncontained concept.

The objectives during the past quarter were to optimize and determine the overall primary system configuration based on ease of maintenance, ease of refueling and ease of erection at the site. During the next quarter, final configuration drawings will be prepared, drawings and specifications for the components of the subsystem will be prepared and vendor contacts established.

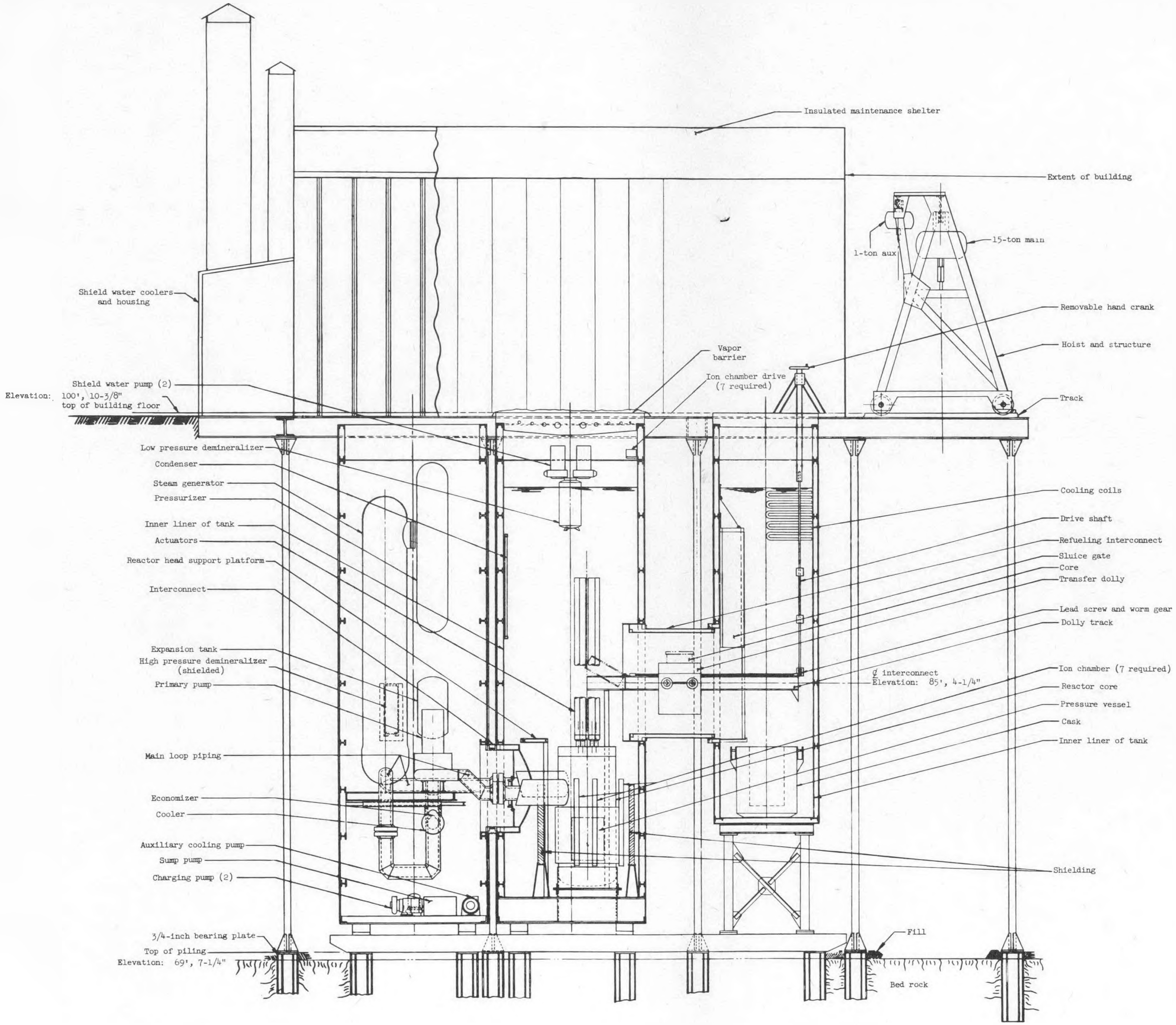

Fig. 4.29. Primary System Arrangement

During the quarter, a review was held with the AEC regarding preliminary design. It was decided then that the use of components located in inaccessible places and requiring maintenance during the 20-year design life period should be eliminated. The present design eliminates inaccessible expansion bellows and flanges from the previous primary system design, thereby reflecting the decision reached at the review meeting.

In addition to a redesign of the piping arrangement, the tanks containing the reactor vessel and steam generator were repositioned for further reduction in lengths of interconnecting piping. A two-flanged connection between tanks may be used to facilitate the 6-inch primary system piping installation at the Sundance site. These flanges are located within the interconnection fitting between the reactor tank and the steam generator tank. They are accessible from within the steam generator tank for maintenance during plant operation.

Rearrangement of components within the tanks was accomplished. In the reactor tank, the reactor vessel has been relocated to approximately the center of the tank and mounted rigidly off the floor. An added section of shielding between the reactor vessel and tank wall reduces the problem of heat generation at the tank wall. The low pressure demineralizer is located at the top of the tank, improving its accessibility and reducing the connecting lengths of small system piping. Similarly, the shield water pumps are located at the top of the tank with the pump motors above the level of shield water. The economizer, cooler, auxiliary coolant pump and high pressure demineralizer have been transferred from the reactor tank to the steam generator tank which reduces to two the number of penetrations at the interconnect fitting and simplifies sealing procedures. Included in the steam generator tank from previous designs are such items as the steam generator, primary pump, two charging pumps, sump pump, pressurizer and expansion tank.

The steam generator and the main coolant pump are mounted on a common floating base. This design, using a roller system, will allow for the thermal expansion of the 6-inch main loop pipe. The floating base also allows the units to be shipped on one position in the tank and installed in a different position to allow for proper alignment. An expansion loop in the main loop piping is included between the steam generator and main pump for thermal expansion between these components. The relocation of the high pressure demineralizer from the reactor tank to the steam generator tank now requires some additional lead or steel shielding around the demineralizer since the shield water is not used. All components within the steam generator containment tank are accessible for maintenance.

Elimination of the expansion bellows was accomplished by the following design. The interconnecting piping between the reactor vessel and the containment tank wall consists of the main loop piping wrapped with 1-1/2-inch insulation and housed within an 18-inch OD conduit acting as a secondary water barrier. The conduit is connected to the reactor vessel and the interconnect fitting by welding prior to shipment. The main loop piping and insulation are free to expand within the conduit. Where the main loop piping extends through the tank interconnect fitting, a replaceable gland seal is utilized for secondary sealing. This design is now more reliable, accessible, lighter in weight and more economical than previous designs.

The noncontained primary plant design described eliminates the problem of field welding although, in the contained primary plant, field welding will be required on the reactor containment tank. Due to weight limitations, this tank would be shipped to the site in half sections with the bottom half, including the reactor vessel and main loop piping, prefabricated. The piping arrangement of the noncontained and contained plants are similar.

In both contained and noncontained versions, a number of varied designs were structurally analyzed.

The contained version was checked for distortion effects due to high local temperature in the containment shell near the reactor. It was found that the 350° F level of heat would not permit the use of a rigid interconnect between tank shells. An expandable type design was needed to avoid high induced loads on the interconnect. The design using bellows fulfills this requirement.

For the noncontained reactor vessel tank, a study was made of the interconnect forces caused by the "hot spot" in the tank shell (350° F). Due to the proximity of the reactor vessel, it was found necessary to provide means for reducing this temperature; this is accomplished by use of auxiliary shielding. The latest temperature estimate is 200° F. Reactor vessel relocation and shielding caused this reduction and the thermal stress effects.

A thermal stress analysis of the primary piping between the steam generator and the primary cooling pump was made and it was determined that a common rigid base structure for the system was satisfactory. No special breathing device would be needed in the primary pipe.

The principal elements of the noncontained reactor vessel tank were estimated and weights were brought up to date accordingly.

The weights of the principal elements (noncontained version) are as follows:

Weight Estimate (pounds)--Vessel Containment

Outer skin	4,400
Inner skin	2,430
Floor	1,650
Internal supports	300
Tie-down fittings	300
Hoist, erection and skid fittings	300
Ring frames	1,560
Lower interconnect, rings and bulkhead	1,300
Skids	900
Roller conveyors	660
Upper interconnect, ring frames and bulkhead	500
Interframe bracing	750
Drain	30
	15,080

Weight Estimate (pounds)--Steam Generator Vessel Containment

Outer skin	4,400
Floor	900
Internal supports	800
Tie-down fittings	300
Hoist, erection and skid fittings	300
Ring frames	1,700
Interconnect, rings and bulkhead	600
Skids	900
Roller conveyors	600
Interframe bracing	740
	11,240

SUBSYSTEM 18--MAIN AND AUXILIARY STEAM SYSTEM

R. Groscup, W. Koch

During the past quarter, the following work was planned and accomplished:

(1) Determination of approximate steam and water flows.

(2) Establishment of pipe sizes.

(3) Establishment of the approximate location of all pipe runs.

During the next quarter, it is planned to:

(1) Establish all piping for the system and complete layouts except for minor dimensional changes required because of vendor certified drawing information.

(2) Submit the subsystem write-up and supporting data to the AEC for approval.

The main and auxiliary steam system transports steam from the steam generator outlet to the main turbine, turbine drive on the condensate pump, turbine drive on the boiler feed pump, gland steam system, evaporator reboiler, steam jet air ejector and deaerator.

The main steam line is a 6-inch schedule 40 carbon steel pipe which carries 34,312 pounds per hour of steam to the secondary system. From this total flow, 26,253 pounds per hour are furnished to the main turbine through 6-inch schedule 40 pipe, 500 pounds per hour go to the turbine drive on the condensate pump through 1/2-inch schedule 40 pipe, 2000 pounds per hour go to the turbine drive on the boiler feed pump through 1-1/2-inch schedule 40 pipe, 342 pounds per hour go to the gland steam system through 1/2-inch schedule 40 pipe, 7859 pounds per hour go to the evaporator reboiler through 4-inch schedule 40 pipe, 200 pounds per hour go to the air ejector through 3/4-inch schedule 40 pipe and 500 pounds per hour go to the deaerator through 1-inch schedule 40 pipe.

All pipe is designed for 585 psig and 500° F. After the exact location and length of the 6-inch main steam line from the steam generator to the main turbine has been established, a stress analysis will be performed on this piping.

SUBSYSTEM 19--MAIN TURBINE AND GENERATOR UNIT

R. Groscup, W. Koch

During the quarter, the following planned work was accomplished:

(1) The turbine expansion curve, turbine generator outline drawing, power quality and system layout were reviewed.

(2) The decision to use an oil purification system for the turbine tube oil was made.

(3) The turbine generator unit, turbine lube oil cooler and turbine lube oil conditioner specifications were received and reviewed.

During the next quarter, the following is planned:

(1) The final turbine generator certified outline drawing will be reviewed.

(2) The turbine-generator unit, turbine lube oil cooler and turbine lube oil conditioner specifications will be finalized, submitted to the AEC for approval and sent out to vendors.

(3) The subsystem write-up and supporting data will be developed and submitted to the AEC for approval.

The nonextraction turbine expansion curve for the PM-1 turbine generator unit was received from Westinghouse and is shown in Subtask 1.6. Also, other final turbine generator information was received and presently is being reviewed.

The decision was made to use an oil purifier for protection of the turbine oil from contamination. The gland seal steam system proposed by Westinghouse has been received and is being reviewed.

Note also that the oil purifier, the oil cooler and possibly the gland seal steam regulator will be shipped separate from the turbine generator.

The details of the Westinghouse efforts on the turbine-generator unit are discussed in Subtask 1.6. The details of the turbine control analysis are discussed separately in Task 4, Subsystem 1.

SUBSYSTEM 20--MAIN CONDENSER AND CONDENSATE SYSTEM

W. Koch

During this quarter, the following planned work was accomplished:

(1) The final condenser model test program was developed by Westinghouse and accepted with minor modifications.

(2) The final condenser model test program arrangements were reviewed and completed with Eglin AFB Climatic Test Chamber personnel.

(3) The condenser, air ejector, hotwell and condensate pump specifications were reviewed and are complete, subject to incorporation of review modifications.

During the next quarter, the following is planned:

(1) The condenser model test will be 90% completed at Eglin AFB.

(2) The main condenser and condensate system layout will be completed except for minor dimensional changes required by vendor certified drawings.

(3) The condenser, air ejector, condensate pumps and hotwell specifications will be finalized, submitted to the AEC for approval and sent out to vendors for bids.

(4) The subsystem write-up and supporting data will be developed and submitted to the AEC for approval.

During this quarter, the final condenser model test procedures were received from Westinghouse and reviewed. This test procedure is discussed in Subtask 1.6.

The layout and specifications for the condenser, air ejector, condensate pumps and hotwell were received from the Gibbs and Hill Company. This data was reviewed and commented on. (See Task 16 for detailed discussion of Gibbs and Hill Company efforts.)

SUBSYSTEM 21--FEEDWATER SYSTEM

L. Hassell, W. Koch

During this quarter, the following planned work was accomplished:

(1) The deaerator, feedwater pumps and feedwater heater specifications were received and reviewed.

(2) The feedwater system layout was received and reviewed.

During the next quarter:

(1) The deaerator, feedwater pumps and feedwater heater specifications will be completed, submitted to the AEC for approval and sent to vendors.

(2) The feedwater system layout will be completed except for minor dimensional changes required by vendor's certified drawings.

(3) The subsystem write-up and supporting data will be developed and submitted to the AEC for approval.

During this quarter, the specifications for the deaerator, feedwater pumps and feedwater heater were received from Gibbs and Hill, reviewed and commented on. They are complete, pending incorporation of review changes.

The preliminary layout of this equipment and associated piping was finished by Gibbs and Hill, reviewed and accepted, subject to details dependent on vendors' certified drawings (see Task 16). One of the major problems encountered with the equipment in the Heat Transfer Apparatus Package is the design of equipment mounting supports which are suitable for shipping and, in turn, do not interfere with the various pipe runs in the package. This will be resolved next quarter.

Controls for the feedwater system are discussed in Task 4, Subsystem 1, "Controls and Instrumentation."

SUBSYSTEM 22--EXTRACTION STEAM AND HEATER DRAIN SYSTEM

L. Hassell, W. Koch

During this quarter, the following planned work was accomplished:

(1) The preliminary layout of this equipment was received from Gibbs and Hill and reviewed.

During the next quarter:

(1) The layout of this system will be completed except for minor dimensional changes required by the receipt of certified equipment drawings from vendors.

(2) The subsystem descriptions and supporting data will be developed and submitted to the AEC for approval.

Work in this subsystem area during this quarter consisted of layout work within the Heat Transfer Apparatus Package by Gibbs and Hill Company (Task 16). The preliminary layout drawing of this system was received, reviewed and accepted pending final design modifications.

SUBSYSTEM 23--COOLING WATER SYSTEM

W. Koch

No work was planned or accomplished in this subsystem area during this quarter.

Next quarter:

(1) The subsystem write-up and supporting data will be developed and submitted to the AEC for approval.

(2) The cooling water requirements of the PM-1 plant equipment will be established and design of the system completed.

SUBSYSTEM 24--MAIN TRANSFORMER AND DISTRIBUTION SYSTEM

W. Koch

During this quarter, the following planned work was accomplished:

(1) The switchgear and power center transformer specification was received from Gibbs and Hill and reviewed.

(2) The electrical one-line diagram was received from Gibbs and Hill and reviewed.

(3) The preliminary switchgear layout in the switchgear package was received from Gibbs and Hill and reviewed.

(4) Preliminary switchgear outline drawings were received and reviewed.

During the next quarter:

(1) The switchgear and power center transformer specification will be completed.

(2) The main transformer and distribution subsystem write-up and supporting data will be developed and submitted to the AEC for approval.

(3) The switchgear layout will be completed except for minor dimensional changes due to vendors' certified drawings.

(4) The one-line electrical diagram will be completed.

SUBSYSTEM 25--STATION SERVICE SYSTEM

W. Koch

During this quarter, the following planned work was accomplished:

(1) The motor control center specification was received from Gibbs and Hill Company and reviewed.

(2) The electrical one-line diagram was received from Gibbs and Hill and reviewed.

(3) Preliminary motor control center drawings were received and reviewed.

During the next quarter:

(1) The motor control center specification will be finalized.

(2) The station service system write-up and supporting data will be developed and submitted to the AEC for approval.

(3) The motor control center layout in the switchgear package will be completed except for minor dimensional changes due to vendors' certified drawings.

(4) The one-line electrical diagram will be completed.

Work during this quarter in this system area consisted of review and comment on the Westinghouse and Gibbs and Hill Company efforts. Also included in this work area was the submission of the PM-1 plant electrical requirements to Westinghouse and Gibbs and Hill Company for incorporation into the motor control center design.

A list of all motors, heaters and other power consuming devices was made (see Table 4.5) to determine plant power requirements and to lay out the motor control center.

TABLE 4.5

Equipment and Service Power Requirements in PM-1 Plant

	Item	Number	Power Requirements (total) (kw)
1.	Condenser fans	8	105
2.	Turbine auxiliary oil pump	1	0.8
3.	Lube oil cooler fans	2	7.6
4.	Feedwater pump	1	23
5.	Condensate pump	1	1.5
6.	Evaporator feed pump	2	1.6
7.	Sump pump	2	0.8
8.	Reactor control rod actuators	6	7
9.	Decontamination vent fan	1	0.4
10.	Primary system vent fan	1	0.8
11.	Auxiliary boiler	1	6
12.	Changing pumps	2	2.2
13.	Shield water cooler fans	4	8
14.	Shield water circulating pumps	2	2.2
15.	Auxiliary coolant pump	1	0.4
16.	Coolant pump	1	42 (hot operation) 53 (cold operation)
17.	Waste disposal pump	2	0.4
18.	Hoist	2	0.8
19.	Static battery charger	1	5
20.	Air compressor	2	7.6
21.	Pressurizer heaters	2	30
22.	Lighting panel	1	12
23.	Maintenance shop	1	15
24.	Vital a-c supply	1	12
25.	Convenience outlet circuit	1	40

SUBSYSTEM 26--LIGHTING AND D-C EMERGENCY LIGHTING

W. Koch

During this quarter, the following planned work was accomplished:

(1) Preliminary lighting design, based on the packaged module concept, was completed.

(2) Illumination levels were selected and fixture type chosen.

(3) Emergency lighting systems were evaluated and selected.

During next quarter:

(1) The lighting design, based on the new secondary building concept, will be completed.

(2) Wiring and mounting system design will be completed.

(3) The bill of material for this system will be completed.

(4) The subsystem description and supporting data will be developed and submitted to the AEC for approval.

During this quarter, the lighting design, based on the packaged module concept, was completed and illumination levels were selected for various plant areas. These values are shown in Table 4.6.

Individual emergency lighting units with self-contained batteries were selected for the emergency lighting system. These units normally operate from an a-c convenience outlet but, upon loss of power, they automatically switch to d-c battery power.

TABLE 4.6

Lighting Levels in PM-1 Plant

Location	Ft-C. Maintained in Service	Controlled from	Emergency Lighting
Control room	40	Lighting panel	Yes
Offices	40	Wall switches	No
Laboratory	40	Wall switches	No
Machine shop	40	Wall switches	Yes
Stock and tool room	25	Wall switches	No
Switchgear area	30	Lighting panel	Yes
Turbine-generator area	20	Lighting panel	Yes
Pump areas	20	Lighting panel	Yes
Lube Oil areas	20	Wall switches	Yes
Air compressors	15	Lighting panel	Yes
Toilet and locker areas	15	Wall switches	No
Battery areas	15	Wall switches	Yes
Open storage	10	Lighting panel	No
Chemical storage	10	Lighting panel	No
Stairway landings	10	Lighting panel	Yes
Walkways (indoor)	10	Lighting panel	Yes
Walkways (outdoor)	10	Wall switch	Yes
Storage tank area	5	Lighting panel	No
First aid	40	Wall switch	Yes
Emergency lighting	3	Automatic	-

SUBSYSTEM 27--PLANT D-C SYSTEM

W. Koch

During this quarter, the following planned work was accomplished:

(1) A battery type was selected for the station battery system.

(2) A battery charger type was selected.

During the next quarter:

(1) The station battery specification will be completed, submitted to the AEC for approval and sent out to vendors for bidding.

(2) The subsystem write-up and supporting data will be developed and submitted to the AEC for approval.

A study was made during this quarter on the comparison of lead-acid and nickel-cadmium batteries for PM-1 station battery use. Due to the cost ratio of approximately 6 to 1 of the nickel-cadmium batteries to the lead-acid type and due also to discharge voltage characteristics of the nickel-cadmium batteries, the lead-acid type was selected. This battery will be sized for 160 ampere-hours at an 8-hour discharge rate and will consist of 60 cells.

SUBSYSTEM 28--EMERGENCY POWER SYSTEM

W. Koch

During this quarter, the following planned work was accomplished:

(1) The auxiliary diesel-generator unit specification was written and reviewed internally.

(2) The d-c bus and vital a-c bus equipment specifications were received from Gibbs and Hill and reviewed.

During the next quarter:

(1) The auxiliary diesel-generator unit specifications will be completed, submitted to the AEC for approval and sent out to vendors.

(2) The d-c bus and vital a-c bus equipment specifications will be completed, submitted to the AEC for approval and sent out to vendors.

(3) The subsystem write-up and supporting data will be developed and submitted to the AEC for approval.

The primary purpose of the diesel generator is to supply emergency power in case of plant shutdown and power for normal startup. A study has shown that, during these periods, 150 kw is sufficient.

Because of the space and weight limitations in the secondary system area, it was determined that a high speed diesel-electric generating set was preferred. This is consistent with the low load factor required of the machine. The weight of this unit will be between 6600 pounds and 7000 pounds with overall dimensions of 99 inches long, 42 inches wide and 60 inches high. This unit will have a speed of 1800 rpm and be equipped with a supercharger. The continuous rated capacity will be 150 kwe with a 10% overload capability. Overload is based on 2 hours' operation at 70° C generator temperature rise at normal elevations. A site elevation of 6500 feet will have some effect on these ratings; these effects are being investigated.

The design criterion of using dc for reliability was retained.

A reliable power system for vital a-c equipment was selected. This system utilizes a vital bus normally supplied through a transformer from the 480-volt bus. The vital bus feeds the system loads and the motor of the inverter-diverter m-g set. The generator charges the battery, but on a-c failure, the d-c machine motors and drives the a-c machine as an alternator.

SUBSYSTEM 29--WATER TREATMENT

R. Groscup, W. Koch

During this quarter, the following planned work was accomplished:

(1) The chemical treatment equipment specification was received from Gibbs and Hill and reviewed.

(2) A study was made of the water treatment necessary for the PM-1 Secondary System.

During the next quarter:

(1) The chemical treatment equipment specification will be completed, submitted to the AEC for approval and sent out to vendors.

(2) The subsystem description and supporting data will be developed and submitted to the AEC for approval.

(3) The layout of this subsystem will be completed except for minor dimensional changes dependent upon vendor's certified drawings.

A study was made of the water treatment necessary for the Secondary System. This study included the evaluation of conditions at the SM-1 and Shippingport pressurized water installations based upon several field trips and evaluation of previous work undertaken by The Martin Nuclear Division. As a result of this study and the Gibbs and Hill effort, the following was established as the design criteria:

(1) pH will be maintained between 8.5 and 9.5 in the steam generator using a mixture of trisodium phosphate and disodium phosphate.

(2) The mixture of trisodium phosphate and disodium phosphate will be determined in the field.

(3) Total dissolved solids in the steam generator shall not exceed 500 ppm. Continuous steam generator blow-down is planned.

(4) The evaporator-reboiler will not have a deaerating section, but the deaerator manufacturer will be required to guarantee the CO_2 content of the feedwater leaving the deaerator.

(5) Morpholine will be used for CO_2 control.

(6) There will be no deaeration of the return drains from the heating system.

(7) Continuously injected hydrazine solution will be used to scavenge oxygen.

(8) Chloride content will be held to less than 0.5 ppm in the steam generator.

SUBSYSTEM 30--CONDENSATE MAKE-UP SYSTEM

W. Koch

During this quarter, the following planned work was accomplished:

(1) The evaporator-reboiler capacity requirements were established.

(2) The approximate evaporator-reboiler size and weight were established, and the unit was located in the Heat Transfer Apparatus Package.

(3) The evaporator-reboiler specification was received from Gibbs and Hill and reviewed.

During the next quarter:

(1) The evaporator-reboiler specification will be completed, submitted to AEC for approval and sent to vendors.

(2) The subsystem description and supporting data will be developed and submitted to the AEC for approval.

(3) The layout of the evaporator-reboiler in the Heat Transfer Apparatus Package will be completed except for minor dimensional changes dependent upon vendor's certified drawing.

The PM-1 evaporator-reboiler is sized to furnish 500 lb/hr of vapor to the deaerator for condensate make-up plus 7×10^6 Btu/hr in the form of 35-psia steam for site heating.

The evaporator-reboiler type selected for the PM-1 plant is a single effect tube-in-shell unit with a removable tube bundle. The evaporator is furnished heat from the main steam line. This unit is located in the Heat Transfer Apparatus Package and is approximately four feet in diameter and seven feet long. Tubes can be pulled from the central aisle area of the Secondary System building.

SUBSYSTEM 31--FIRE PROTECTION SYSTEM

W. Koch

No effort was planned during this quarter in this subsystem area.

During the next quarter:

(1) The fire protection system requirements, equipment requirements and layout will be completed.

(2) The subsystem write-up and supporting data will be developed and submitted to the AEC for approval.

SUBSYSTEM 32--AUXILIARY STEAM SYSTEM

W. Koch

No effort was planned during this quarter in this subsystem area.

During the next quarter:

(1) The auxiliary steam system requirements, equipment requirements and design will be completed.

(2) The subsystem write-up and supporting data will be developed and submitted to the AEC for approval.

SUBSYSTEM 33--HEATING AND VENTILATING SYSTEMS

W. Koch

During the quarter, the following planned work was accomplished:

(1) The PM-1 plant central heating system preliminary requirements were established.

(2) A preliminary plant heating flow diagram was developed.

During the next quarter:

(1) The PM-1 plant heating and ventilating system designs will be completed except for detailed layout.

(2) The subsystem description and supporting data will be developed and submitted to the AEC for approval.

Design effort was directed toward establishing one central heating and ventilation system for the entire PM-1 plant including primary, secondary and decontamination buildings.

The heating system is to consist of a central steam supply, either the auxiliary steam boiler or the evaporator-reboiler and sufficient space heaters to keep the building at a uniform temperature of 70° F with a -55° F ambient temperature. The heating system will also include local controls necessary to accomplish this.

Evaluations of the heat losses from the secondary building were made assuming a true arctic building in an arctic environment. The building was taken to be 32 feet wide, 64 feet long and 10 feet high, with a center peak height of 16 feet, having an overall coefficient of heat transfer established at 0.09 Btu/hr-ft^2-°F. An outside temperature of -55° F was assumed with an inside temperature of +70° F. Using the above-stated conditions, the heat loss through the walls, roof and floor was found to be 74,500 Btu/hr. The heat loss due to infiltration was found to be 160,000 Btu/hr, assuming two air changes per hour. This gives a total heat loss for the secondary building of approximately 235,000 Btu/hr.

It is planned to use horizontal unit heaters equipped with electric fans of approximately 1/30 hp. There will be four heaters required in the secondary building. These heaters will use steam furnished from the evaporator-reboiler during normal operating conditions and steam from an auxiliary boiler during shutdown periods (see Fig. 4.30). The steam will be supplied to the heaters at 35 psia. Each fan will be provided with an adjustable-louver fin diffuser. Vertical fins are adjustable to provide air deflection at any degree in the horizontal plane. Horizontal louvers will allow air to be controlled in the vertical plane.

It is planned to use individual thermostatic control for certain heaters. Each thermostat will control the heat in its particular zone.

There will be a condensate return system tank and a condensate pump for feedwater return to the reboiler or the auxiliary steam boiler.

An evaluation was made of heat losses from the decontamination building. The buildup itself will be of the integral housing type construction. The size of the building is 8 feet, 8 inches wide, 30 feet long, 8 feet, 3 inches high on one side and 8 feet, 6 inches high at the other. Overall U value is 0.10 maximum, giving a heat loss of 15,500 Btu/hr. The heat loss due to infiltration was calculated to be 6727 Btu/hr, also assuming two air changes per hour in this building. Thus, the total heat requirement for the decontamination building is approximately 22,000 Btu/hr.

The primary building will not normally be heated as a working space but may require heat during emergency repairs to the Primary System. The building will be approximately 16 feet by 32 feet by 14 feet at the eave with a peak height of 17 feet and an overall U value of 0.2. No attempt will be made to hold air temperatures above 60° F with an ambient of -55° F. Under these conditions, heat losses are approximately 58,000 Btu/hr through the walls and 45,000 Btu/hr due to air changes (2 per hour). This brings the total primary building losses to approximately 103,000 Btu/hr.

Total heat requirement for the three areas is approximately 360,000 Btu/hr when heating all areas. Normal load in coldest weather would only be 255,000 Btu/hr for the secondary building and decontamination building.

Additional requirements arise for the waste disposal evaporator, walkway heating, greater air infiltration losses in high wind steam tracing, etc. Full-load operation of the waste disposal system evaporator requires over 300,000 Btu/hr. This will not normally be accommodated during full heating of all three building areas. A maximum reasonable rating for the auxiliary boiler has, therefore, been established at 500,000 Btu/hr. The unit will supply 100-psi steam because of the waste disposal evaporator. Heating steam will be pressure-reduced.

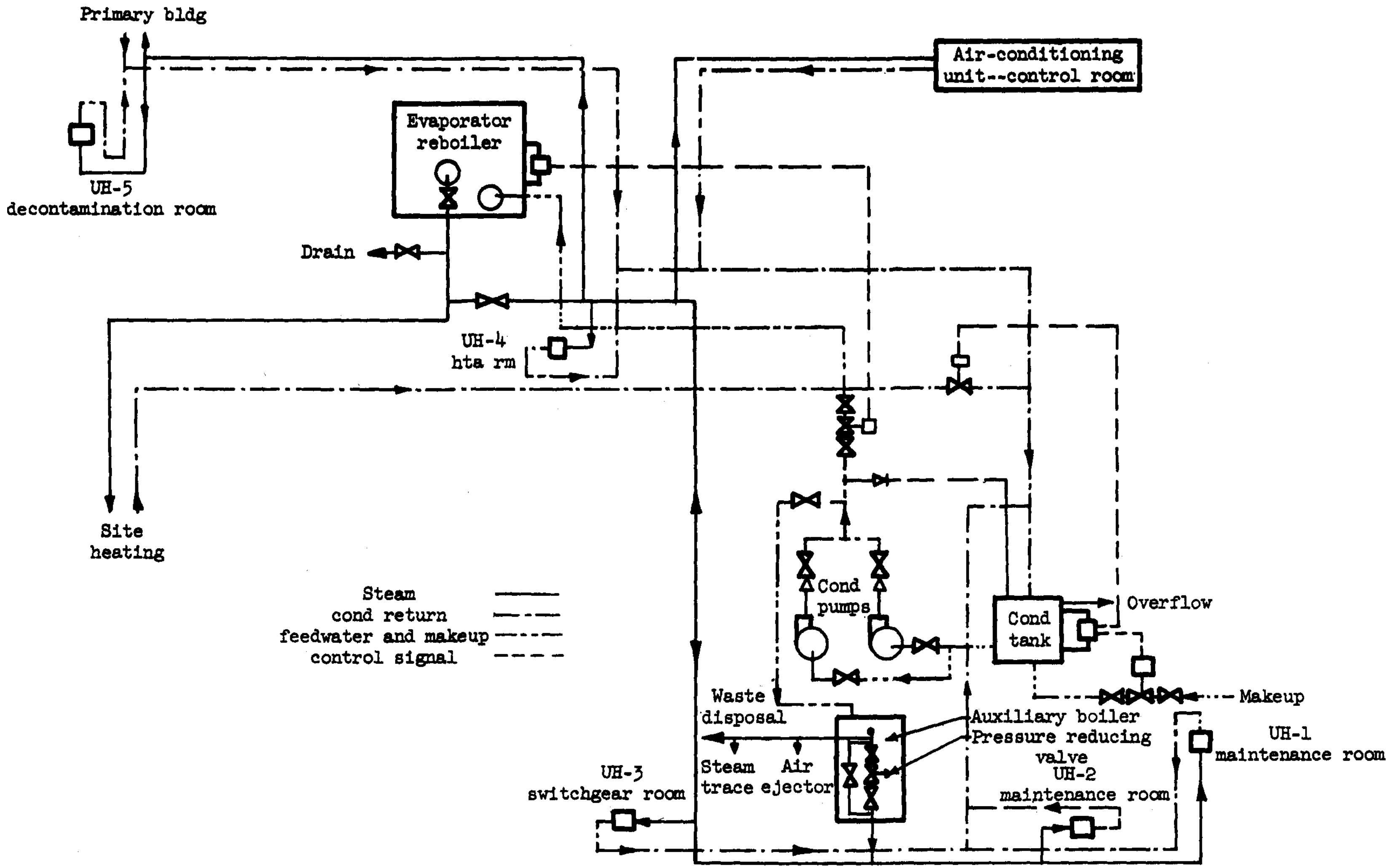

Fig. 4.30. Flow Diagram--PM-1 Plant Heating

The control room heat losses are about 80% of those for the decontamination building. It is proposed to install a combination summer-winter air-conditioning system in this room. For heating purposes, a steam heating coil will be placed in the air discharge passage of the air-conditioning unit for heating the air during the winter season. From preliminary investigations, a 3-ton air-conditioning unit should be sufficient for this room. This room will also be thermostatically controlled to allow either heating or cooling from the same unit.

During the next quarter, it is planned that sizes of all equipment, layout of equipment, flow diagrams, piping, specifications and equipment procurement data will be completed and vendors will be selected.

SUBSYSTEM 34--PRIMARY LOOP BUILDING

J. Todd, A. Layman

During the quarter, the following planned work was accomplished:

(1) The envelope dimensional requirements for the primary loop building were established as 16 feet wide, 32 feet long and 14 feet high at the eave.

(2) The relative location of tanks, loading dock, crane and doorways was established in a preliminary arrangement which is now being studied with respect to site work before being frozen.

Next quarter, the building relative location and detailed requirements will be established, and the subsystem description and specifications will be submitted to the AEC for approval. A vendor will be selected.

SUBSYSTEM 35--SECONDARY SYSTEM BUILDING

A. Layman

During the quarter, it was planned to continue with the design of integral housing for the Secondary System. This was dropped except for the decontamination package which will still be of the integral housing design. A program review of integral housing at a review meeting 29 October 1959 in Germantown, concluded that secondary equipment other than the decontamination package would be housed in a separately shipped building and that equipment would be shipped in truss-type packages as proposed. Martin was instructed to make specific recommendations as to type of building and did so late in the quarter. Final resolution of the Secondary System building type, size and erection schedule will be accomplished next quarter, and final building specifications will be completed and submitted to the AEC for approval and to vendors for bidding.

SUBSYSTEM 36--DECONTAMINATION EQUIPMENT

W. Koch

During this quarter, the following planned work was accomplished:

(1) The decontamination equipment requirements were established.

(2) The preliminary layout of the decontamination equipment was modified to incorporate new equipment data.

During the next quarter:

(1) The design of the decontamination system will be completed.

(2) The subsystem description and supporting data will be developed and submitted to the AEC for approval.

The decontamination package is a separate building of the Secondary System, located adjacent to the Heat Transfer Apparatus Package and connected to the Primary System area. The purpose of the decontamination package is to provide:

(1) An area to decontaminate parts, equipment and tools.

(2) An area to decontaminate personnel and their protective clothing.

(3) An area to house the water analysis equipment and Health Physics instrumentation.

(4) An enclosed transportation route for personnel and equipment between the Primary and Secondary System areas.

The areas for decontamination of parts, equipment, tools and personnel represent the "hot" side of the package nearest the Primary System. The cold side contains the water analysis area, Health Physics instrumentation and a clothing change area for personnel. The hot side is further subdivided by a barrier incorporating a sliding door which separates the equipment decontamination area from the personnel cleanup area.

Most hot side decontamination work will be done on a stainless steel pad measuring 3-1/2 feet by 6 feet. A double-tub, double-drainboard stainless steel sink, equipped with knee operated water and drain controls, will be utilized for decontamination of small parts, tools, rubber gloves and hands. A combination automatic washer-dryer will be used to decontaminate protective clothing. A stainless steel walk-through shower may be used, if required, by personnel passing from the hot side to the cold side.

The water analysis area on the cold side will consist of a chemical lab stainless steel sink and work bench and a stainless steel fume hood required to evaporate water samples. Six lockers will provide storage of street clothes and a dressing bench adds to the convenience of changing clothing. Instrumentation used for the detection of radiation, which will be installed or stored in the decontamination package, includes a constant air monitor, neutron survey equipment, a portable air sampler and personnel dosimeter. A detector will be located at the hot-cold demarcation for personnel and equipment checks when passing from the hot side to the cold side.

Air movement will be maintained from the cold side to the hot side by drawing inlet air from the Secondary System buildings and/or the outside. Suitable filtration will be installed upstream of the exhaust fan at the hot side to prevent release of contaminated particles to the atmosphere. The washer-dryer will be vented through the exhaust fan filters, but the fume hood in the water analysis area will be separately vented through its own filter. All filters will be checked periodically for radiation buildup and pressure drop.

Hot and cold water will be distributed in the decontamination package where required. Separate contaminated and uncontaminated drain lines will be installed. The contaminated drain will go to the waste disposal system and the uncontaminated or clean drain will enter the sanitary sewer. All plumbing will be routed inside the package above the floor line to prevent freezing at low temperature. This requires elevation of the decontamination pad, washer-dryer (which will rest in an overflow drain pan) and the shower.

Several types of floor covering material were considered. Asphalt block tile coated with an epoxy paint was selected for good wearing qualities. It can be readily decontaminated and repainted. This type of covering can also be removed and replaced if it becomes highly contaminated.

Ample facilities will be provided for storage of equipment required for decontamination of parts, tools and personnel and for performance of water analysis. In addition, storage of radiation detection instruments and protective equipment, including filter-type respirators and portable self-contained air supplies, will be provided.

During the coming quarter, procurement action for the equipment contained in the decontamination package will be started.

SUBSYSTEM 37--MAINTENANCE EQUIPMENT

R. Groscup, R. Stuenes

During the period, it was planned to continue studies of maintenance requirements and selection of types of maintenance equipment required. This was accomplished and a preliminary tools and equipment list has been developed. The maintenance package is planned to contain a work bench with small tool storage cabinets, lathe, grinder and tool truck. In addition, this package will contain auxiliaries and service equipment, including the 150-kw diesel generator unit, instrument air compressors with driers and receivers, auxiliary boiler unit with condensate return tank and pumps, and the men's room. It is planned that some additional equipment be shipped in this package and relocated at the site; these items include welding equipment and a vacuum cleaner.

The principal considerations for selection of equipment within the maintenance package are as follows:

(1) Types of maintenance work anticipated.

(2) Tool unit sizes according to the size of the equipment to be repaired.

(3) Use of tools which are as universal as possible for weight and space savings.

In accordance with these factors, the following decisions have so far been made:

(1) The shaper proposed in the preliminary design can be eliminated. Little work requiring this machine is expected and all such work anticipated can be handled by providing the lathe with milling attachments.

(2) A large service air compressor will not be needed. Present plans are to use electric impact tools. A small portable compressor will be sufficient for general maintenance work, painting, etc.

(3) The fresh fuel element storage locker has been removed from the package due to limited space and will be shipped in the decontamination package.

(4) The drill press will not be a separate unit. Rather, it will consist of a portable 1-inch electric drill with a bench stand for mounting on the work bench.

Features of the major maintenance equipment presently being planned for shipment in the maintenance package are as follows (modification will be made at a later date when the make and model of all equipment is established):

(1) One lathe, which will be of approximately 10-inch swing and 36-inch center distance, will hold the largest shafts and pipe sections expected to be repaired at the site. The lathe will be mounted on a bench-type pedestal which has provisions for tool storage.

(2) One grinder, which will be a 7-inch bench type, mounted on a floor pedestal.

(3) One work bench with drawers for tool storage for small repair work. The drill press, a machinist's vise and a small hydraulic press will be mounted on the bench top. The hydraulic press will be a portable type with attachments for pipe bending, bearing pulling, etc.

(4) One 300-amp ac-dc are welding machine which will be large enough for general welding.

(5) One cylinder truck for a gas welding-burning rig.

(6) One storage cabinet for general mechanic's repair tools, wheel-mounted for easy transportation to working areas.

(7) One portable crane. No decisions have yet been made regarding size or shape of this crane. This will be resolved after all major plant equipment has been selected.

A general layout of the maintenance area has not been completed as the sizes of some major units still are to be determined. Final layout will follow equipment selection.

It is planned next quarter to complete the selection of all major maintenance equipment and to begin the final detailed layout of the maintenance package.

TASK 4--GENERAL STUDIES

The following four subsections report studies and analyses which do not lend themselves to easy classification by subsystem. They are:

A. Nuclear Analysis Studies.

B. Shielding Studies.

C. Secondary System Studies.

D. Miscellaneous Studies.

A. NUCLEAR ANALYSIS STUDIES

Project Engineer--R. J. Akin
E. Scicchitano, R. Hoffmeister, P. Altomare, F. Todt

Nuclear analysis performed during the third quarter consisted of studies to establish final core design specifications. These studies consisted of:

(1) Core design studies.

(2) Fuel element loading studies.

(3) Lumped burnable poison studies.

(4) Control studies.

(5) Power density distribution studies.

The basic core geometry was established. Nonuniform burnup studies to determine fuel element specifications were completed. The resultant fuel loading specification is $38.6\,^{+1.5}_{-0}$ grams of U-235 per fuel element. Studies to determine lumped poison rod specification and rod distribution continued. Control requirements based on fuel loading studies are being evaluated. Control rod design geometry was established. Eu_2O_3 in stainless steel was selected to be the control rod absorber material. Studies to establish the Eu_2O_3 weight specifications were initiated. Studies to determine gross power distribution for the core, including effects of rod insertion, were completed.

During the next quarter, final design specification studies will be completed and design analysis studies will continue. The studies to be performed include:

(1) Determining the effect of fuel loading specification tolerances on core life and control requirements.

(2) Determining lumped poison rod specifications.

(3) Determining control rod material specifications.

(4) Nonuniform lumped poison rod distribution studies and reactor kinetic studies.

In addition, nonuniform burnup, control rod worth and gross and fine flux and power distribution design analysis studies will be performed.

1. Core Design Studies

The PM-1 basic core geometry was established. The core nuclear design characteristics are summarized in Table 4.7.

A top view of the reference core, showing the basic core configuration, control rod location, preliminary lumped poison rod locations, shroud, thermal shields and pressure vessel, is shown in Fig. 4.31.

Figure 4.32 is a top view of the core showing a fuel element cell.

The nuclear characteristics given in Table 4.7 are those obtained in the final design studies. Since the core design was not completed while these studies were being performed, these characteristics, in some cases, contain preliminary design assumptions. Design analysis studies refining the core nuclear characteristics set forth below are in progress.

TABLE 4.7

Nuclear Analysis Design Characteristics

Overall Performance Data	
Reactor thermal power output	9.35 megawatts
Core life requirements	18.70 megawatt-years
Design core life	18.70 megawatt-years

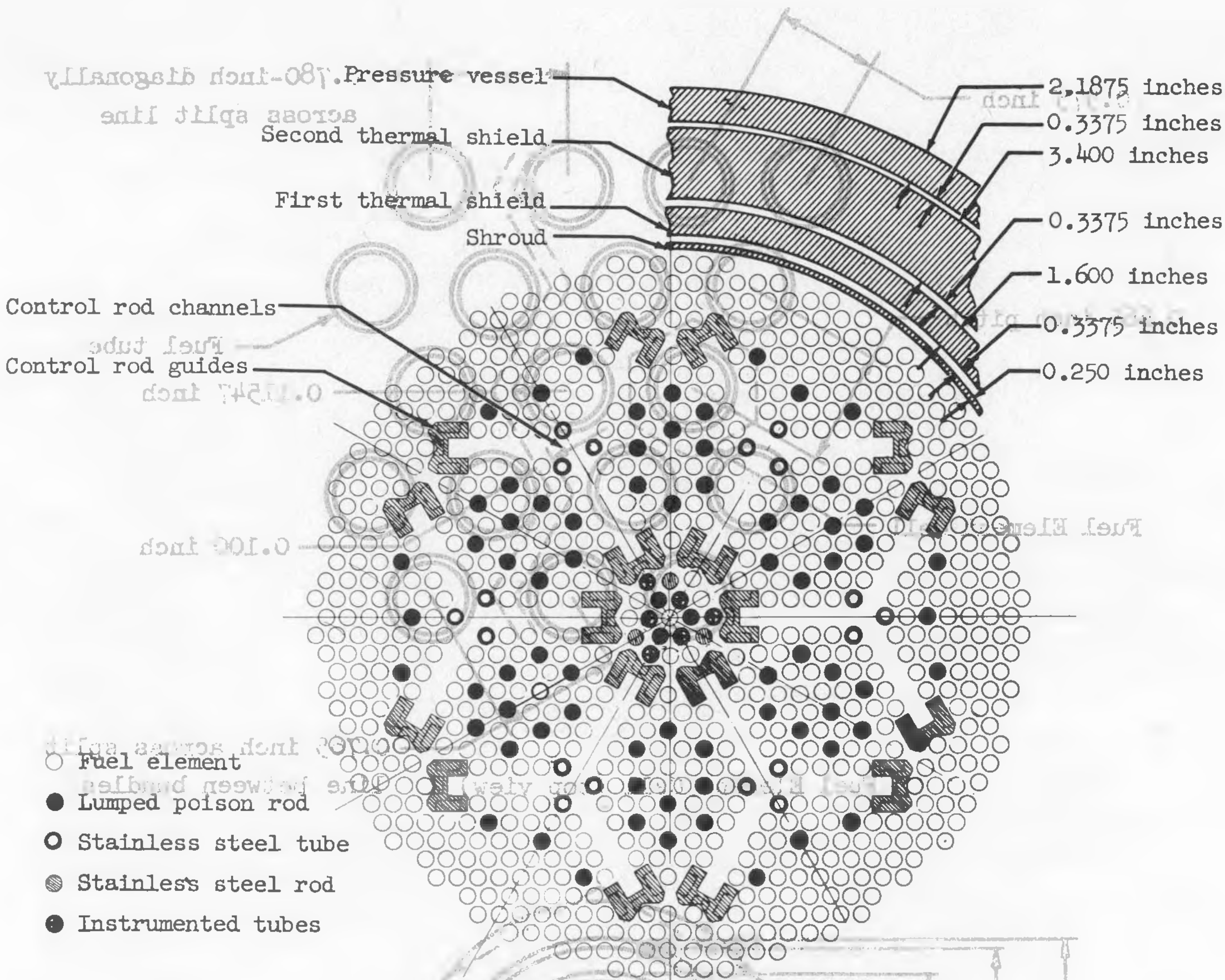

Mean Diameters	Diameter (inches)		
Equivalent core diameter	22.48	Number of fuel elements	727
Outer edge of outer fuel element	22.80		
Shroud ID	23.100	Number of lumped poison rods	75
Shroud OD	23.600		
First thermal shield ID	24.275	Fuel element spacing	
First thermal shield OD	27.475	(except across split line)	0.665 inches
Second thermal shield ID	28.150		
Second thermal shield OD	34.950	Core loading	
Pressure vessel ID	35.625		
Pressure vessel OD	40.000	U-235	28.062 kg
Active core height	30.000	Number of control rods	6

Fig. 4.31. PM-1 Core Configuration (top view)

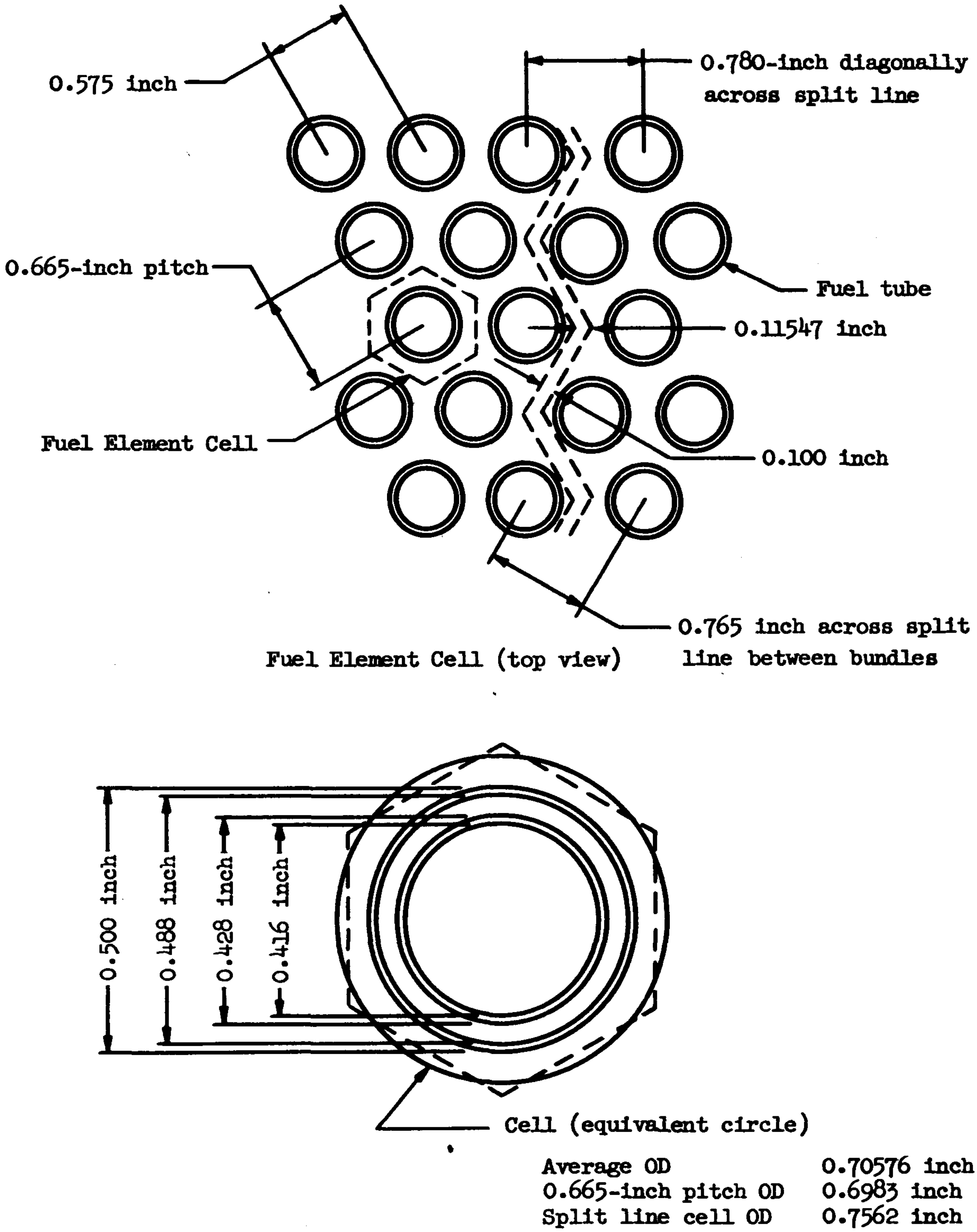

Fig. 4.32. Section of Core Showing A Fuel Element Cell

TABLE 4.7 (continued)

Average core coolant temperature	463° F
Core Design Characteristics	
Geometry, right circular cylinder (approximately)	
Diameter	23 inches
Height (active)	30.0 inches
Moderator, coolant and reflector	H_2O at 1300 psia
U-235 inventory	28.062 kilograms
U-235 burnup (18.7 megawatt-years)	9.0 kilograms
Fuel Element Data	
Tubular, cermet-type	
Pitch, triangular	0.665 inch
Outside diameter	0.500 inch
Inside diameter	0.416 inch
Clad thickness	0.006 inch
Clad material	Modified AISI-347 SS
Meat thickness	0.030 inch
Meat composition	
U-235	38.6 grams
UO_2	26.12 wt %[1]
SS (AISI-304)	73.88 wt %[1]
Length of fuel element (active)	30.0 inches
Number of fuel elements	727

[1]Based on theoretical densities of material; actual densities will be determined later pending packing fraction data.

TABLE 4.7 (continued)

Control System Characteristics	
Control rods	
Number of Y-shaped rods	6
Composition[2]	Eu_2O_3 in SS
Length (absorber)	30.0 inches
Blade width (absorber)	3.5 inches
Blade thickness (absorber)	0.25 inch
Lumped poison rods	
Number	75
OD	0.50 inch
Material	Boron steel
Composition	0.04 gram of natural boron per cubic centimeter

2. Fuel Element Loading Studies

The objective to be met was the determination of fuel loading specifications. The design conditions are that the heat production rate be 9.35 megawatts and the core life be 18.70 megawatt-years. The cold core temperature is 68° F and the hot core temperature is 463° F. Moderator (and coolant) is water at 1300 psia.

Results of the preliminary design studies established the general design of the core to be as follows:

Geometry, right circular cylinder	(approximately)
Diameter	23.0 inches
Equivalent core diameter	22.48 inches
Height (active)	30.0 inches

[2]Specification studies are in progress

Fuel element OD	0.50 inch
Fuel element ID	0.416 inch
Fuel matrix thickness	0.030 inch
Clad thickness	0.006 inch
Pitch, triangular	0.665 inch

In this study, the four basic cores shown in Fig. 4.33 were investigated. The variables considered were:

(1) UO_2 concentration in the fuel matrix.

(2) Number of fuel elements.

(3) Number and location of stainless steel tubes.

(4) Number of lumped poison rods.

(5) Two different control rod guide designs.

The fuel loading was so established that, in addition to the hot clean critical mass, enough fuel was included for an 18.7-megawatt-year life to overcome fission product poisons and to override the effect of the burnable poison which does not burn out. The stainless steel contained in the lumped poison rod and various other miscellaneous materials in the core are taken into account when determining the hot clean critical mass.

The fuel used is uranium dioxide (UO_2) where the uranium is enriched to 93.12% in the isotope U-235. Fuel depletion occurs at the rate of approximately 1.32 grams of U-235 per megawatt-day for a total burnup of 9.0 kilograms of U-235 in 18.7 megawatt-years.

Reactivity versus core life was calculated considering spatial nonuniform burnup of fuel and burnable poison in the core and nonuniform spatial buildup of fission product poisons. The calculation used a burnup code (programmed for an IBM-709 machine) which links a multigroup criticality code with a three-group multiregion, one-dimensional code and which calculates burnup and buildup of the different materials, including burnup of the lumped burnable poison.

Fuel Loading (kg U-235)

U-235 in FM* (wt %)	25	26	27	26.12
Core				
I and I-A	26.7	27.8	29.0	
II and II-A	27.6	28.8	30.0	
III and III-A	26.3	27.4	28.5	
IV				28.1
U-235 per tube (gm)	36.825	38.415	40.015	38.600

* Based on theoretical densities

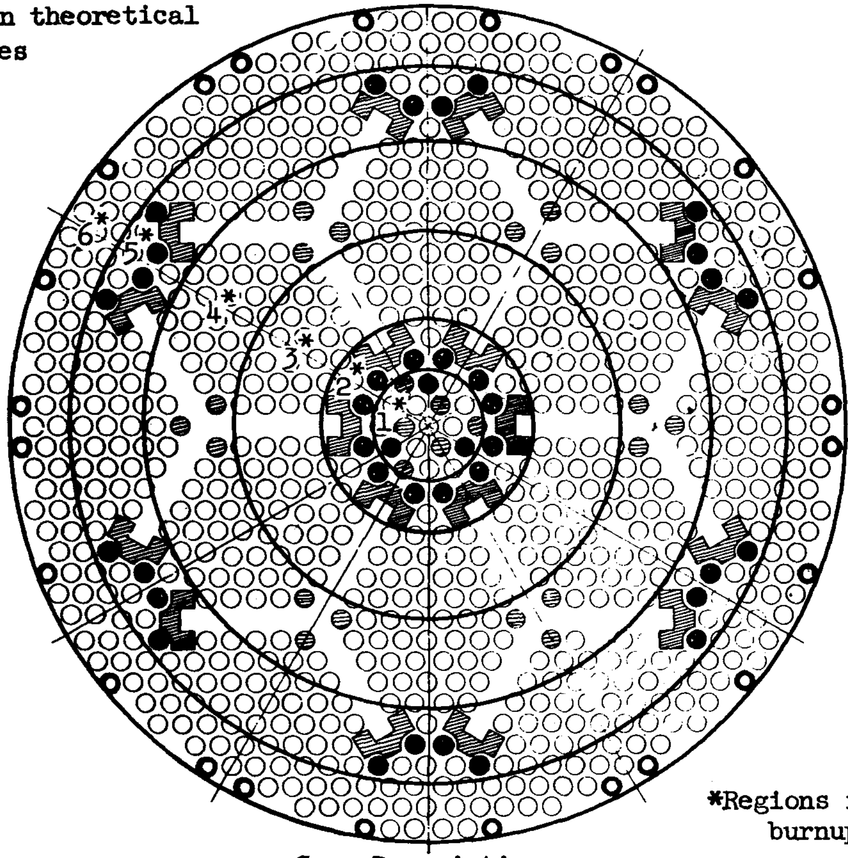

*Regions for nonuniform burnup studies

Core Description

Core	I	I-A	II	II-A	III	III-A	IV
⊜ (24 tubes)	SS	SS	SS	SS	SS	SS	SS
○ (24 tubes)	SS	SS	Fuel	Fuel	Fuel	Fuel	Fuel
● (36 tubes)	Fuel	Fuel	Fuel	Fuel	H_2O	H_2O	H_2O
Fuel elements	725	725	749	749	713	713	727
Lumped poison rods	89	77	89	77	89	77	75
Stainless steel rods (center bundle structure)	3	3	3	3	3	3	3
Stainless steel tubes	48	48	24	24	24	24	24
Control rod guides (cells)	54	54	54	54	54	54	90
Control rod H_2O channels (cells)	96	96	96	96	96	96	96
H_2O cells	0	12	0	12	36	48	0
Equivalent core OD	22.48 inches						

Fig. 4.33. Fuel Element Loading Studies--Core Description

The core was divided into six regions in both the radial and axial directions. The flux distribution in the core was obtained for the initial core loadings, followed by calculation of the burnup of fuel and burnable poison and of the formation of fission product poisons for each region over a given time interval (100 days at operating power). The new concentration of each material in each region was then determined, and the new flux distribution in the core was obtained. The entire process was repeated until the end of core life was reached.

The effect of nonuniform spatial burnup of reactivity versus core life for Core 4 (Fig. 4.33) is shown in Fig. 4.34. These curves are for the hot operating core conditions (equilibrium xenon and other fission product poisons). Curve 1 is for uniform burnup of fuel and burnable poison in a homogeneous core, and Curve 3 is for axial nonuniform burnup in a homogeneous core. Curve 2 is for radial nonuniform burnup of the reference core. The combined effects of radial and axial nonuniform burnup of the reference core are shown as Curve 4.

For the above burnup calculations, the lumped burnable poison was distributed as shown in Fig. 4.31.

Results of these nonuniform burnup fuel loading studies are given in Fig. 4.35 which shows the core life as a function of the weight percent loading of UO_2.

Analysis of these curves resulted in the fuel element specification of 38.6 grams of U-235 per fuel element.

3. Lumped Burnable Poison Studies

Preliminary design burnable poison studies indicated that an all lumped burnable poison system with boron concentrations of approximately 0.04 to 0.06 grams of natural boron per cc in poison rods would be suitable for a burnable poison system.

Final design studies initiated during the past quarter consisted of analysis to optimize the size and poison concentration specifications in order to minimize control requirements and maximize core life. Fuel loading studies described above, in which a nominal 0.04 gram of boron per cc of rod was used for the lumped poisons, included some nonuniform spatial placement of the rods in the core.

Uniform burnup studies evaluating three different size rods were completed, assuming uniform distribution of the lumped poison. The lumped poison rods were 0.50, 0.485 and 0.470 inches OD (including a 0.007-inch clad). This range in OD was chosen so that it would be con-

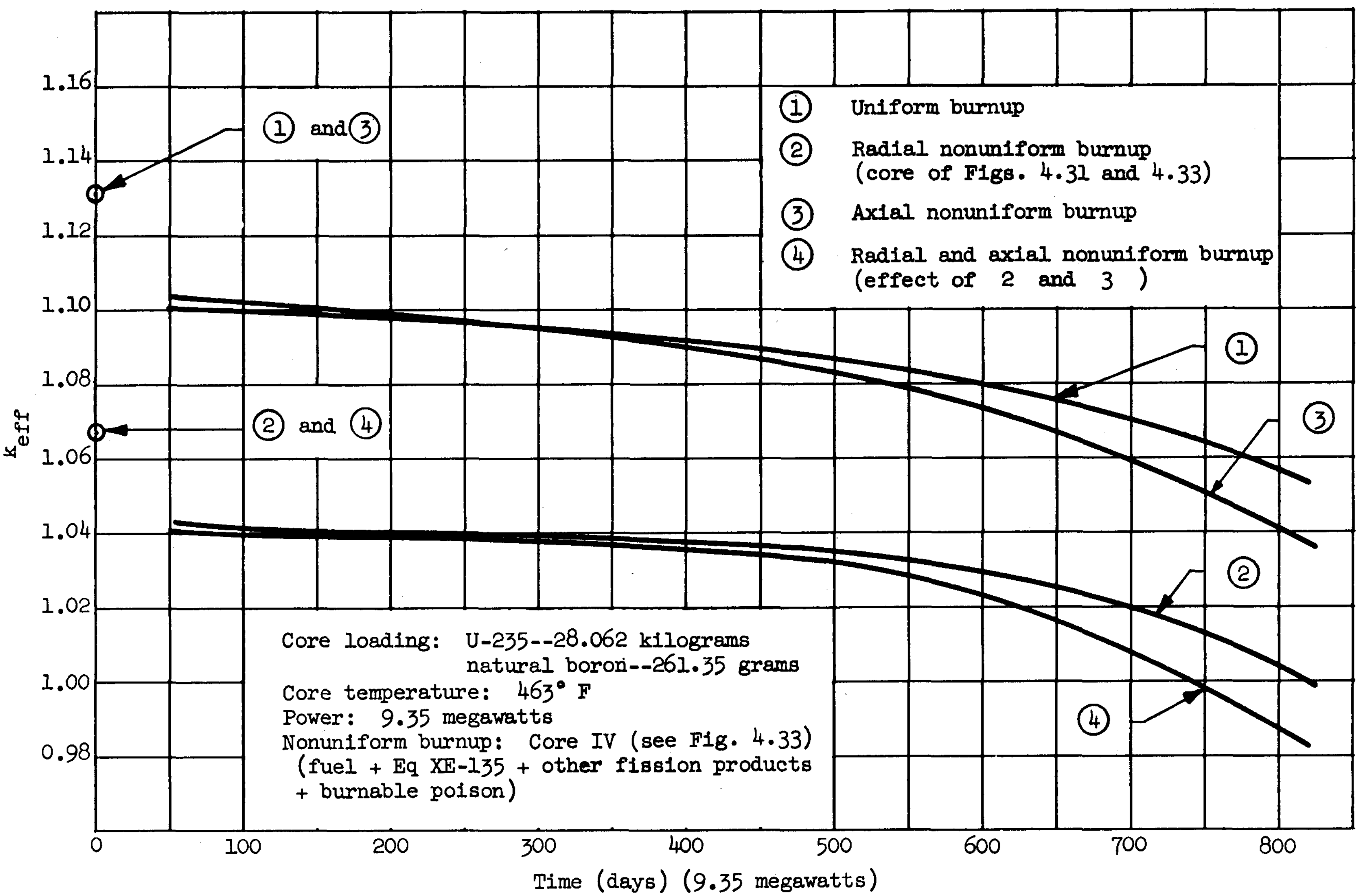

Fig. 4.34. k_{eff} Versus Time

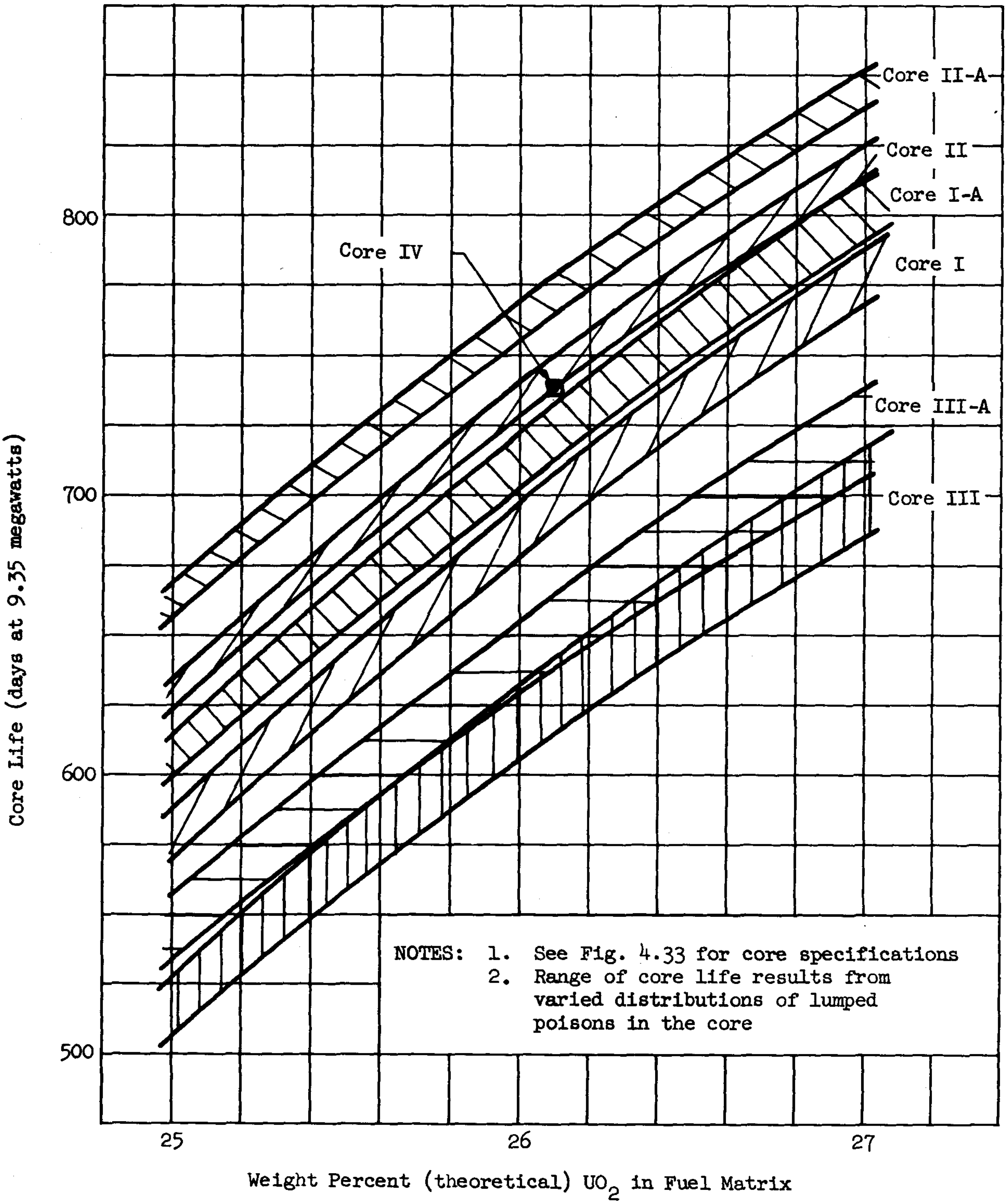

Fig. 4.35. Core Life Versus UO_2 Concentration

sistent with the final core design and coolant flow rates. The poison concentrations in rods were varied from approximately 0.03 to 0.07 grams of natural boron per cc of the poison section of the rods.

Results of these studies are shown in Figs. 4.36, 4.37 and 4.38. All curves are for operating conditions. Figure 4.36 shows k_{eff} versus core life for different poison concentrations in the 0.5-inch OD rod. Figures 4.36 and 4.37 show k_{eff} versus core life for different poison concentrations for the 0.485-inch and 0.470-inch OD rods, respectively. Curve 1 represents k_{eff} versus time for the core with no burnable poison. The effect of the stainless steel in the lumped poison rods is shown by Curve 2. These curves represent the condition of having the stainless steel rods associated with the lumped poison rods (without the poison) in the core. Curves 3, 4, 5 and 6 show the effects of various boron concentrations.

Data which indicate the relative effect on core life and control requirements for the different systems are being evaluated. Further studies initiated include nonuniform burnup evaluation for systems of interest. Additional nonuniform distribution studies will be performed.

Rod design and worth. Rod geometric design studies were completed. The rod configuration and locations, consistent with fuel element locations, rod guides, etc., are shown in Figs. 4.31 and 4.39. The poison section of each arm of the rods is 0.25 inch by 3.50 inches by 30.0 inches. The control rod poison material is Eu_2O_3 in stainless steel and is clad with 1/32-inch stainless steel as shown in Fig. 4.39.

Studies to determine the worths of 4-, 5- and 6-rod banks are in progress. Because of the increase in arm width (3.25 inches to 3.5 inches) and relocation (radius to center of rod from 6.16 inches to 6.10 inches), the worth of these banks will be greater than those given in the second quarterly progress report. The change from boron to europium will not significantly change the worth.

4. Control Studies

Evaluation of the control requirements for the preliminary design core was completed. Results were described in the preliminary design technical report. Design analysis studies to establish control requirements for the core described in Fig. 4.31 include determining the following:

(1) Cold clean core reactivity as a function of time.

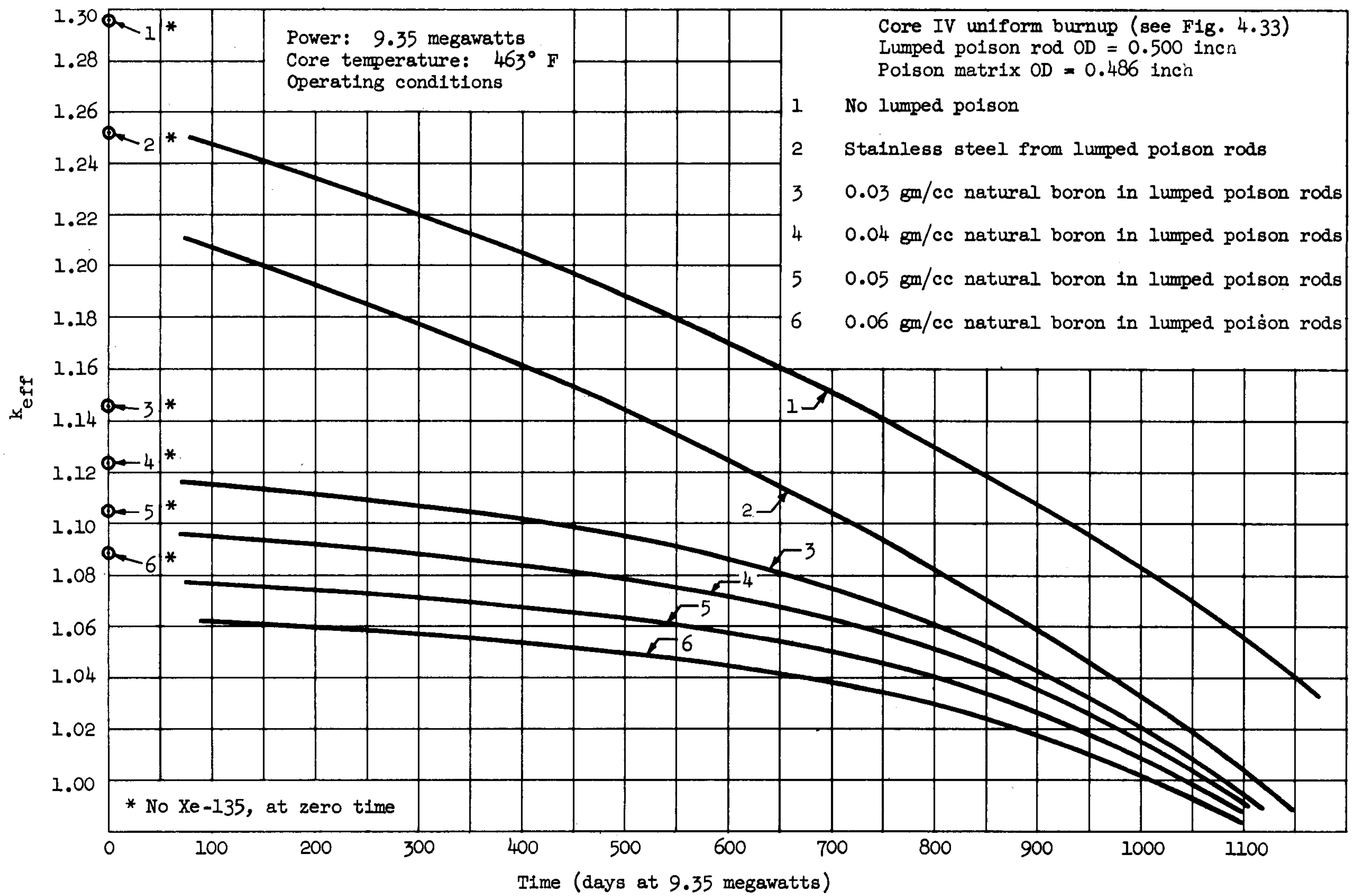

Fig. 4.36. k_{eff} Versus Time for Different Lumped Poison Concentrations

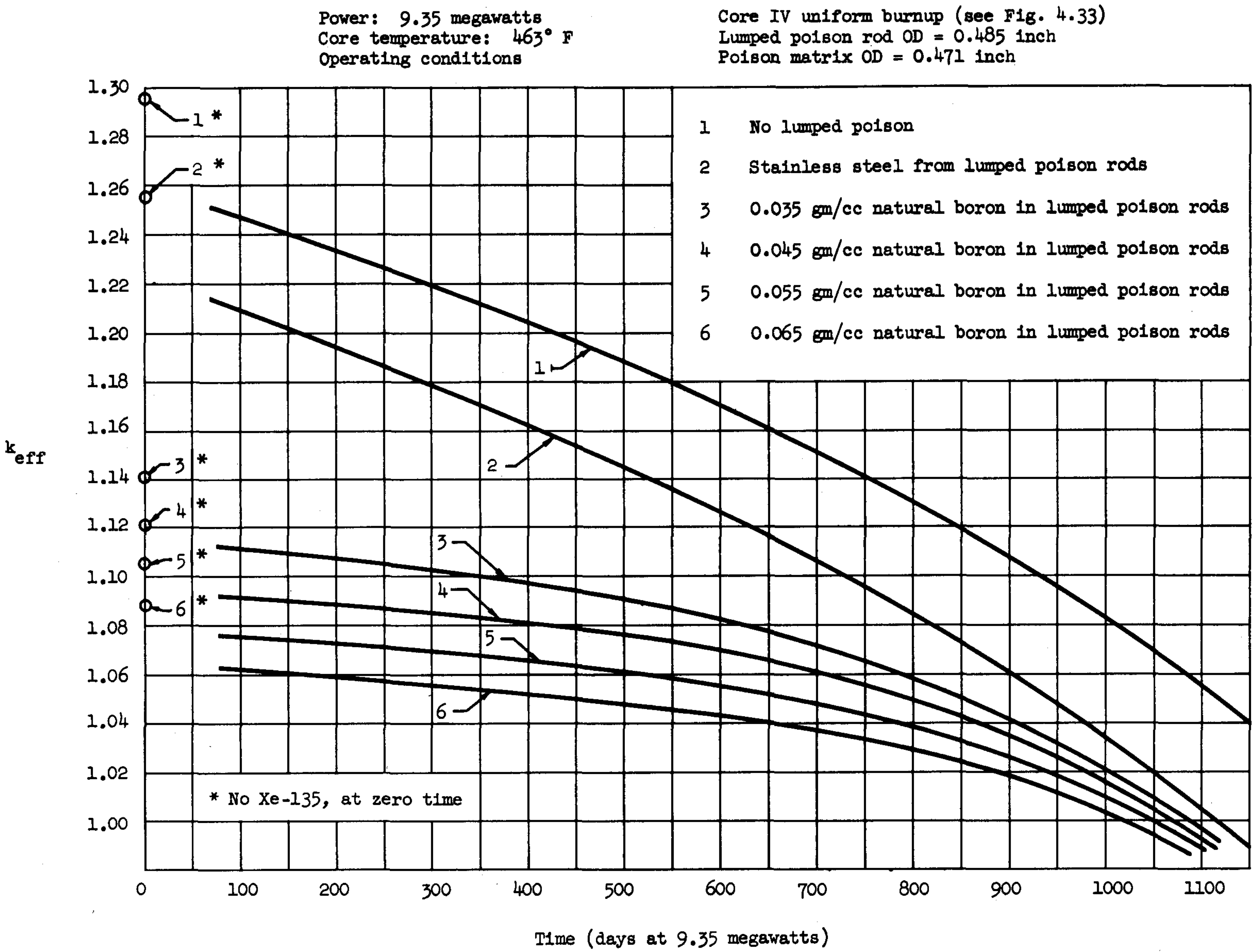

Fig. 4.37. k_{eff} Versus Time for Different Lumped Poison Concentrations

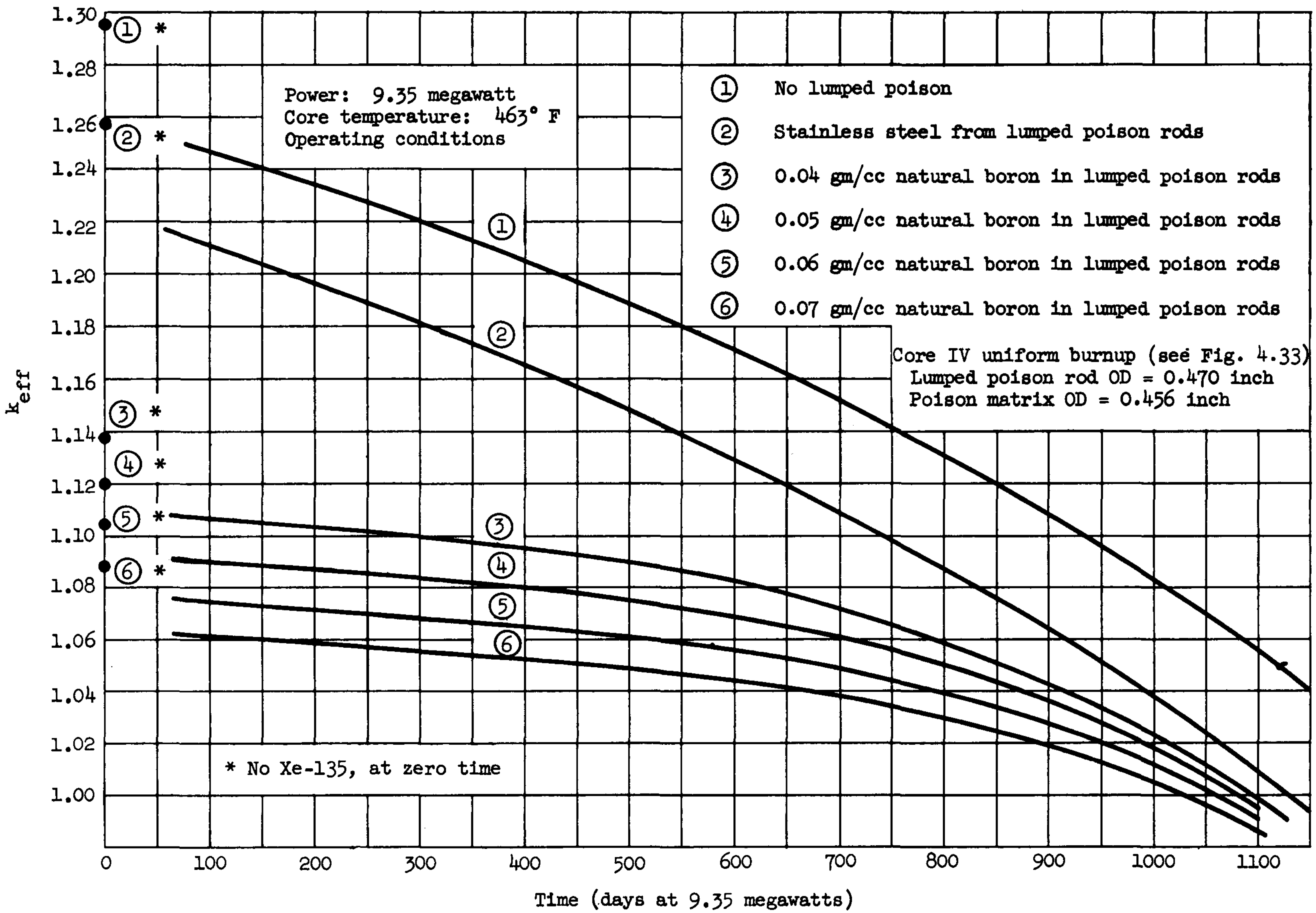

Fig. 4.38. k_{eff} Versus Time for Different Lumped Poison Concentrations

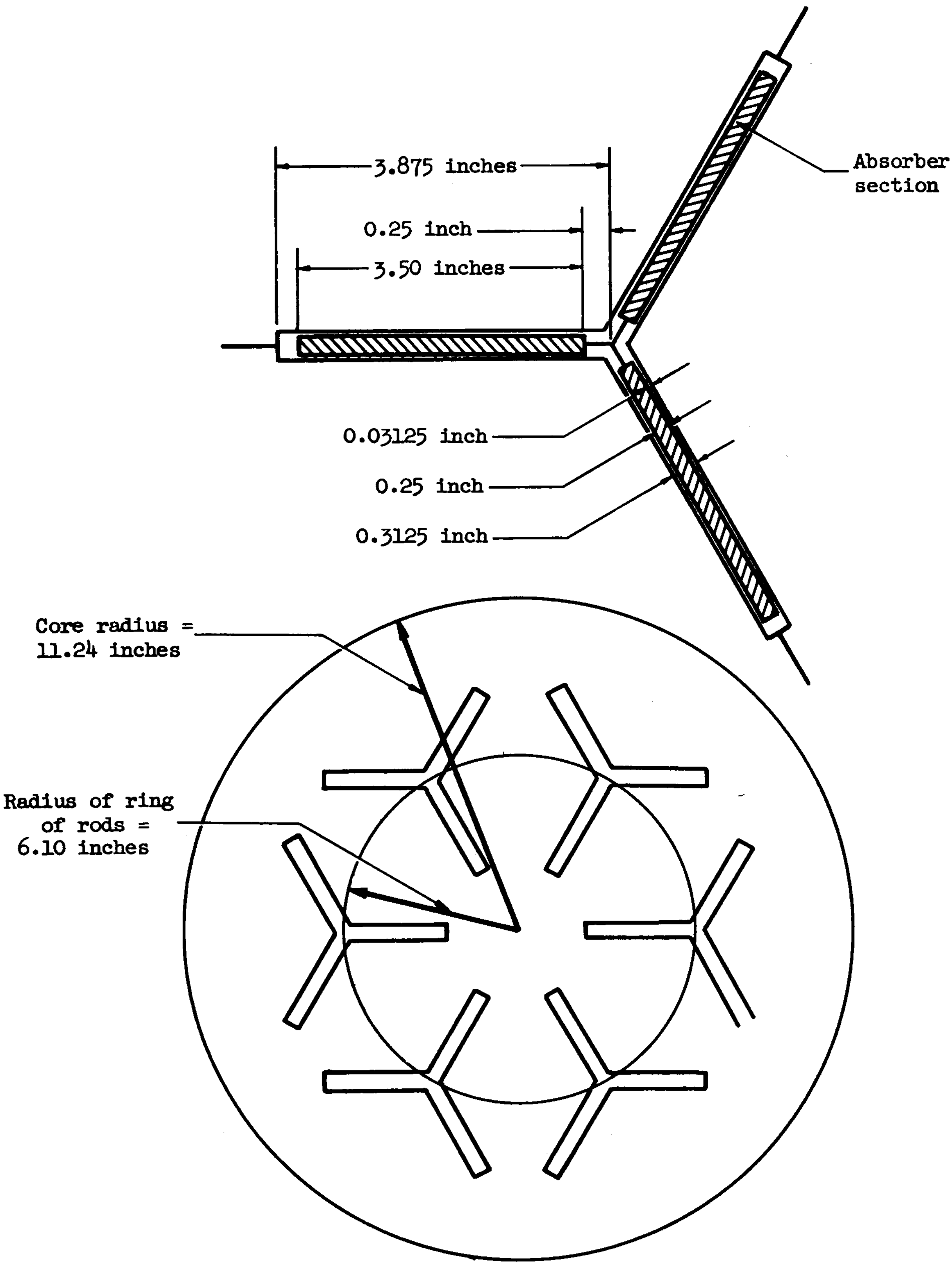

Fig. 4.39. Rod Configuration and Location

(2) Hot operating condition core reactivity as a function of time.

(3) Equilibrium and maximum xenon control requirements.

(4) Effect of fuel loading specifications on control requirements.

These studies will be completed during the next quarter. Evaluation of stuck rod conditions in terms of rod worth and rod requirements will also be completed during the next quarter.

Control rod material. Preliminary nuclear studies have shown that a number of materials, such as boron, hafnium, cadmium-silver-indium, europium and gadolinium-samarium, satisfy the nuclear requirements for control rod materials. Consideration of availability, metallurgical fabricability, radiation damage and other mechanical properties have led to the selection of europium (Eu_2O_3 in stainless steel) as the control rod material.

Studies to establish the europium weight fraction specification for the rod design given above were started. A preliminary evaluation similar to studies described in the Second Quarterly Progress Report (MND-M-1813) was completed. A more detailed study to determine the thermal macroscopic absorption cross section as a function of core life is in progress.

Results of the initial evaluation of the nuclear characteristics of the rod material for different weight concentrations of europium are summarized in Table 4.8. The initial thermal, epithermal (0.0322 to 2.4×10^4 ev), and fast (2.4×10^4 to 1×10^7 ev) macroscopic absorption cross sections for the 15, 20, 25, 30 and 35 wt % Eu_2O_3 in stainless steel are given in Columns 3, 4 and 5. The epithermal and fast cross sections were weighted by the average energy dependent fluxes in the rod before being reduced to epithermal and fast constants.

A measure of the initial thermal "blackness" for the different concentrations is given in Column 7. This represents the fraction of incident flux transmitted through a thickness x calculated from the expression:

$$\frac{I}{I_0} = e^{-\Sigma_a x}.$$

TABLE 4.8

Nuclear Characteristics of Different Weight Concentrations of Europium

1	2	3	4	5	6	7	8	9	10	11	12
		Initial Σ_a (cm^{-1})						k_{eff} = 1.04		k_{eff} = 1.08	
Weight Percent Eu_2O_3 in Europium Oxide-Stainless Steel	Important Isotope (σath = 7800 Barns)	Fast (2.4×10^4 - 1×10^7 ev)	Epithermal (0.032 - 2.4×10^4 ev)	Thermal	$\frac{\phi_{poison}}{\phi_{core}}$	$e^{-\sigma a g \phi t}$	Σ_{ath} at t = 2 yr	$\frac{N}{N_o}$	Σ_{ath} at t = 2 yr	$\frac{N}{N_o}$	Σ_{ath} at t = 2 yr
15	E_u-151	0.008	0.580	13.92	0.034	0.875	12.20	0.92	12.88	0.85	11.84
20	E_u-151	0.010	0.692	17.82	0.026	0.901	16.06	0.94	16.81	0.89	15.82
25	E_u-151	0.012	0.790	21.44	0.022	0.917	19.67	0.95	20.48	0.91	19.51
30	E_u-151	0.014	0.878	24.62	0.019	0.928	23.03	0.96	23.89	0.92	22.96
35	E_u-151	0.015	0.956	27.98	0.017	0.935	26.18	0.97	27.08	0.94	26.18

As in the analysis described in the Second Quarterly Progress Report, MND-M-1813, two different methods were used for evaluating rod burnup. In both methods, however, only the thermal cross sections were considered. Essentially, the first method consisted of calculating the concentration of the absorbing isotope at time t from the expression:

$$\frac{N}{N_0} = e^{-\sigma_a g \phi t}$$

where.

$\frac{N}{N_0}$ = fraction of concentration remaining after time t (Column 7, Table 4.7

$g = \frac{\bar{\Phi}\text{ poison}}{\bar{\Phi}\text{ core}}$ = ratio of average flux in the poison to average core flux (Column 6, Table 4.8)

σ_a = thermal microscopic absorption cross section

ϕ = average core thermal flux = 8.0×10^{12}.

Then, the macroscopic thermal absorption cross sections were recalculated for t = 2 years. These values are shown in Column 8, Table 4.8.

In the second method, the concentration of absorbing nuclei at time t = 2 years was calculated by subtracting one nuclei for each neutron absorbed from the initial concentration. The number of excess neutrons that must be absorbed was calculated by multiplying the number of fissions required for two years of operation at full power by the excess number of neutrons that must be absorbed. Two cases were considered: (1) an average k_{eff} at operating conditions of 1.04 (0.04 excess neutrons per fission) and (2) k_{eff} = 1.08. The ratios of final-to-initial concentrations of the absorbing isotopes are given in Columns 9 and 11 of Table 4.8. The new Σa_{th} are given in Columns 10 and 12.

In the above studies, the high cross-section daughter formations were neglected, the isotope Eu-151 was assumed to be the sole absorber and the complete rod system was used to absorb the neutrons.

A detailed study to determine the change in the total macroscopic cross section over core life, considering the decay chain for Eu-151, was started (see Table 4.9).

TABLE 4.9

Europium-151 Decay Chain

$$
\begin{tikzcd}
 & \text{Gd-152} \arrow[r] & \text{Gd-153} \arrow[d] & \text{Gd-154} & \text{Gd-155} & \text{Gd-156} \arrow[r] & \text{Gd-157} \arrow[r] & \text{Gd-158} \\
\text{Eu-151} \arrow[r] & \text{Eu-152} \arrow[r] \arrow[u] \arrow[d] & \text{Eu-153} \arrow[r] & \text{Eu-154} \arrow[r] \arrow[u] & \text{Eu-155} \arrow[r] \arrow[u] & \text{Eu-156} \arrow[u] & & \\
 & \text{Sm-152} \arrow[r] & \text{Sm-153} \arrow[u] & & & & &
\end{tikzcd}
$$

Equations for determining the atomic densities of the isotopes have been written and programmed for numerical solution on the IBM-709 computer. These equations are of the form:

$$N_1(t) = N_1(t=0)\, e^{-(\sigma_1 \phi + \lambda_1)t} \tag{1}$$

$$N_L(t) = N_1(t=0) \prod_{J=1}^{L-1} \sigma_J \sum_{J=1}^{L} \frac{e^{-(\sigma_J \phi + \lambda_J)t}}{\left[\prod_{K=1}^{J} \left(\sigma_K + \frac{\lambda_K}{\phi} - \sigma_J - \frac{\lambda_J}{\phi}\right)\right]}$$

$$\times \frac{1}{\left[\prod_{M=J+1}^{L} \left(\sigma_M + \frac{\lambda_M}{\phi} - \sigma_J - \frac{\lambda_J}{\phi}\right)\right]}$$

where

$$K \geq J, \quad \left[\prod_{K=1}^{J} \left(\sigma_K + \frac{\lambda_K}{\phi} - \sigma_J - \frac{\lambda_J}{\phi}\right)\right] = 1.0$$

$$M > L, \quad \left[\prod_{M=J+1}^{L} \left(\sigma_M + \frac{\lambda_M}{\phi} - \sigma_J - \frac{\lambda_J}{\phi}\right)\right] = 1.0$$

where:

$N_1(t=0)$ = atomic density of the natural isotope at time zero

$N_1(t)$ = atomic density of the natural isotope at time t

$N_L(t)$ = atomic density of the L^{th} isotope at time t

σ_L = microscopic cross section of the L^{th} isotope

λ_L = decay constant for the L^{th} isotope

ϕ = thermal flux

t = time.

Checkout of the code is in progress. This study will be completed during the next quarter.

5. Power Density Distribution

Studies to determine power density distribution for the core, including the effect of rod insertion and burnup, were completed. These studies were undertaken to determine the axially integrated radial power distribution as a function of core lifetime. From this data, "peak power" fuel elements were located for coolant flow requirement evaluation.

Gross power density distribution obtained from these studies include:

(1) Two-dimensional radial power density distribution for the core without control rods (Fig. 4.40).

(2) Two-dimensional radial power density distribution for the core with six rods fully inserted (Fig. 4.41).

(3) Two-dimensional radial power density distribution for the core with three rods fully inserted (Fig. 4.42).

(4) One-dimensional "window shade" model axial power density distribution with three and six rods partially inserted for different insertions of the rod banks.

(5) One-dimensional power density distributions for the core without rods as a function of time.

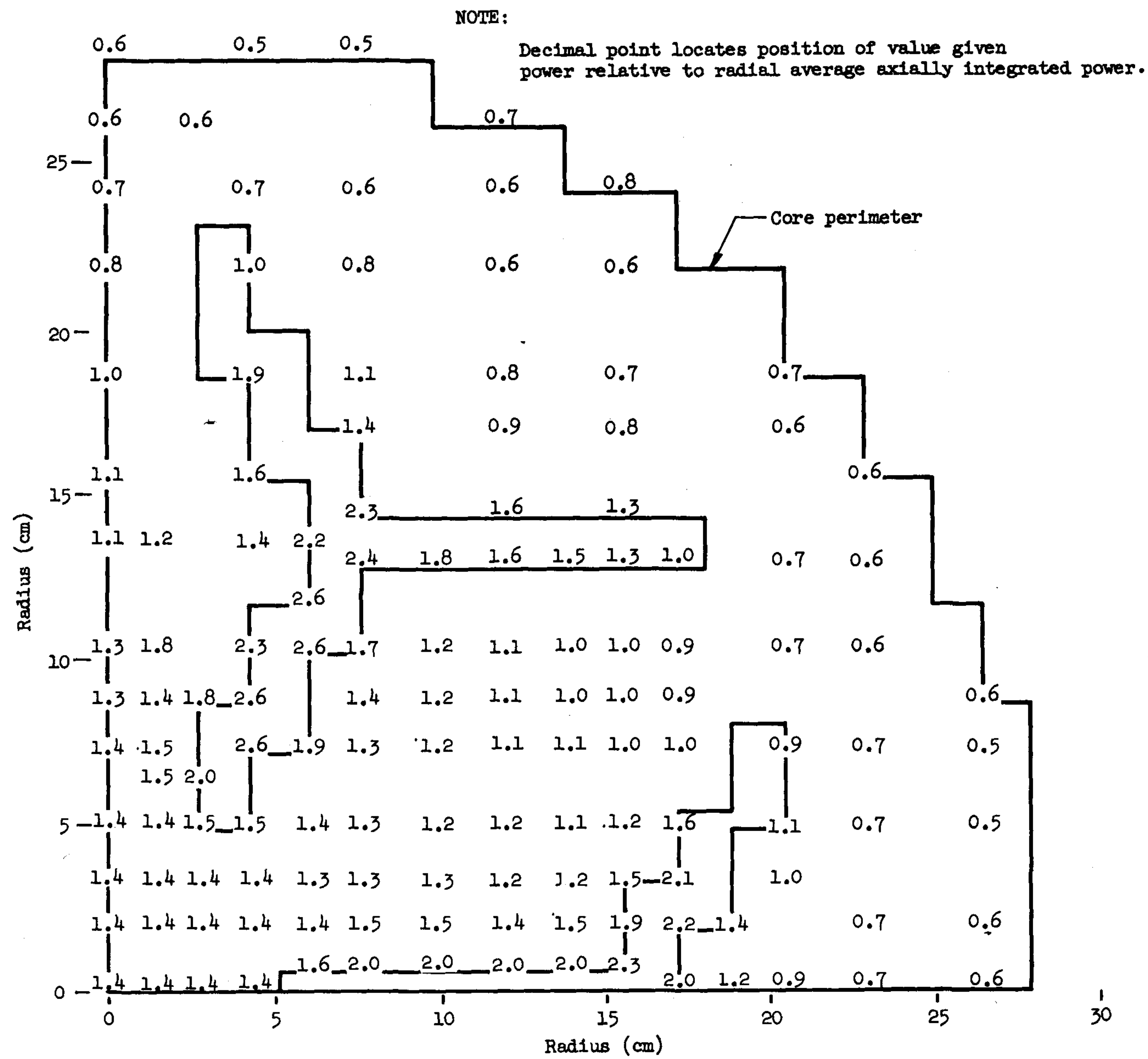

Fig. 4.40. Radial Power Density Distribution with Control Rods Fully Withdrawn

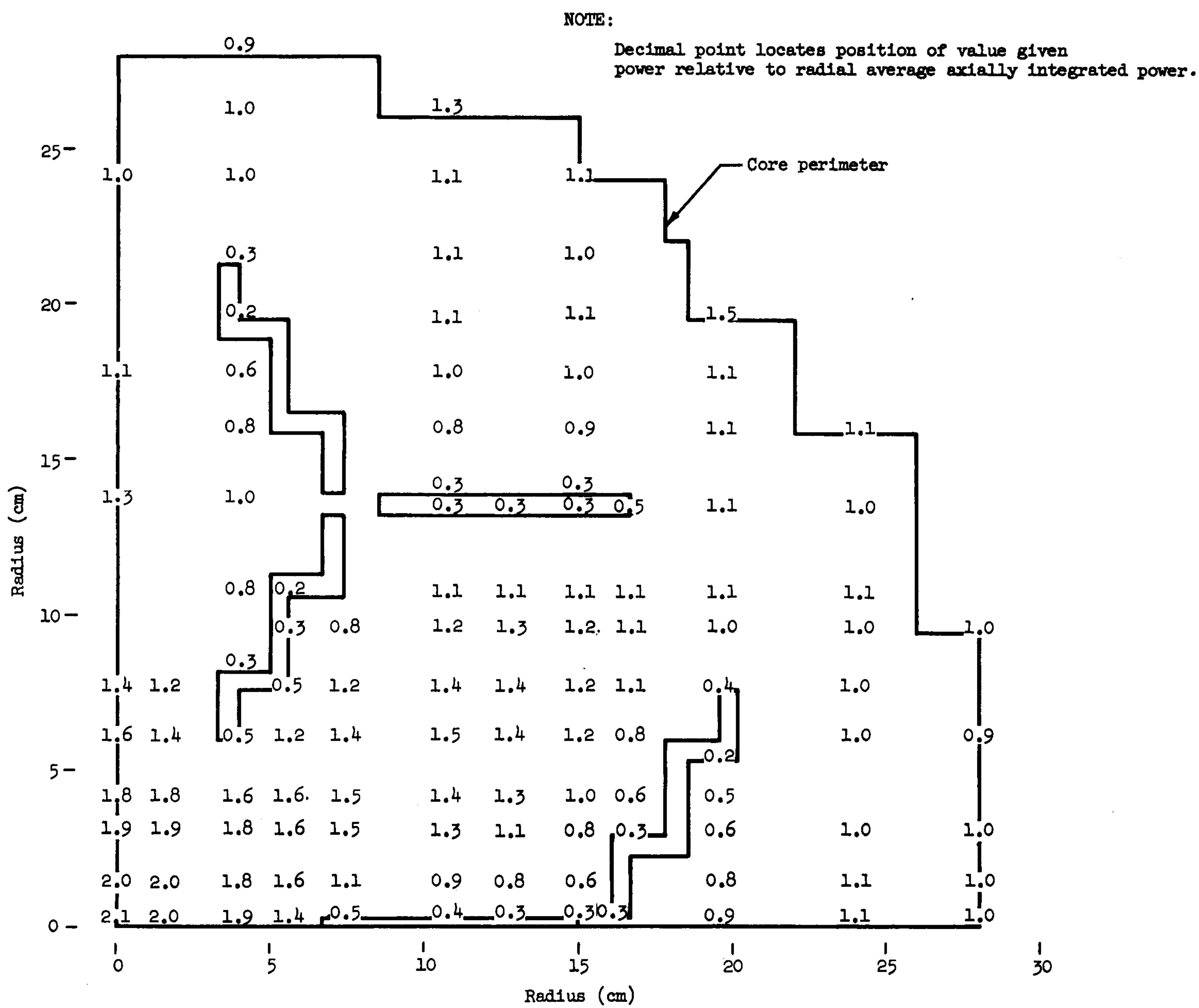

Fig. 4.41. Radial Power Density Distribution with Six Control Rods Fully Inserted

NOTE:

Decimal point locates position of value given power relative to radial average axially integrated power.

① Control rod inserted.
② Water channel.

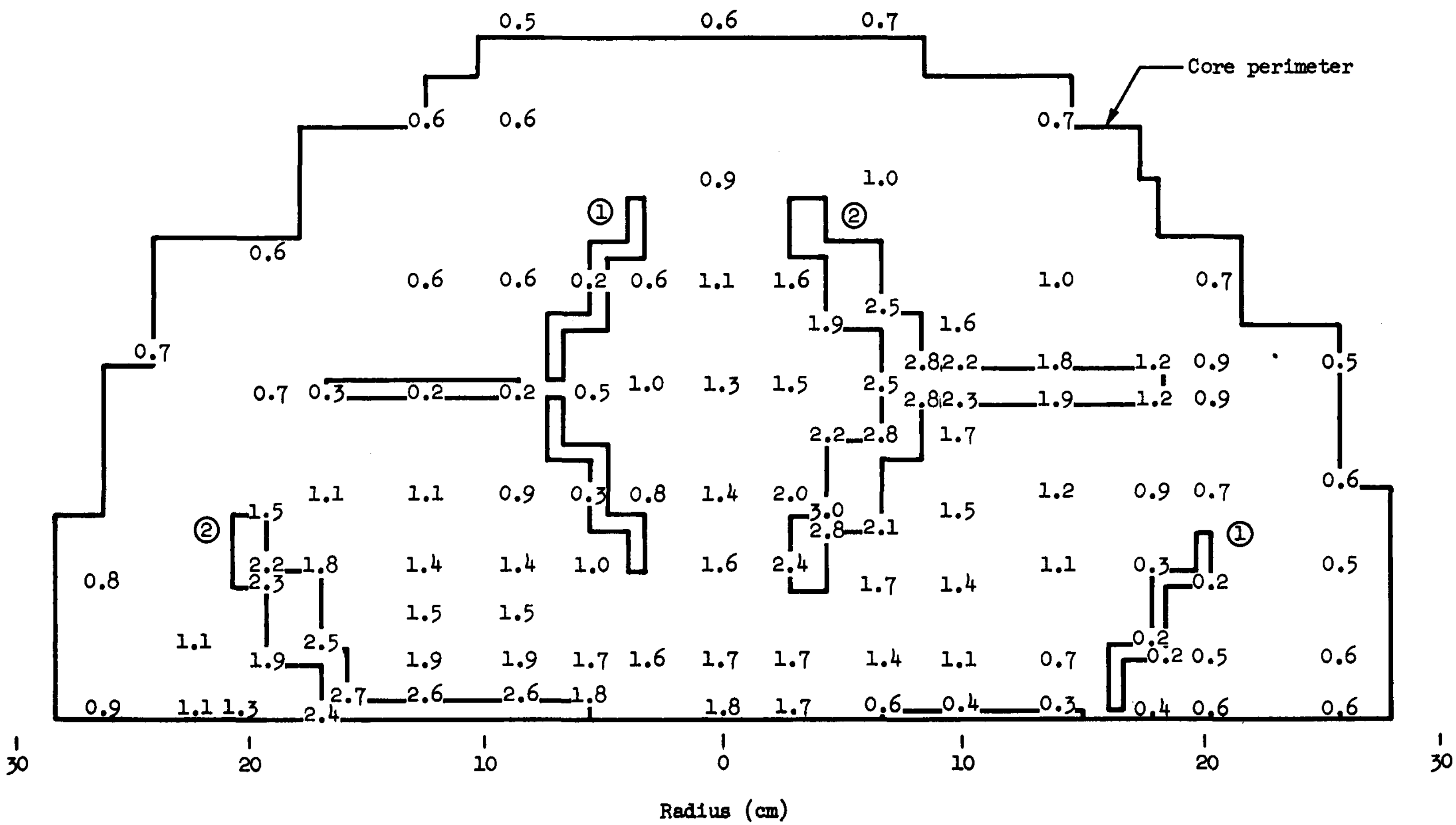

Fig. 4.42. Radial Power Density Distribution with Three Control Rods Fully Inserted

The ratios of the power developed in a fuel tube to the power developed in an average fuel tube for representative "peak" locations are given in Table 4.10. The approximate fuel element locations are shown in Fig. 4.43.

TABLE 4.10

Relative Radial Power Distribution

Fuel Element Location (see Fig. 4.43) 1	2	3	4	5	Percent of Control Rod Bank Insertion
6 Control-Rod Bank					
0.6	1.0	1.2	1.5	2.2	100.0
1.6	1.6	1.7	1.3	1.7	72.2
1.8	1.7	1.7	1.3	1.7	65.6
2.1	1.9	1.9	1.3	1.6	45.9
2.3	2.0	2.0	1.3	1.5	19.7
2.4	2.1	2.1	1.2	1.4	0.0
3 Control-Rod Bank					
2.9	2.6	2.7	1.3	1.8	100.0
2.7	2.5	2.5	1.2	1.7	80.0
2.6	2.3	2.3	1.2	1.6	49.9
2.5	2.2	2.2	1.2	1.5	26.2
2.4	2.1	2.1	1.2	1.4	0.0

NOTE: Power relative to average power per fuel element.

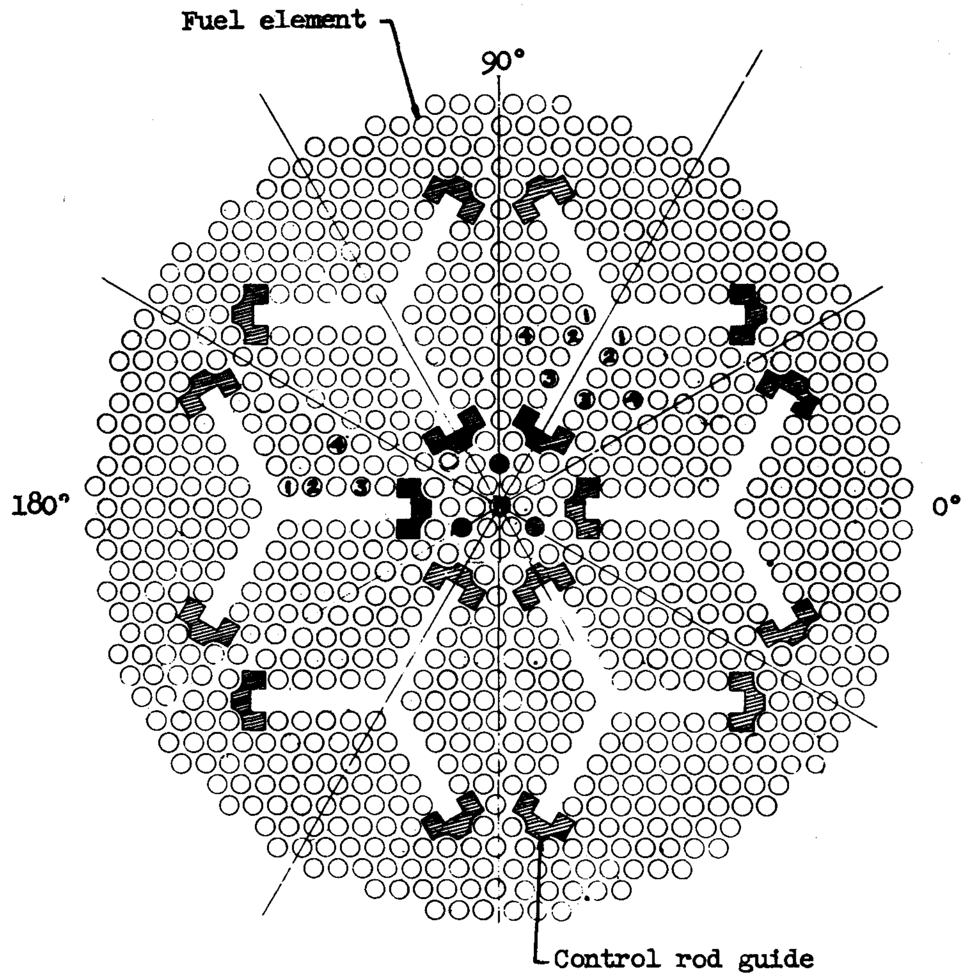

Fig. 4.43. Location of Fuel Elements for Power Distribution Studies

Essentially, the procedure used to obtain the above data was as follows:

(1) The power ratios in the rodded and nonrodded core were calculated for different rod insertions of the two banks from results of one-dimensional "window shade" power density distributions.

(2) The two-dimensional radial power density distributions shown in Figs. 4.40 and 4.41 (or Figs. 4.40 and 4.42 for the three-rod banks) were weighted according to information obtained in (1).

(3) A lifetime weighting factor for (2) was determined from one-dimensional temporal power density distributions obtained in the nonuniform burnup lifetime studies.

The "hottest" fuel elements are located near the control rod water channels, the center of the core and in the regions between the control rods. Since preliminary analysis (Second Quarterly Progress Report, MND-M-1813) indicated that there may be excessive power peaking in the fuel element located at the vertices of the control rod water channels (Fig. 4.43, Location 1), this fuel element has been replaced by a stainless steel tube (see Fig. 4.31). If detailed studies confirm this peaking, the stainless steel tube will be used (or a lumped poison rod if this does not adversely affect the rod worth).

Coolant flow rate calculations, described previously, were based on peak-to-average radial power of 1.9 for fuel elements other than those along the water channels and 2.1 for a fuel element along the rod channel.

From the results of Table 4.10 and Curve 4 of Fig. 4.34, it can be seen that under operating conditions:

(1) At no time in core life is there any excessive peaking for a six-rod bank operation after replacing the Location 1 elements.

(2) A three-rod bank can be used for at least the latter half of core life if the other three rods are partially inserted.

B. SHIELDING STUDIES

D. Owings, E. Divita, E. Koprowski

Shielding analysis performed during the third quarter consisted of:

(1) Thermal shield and reactor vessel studies.

(2) Determination of radiation heating after shutdown.

(3) Spent fuel removal and shipping cask design studies.

(4) Biological shield design.

(5) Studies of activation of the primary loop by corrosion products.

(6) Determination of radiation heating in shield water.

Thermal shield and reactor vessel studies are 80% complete. During the next quarter, radiation heating rates will be determined in the reactor vessel base and in the region of the inlet nozzle. After-shutdown radiation heating and shipping cask design studies are complete. Primary loop corrosion product studies will be extended to include determination of biological dose rates at points of interest throughout the Primary System packages and housing.

In addition, the following studies will be initiated during the next quarter:

(1) Determination of operating and after-shutdown dose rates within the primary packages and t e containment tanks of the final design.

(2) Determination of radiation heating rates within control rods and control rod guides.

(3) Earth shield activation studies.

1. Thermal Shield and Pressure Vessel Design

Neutron flux determination. Previously, neutron flux within the pressure vessel-thermal shield configuration has been determined by use of GE diffusion theory codes (Programs C and F) directly without modification. Although the neutron flux thus obtained may be correct within the fuel region to ±20%, greater error can be expected in regions where neutron inelastic scatter is significant. Basic cross-section data, used by Program C to complete diffusion constants for flux determination, do not include inelastic scatter cross sections. It may be expected that, in material such as iron where inelastic scatter is significant, an overestimate of flux with energy above the inelastic scatter threshold will occur with a corresponding underestimate of flux below the threshold energy.

An attempt has been made to account for inelastic scatter neutron energy degradation in iron by modifying the macroscopic neutron group constants obtained from Program C by the data of Ref. 1. Curves of the energy distribution of neutrons inelastically scattered by iron, as a function of incident neutron energy, were numerically integrated to determine inelastic "transfer" cross sections. Two cross sections may be defined to represent scatter to emitted neutron energies where inelastic scatter may reoccur or scatter to emitted neutron energies below the threshold energy for this event.

By definition:

$\sigma_{in_{TR}}(E_0)$ = the microscopic inelastic transfer cross section for inelastic scatter events in which the emitted neutron energy is less than the threshold for inelastic scattering

$\sigma_{in_{E\rightarrow E}}(E_0)$ = the microscopic inelastic transfer cross section for inelastic scatter events, in which the emitted neutron energy is greater than or equal to the threshold energy for inelastic scatter.

The total inelastic cross section at the incident energy E_0 is:

$$\sigma_{in}(E_0) = \sigma_{in_{TR}}(E_0) + \sigma_{in_{E\rightarrow E}}(E_0).$$

Fission spectrum weighed inelastic scatter cross sections were obtained for neutrons in iron above the threshold energy (0.85 mev) as:

$$\bar{\sigma}_{in_{TR}} = \frac{\int_{0.85\text{ mev}}^{\infty} \sigma_{in_{TR}}(E) \,;\, N(E)\,dE}{\int_{0.85\text{ mev}}^{\infty} N(E)\,dE}$$

and

$$\sigma_{in_{E\rightarrow E}} = \frac{\int_{0.85\text{ mev}}^{\infty} \sigma_{in_{E\rightarrow E}}(E) : N(E)\,dE}{\int_{0.85\text{ mev}}^{\infty} N(E)\,dE}$$

where N(E) is the fission neutron spectrum represented as:

$$N(E) = 0.453\ e^{-E/0.965}\ \sin h\ (2.29E)^{1/2}$$

Neutron diffusion constants for iron were obtained from Program C for three neutron energy groups of thermal, thermal to 0.85 mev and above 0.85 mev. Constants for the fast neutron group (above 0.85 mev) were modified as follows.

Scattering out cross section:

$$\Sigma^*_S = \Sigma_{S_{elastic}} + \bar{\Sigma}_{in_{TR}}.$$

Diffusion constant:

$$D^* = \frac{1}{3(\Sigma^*_{TR} + \Sigma_a)}$$

where

$$\Sigma^*_{TR} = \left[\Sigma_{S_{total}} + \Sigma_{in_{E \to E}}\right]\left(1 - \frac{2}{3A}\right)$$

$$\Sigma_{S_{total}} = \frac{\frac{1}{3D} - \Sigma_a}{1 - \frac{2}{3A}}$$

and A = atomic weight of the scattering nuclear. The constants $\Sigma_{S_{elastic}}$ and Σ_a are taken directly from Program C results. The modified constants Σ^*_S and D* are used as input for Program F which computes three energy group space distributed neutron flux.

Thermal shields and pressure vessel steel exterior to the active core are assumed to be iron for computation of neutron flux. Modified cross sections, computed by the above outlined procedure are used for neutrons of energies greater than the inelastic scatter threshold energy. Thermal neutron flux distribution through the thermal shields and pressure vessel, computed by the above methods, are given in Fig. 4.44.

Exterior flux suppressor effects. A significant amount of the total radiation heating within the reactor vessel along the core midplane is being produced by absorption of thermal neutron capture gammas created within the reactor vessel. Neutron moderation by shield water exterior to the reactor vessel produces a significant rise in the thermal neutron flux near the outer surface of the vessel. The effect on the thermal flux of placing a steel flux suppressor exterior and adjacent to the vessel insulation is shown in Fig. 4.45 for various flux suppressor thicknesses. The fluxes of Fig. 4.45 were computed, assuming a total of 5.25 inches of thermal shield between the reactor vessel and core. Gamma heating of the reactor vessel from thermal neutron capture gammas created in this region, assuming no exterior flux suppressor and a one-inch exterior flux suppressor, is shown in Fig. 4.46. Total radiation heating density in the reactor vessel may be expressed as a sum of exponentials of the form:

$$Q\,(X) = \sum_i Q_{0_i}\, e^{-\beta_i x}$$

where

$Q\,(X)$ = total heating rate at a distance x from the inner surface of the reactor vessel measured radially

Q_0 = heating rate at the inner surface

β = an attenuation factor through the vessel and is equal to $-\frac{1}{t}\ln\frac{Q_t}{Q_0}$

and t = the thickness of attenuator.

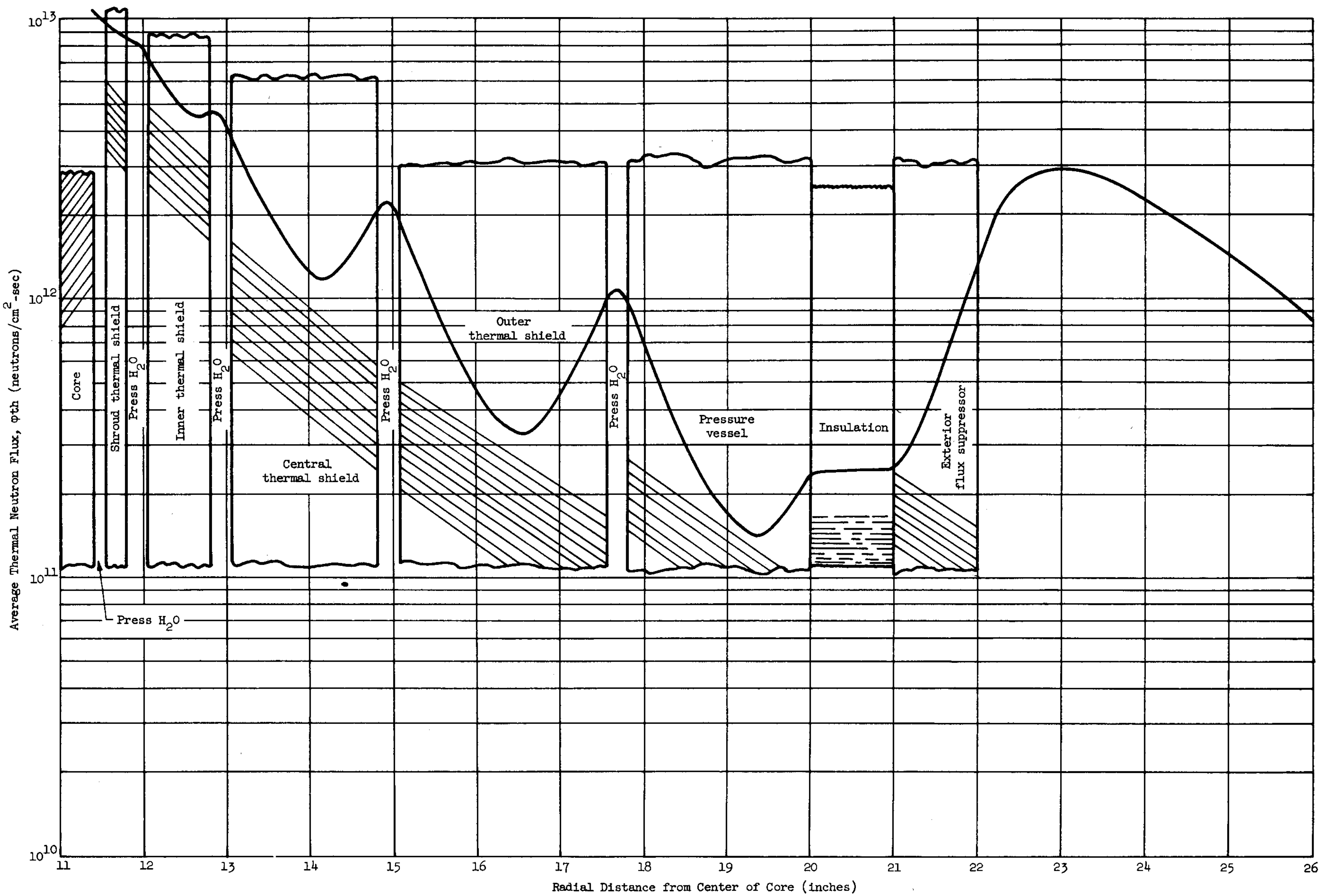

Fig. 4.44. Thermal Neutron Flux Exterior to Core Versus Radial Distance from Core Center (10-megawatt operation)

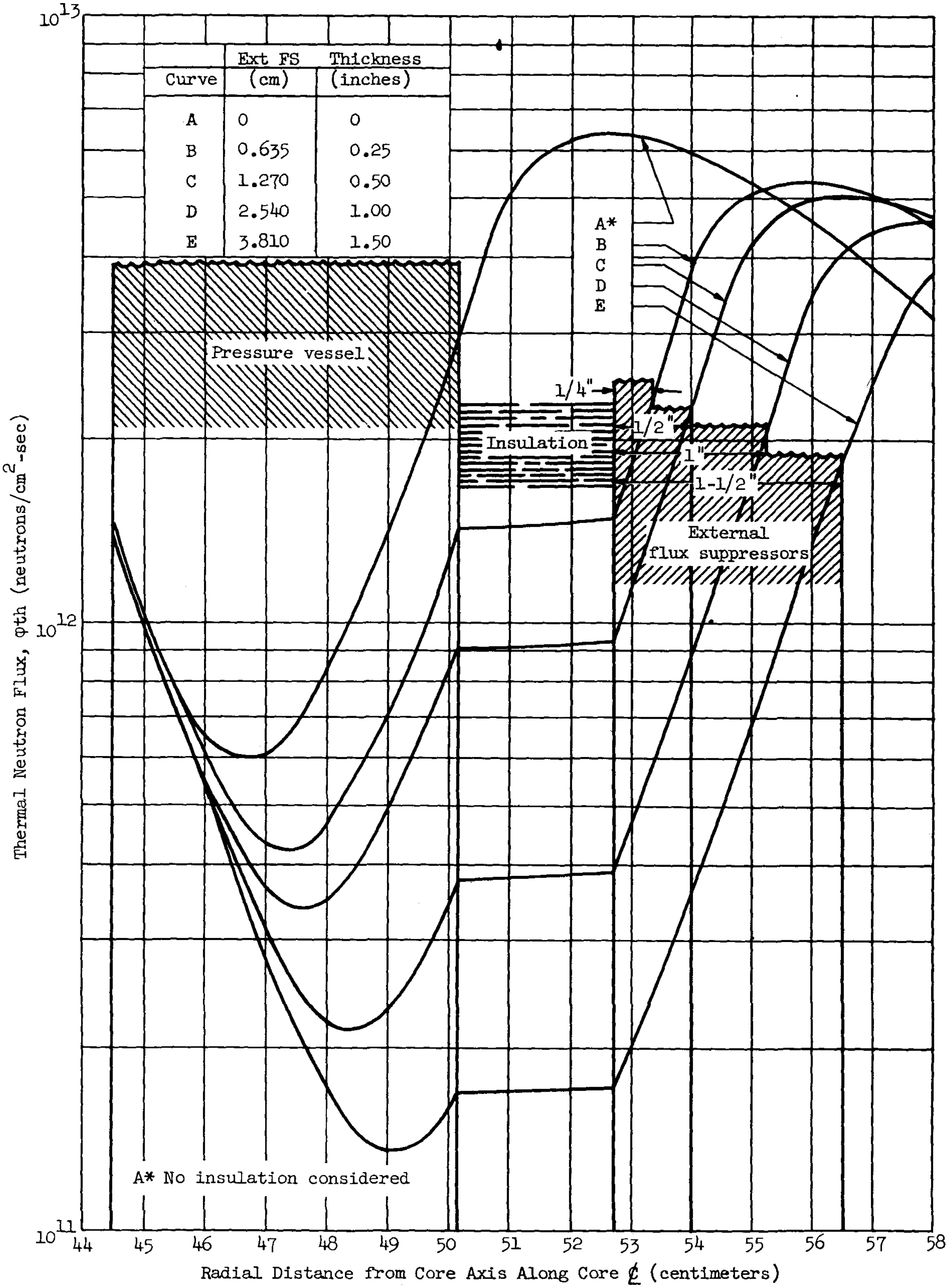

Fig. 4.45. Thermal Neutron Flux in Reactor Pressure Vessel for Various External Flux Suppressor Thicknesses (10-megawatt operation)

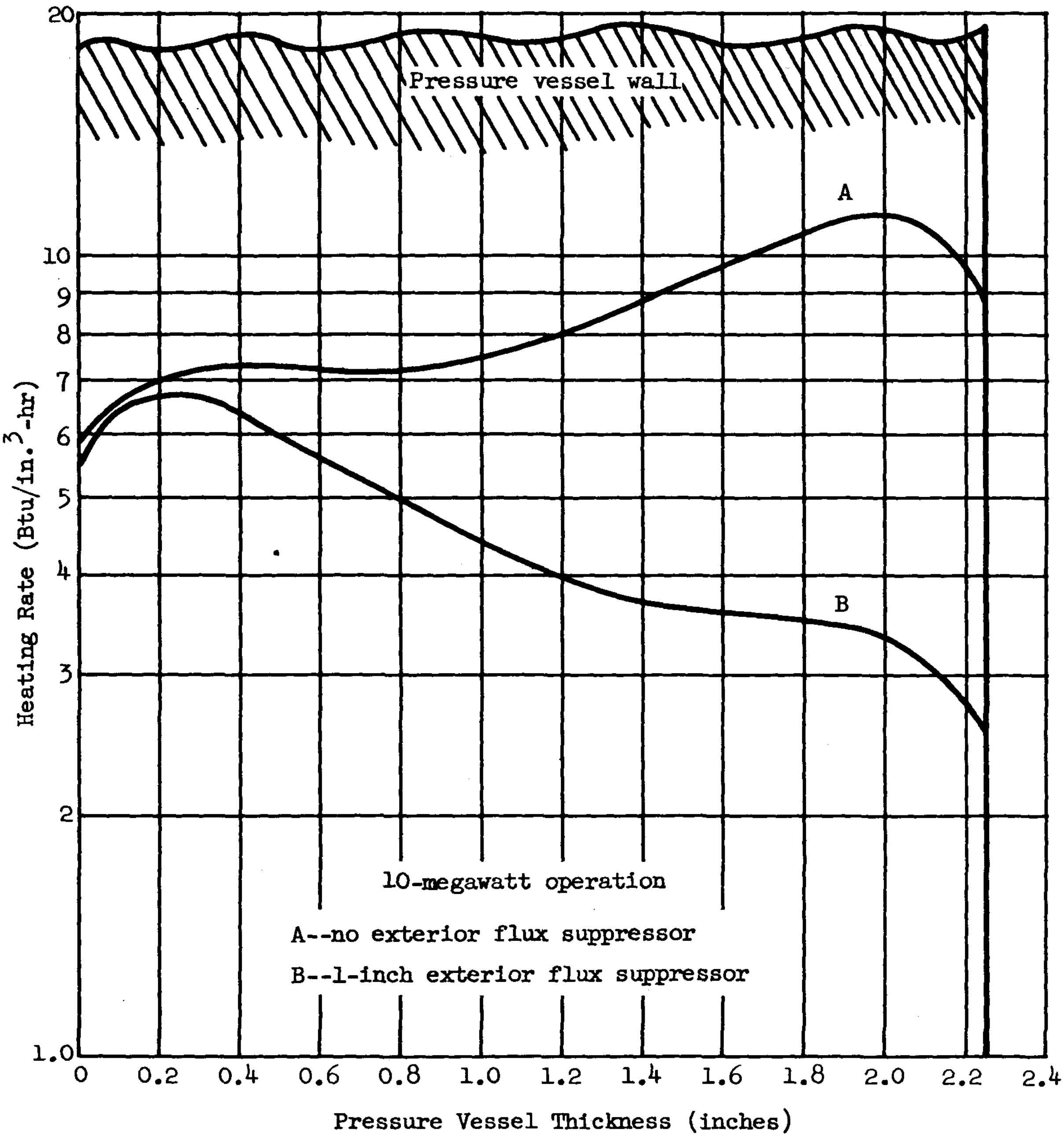

Fig. 4.46. Heating in Reactor Vessel from Thermal Neutron Capture Gammas Originating in the Reactor Vessel

Since thermal neutron capture gamma heating is a significant component of the total heating, it can be seen from Fig. 4.46 that the effect of the external flux suppressor is to increase β, since the ratio $\frac{Q_t}{Q_0}$ decreases. To a first approximation, the tangential thermal stress is proportional to $\frac{1}{\beta^2}$. Thus, the overall effect of adding the exterior flux suppressor is a decrease in tangential thermal stress.

It was determined that a total radial thickness of 5.25 inches of thermal shield placed within the reactor vessel and a 1-inch exterior flux suppressor is sufficient to reduce thermal stress in the core midplane region of the reactor vessel to tolerable values during normal 10-megawatt operation.

Heating rates in thermal shields and reactor vessel along core radial midplane. Radiation heating rates have been determined along the core radial midplane within components of a thermal shield pressure vessel configuration. The results are plotted in Fig. 4.47 which shows gamma heating rates during 10-megawatt core operation. The configuration consists of three interior thermal shields, pressure vessel and exterior flux suppression. Results of this analysis will be used to determine the final thermal shield configuration.

The dominant contributor to the total heating rates within the inner thermal shield is radiation originating in the core. In estimating core source strengths, it was assumed that the core had operated continuously at full power for two years. At this time, fission product activity and thermal neutron capture gamma activity will be at a maximum. Core gamma contribution to the total heating rate decreases significantly in regions beyond the central thermal shield. Thermal neutron capture gammas originating in the stainless steel regions exterior to the core become the dominant contributor to the total heating rate in the outer thermal shield, pressure vessel and exterior flux suppressor. Of less importance are gammas from inelastic scatter of fast neutrons and heat generation from elastic scattering of neutrons.

Neutron flux used to determine gamma source strengths was obtained by use of diffusion theory machine codes with the modifications previously described. Core constants were chosen to represent the condition of highest neutron flux over the practical life of the core.

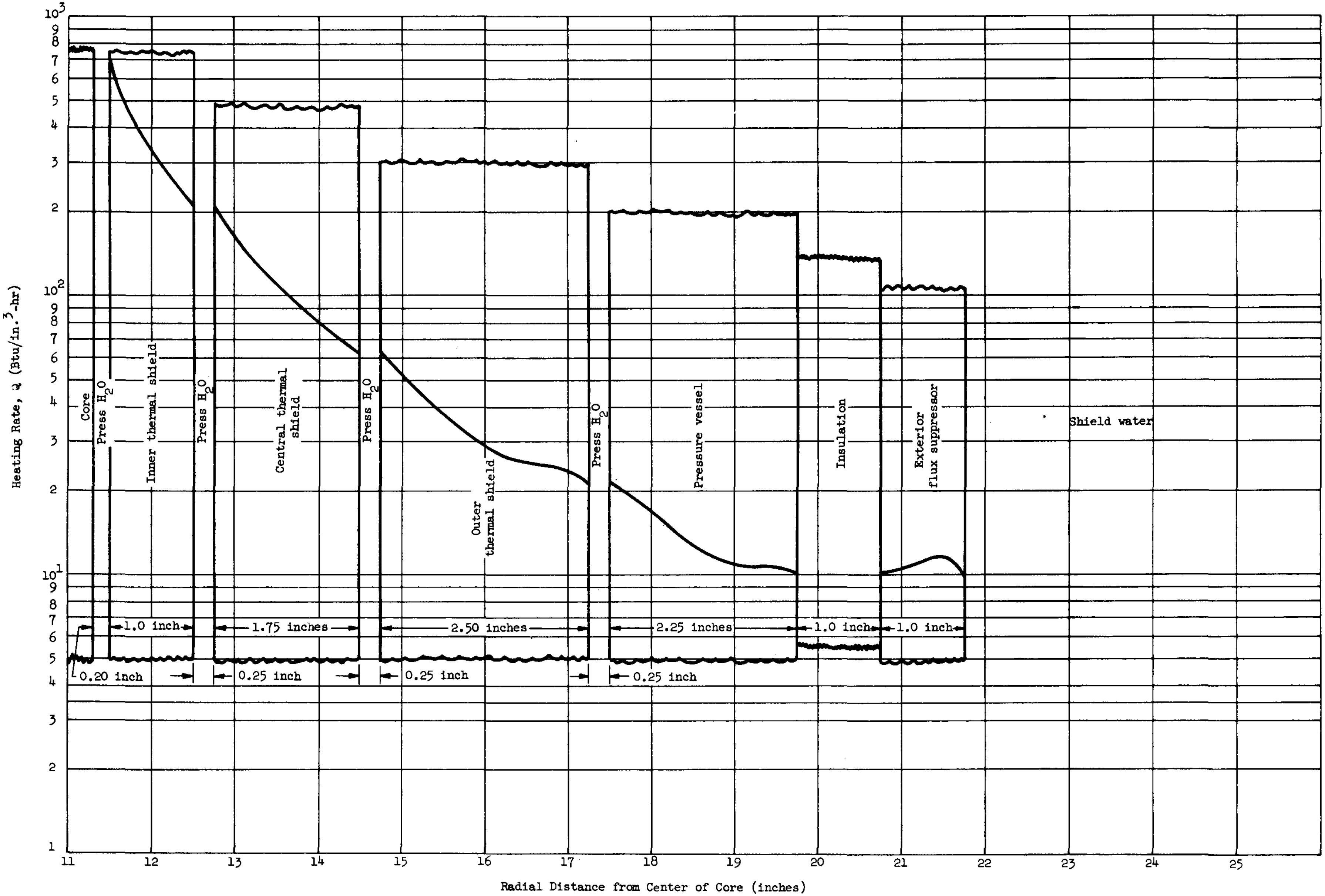

Fig. 4.47. Total Radiation Heating Along Core Radial Centerline
(10-megawatt operation)

For attenuation of core gammas, the core was assumed to be a homogeneous uniform cylindrical source. The cylinder was replaced by an equivalent line source with an appropriate self-attenuation factor by methods described in Rockwell (Ref. 2). Regions exterior to the core were assumed to be semi-infinite slab sources with exponential source strengths equivalent to the actual source strength along the reactor midplane. An exponential representation of the infinite medium energy absorption buildup factor for iron was used in all attenuation calculations.

Computed heating rates should represent a conservative estimate of the maximum values attained over the useful core life.

Radiation heating rates within the reactor vessel. Approximate radiation heating rates within the reactor vessel were determined in the regions indicated in Fig. 4.48. Heating rate distributions expressed in single exponential form as:

$$Q\ (X) = Q_0\ e^{-\beta x}$$

where

x = distance along the specified line, measured from the inner surface of the vessel

Q_0 = heating rate at the inner surface

β = attenuation factor.

are as follows:

Line	Q_0 (Btu/in.^{3}-hr)	β (in.$^{-1}$)
AA'	19.5	0.31
BB'	14.5	0.25
CC'	25.9	0.76
DD'	1.01	0.63

These values assume 10-megawatt operation.

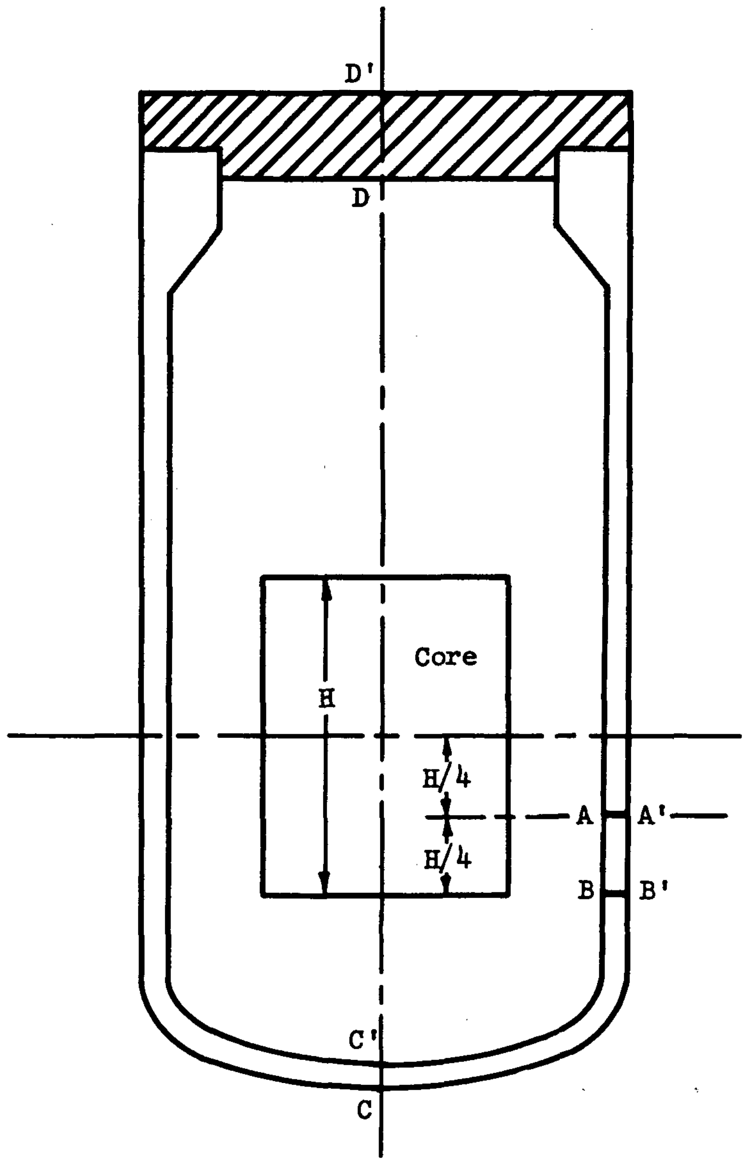

Drawing
not to scale

Fig. 4.48. Reactor Pressure Vessel Heating Rate Regions

Radiation heating rates were computed at the inner and outer surfaces of the reactor vessel along each line of interest. The attenuation factor β is given by:

$$\beta = -\frac{1}{t} \ln \left(\frac{Q_t}{Q_0} \right)$$

where

t = thickness of the vessel

Q_0 = heating rate at the inner surface

Q_t = heating rate at the outer surface.

Generally, representation of the spatial distribution across the reactor vessel by a single exponential term gives a conservative estimate of heating rates at points within the vessel.

Sources of radiation considered within the reactor core were prompt fission gammas, fission product gammas, thermal neutron capture gammas in the fuel, fuel cladding and moderator, and gammas from decay of induced radioactivity. Exterior to the core, the major source of radiation was thermal neutron capture gammas created within the thermal shields and reactor vessel. Hydrogen capture gammas in the coolant and gammas from inelastic scatter of fast neutrons were neglected for this calculation.

Attenuation calculations were performed by use of the IBM-709 Cylindrical Volume Source Code which numerically integrates over the volume of the source. The infinite medium point isotropic energy absorption buildup factor for water was applied over the total number of mean free paths from source to dose point. A uniform source distribution was assumed for the core. The thermal shield pressure vessel region source distribution was taken to be uniform in the axial direction and radially proportional to the thermal neutron flux of Fig. 4.44.

Integrated neutron flux in the reactor vessel and thermal shields. The integrated neutron flux values of Table 4.11 represent maximums on the inner and outer surface of the specified regions. Values were obtained from modified multi-energy group one-dimensional neutron flux calculations described earlier in this report and were prepared for use as a guide to determine possible neutron damage in these regions.

TABLE 4.11

NVT for One Year at Ten-Megawatt Operation in Thermal Shields and Pressure Vessel Along Core Radial Centerline

NVT (neutrons/cm^2)

Region	IR (inches)	OR (inches)	Inner Surface: Thermal $\leq$ 0.04 mev	Inner Surface: Epithermal Th to 0.8 mev	Inner Surface: Fast $\geq$ 0.8 mev	Outer Surface: Thermal $\leq$ 0.04 mev	Outer Surface: Epithermal Th to 0.8 mev	Outer Surface: Fast $\geq$ 0.8 mev
Core shroud	11.550	11.800	4.1×10^{20}	1.7×10^{21}	9.1×10^{20}	3.7×10^{20}	1.6×10^{21}	7.8×10^{20}
Inner thermal shield	12.0535	12.8035	3.0×10^{20}	1.6×10^{21}	7.4×10^{20}	2.0×10^{20}	1.5×10^{21}	4.8×10^{20}
Central thermal shield	13.0565	14.8065	1.7×10^{20}	1.4×10^{21}	4.5×10^{20}	8.6×10^{19}	1.0×10^{21}	1.7×10^{20}
Outer thermal shield	15.0595	17.5595	8.2×10^{19}	9.8×10^{20}	1.7×10^{20}	4.1×10^{19}	5.4×10^{20}	4.4×10^{19}
Pressure vessel	17.8125	20.000	4.0×10^{19}	5.0×10^{20}	4.2×10^{19}	1.0×10^{19}	2.3×10^{20}	1.1×10^{19}
Exterior thermal shield	21.000	22.000	1.0×10^{19}	2.2×10^{20}	1.1×10^{19}	5.5×10^{19}	1.4×10^{20}	4.5×10^{18}

2. Energy Release from Radiation After Reactor Shutdown

Fission products. Total energy release from fission products as a function of time after shutdown was computed, assuming that the PM-1 core had operated continuously for two years at a power of 10 megawatts. Results plotted in Fig. 4.49 represent total energy of beta and gamma radiation released from radioactive decay of fission products and daughter product activity. Approximately 50% of the total energy is from emitted betas and it may be assumed that all of this energy is released as heat within the fuel and fuel cladding. Gammas will be absorbed within the core and surrounding material. More than 95% of the gamma radiation will be absorbed within the core material and thermal shields while the core remains in operating position or within the core and lead shipping cask after core removal from the Primary System.

For shutdown times greater than 0.43 hour, the data compiled by Perkins and King (Ref. 3) were used directly with an IBM-704 code for computation of fission product activity (Ref. 4) to compute total activity. For times less than 0.43 hour, the short-lived activities not considered in the above data are significant; therefore, total energy during this period was estimated by the data of Ref. 2 as follows:

For 1.5 seconds after shutdown, $\frac{P}{P_0} = 0.048$

where

P = energy release from fission products

P_0 = operating power of the reactor.

$$\text{Thus, } P_{1.5} = \frac{0.048 \times 10^{7} \text{ watts}}{1.6 \times 10^{-13} \text{ watt-sec/mev}} = 3.0 \times 10^{18} \text{ mev/sec.}$$

From times 1.0 second to 1550 seconds (0.43 hour) after shutdown, assume $P = 3.2 \times 10^{18} t^{-0.141}$ mev/sec.

Time-dependent energy release from fission products was integrated over a one-year period from shutdown to obtain a total energy release of 1.24×10^{24} mev (5.52×10^{4} kilowatt-hours) during this period.

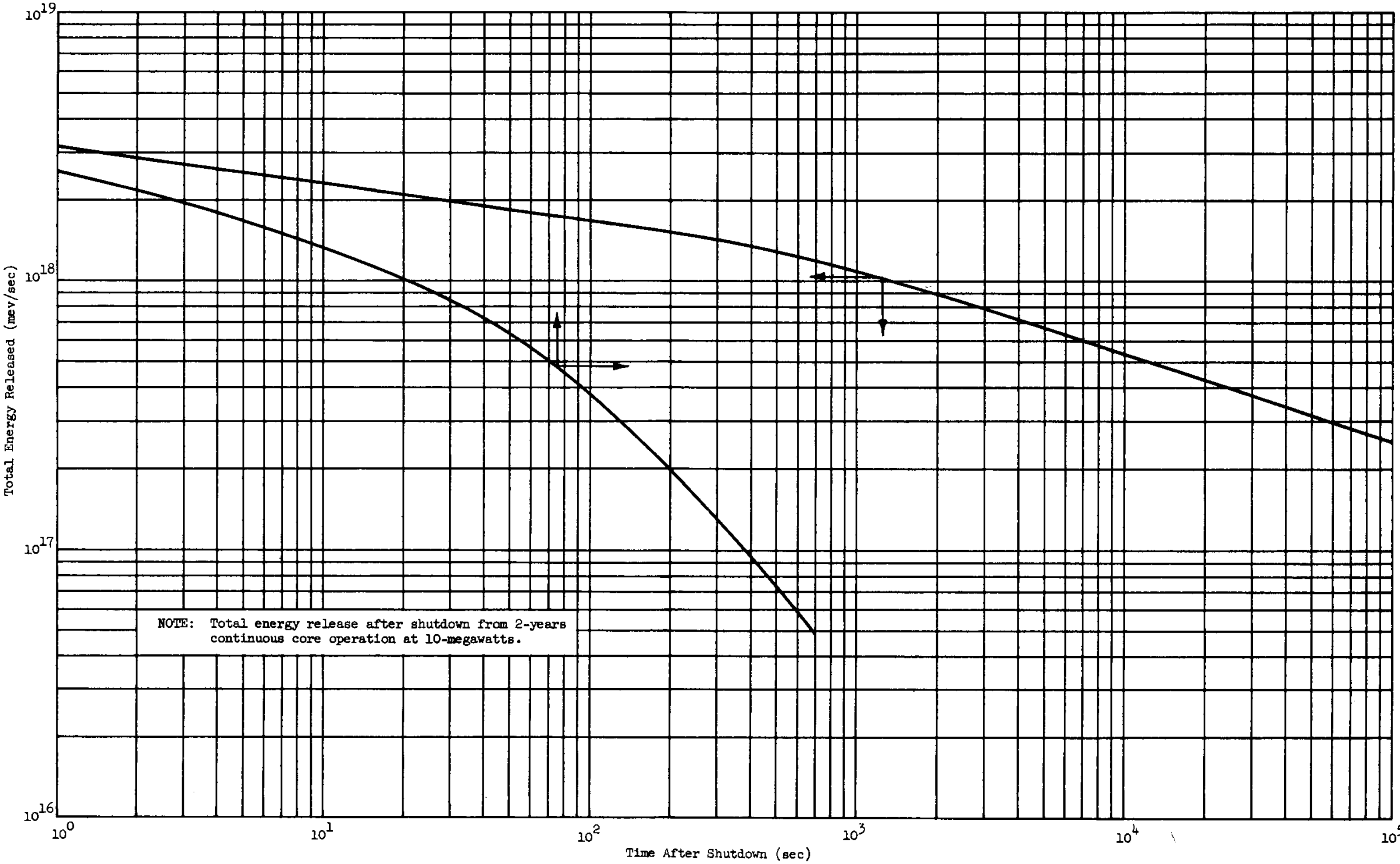

Fig. 4.49. Fission Product Decay Energy

Thermal neutron induced activity in the stainless steel fuel cladding. The total integrated energy release by the radioactive decay of the stainless steel fuel cladding for a time period of from shutdown to one year after shutdown was computed to be 4.1×10^{21} mev (183 kilowatt-hours). Significant radioactive isotopes produced in the clad are Cr-51, Fe-59, Mn-56, Ta-182 and Co-60. Specific activity of these isotopes for various times after shutdown is shown in Figs. 4.50 through 4.53. The reactor was assumed to have operated continuously at 10 megawatts for two years. For conservatism, the thermal neutron flux averaged over the volume of the core at the end of core life was assumed to have existed in the core over the full period of operation considered. Actually, the average flux varies from 0.86×10^{13} to 1.6×10^{13} neutrons/cm^2-sec over the period of operation.

All stainless steel in the core was assumed to be type AISI-348 stainless steel. Activity was computed by the standard methods for buildup and decay as given in Ref. 2. Thermal neutron activation cross sections were taken from BNL 325, second edition (Ref. 5).

Induced activity in europium control rods. The use of europium for control of the core will result in the formation of radioactive Eu-152, Eu-154, Eu-155, Eu-156, Gd-153 and Sm-153. Equations for the buildup and decay of the various isotopes of europium, samarium and gadolinium during neutron irradiation have been coded for the IBM-709. When code checkout is complete, total energy release from decay of the above-mentioned isotopes for various times after shutdown will be determined. A preliminary estimate indicates decay energy release after core operation for two years at 10 megawatts to be 5×10^{16} mev/sec. Final analysis will be completed during the next quarter.

3. Spent Fuel Removal and Shipping Cask Design Dose Rates in Water Above the Core

Previously estimated after-shutdown dose rates (see Fig. III-31, p III-71, Ref. 6) in water on the axis of the spent core were computed, assuming the water within the core to have a density of 0.82 gram/cm^3. A revised estimate, assuming core water density of 1.0 gram/cm^3, is presented in Fig. 4.54.

Dose rates were computed, assuming a homogenized core of uniform source strength. In reality, the nonuniform source distribution is higher near the center of the core. Thus, uniform source strength is a conservative assumption. The assumption of a homogeneous core ignores possible gamma streaming through the water surrounding and within the individual fuel tubes.

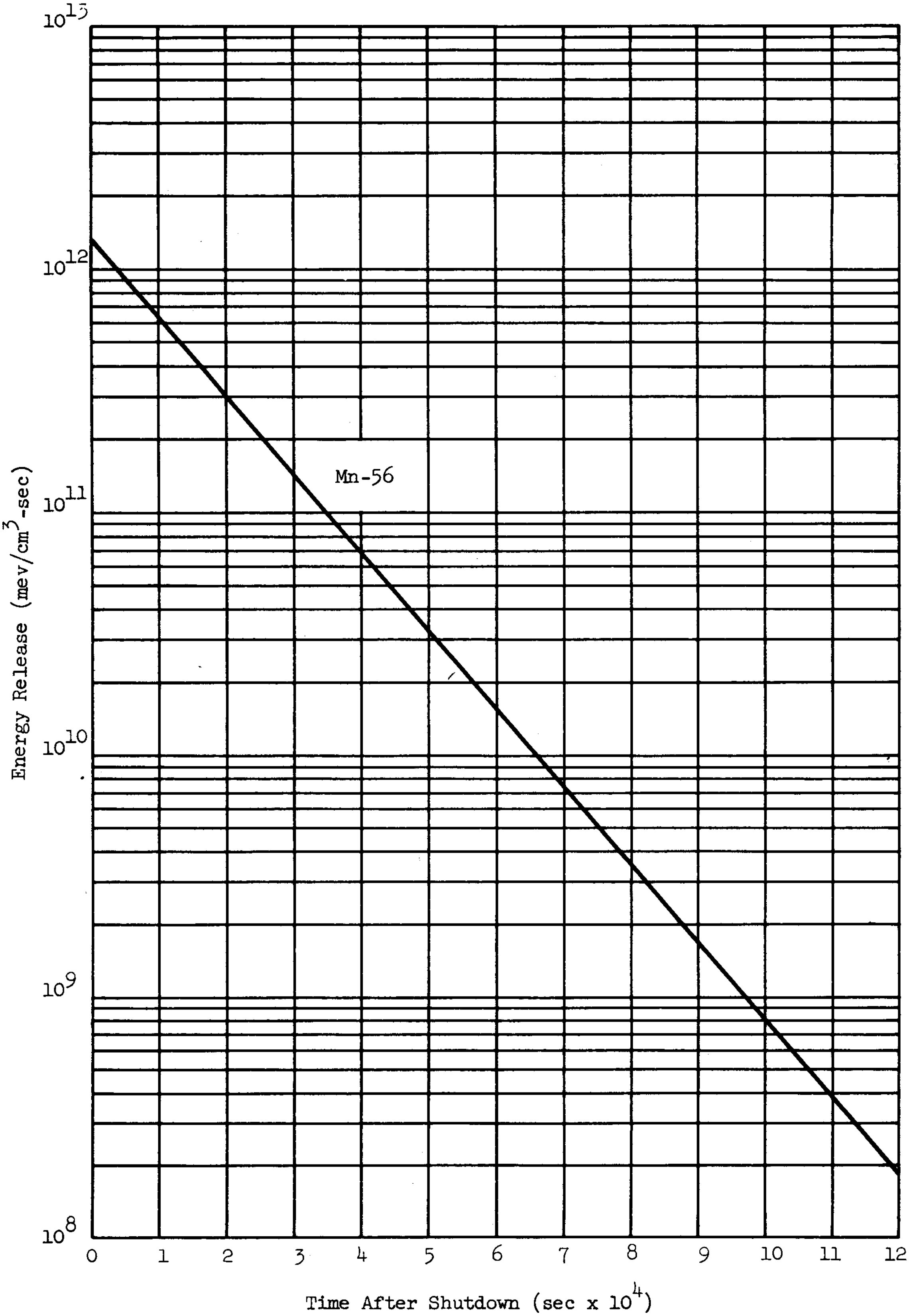

Fig. 4.50. Energy Release per Unit Volume of Stainless Steel by Decay of Mn-56 in PM-1 Core

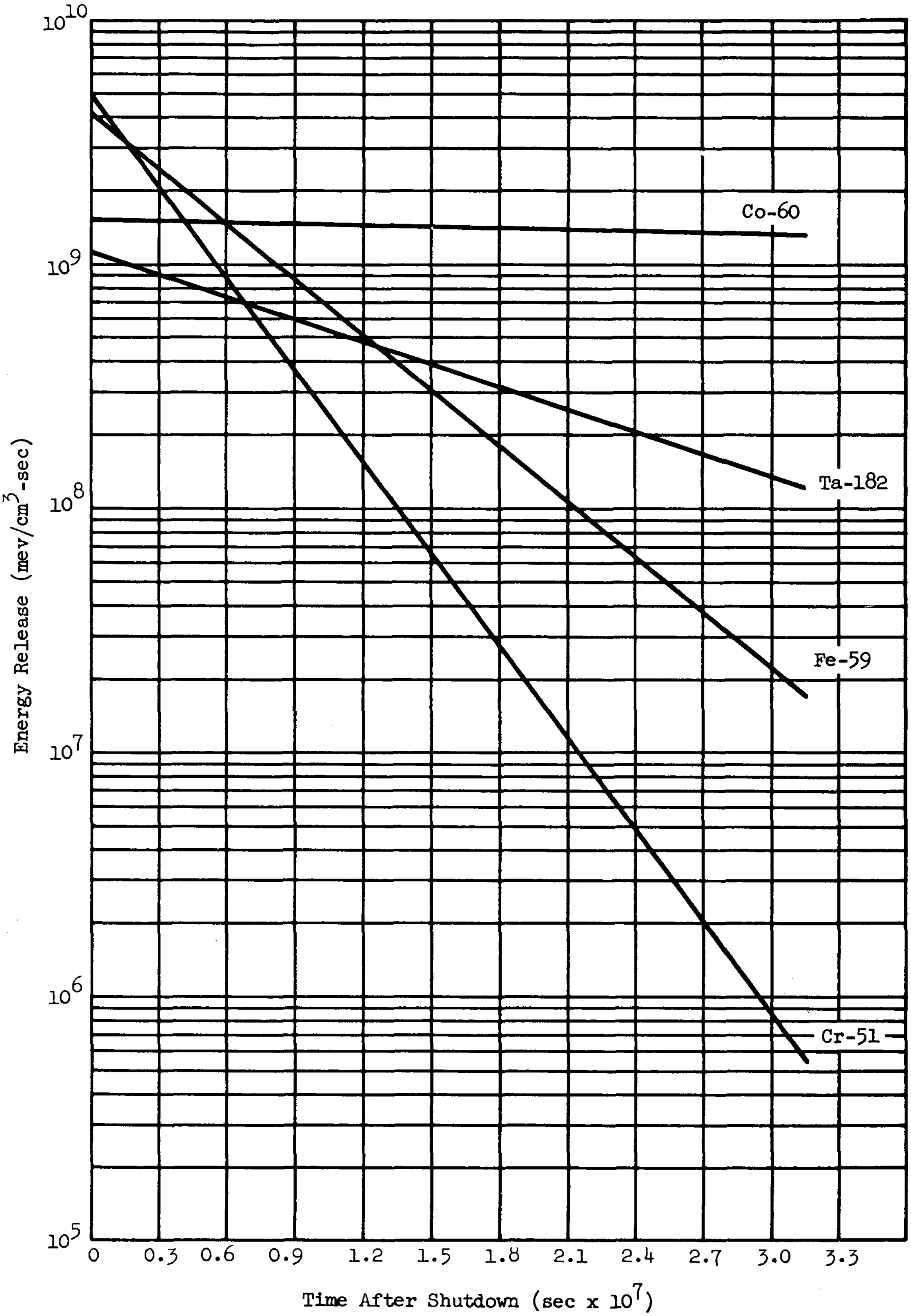

Fig. 4.51. Energy Release per Unit Volume of Stainless Steel by Decay of Cr-51, Fe-59, Ta-182 and Co-60 in PM-1 Core

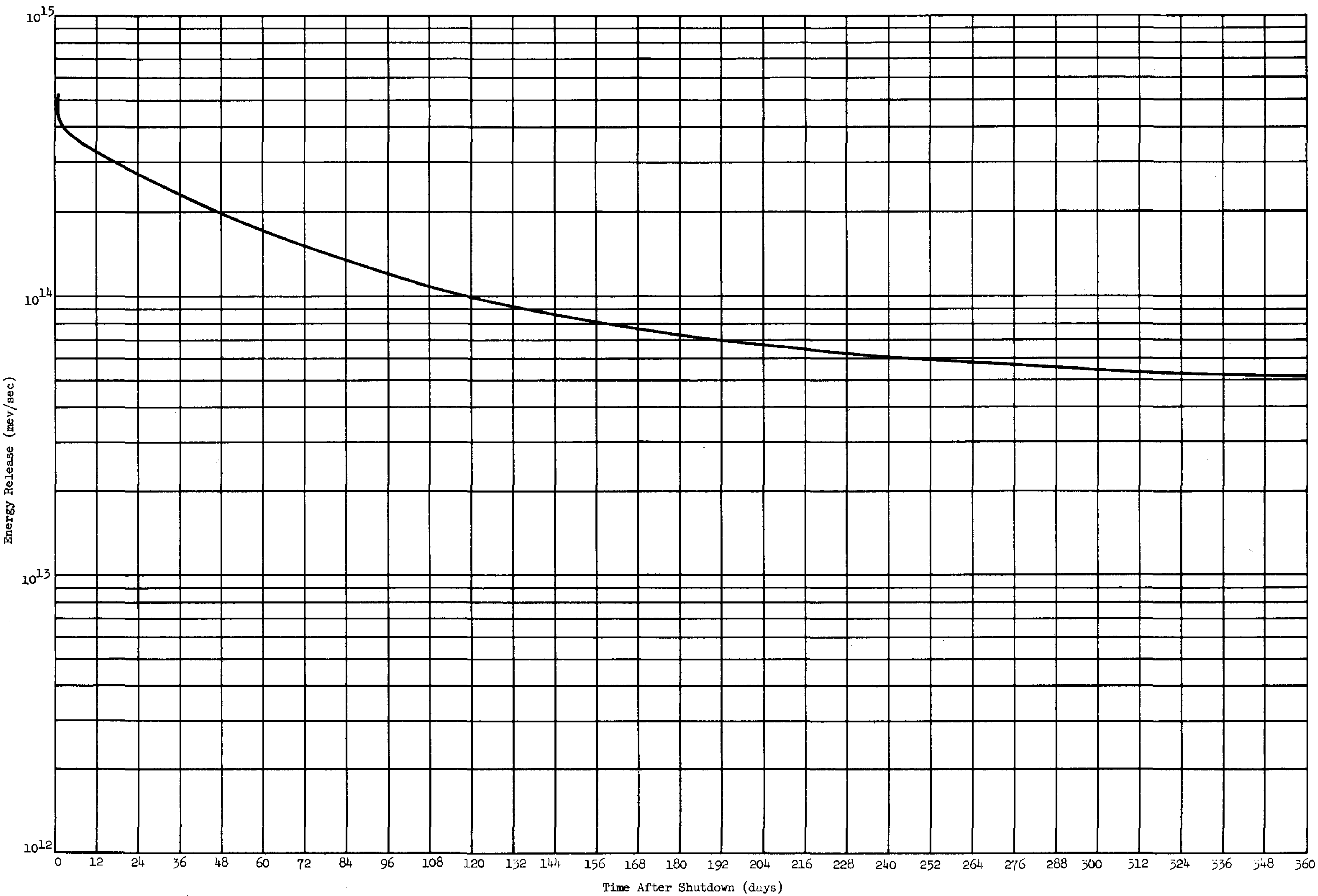

Fig. 4.52. Total Energy Release per Unit Time Versus Time After Shutdown by Decay of Mn-56, Cr-51, Fe-59, Ta-182 and Co-60 in PM-1 Core

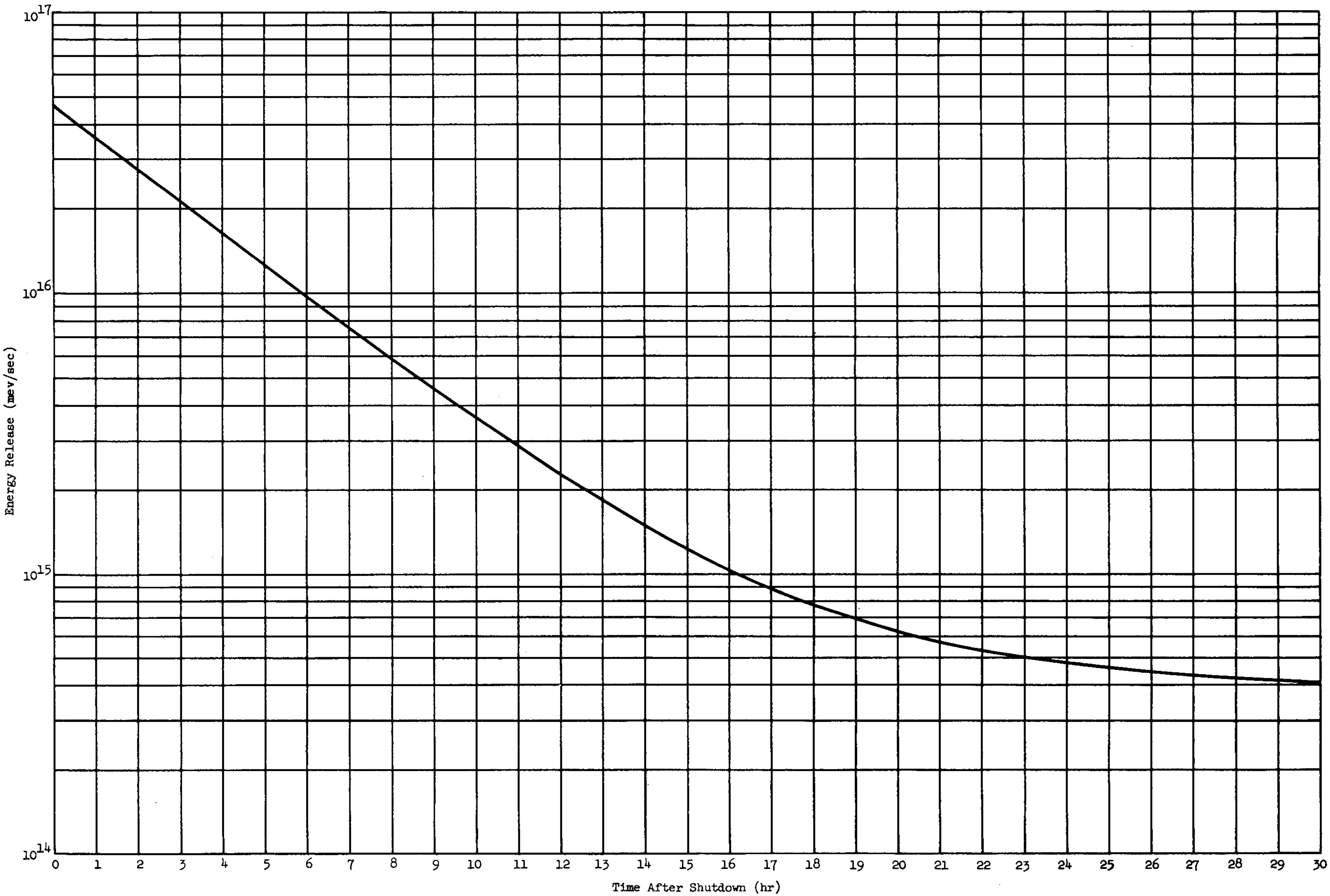

Fig. 4.53. Total Energy Release per Unit Time Versus Time After Shutdown by Decay of Mn-56, Cr-51, Fe-59, Ta-182 and Co-60 in PM-1 Core

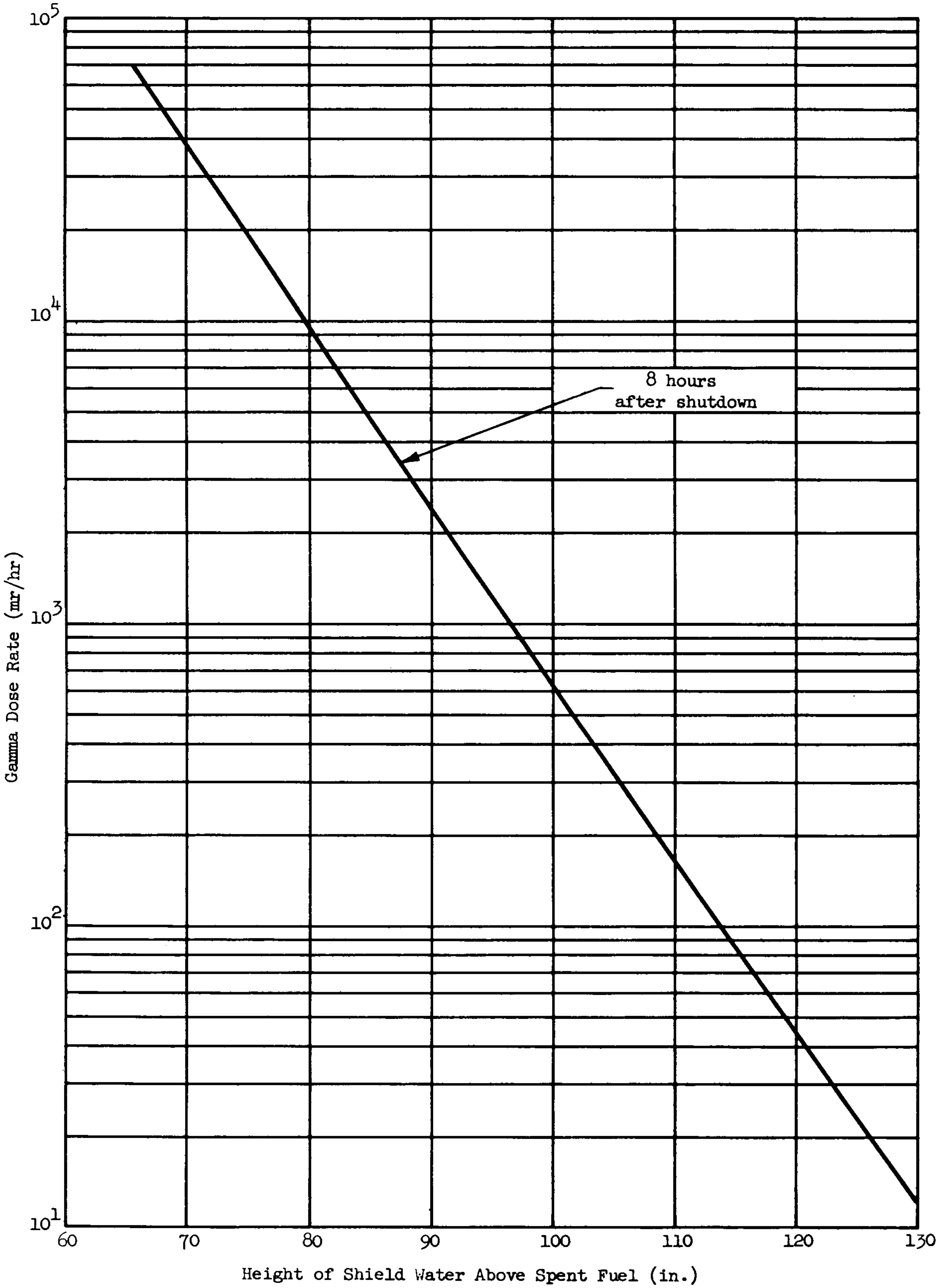

Fig. 4.54. Dose Rate in Shield Water from Core Fission Product Decay Gammas

Effect of the use of europium for core control on shipping cask design. A study to determine the effects of induced radioactivity in europium control rods on core storage and shipping cask design was completed during this quarter. The isotopic abundance of the radioactive isotopes of europium, samarium and gadolinium produced over the two-year core life were computed at the end of this period. The intensity of the activity after two years of operation was computed to be 7.3×10^5 curies. This value was calculated by assuming that 25% by volume of the rods was exposed to an average thermal neutron flux of 10^{13} neutrons/cm^2-sec.

The induced gamma activity in the europium rods was grouped according to gamma energy with the corresponding spent fuel activity energy groups, and the new source strengths were used to re-estimate core shipping cask lead thickness.

The results indicate that a new cask thickness 0.25 inch greater than the present cask thickness for spent fuel with Boron-10 rods will be required if europium is used as the control material.

4. Biological Shield Design

Package interconnect shield. A compact gamma shield placed between the reactor vessel and package interconnect will be required, in addition to the shield water in this area, to protect maintenance personnel while in the vicinity of the lower package interconnect after core shutdown. The approximate dimensions of a lead shield (density = 11.35 grams/cm^3), which would lower the dose rate from induced activity of reactor vessel and internal components and fission product radiation eight hours after shutdown to less than 200 milliroentgens per hour, are 5.0 inches thick by 51 inches high surrounding approximately 120 degrees of the reactor vessel facing the interconnect. This shield would probably be permanently mounted and constructed of either cast lead or lead brick and encased in a protective metal. A temporary shield could not be lowered into place when needed because of piping in this region. Small lead shields may be necessary to prevent direct radiation streaming through the primary piping.

Should the present interconnect design be incorporated in the Primary System final design, further analysis will be performed to determine the exact dimensions and extent of shielding required in this area.

Radiation heating rates within the earth shield. Radiation heating rates along the midplane of the reactor core within the earth shield adjacent to the reactor package have been computed. Results obtained to date are shown in Fig. 4.55 for three shield configurations. For these computations, it was assumed that the reactor was operating at 10 megawatts.

All significant heating is produced by absorption in earth of thermal neutron capture gammas created within the thermal shields and reactor vessel. Attenuation calculations were performed by use of the IBM-709 cylindrical volume source code to numerically integrate over the volume of the source.

A design criteria of this study is that the temperature at any point within the earth surrounding the primary packages will not exceed 200°F. Heating rates will be analyzed to determine maximum temperatures, and a final shield will be designed such that this condition is met. This work will be completed during the next quarter.

5. Activation of the Primary Loop by Corrosion Products

Activity buildup code. An IBM-709 code for determination of the buildup of corrosion product activity in the Primary System of a pressurized reactor was developed. The code evaluates the equations of buildup of deposited activity as given in Ref. 7. These coded equations, which solve for the surface activity due to any individual radioactive isotope, contain the following approximations for corrosion rate of the system:

(1) A variable corrosion rate may be assumed for the entire primary loop during the first year of activation.

(2) A constant corrosion rate is used for the entire primary loop during and after the second year of activation.

(3) After core replacement, the corrosion rate of the core portion of the primary loop is assumed to be variable for the first year and constant for the second year.

To date, machine results have been checked out with hand computations. Accuracy of the results is limited only by the accuracy of input data.

Effect of varying amounts of tantalum and cobalt in core clad and reflector materials. An evaluation of the activity deposited on the surfaces of the Primary System due to the low impurity reactor materials along with other basic constituents was performed for the present Pri-

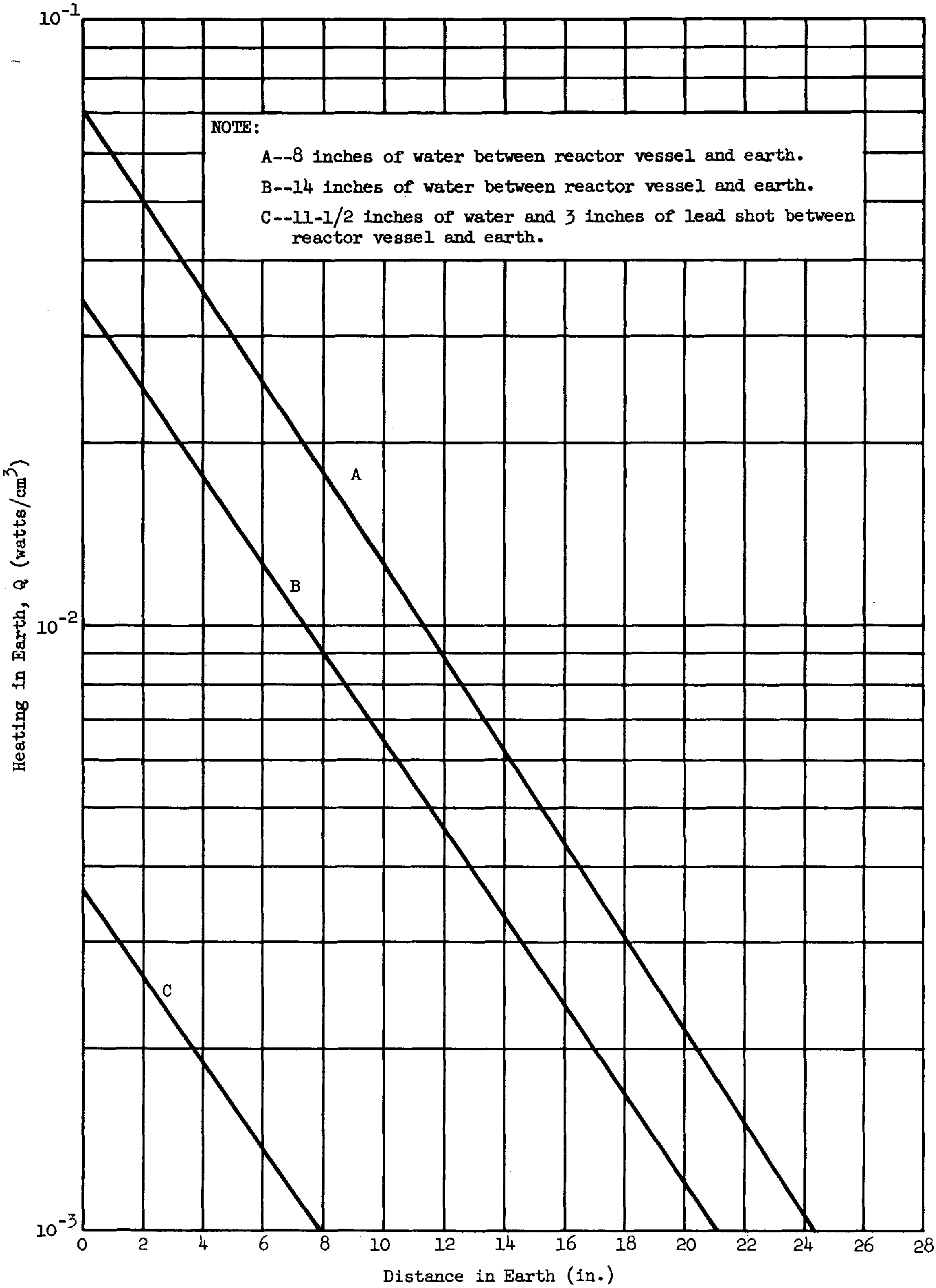

Fig. 4.55. Radiation Heating Rates in Earth Along Core Radial Centerline--10-Megawatt Operation

mary System design. Materials making up the various reactor components were Types 347 and 304 stainless steel. The basic constituents referred to, which form significant amounts of radioactive isotopes in these steels, are chromium, nickel, iron and manganese. The amount of basic materials was assumed to be the same for both stainless steels. Cobalt and tantalum are the low impurity materials considered. Concentrations of cobalt and tantalum in core cladding were varied. Concentration of cobalt in the reactor materials was varied, and it was assumed that the reflector contained no tantalum.

The total activity in the Primary System at any time is due to the activity from the core cladding from both the present and previous cores and the activity from the fixed components of the reactor. Values of surface activity due to the various isotopic concentrations versus time of reactor operation up to 20 years are presented in Fig. 4.56. By applying a concentration ratio to the plotted values, it is possible to determine the effects of changing the concentrations. The curve representing the activity from the basic constituents remains the same as long as the materials are not changed. Curves in Fig. 4.57 show the change in isotopic surface dose rate (obtained by direct conversion of surface activity) as a function of concentration. By use of Fig. 4.57, it is possible to estimate optimum initial concentrations of low impurities.

The IBM-709 Activity Buildup Code was used to compute the various contributions of surface activity from the deposited radioactive isotopes formed during 20 years of operation. The coded solutions include the contributions resulting from thermal neutron (n, γ) reactions, fast neutron (n, p) reactions and an effective fast neutron reaction which involves using the resonance integral values of cross sections and flux.

In computing the neutron fluxes, the three-group diffusion program (F-3) was used, which sets 0.04 ev, 0.84 mev and infinite energy limits on the thermal, epithermal and fast fluxes, respectively. In computing the flux for the fast reactions, it was necessary to add the epithermal and fast flux to obtain a more representative fast flux. The effective fast flux used with the resonance integral cross sections was obtained by the following relation which is derived in Ref. 7:

$$\phi_{Fe} = \frac{\phi_f}{\int_{0.4\ \mathrm{ev}}^{2 \times 10^6\ \mathrm{ev}} \frac{dE}{E}} = 0.065\ \phi_f .$$

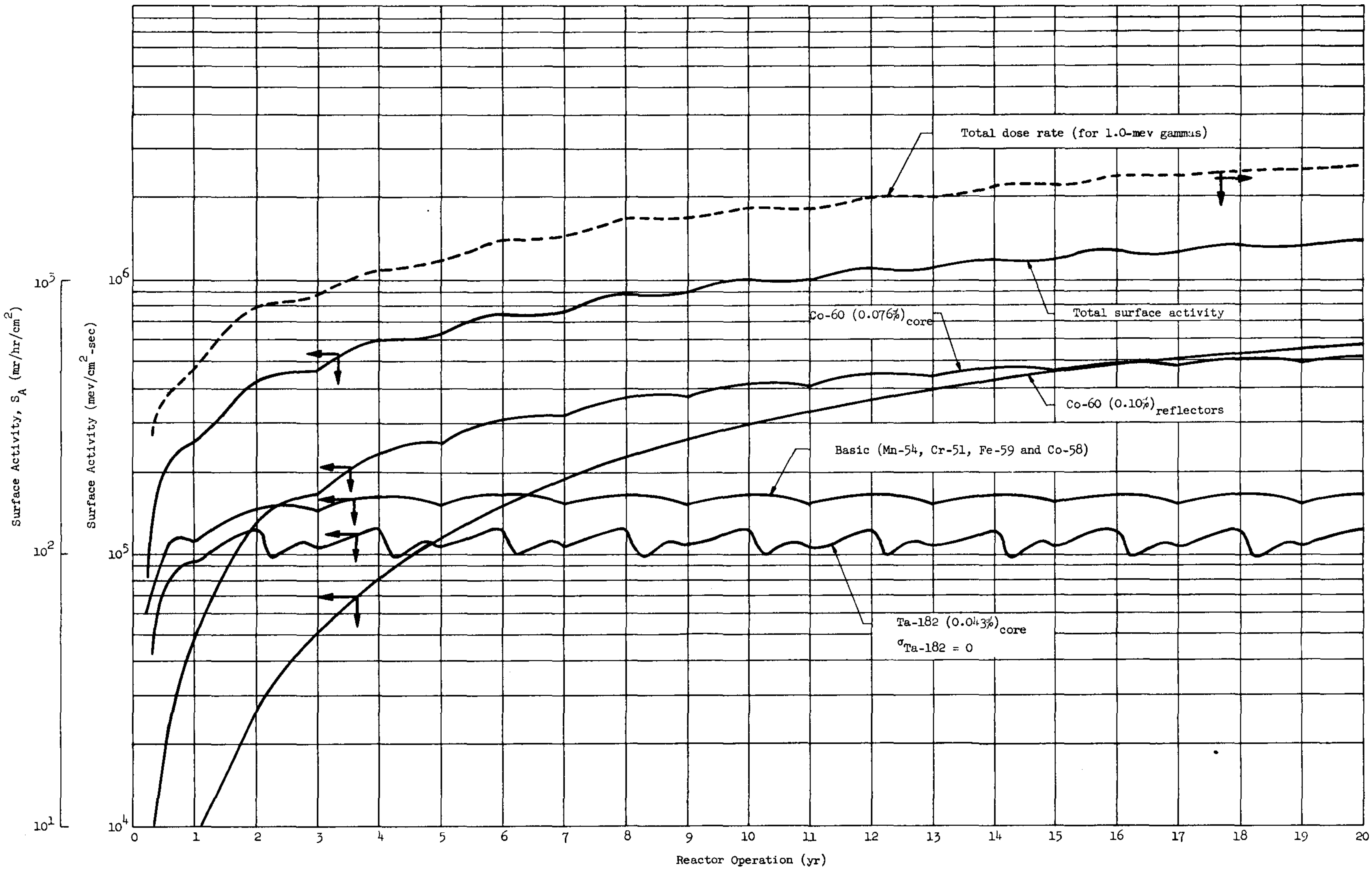

Fig. 4.56. **Primary System Surface Activity over 20-Year Period for PM-1 Reactor, Core Life--2 Years** (Core A)

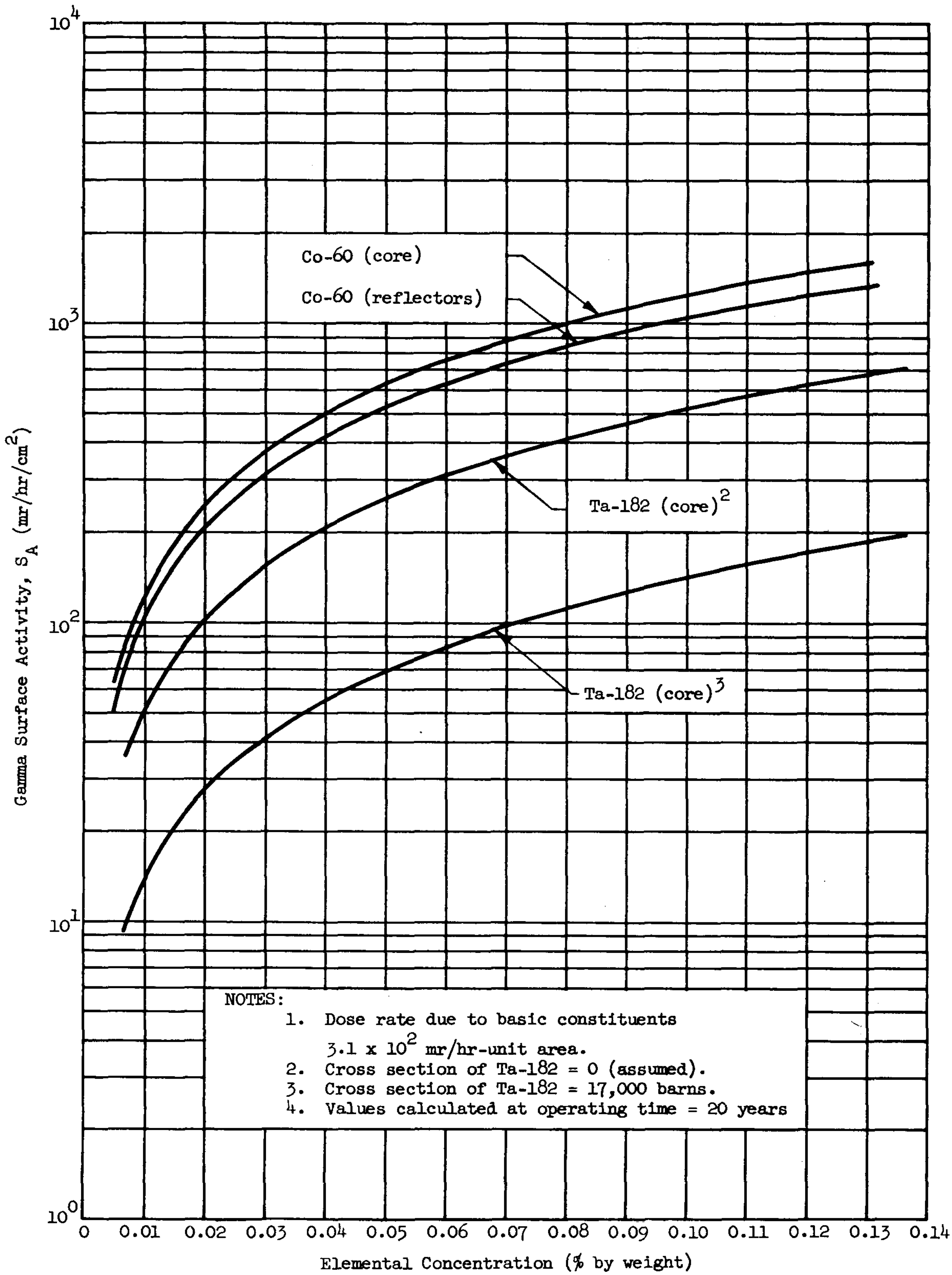

Fig. 4.57. Variation of Surface Activity with Elemental Concentration

6. Determination of Heating in Shield Water

The radiation heating in the shield water of the PM-1 reactor containment was determined by assuming a cylindrical annulus of water surrounding the reactor vessel and having a thickness and height of 12 inches and 30 inches, respectively. The reactor configuration is that of the present design, which has a 40-inch OD pressure vessel, a total thickness of 5.25 inches of internal thermal shields, an 11.3-inch radius by 30-inch height core and a 1.0-inch exterior thermal shield. The total heating in the shield water is 4.78×10^{17} mev/sec (76.4 killowatt). This value neglects the heat escaping radially above and below the core and also that part which is emitted through the top and bottom of the reactor vessel. The contribution of the neglected areas was estimated to be lower than that of the region considered.

The sources of radiation considered are prompt fission and fission product gammas from the core, iron and water capture gammas and fast neutrons. The core gammas and capture gammas were machine calculated using either the IBM-709 cylindrical volume source code or the slab source code. The equations given by Rockwell (Ref. 2) for heating by elastically scattered neutrons with slight modification were used to calculate the contribution due to fast neutron moderation.

In computing the contribution from the sources within and including the exterior iron ring, a total surface gamma energy flux was determined on the surface of the iron ring and integrated over the surface of the iron ring, assuming a height of 30.0 inches. Heating due to elastically scattered neutrons in the shield water was found to be significant in shield water regions up to 12 inches beyond the outer surface of the exterior thermal shield. The equation of Ref. 2 for the specific rate of heating due to elastic scattering of fast neutrons is given as:

$$H(r) = \sum_i N_i \frac{2A_i}{(A_i + 1)^2} \sigma_i (1 - \mu_{1_i}) \phi_f (r) \int_0^\infty N(E)\, E\, dE,$$

This equation was reduced to the form:

$$H(r) = C\phi_f e^{-Ar}$$

where C is a constant relating energy release in water to the fast neutron flux and $_f e^{-Ar}$ is given by multiplying the volume of the shield water considered by the average radial flux. Thus:

$$H_T = VC\,\phi_f \frac{\int_{r_i}^{r_0} r e^{-Ar}\,dr}{\int_{r_i}^{r_0} r\,dr}$$

In the above equations:

H_T	=	total heating contribution from elastically scattered neutrons, mev/sec
$H(r)$	=	power density in shield water due to fast neutron moderation, mev/cm^3-sec.
N_i	=	number density of the ith element of the medium being considered, atoms/cm^3
Ai	=	atomic mass of the element in atomic mass units, atoms/g-atom
σ_i	=	elastic scattering cross section, cm^2
μ_{1_i}	=	mean cosine of the scattering angle.
E	=	neutron energy, mev
ϕ (r)	=	$\phi_f e^{-Ar}$ exponential representation of neutron flux as a function of radius, neutrons/cm^2-sec
$\int_0^\infty N(E)\,dE$	=	integral spectrum of neutron energy (fission neutron spectrum)

V = volume of shield water being considered, cm^3

r_i = inner radius of shield water, cm

r_o = outer radius of shield water, cm.

The heating due to hydrogen capture gammas in the 12-inch thick shield water region was determined using the slab source code which computed the gamma flux at various points throughout the water region. Radial gamma flux was represented by a single exponential and then averaged over the radius using an equation similar to that shown above for elastically scattered neutrons.

C. SECONDARY SYSTEM STUDIES

W. Koch, R. Groscup, L. Hassell

1. General PM-1 Secondary System Layout

During this quarter, the following work was planned and accomplished: Secondary System layout, including the decontamination package, was revised for the PM-1 site conditions.

During the next quarter, it is planned that the PM-1 layout will be completed except for minor dimensions which depend on data from vendors' certified drawings.

The revision of the PM-1 Secondary System layout was made in order to improve the PM-1 plant arrangement for the Sundance site and in accordance with directions given in an AEC Review Meeting on packaging held on 15 October 1959. This revised arrangement is shown in Fig. 4.58.

The heat transfer apparatus, switchgear, maintenance, control and turbine-generator unit packages are housed in a prefabricated building with inside clearances of 34 feet by 62 feet. The decontamination equipment is located in an integrally housed-type package which is nominally 8 feet, 8 inches by 8 feet, 8 inches by 30 feet (overall dimensions).

The major portion of the pipe runs from the primary loop to secondary loop originate or terminate in the heat transfer apparatus package. Therefore, this package has been located closest to the primary loop. Also, it is now planned to run the control and instrument cables directly from the primary loop area to the control room. With the present arrangement, the length of these runs is kept to a minimum.

The power tie cable to the base will run through the enclosed walkway from the base. This tie will, therefore, be made in the northwest corner of the switchgear package.

The maintenance package is located in the least congested area in the secondary building and also near the truck access door.

The heat transfer apparatus package contains the separate condenser hotwell (tank) condensate pumps, feedwater heater, air ejector, deaerator, feedwater pumps, evaporator, condensate storage tank and the associated valves, piping and control stations. The various power and control cables to the decontamination package and Primary System are carried in a cable tray through the heat transfer apparatus package. Equipment arrangements have been carried as far as practical prior to approval of final equipment specifications and vendors.

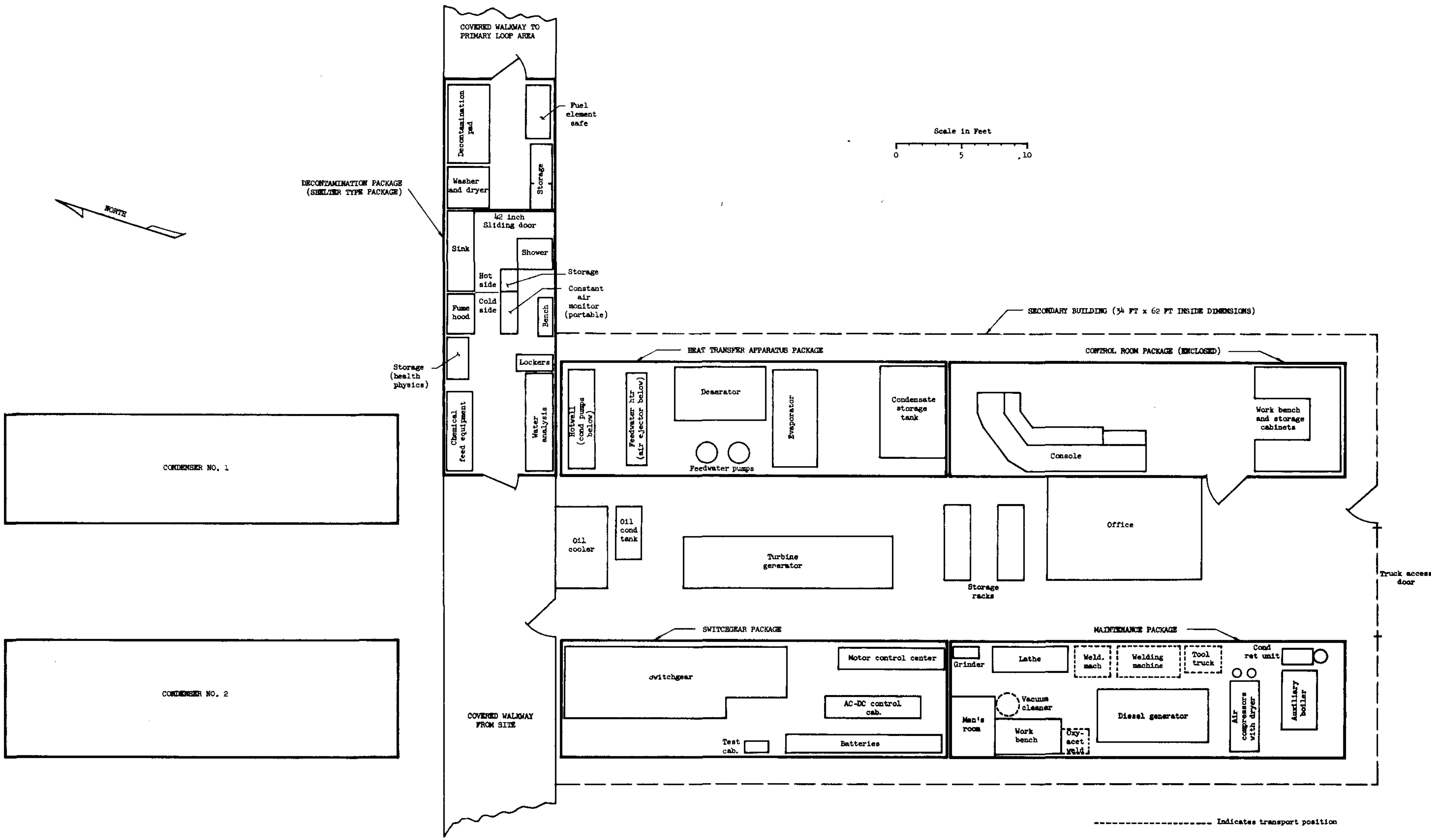

Fig. 4.58. PM-1 Secondary System Layout

The switchgear package contains the high- and low-voltage switchgear, static excitation system, motor control center, vital a-c and d-c control cabinet (including static battery charger and inverter-diverter pole m-g set), batteries and breaker test cabinet. Layout in this package has been rearranged during the quarter to accommodate design data developed by Westinghouse under Subtask 1.6.

The maintenance package contains the plant maintenance equipment plus other auxiliary and service equipment. This package is discussed in detail under Subsystem 37.

The control room will contain the control console and the electronics repair area with work benches and storage cabinet. The control room will be enclosed and air conditioned. No basic changes have developed in this package except for removal of the water chemistry laboratory.

A minimum amount of equipment is located in the central aisle area. This equipment includes the turbine-generator unit with its associated oil cooler and oil conditioner, storage racks and an office space suitable for a maximum of two desks and two file cabinets. A truck access door and personnel door are provided on the south end of the secondary building and a personnel door is also provided on the north end of the building, opening into the covered walkway to the decontamination package and to the base.

2. Secondary System Controls and Instrumentation

See Task 4, Subsystem 1.

3. Secondary System Package Design

A. Layman, R. Dugas, L. Noyes

During the third quarter, the major efforts planned in the packaging design program were to complete the design of a basic integral housing package after final resolution of the package design criteria. The final design of specific plant modules was then to be started, incorporating the specific equipment mounting, wall penetration and skid reinforcing features peculiar to the equipment in each package while utilizing the basic design features of integral housing.

Actual accomplishments were:

(1) Design criteria were resolved along the lines proposed in the preliminary design with respect to integral shipping and housing design. This included the previously reported limits on dimensions, weight, center-of-gravity, shipping and handling loads and vibration, tie-down, jack and hoist provisions and minimum deflection of the package.

(2) During the first two months of the quarter, the basic design of a package shelter was developed in considerable detail. This design was then applied to the structural test package which was detailed and submitted to manufacturing under Task 1.1. Figures 4.59 through 4.62 (Drawing 372-9090001 Sheets 1, 3, 4 and 8) show the proposed package assembly and major details (i.e., the walls, roof, ends and skid base).

(3) A number of changes were incorporated into the basic truss package design during this period. These included the following:

 (a) The redundant X-type truss was replaced by a K-type panel design which is more efficient both weightwise and from a manufacturing cost standpoint.

 (b) The longitudinal skid members were made slightly deeper to keep limit binding stresses below 36,000 psi.

 (c) Diagonal tie-rods were added to the pallet framework to provide lateral shear strength and help carry internal equipment inertia loads to the skids.

 (d) Auxiliary internal space bracing was designed to supplement the equipment pedestals in supporting longitudinal and lateral inertia loads resulting from transportation accelerations.

(4) Structural data for the C-130 airplane, pertaining to fuselage flexure and internal cargo tie-down characteristics, were obtained. Preliminary appraisal of the data in relation to carrying Secondary System packages indicates that the tie-down devices would be able to accommodate the redistribution of tie-down forces caused by fuselage binding.

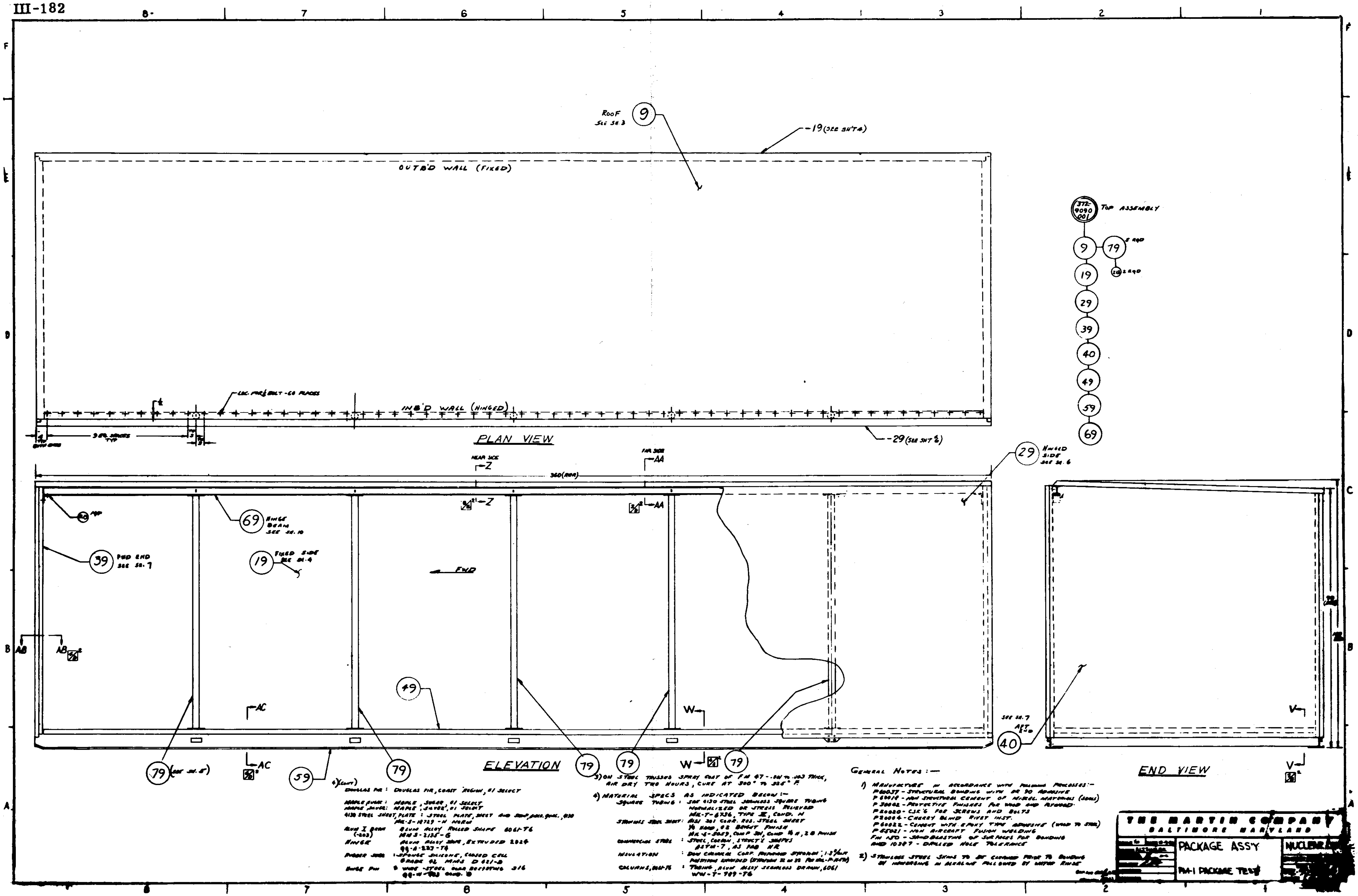

Fig. 4.59. Package Assembly Drawing

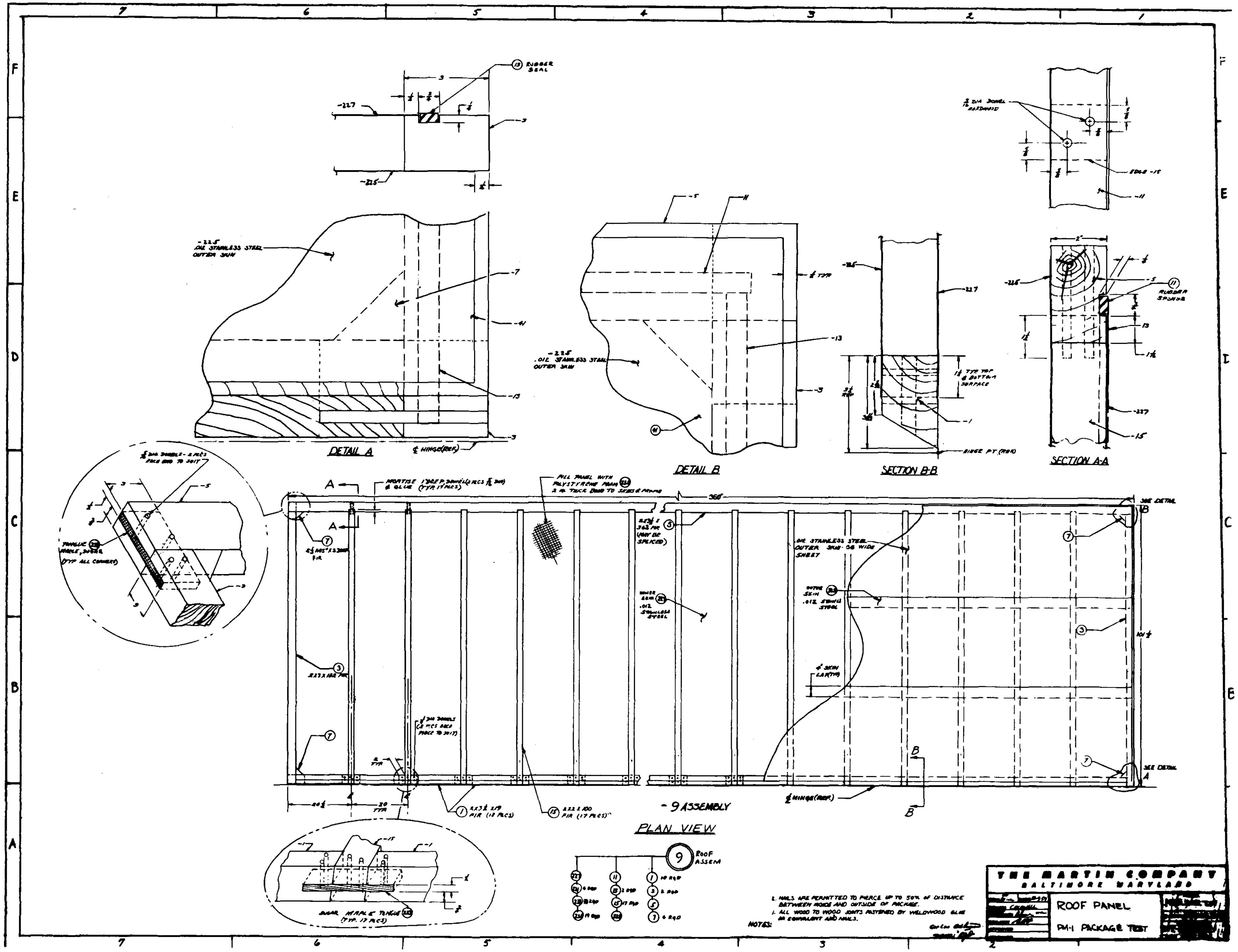

Fig. 4.60: Roof Panel Drawing

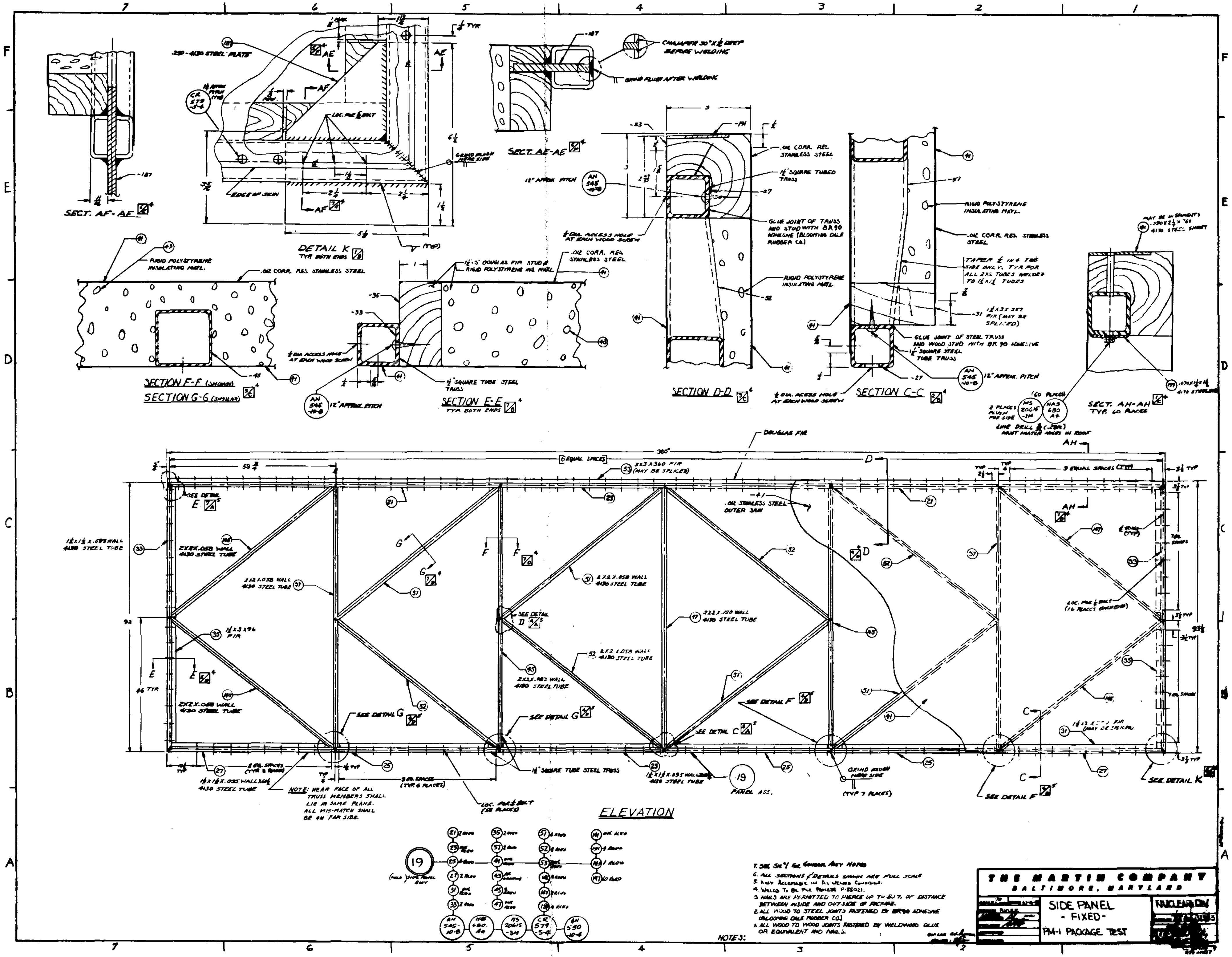

Fig. 4.61: Side Panel Drawing

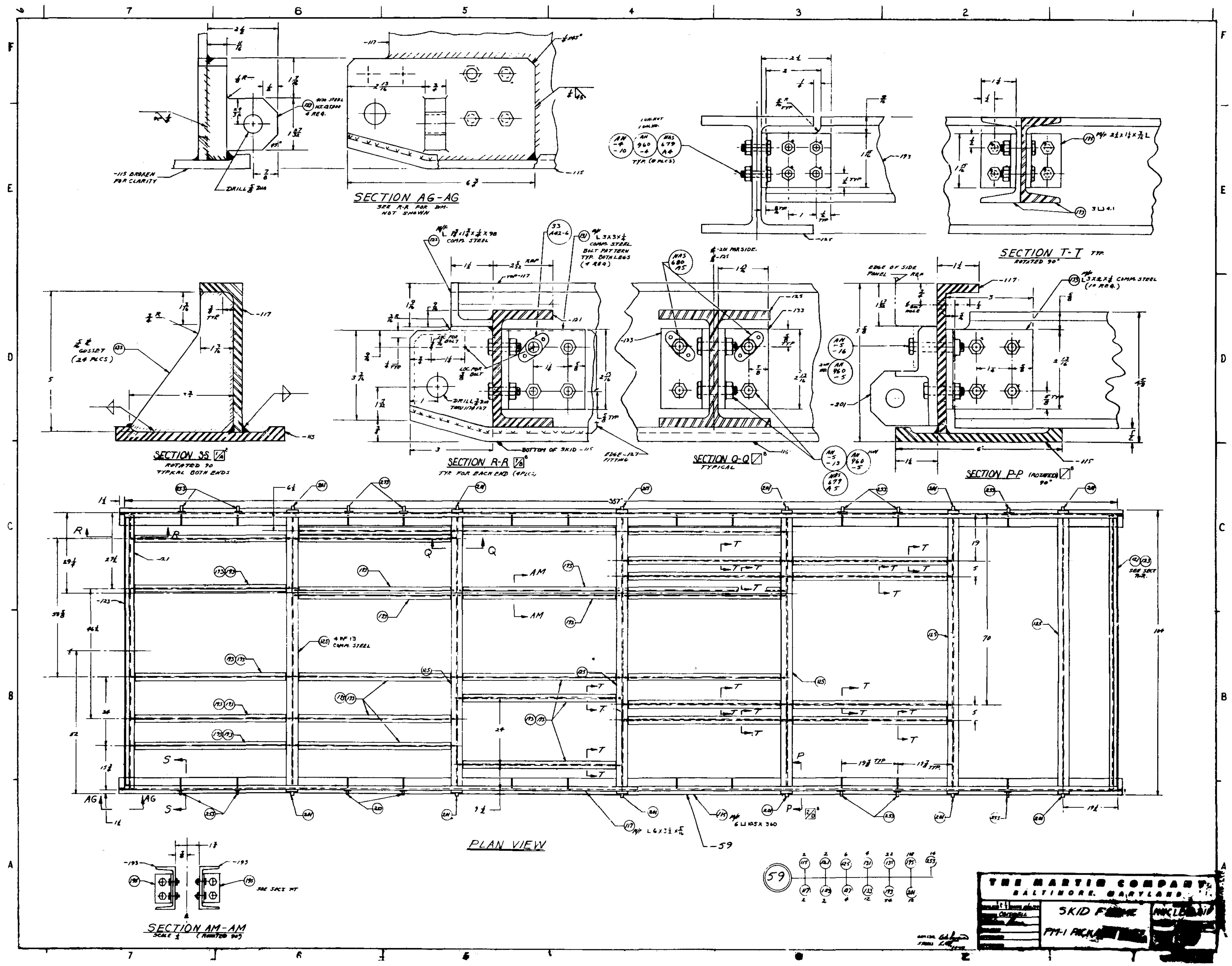

Fig. 4.62. Skid Frame Drawing

(5) Analysis of the dynamic response of the heat transfer package prompted the recommendation that floor members be made to have natural frequencies of 25 cps or greater in order to avoid resonance and amplification of load factor effects. This criterion was made in conjunction with the necessity for rigid (strut) bracing of the internal equipment, the design of which is now completed.

(6) The above changes, combined with the decision to drop integral housing for the Secondary System equipment packages (see Sub-system 35), led to a recall of all drawings and complete revisions were made. The revised design retains all of the original steel design but omits integral housing features, being only a shipping package in the revised form. The revised side panels and ends are covered with plywood. The floor is of plywood. The roof was kept as a sandwich panel since this gives minimum weight, but its faces were changed from stainless steel to 2024 aluminum alloy. The new design was formulated for the test package program under Task 1.

Figures 4.63 through 4.66 (Drawing 372-9090030, Sheets 2, 3, 5 and 9) show those construction details of the shipping package assembly which contain the most significant design modifications: the skid, side panels and details involved in use of a 3/4-inch plywood floor.

This change in plans requires an intensified effort during the coming period to complete the final design by the original scheduled date of 9 March 1960. During the next quarter, the final design drawings will be prepared for each secondary package after completion of a detailed review of design criteria costs and the effects of abandonment of integral housing features for the Sundance installation.

The end result of the above efforts has been to produce the basic design data needed for both the decontamination package and the shipping packages for heat transfer apparatus, control room, maintenance package and switchgear package.

D. MISCELLANEOUS STUDIES

P. Mon

1. Primary System Plant Erection Study

The objective of this study was to determine a means for erecting the PM-1 Power Plant as expeditiously as possible without the use of special hoisting equipment.

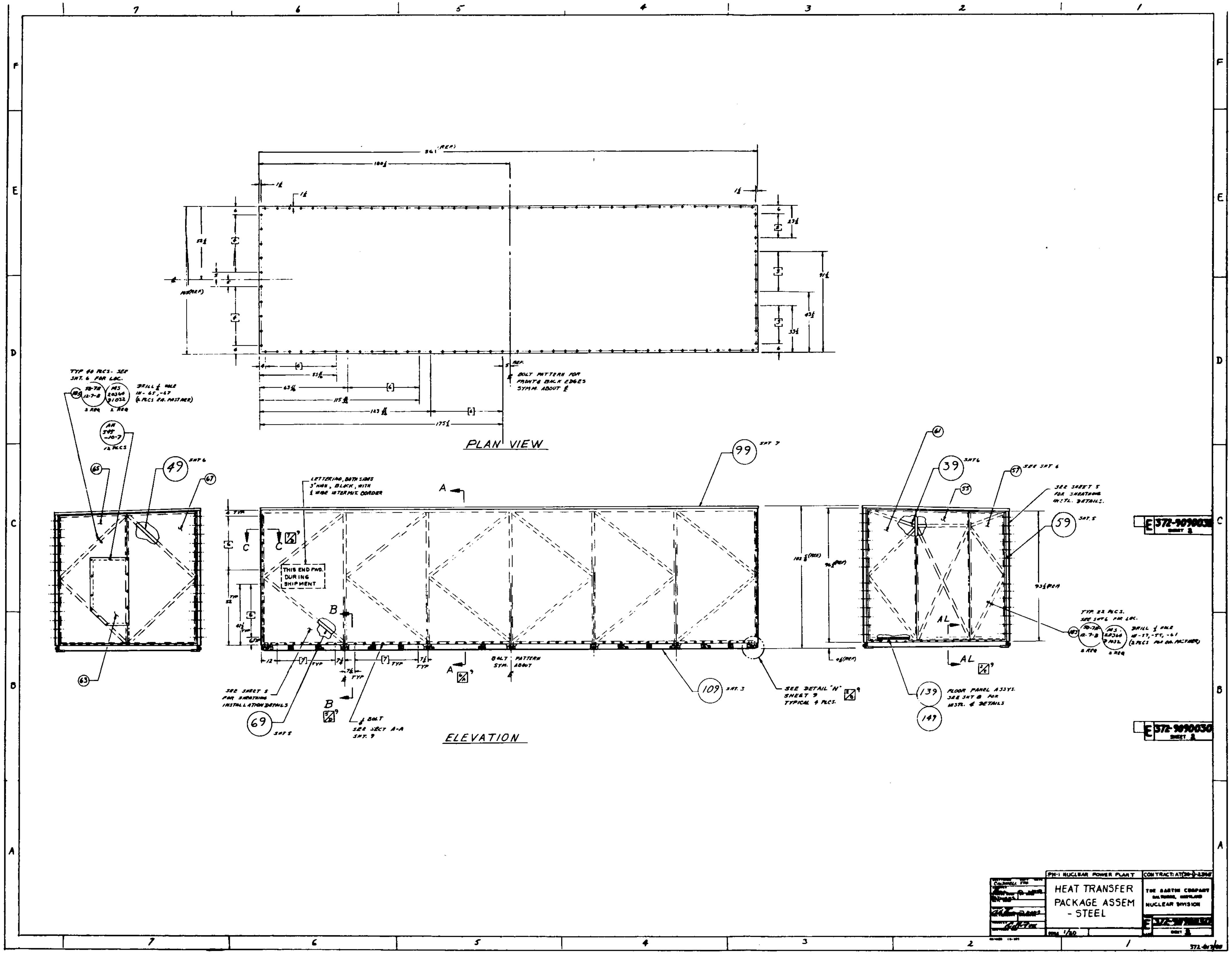

Fig. 4.63. Heat Transfer Package Assembly Drawing

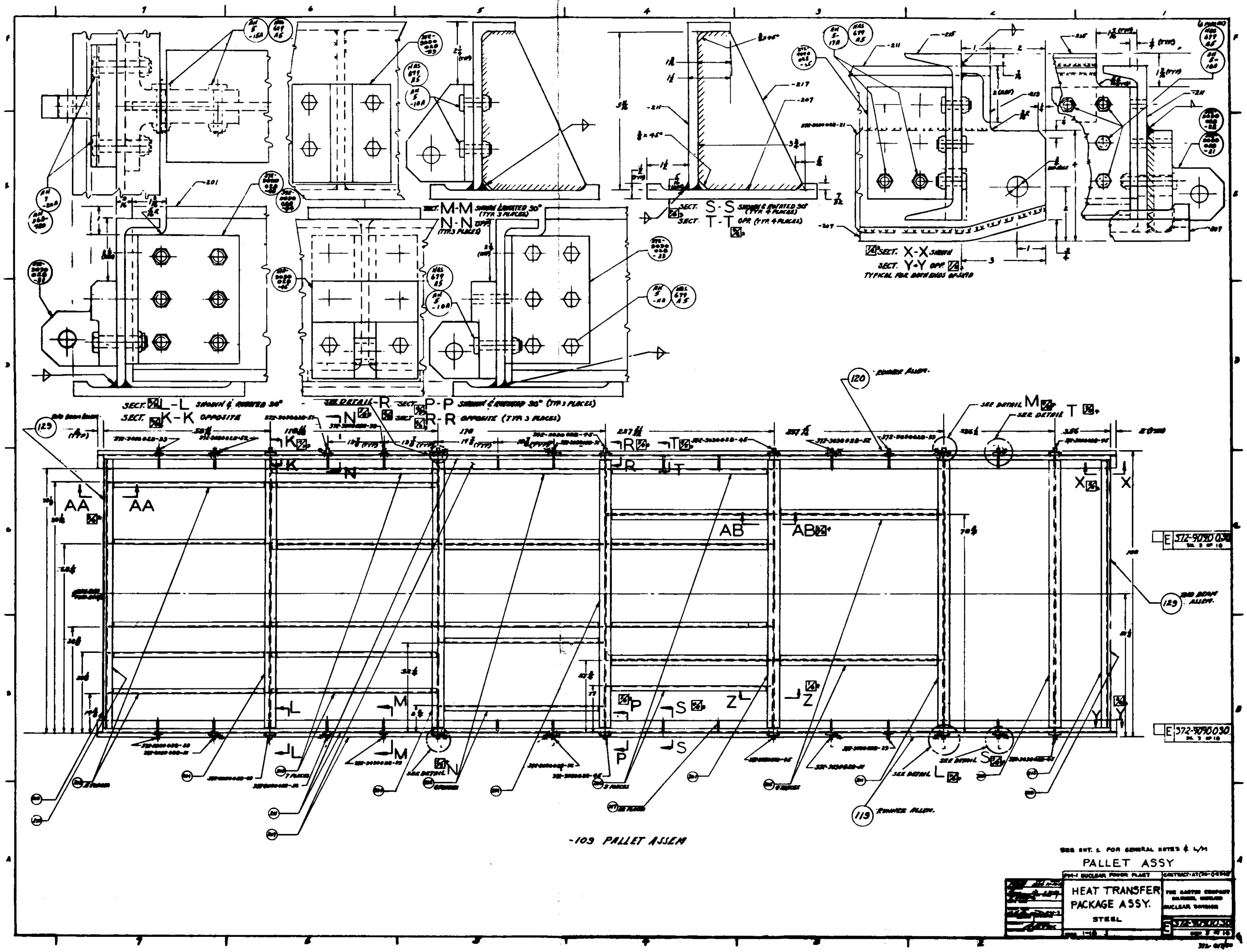

Fig. 4.64. Heat Transfer Package Assembly Drawing (Pallet Assembly)

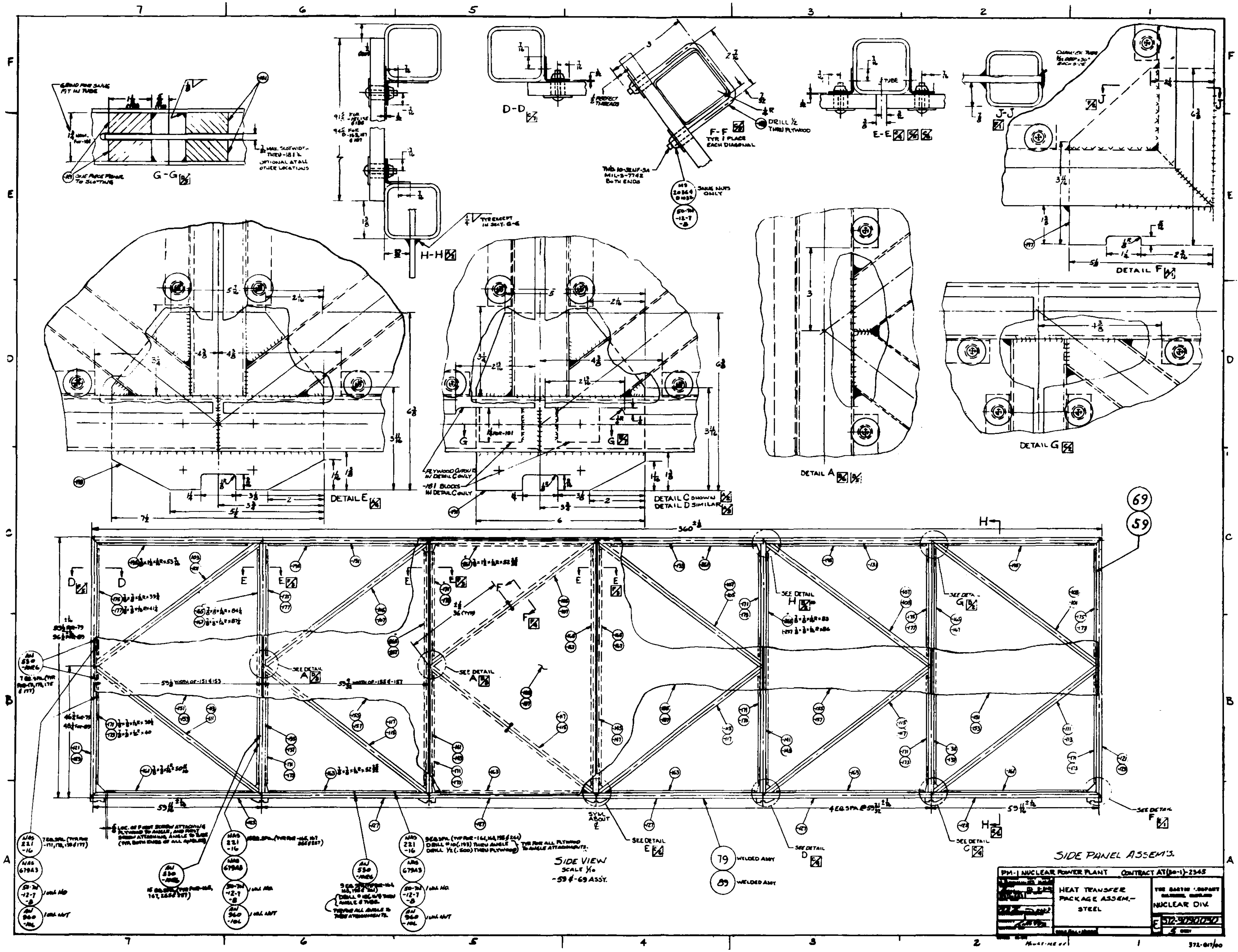

Fig. 4.65. Heat Transfer Package Assembly Drawing (Side Panel Assemblies)

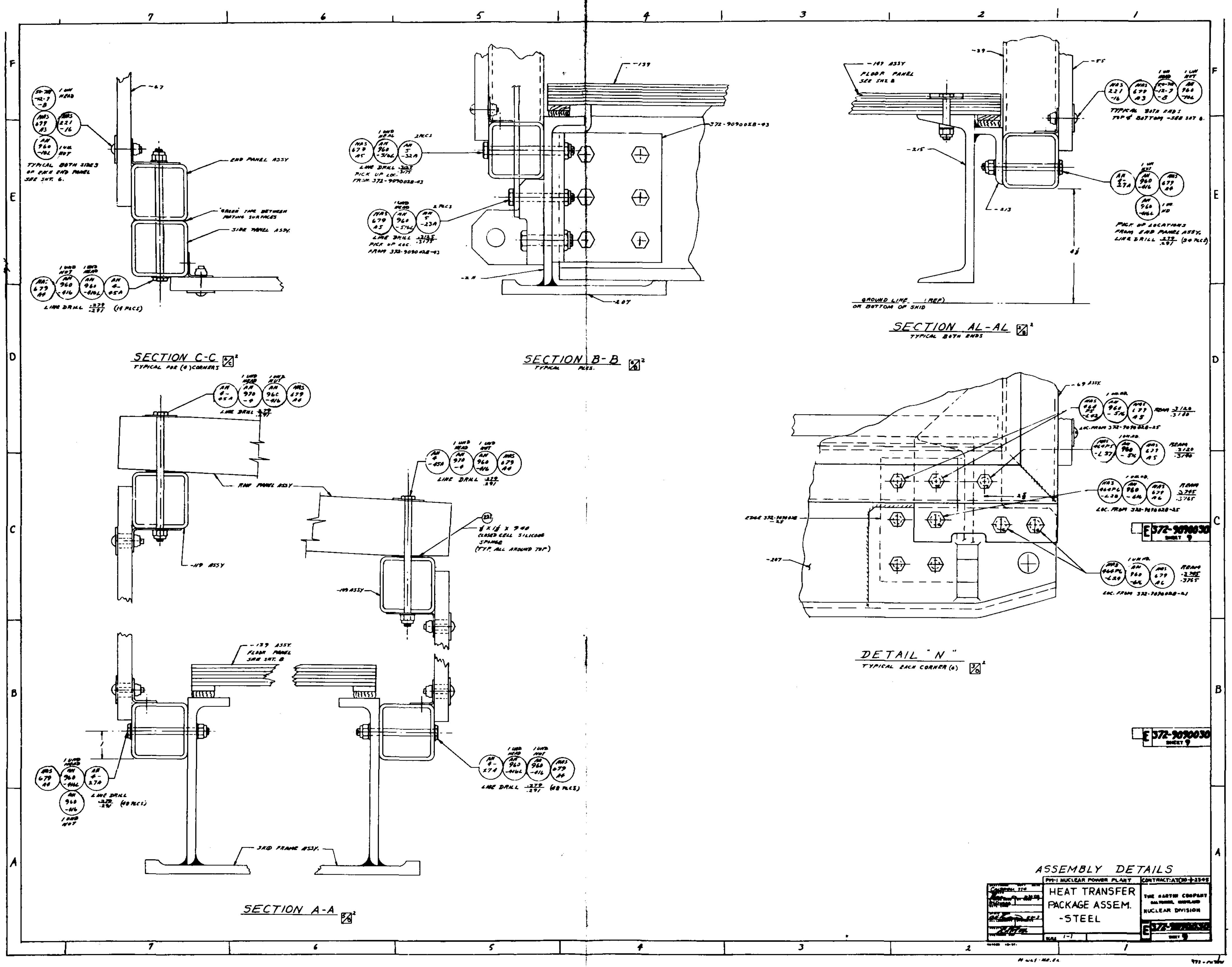

Fig. 4.66. Heat Transfer Package Assembly Drawing (Assembly Details)

During the next quarter, final methods and procedures will be established for installing and erecting the primary plant. The drawings needed to describe the erection method adequately will be prepared.

The basic methods for erecting the noncontained plant utilize, in the following sequence, the gantry and hoist normally used for plant maintenance and refueling.

a. Noncontained version

(1) After the primary plant superstructure and hoisting gantry are installed, the spent fuel storage tank is skidded into place and raised to a vertical position as noted in Fig. 4.67. The spent fuel tank is temporarily supported until the base is installed.

(2) The support frame for the reactor and steam generator packages is positioned on the foundation, leveled and bolted down.

(3) The trunnion fittings, sheaves and hoisting cables are rigged to hoist the reactor package to a vertical position as shown in Fig. 4.68.

(4) A snubbing device is installed to ease the package past the vertical centerline of the hoisting trunnion to the rest position.

(5) The package (shipped with the reactor pressure vessel in position) is rotated 180 degrees to align it properly with the steam generator package interconnect. This operation is accomplished by using the overhead hoist and swivel hook to lift and rotate the package.

(6) The hoisting trunnions, sheaves and cables are rigged for erecting the steam generator package as shown in Fig. 4.69. The steam generator package erection procedure is similar to that used with the reactor package except for the rotation of the package.

(7) After the final positioning of the two packages, the hoisting equipment is removed and the interconnect is positioned between the reactor package and the spent core storage tank.

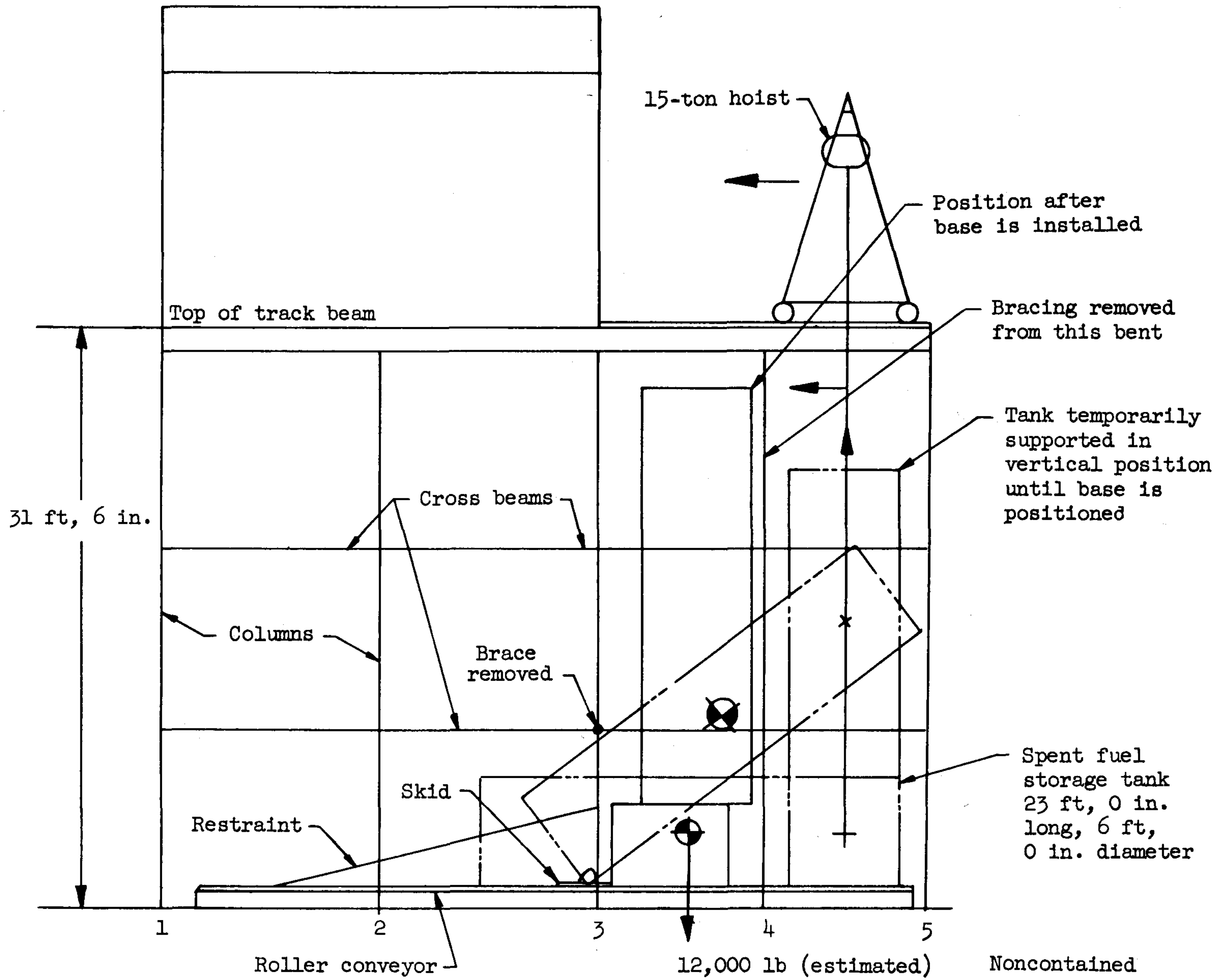

Fig. 4.67. Hoisting Spent Fuel Storage Tank

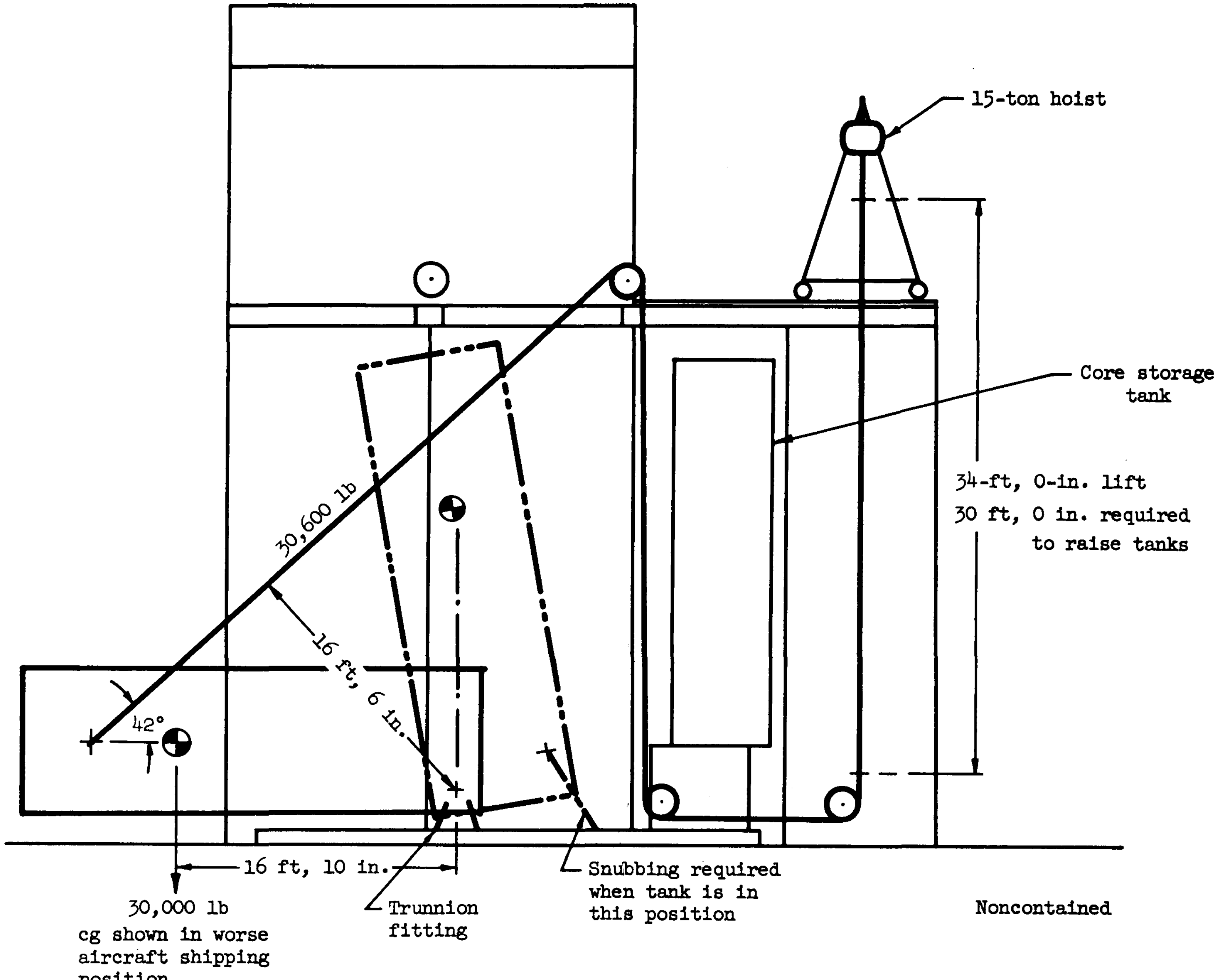

Fig. 4.68. Hoisting Reactor Package

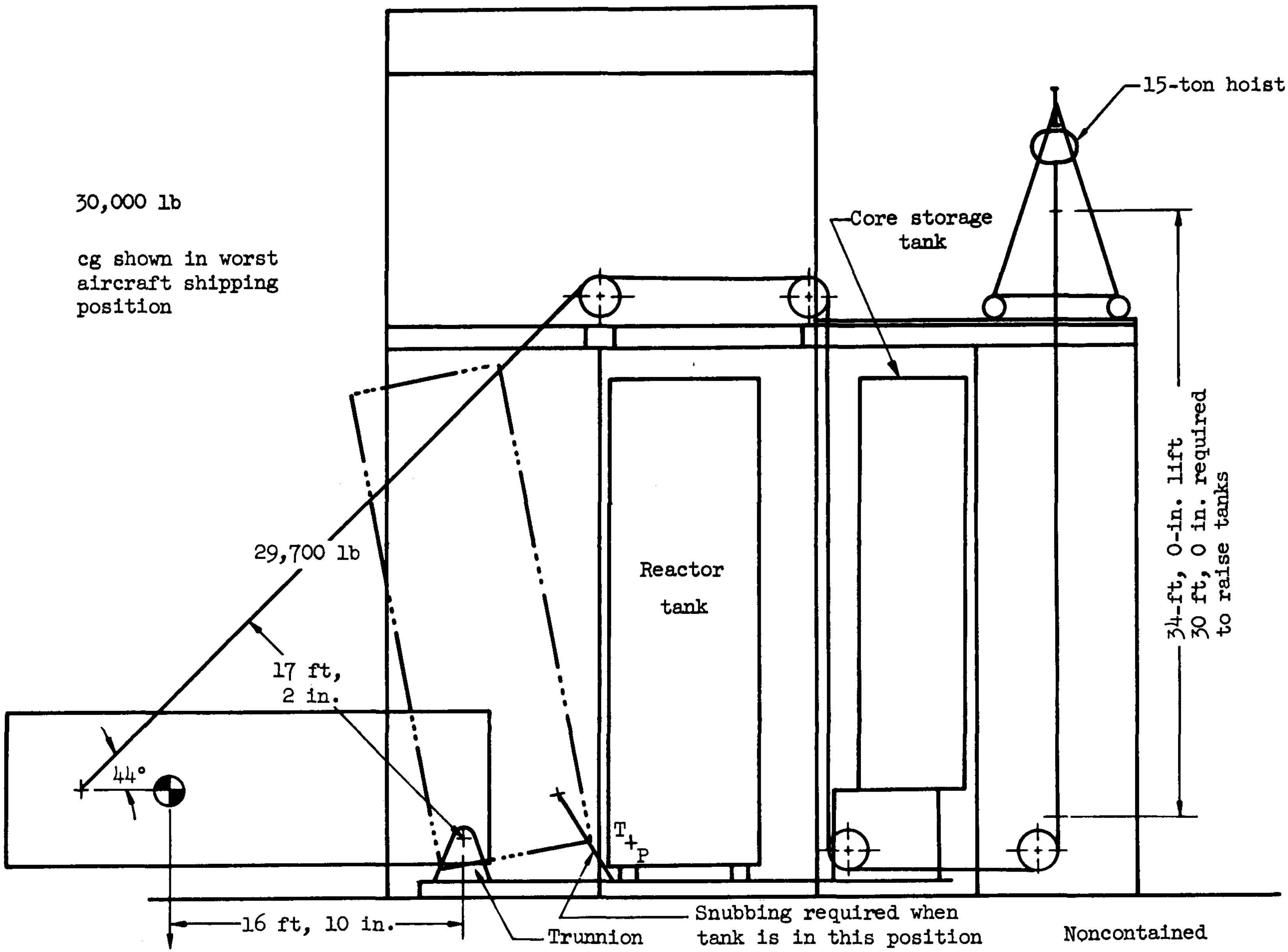

Fig. 4.69. Hoisting Steam Generator Package

(8) The interconnect to the reactor is an attached package (see Fig. 4.70).

(9) After positioning and bolting the interconnect to the reactor package, the spent core storage tank is positioned as shown in Fig. 4.70.

An alternate method considered for arranging the hoisting sheaves is shown in Fig. 4.71. This method is not contemplated since it induces undesirable loads in the gantry structure. The weight increase in the structure, necessary for carrying these loads, would hamper its assembly at the site.

b. Contained version

Basically, the same method is used for erecting the contained version of the primary plant. The contained version reactor package is hoisted in two separate halves. It is, then, necessary to rerig for hoisting of the steam generator packages due to the large weight of the total package.

The reactor package is skidded into place and hoisted to a vertical position. The interconnects between the reactor and steam generator packages are temporarily positioned.

The combined steam generator package (containment tank plus frame on which equipment is mounted) is skidded into place, and the hoisting equipment is rigged for the first lift (see Fig. 4.72). The package is hoisted to an intermediate position, and support cables are attached in order to rerig as shown in Fig. 4.73. A snubbing device is used when the package approaches the vertical centerline of the hoist trunnions as shown in Fig. 4.74. Jacks are used for the final positioning and leveling of the package.

There are distinct disadvantages to erecting the contained plant as compared to the noncontained. The limited shipping weight requires the insertion of the steam generator package into the containment vessel at the site. The combined weight (approximately 50,000 pounds) requires special handling, such as multiple sheaving, which requires two-phase erection.

2. Primary System Component Packaging

W. Dallam

During this quarter, a running tabulation of component weights was established, and components were grouped into packages for shipping purposes.

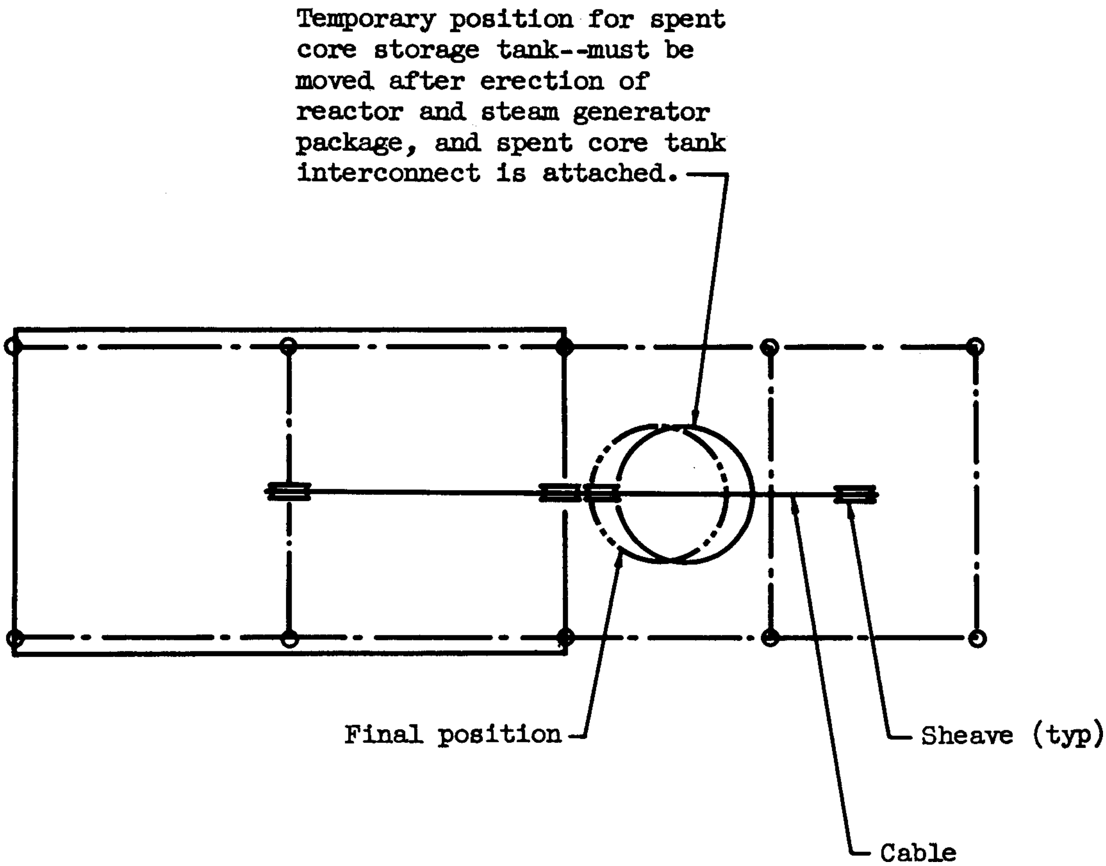

Plan view

Noncontained

Fig. 4.70. Interconnect Attachment

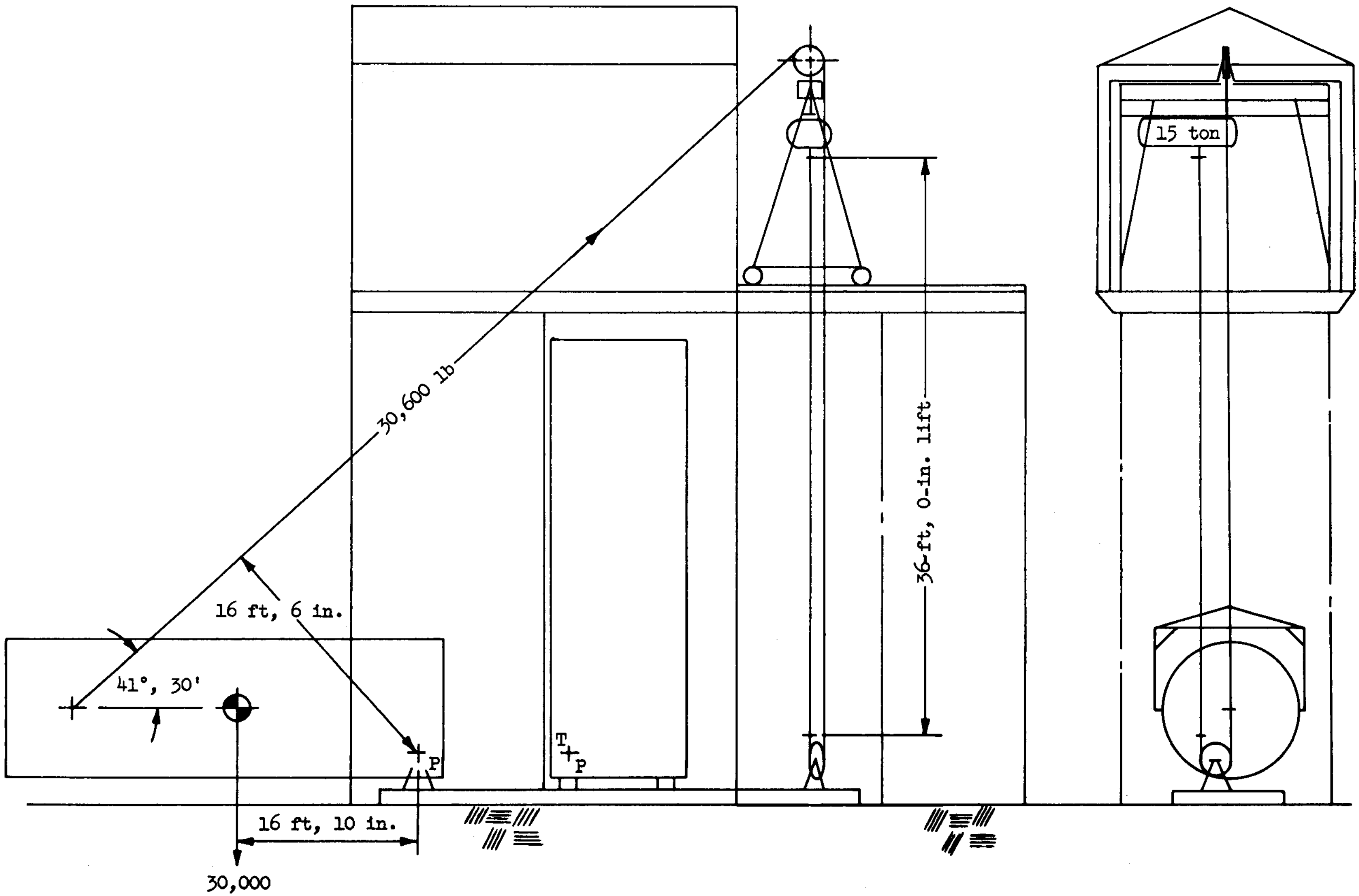

Fig. 4.71. Alternate Method of Hoisting Tanks (steam generator package shown)

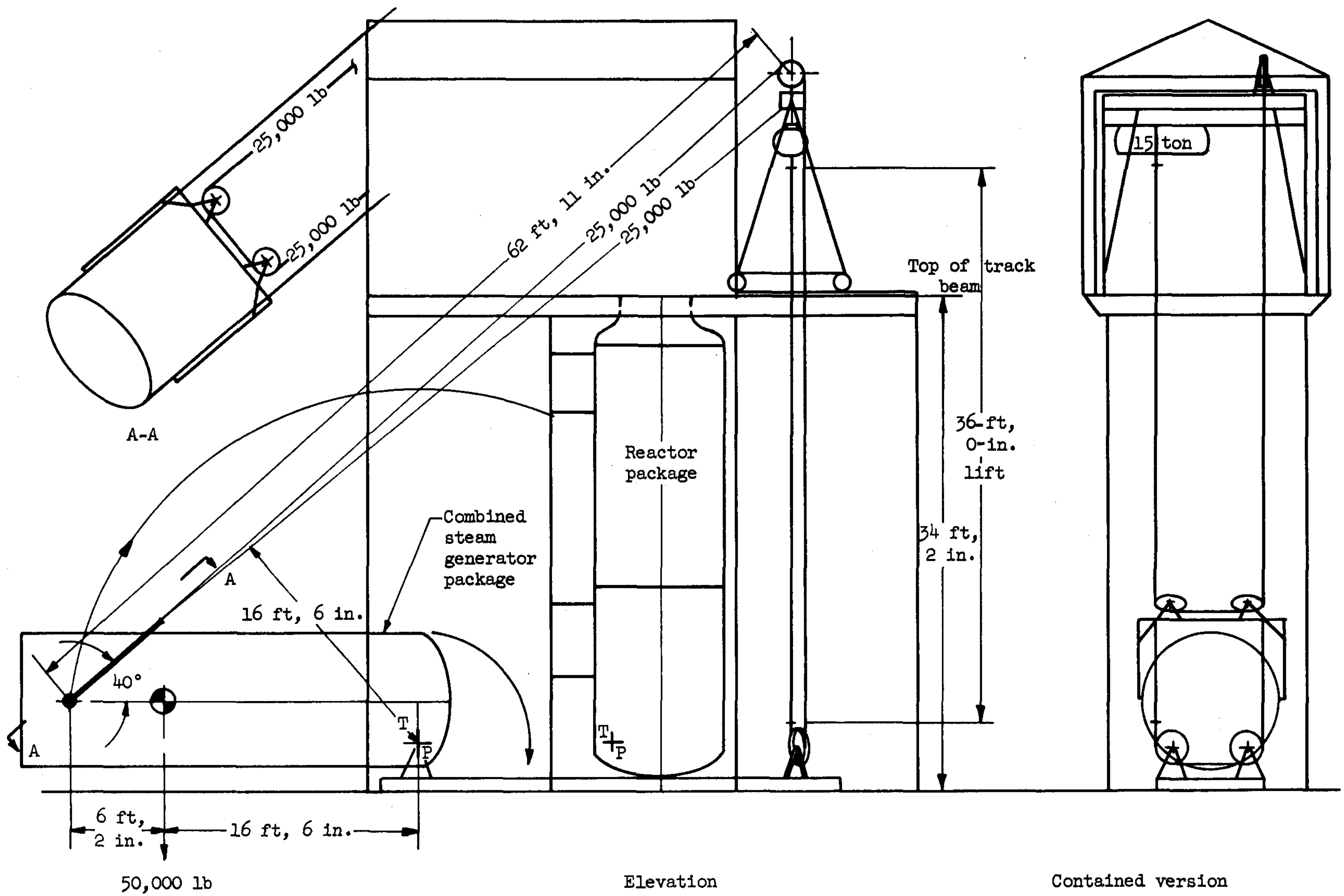

Fig. 4.72. Hoisting Steam Generator Package

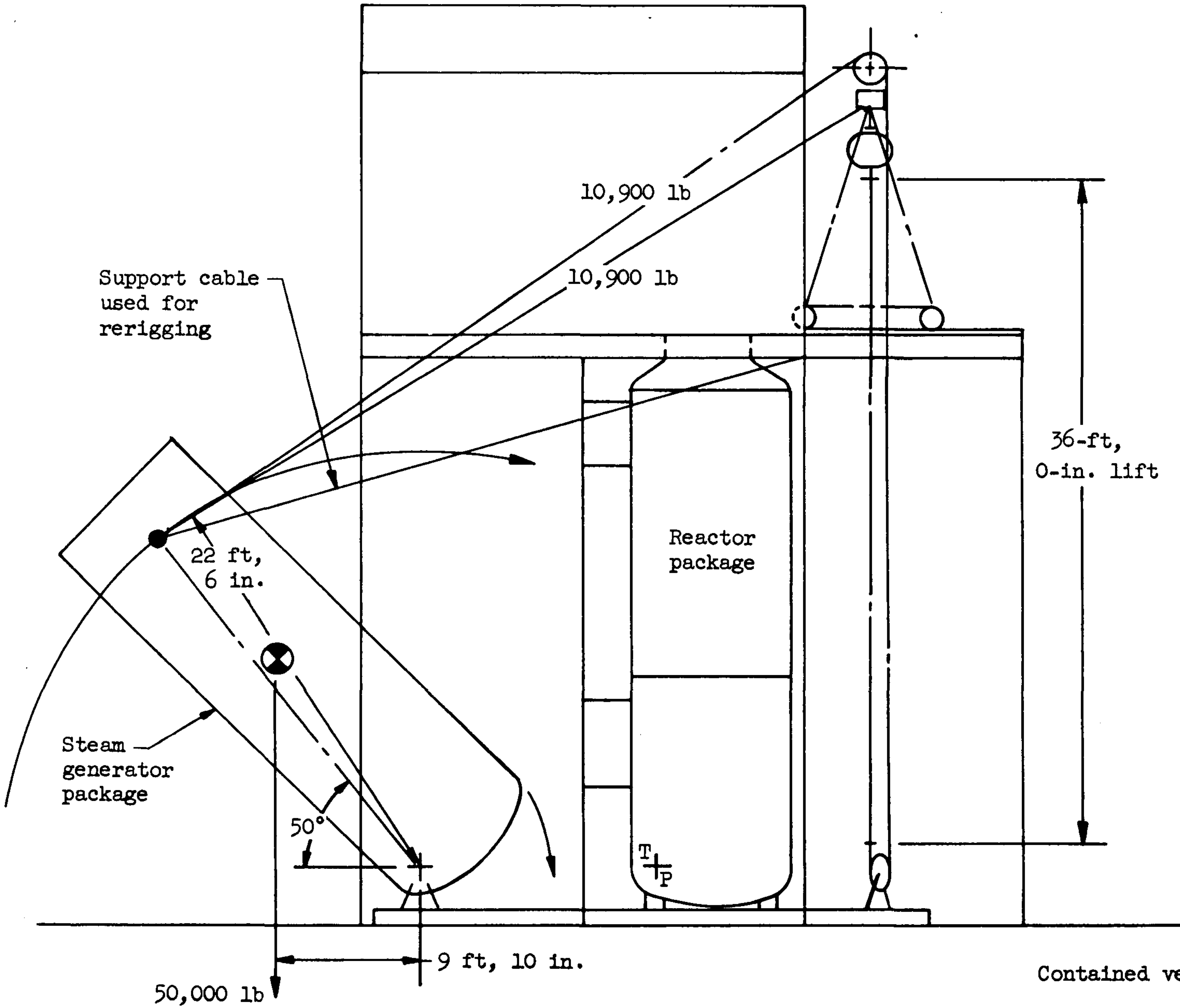

Contained version

Fig. 4.73. Rerigging Position 2

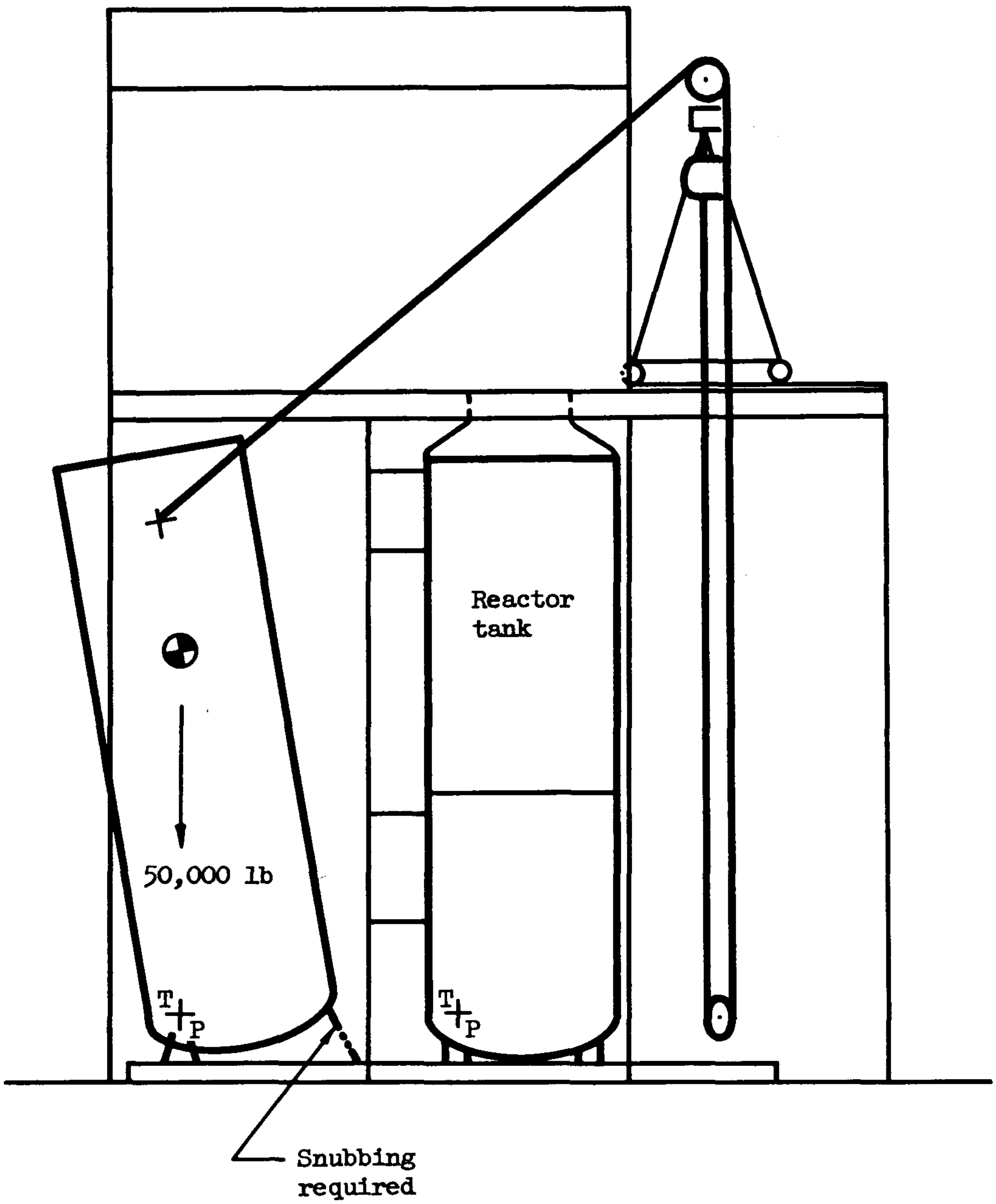

Contained version

Fig. 4.74. Snubbing Position

During the next reporting period, layouts of the individual packages will be completed, and package weights will be confirmed. The running weight balance will be modified as additional equipment weight and size data become available.

The weight tabulation and package arrangements include the entire primary system, including the superstructure and the plant building, with the exception of the spent fuel shipping cask.

The packaging list that follows was prepared on the basis of gross shipping weight; changes may be made when layouts are completed, and space per component is evaluated against the gross volume of the individual packages. It appears, from a weight standpoint, that the noncontained plant to be flown to the site in 1961 will utilize six packages (as presented in Fig. 4.75) and the contained version will require eight packages (as presented in Fig. 4.76).

If certain items are shipped in 1960 and installed during site erection work, the noncontained plant will require only that the five packages shown in Fig. 4.77 be flown to the site.

3. Reliability

J. Stegemerten

The general objectives for reliability effort during the third quarter placed emphasis on review of overall plant reliability, including:

(1) Review of equipment specifications for adequate reliability requirements and review and filing of equipment data received.

(2) Component reliability studies to support specifications.

(3) Liaison with subcontractors.

Data was received from the three subcontractors and reviewed. A detailed study and statistical summary of SM-1 operating history was started.

The expected work for the next quarter will be confined to efforts having direct effect on the final equipment design. This will include general specification language for reliability of all procured equipment and component reliability studies only on specific items where the type or quantity may be affected in final design.

Reactor Package 01	
Item	Weight (lb)
Double wall tank	14,560
Reactor vessel shell	8,426
Insulation	1,725
Water box	250
Mounts	500
Main loop pipe and interconnect insulation and conduit pipe	855
Water barrier and interconnect fitting	1,805
Auxiliary piping	200
Shield water pumps (2) and mounts	120
Low pressure demineralizer	270
Condenser coil	60
Ion counter package	125
Roller conveyors	660
Gross shipping weight	29,556

Steam Generator Package 02	
Item	Weight (lb)
Steam generator tank	13,700
Steam generator	9,900
Primary coolant pump	1,500
Expansion tank	200
Charging pumps (2)	600
Auxiliary piping and valving	500
Economizer	800
Cooler	180
Auxiliary coolant pump	80
High pressurizer demineralizer	350
Sump pump	250
Main loop pipe	860
Gross shipping weight	28,920

Equipment Package 11	
Item	Weight (lb)
Support skid and roller conveyor	7,660
Reactor head	3,075
Pressurizer	4,200
Pump motor	2,150
Hoisting trunnions	1,300
Air blast cooler	3,700
Tank interconnect	3,000
Tank extensions	1,400
Air blast cooler duct	3,000
Gross shipping weight	29,485

Equipment Package 13	
Item	Weight (lb)
Support skid and roller conveyor	7,660
Super structure (columns and bracing)	9,820
Super structure deck	10,660
Hoisting cables	1,000
Chocks and shoring	500
Gross shipping weight	29,640

Equipment Package 12	
Item	Weight (lb)
Support skid and roller conveyor	7,660
Building (crated)	5,390
Gantry structure	2,100
Sheaves and hardware	1,500
15-ton hoist	2,000
Hoisting trunnions (2)	1,300
Common support frame	9,000
1-ton hoist	200
Chocks and shoring	500
Gross shipping weight	29,650

Waste Disposal Package 23	
Item	Weight (lb)
Plywood shipping packages and roller conveyor	7,660
Spent fuel storage tank	7,700
Fuel transfer equipment	1,000
Reservoir tank (1400 gallon)	2,200
Waste tank (500 gallon)	1,020
Evaporator, piping and fittings	1,200
Condenser, piping and fittings	1,200
Condensate pump and piping	250
Lead shielding	7,590
Gross shipping weight	29,820

Items to be Shipped with Secondary System	
Maintenance and special tools	1500
Lead shielding	2500
Miscellaneous core parts	1850
Reactor thermal shields	4800
Actuator packages	4500
Tank covers	2680

Fig. 4.75. PM-1 Noncontained Shipping Arrangement (all equipment air shipped)

Reactor Package 11	
Item	Weight (lb)
Double wall tank	14,465
Tank cover	1,477
Shield water pumps (2)	140
Internal hoist	650
Condenser coil	60
15-ton hoist	2,000
Ion chamber	300
Electrical junction boxes	900
Auxiliary piping and valves	200
Sheaves and hardware	1,500
Skids	600
Shipping cover	300
Thermal shields	1,300
Roller conveyors	440
Tie down fittings	200
Hand trolly	600
Actuators	4,500
Gross shipping weight	29,632

Steam Generator Package 12	
Item	Weight (lb)
Shipping container	8,410
Steam generator	9,900
Primary coolant pump	1,500
Primary main loop pipe	860
Expansion tank	200
Charging pumps (2)	600
Auxiliary piping valving	500
Economizer	800
Cooler	180
Auxiliary coolant pump	80
HP demineralizer	350
Sump pump	250
Roller conveyors	660
Steam generator mounts	1,500
Pressurizer	3,500
Gross shipping weight	29,290

Reactor Package 01	
Item	Weight (lb)
Reactor vessel	11,361
Double wall tank	14,911
Main loop pipe	855
Tie down fittings	200
Skids	600
Shipping covers	120
Roller conveyors	440
Miscellaneous core parts	1,000
Gross shipping weight	29,487

Steam Generator Package 02	
Item	Weight (lb)
Container tank with skids	19,430
Building crated	5,390
Bridge crane structure	2,100
Rail beams	2,160
Roller conveyors	660
Gross shipping weight	29,740

Miscellaneous Equipment Package 13	
Item	Weight (lb)
Skid frame and cover	7,000
Air blast cooler	3,500
Thermal shields	3,000
Primary coolant pump	2,150
Reactor head	3,075
Expansion joints (3)	5,640
Ion counter package	125
Roller conveyors	660
Hoisting trunnions	1,300
Container head	2,410
Chocks and shorings	1,000
Gross shipping weight	29,860

Miscellaneous Equipment Package 14	
Item	Weight (lb)
Skid frame and cover	7,000
Floor beams	3,125
Building structure	8,922
Support frame	9,000
Gantry rails	720
Roller conveyors	660
Gross shipping weight	29,427

Waste Disposal Package 23	
Item	Weight (lb)
Skid frame and cover	7,660
Reservoir tank (1400 gallon)	2,200
Waste tank (500 gallon)	1,020
Evaporator	1,200
Condenser unit	1,200
Condensate pump	250
Spent fuel storage tank	7,700
Lead shielding	6,740
Fuel transfer equipment	1,000
Miscellaneous core parts	850
Gross shipping weight	29,820

Void Containment Tank 26	
Item	Weight (lb)
Void tank	19,850
Chocks and shoring	1,000
Building floor	2,700
Leveling jacks	300
Maintenance and special tools	1,500
Lead shielding	2,400
Roller conveyors	660
Hoisting cables	1,000
Gross shipping weight	29,410

Fig. 4.76. PM-1 Contained Shipping Arrangement (all equipment air shipped)

Package 01	Weight (lb)
Containment vessel	14,560
Reactor vessel	10,901
Main loop pipe	2,660
Auxiliary piping	200
Shield water pumps	120
LP demineralizer	270
Condenser coil	60
Ion counter package	125
Roller conveyors	660
Total weight	29,556

Package 02	Weight (lb)
Containment vessel	13,700
Steam generator	9,900
Primary coolant pump volute	1,500
Main loop pipe	860
Expansion tank	200
Charging pumps	600
Auxiliary piping	500
Economizer	800
Cooler	180
Auxiliary coolant pump	80
HP demineralizer	350
Sump pump	250
Total weight	28,920

Package 11	Weight (lb)
Skid and conveyor	7,660
Reactor head	3,075
Pressurizer	4,200
Pump motor	2,150
Air blast cooler	3,700
Tank extensions	1,400
Hoisting trunnions	1,300
Interconnect	3,000
Air blast cooler duct	3,000
Total weight	29,485

Package 12	Weight (lb)
Support frame	9,000
Thermal shields	4,800
Maintenance and special tools	1,500
Actuator packages	4,500
Miscellaneous core parts	1,850
Roller conveyor	660
Chocks, shoring and supports	2,000
Tank covers	2,680
Lead shield	2,500
Total weight	29,490

Package 23	Weight (lb)
Shipping skid	7,660
Spent fuel storage tank and demineralizer equipment	7,700
Fuel transfer equipment	1,000
Reservoir tank (1400-gallon capacity)	2,200
500-gallon waste tank	1,020
Evaporator	1,200
Condenser	1,200
Condensate pump	250
Lead shielding	7,590
Total weight	29,820

Equipment Shipped Pre-Site Items Shipped 1960			
	Weight (lb)		Weight (lb)
15 ton hoist	2,000	Super structure (columns and bracing)	9,820
1 ton hoist and trolley	200	Super structure deck (stringers, beams and grating)	10,660
Sheaves and hardware	1,500	Guys, ropes, block and tackle	1,000
Gantry structure	2,370	Erection equipment (wrenches, jacks and gin pooles)	1,500
Hoisting cables	1,000		
Building crated (32-foot building)	6,850		
Total weight less shipping skids--36,900 lb			

Primary System Packages

5 shipping packages (shipped 1961)
- 01 reactor
- 02 steam generator
- 11 miscellaneous equipment
- 12 miscellaneous equipment
- 23 waste disposal

Total shipping weight, 147,270 lb

Pre-site equipment (shipped 1960)
Total shipping less skids, 36,900 lb

Fig. 4.77. PM-1 Noncontained Version Shipping Arrangement (site preparation equipment shipped separately)

Among the equipment for which specifications were issued during the quarter, the primary coolant pump was of particular interest. In response to the outline specification issued to vendors, several proposals contained reference to reliability records of existing installations. Data covering four years of operating experience with a canned motor pump installation was obtained at the Possum Point Power Station of Virginia Electric and Power Company. This information was reviewed to determine a most desirable mean-time-between-failure goal to be used in the final specification. The Possum Point report revealed some initial difficulties with bearings which required inspections and replacements; however, redesign of the bearings appeared to eliminate this problem. Considering this initial difficulty, the pump recorded a maximum of 6300 hours between inspections and a maximum accumulated operating time of 11,300 hours between bearing maintenance. In submarine service, Westinghouse reported that six Nautilus canned pumps logged from 10,000 to 15,000 hours each without maintenance. In consideration of this and previous information and the established scheduled down time allowed for PM-1 inspection and maintenance, it was determined that 8760 hours (one year) would be a reasonable mean time between failures (MTBF) with one spare pump available for immediate replacement in case of failure. An annual allowable down time of 16 hours for pump failure was estimated, including 8 hours for Primary System cooling and startup. On this basis, an additional requirement was included in the specification that the design allow for removal and replacement of the pump from its volute casing in a total span time of 4 hours.

It was determined from a preliminary investigation of the pressurizer design that no failures causing significant down time should be expected from the well-type heaters due to the redundancy of installed spares.

The requirements for reliability data from Westinghouse, as specified in the revised statement of work issued to them, were reviewed. The types of information most useful in making a reliability evaluation of the equipment concerned were enumerated as failure rates or failure history, operating time of existing installations, modes of failure, maintainability records and effects of storage degeneration. Predictions of annual maintenance and down time were requested in final report form, supported by data from existing installations of similar equipment.

The statement of work previously issued to Stromberg-Carlson calls for a complete reliability analysis of the control system that they are developing. Progress data was reviewed during the quarter, and comments forwarded.

REFERENCES

1. Kavanaugh, D. L., and Mandeville, C. E., "Elastic and Inelastic Neutron Cross Sections," CWR 4040, June 1958.

2. Rockwell, T., Editor, "Reactor Shielding Design Manual," TID 7004, March 1956.

3. Perkins, J. F., and King, R. W., "Energy Release from the Decay of Fission Products," Nuclear Science and Engineering, Vol. 3, pp 726 to 746, 1958.

4. Owings, W. D., "A Program for the Computation of Fission Product Activity," MND-1721, March 1959.

5. Hughes, D. J., and Schwartz, R. B., "Neutron Cross Sections," BWL 325, 1 July 1958.

6. "PM-1 Nuclear Power Plant Program--Second Quarterly Progress Report, 1 July to 31 August 1959," MND-M-1813, 5 October 1959.

7. "Evaluation of Low Impurity Core Material in the SM-2," APAE Memo No. 214, August 1959.

IV. TASK 5--CORE FABRICATION

Project Engineer--Subtask 5.1, 5.2, 5.3: J. F. O'Brien

The overall objectives of Task 5 are to develop and fabricate the fuel elements for the PM-1 Flexible Zero-Power Test and the final PM-1 core.

A. SUBTASK 5.1--FABRICATION OF CORE

S. Furman, J. Neal, B. Sprissler

During this quarter, fabrication of the PMZ-1 fuel elements was initiated.

At the completion of the next quarter, fabrication should be approximately 90% complete.

Studies to determine the fuel loading for the PMZ-1 core were completed. Fuel specifications established were $38.6^{+1.5}_{-0}$ grams of U-235 per fuel element. The nonuniform burnup studies performed to determine the fuel loading are described under Task 4 in this report.

The criticality amendment* to the PM-1 manufacturing feasibility report was completed. Criticality limits for the different forms of materials were determined on the basis of nuclear calculations**.

An allowable limit for the manufacturing of the fuel elements, consistent with calculated limits and manufacturing requirements, was established.

Nuclear studies for the design of the fuel element storage boxes were completed. The container dimensions (in inches) are 15 by 15 by 42. Each container can store up to 25 fuel elements.

Low Cobalt-Low Tantalum Material Study

The degree of attainable purity in stainless steel cladding material with respect to cobalt and tantalum content depends, to a great extent, upon the degree of purity of the raw materials used and their subsequent handling. To examine this aspect of the problem, three 18-pound heats

* Criticality Precautions Manual, Amendment A, MND-1063, 5 November, 1959.

** Chernick, "A Guide to the Calculation of Criticality Limits for Enriched Uranium," January 1959.

of type 347 stainless steel were prepared by the Special Alloys Section, Metallurgical Products Division of the General Electric Company. The grades of raw material shown in Table 5.1 were used. The raw material impurity contents are given only for cobalt and tantalum since the analyses for the other impurities remained essentially the same. Heats Nos. X1551, X1552 and X1553 were prepared using vacuum-induction melting. The results of these melts are given in Table 5.2. The results indicate that good impurity levels can be obtained with intermediate purity grade raw materials. The technical grade raw material used is of a higher purity than commercial grade raw material. The results for heat No. X1553 indicate the level of purity attainable with the best raw materials available.

Several points of importance should be noted regarding the production of high purity material. It is essential that steels of the purity levels desired be vacuum-induction melted rather than air melted. Air melting allows less control of impurity content and excessive oxidation as well as large accumulations of slag and very little outgassing of the melt. All casting must be done in a vacuum with attention given to preconditioning of the mold in a high temperature furnace. Metal molds must be used since sand molds contain excessive moisture which leads to oxidation.

TABLE 5.1

Analysis of Raw Materials Used for Experimental Heats

Raw Material	X1551 Technical Grade Co	X1551 Technical Grade Ta	X1552 Intermediate Co	X1552 Intermediate Ta	X1553 High Purity Co	X1553 High Purity Ta
	Weight %		Weight %		Weight %	
Fe	0.007	ND*	0.005	ND*	0.002	ND*
Cb	--	1.5	--	0.5	--	0.16
Si	Nil	Nil	Nil	Nil	Nil	Nil
Mn	Nil	Nil	Nil	Nil	Nil	Nil
Ni	0.001	Nil	0.001	Nil	0.001	Nil
C	Nil	Nil	Nil	Nil	Nil	Nil

*ND--not detectable.

TABLE 5.2

Results of Experimental Heats* (as cast)

Heat Number	Weight % C	Cb	Co	Ta
X1551	0.05	0.76	0.008	0.008
X1552	0.02	0.74	0.006	0.005
X1553	0.06	0.76	0.005	0.005

*Analysis of other materials same as standard type 347 stainless steel.

The dew point of the vacuum furnace must be maintained at better than -125°F. Inert gas atmospheres are neither desirable nor practical.

B. SUBTASK 5.2--CONVERSION OF UF_6 TO UO_2

W. Thompson

Delivery of approximately 15 pounds of UO_2 was completed during this quarter.

At the end of the next quarter, conversion of all UF_6 will be complete and delivery will be 75% complete.

C. SUBTASK 5.3--FUEL ELEMENT DEVELOPMENT

B. Sprissler, J. Kane, J. Neace, D. Grabenstein, H. Barr

The general objectives of this subtask are to determine the limits of control rod and tubular fuel element fabrication techniques and to determine what refinements of technique can be made. During this quarter, efforts were planned and accomplished for:

(1) Establishment of final fabrication parameters for fuel elements and the development of tooling for production runs.

(2) Establishment of ultrasonic testing standards for production elements.

(3) Completing boron loss tests.

(4) Investigation of methods of stabilization of the rare earth oxides against hydration.

During the next quarter:

(1) Ultrasonic testing standards will be completed.

(2) An expanded program to investigate stabilization of the rare earth oxides for use as control materials will be initiated.

1. Fuel Element Fabrication

Development of the tools required for fuel element fabrication evolved from the production of full length and segmented irradiation samples. The most significant change in tooling was the elimination of the swaging operation which was always objectionable from the standpoint of contamination and UO_2 losses. This operation was eliminated by utilizing a set of formed rolls on a Niagara bench roller to form the core. The other change is the successful use of the restrained mandrel for better control of the inside diameter of the tube along with a better surface finish.

During the fabrication of fuel elements in a preproduction run consisting of ten lots of eight natural tubes each, some process changes were required. The first change was necessitated by the fuel loading change which brought the weight percent of UO_2 into the upper limits as far as formability of the core tube was concerned. It was necessary to increase the annealing temperature of the strips to 2150° F for 45 minutes and, with this heat treatment, the strips formed successfully. Production forming tools were used for the majority of the core tube forming work. During the drawing and elongation of the tubes, it was found that the most significant changes in elongation were influenced by the thickness of the fuel strip used. A close tolerance, therefore, is required on fuel strip thickness. After the drawing procedure and die selection were resolved, the length control was not a serious problem.

A technique for pointing the tubes for the second drawing operation, utilizing the draw bench, eliminated the necessity for transporting material from one work area to another.

Ultrasonic testing uncovered a bonding problem during this run. It was found that any appreciable amount of forming after the leaching operation caused an objectionable amount of new fuel to break up and contaminate the interface between the core and clads. A change in the cleaning cycle eliminated this difficulty.

Ultrasonic and metallographic inspection indicated that the seam along the dead end was also a problem area. More control during the shearing of strip to single widths has alleviated this problem.

After furnace modifications were completed, the furnaces were certified for use. Further modifications to lengthen the cooling chambers were required. It was found that the length of the boats dictated by the work load kept one end too close to the hot zone and prevented adequate cooling, resulting in oxidation and contamination on removal from the furnace. Two modified furnaces will be recertified. The tooling for the brake forming operations was received and checked.

2. Ultrasonic Testing

Some difficulty was encountered in fabricating a satisfactory internal probe. Several were made of tubing with an OD of approximately 0.110 inch. Tests utilizing these probes showed that a 5-mc crystal gave best results. However, these small diameter probes proved too fragile and broke constantly. A satisfactory internal probe was, therefore, fabricated using 0.200-inch OD tubing and a 5-mc crystal. To date, this probe has been able to withstand the rigors of constant use.

During preliminary testing, a fuel element (1372-1) was chosen as the standard defect fuel tube. Three flat bottom holes (1/16, 1/8 and 3/16 inch in diameter) were drilled on the surface and filled with a mixture of epoxy resin and microballoons (an excellent absorber of sound) to simulate unbonded areas. Figure 5.1 shows the DCP* trace of this fuel element. The trace shows that the 3/16- and 1/8-inch holes are clearly visible while the 1/16-inch hole can hardly be seen. The trace accompanying the DCP recording is a double wall trace. All three holes show up distinctly. It is noted that this type of trace shows no information on the shape of the defect.

Figure 5.2 shows the effect of gain on the appearance of the DCP recording. For the actual test run, a gain of 300 was chosen. The six sections marked were examined metallographically and all appeared to be well bonded. Therefore, the clearest trace, i.e., gain 300, was chosen.

Figure 5.3 shows a cross section of element 1029-3. This photo reveals that all except about 90° of the tube is unbonded. Figure 5.4 is a photograph of the DCP recording of the same tube showing the section which was metallographically examined. The correlation is excellent since the DCP also shows the tube to be bonded for approximately 90° around the wall.

Figure 5.5 presents a section of element K-5 and shows how a cracked core appears on the DCP recording. Figure 5.6 shows how a cracked dead end weld appears on the DCP recording.

* Direct contour plot.

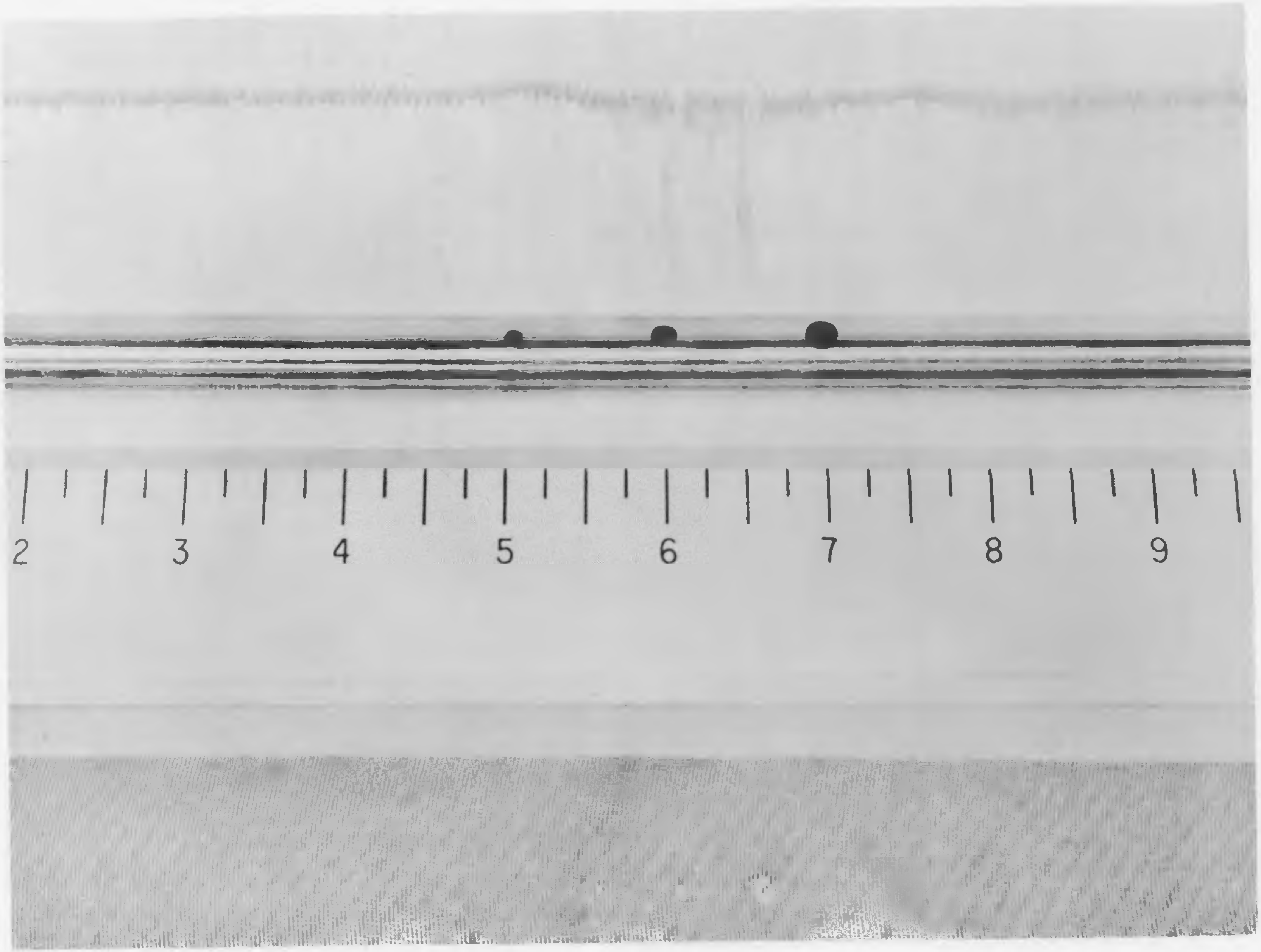

Fig. 5.1. Direct Contour Plot of Standard Defected Fuel Element

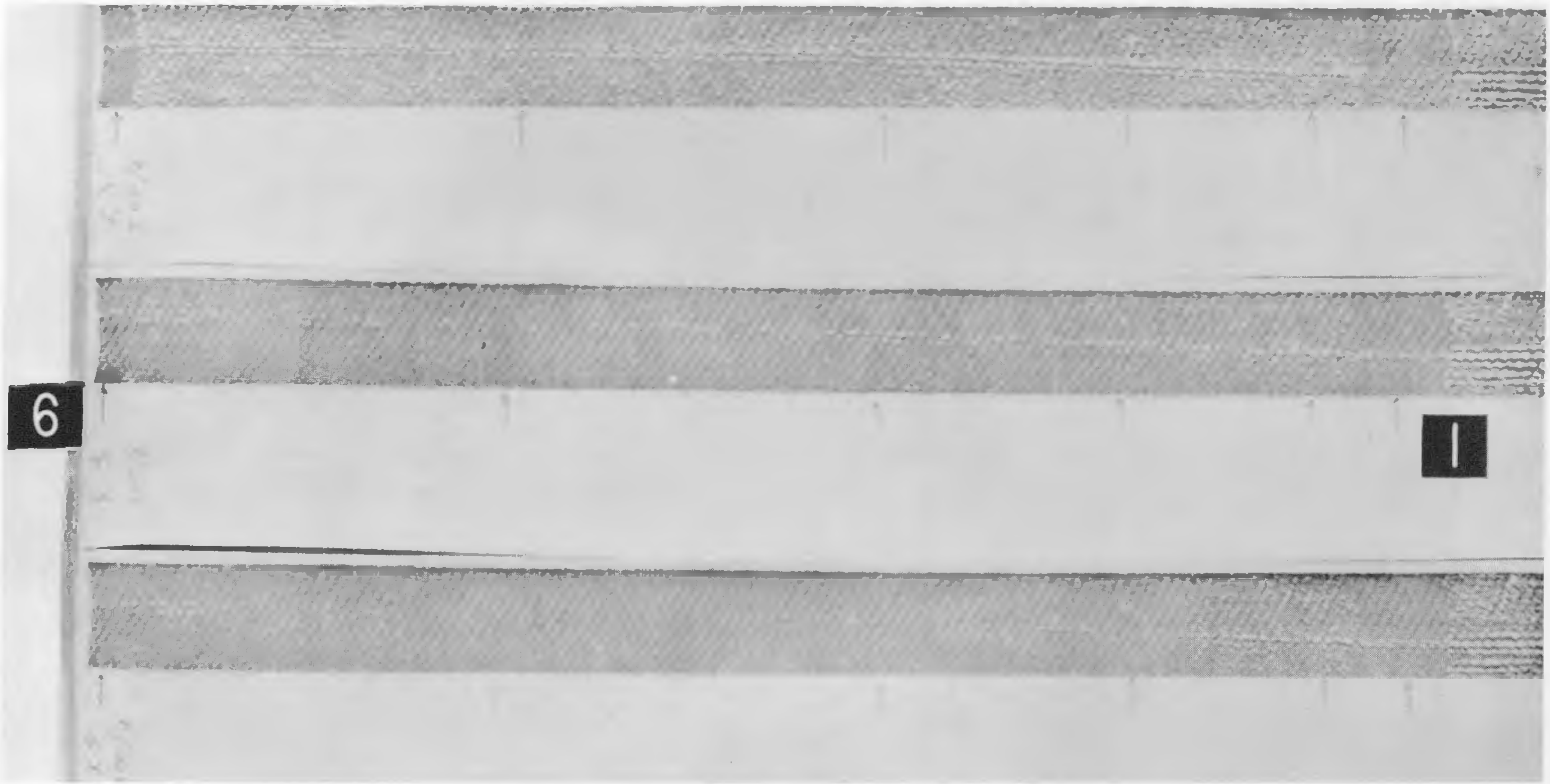

Fig. 5.2. Effect of Electronic Gain on DCP Recording

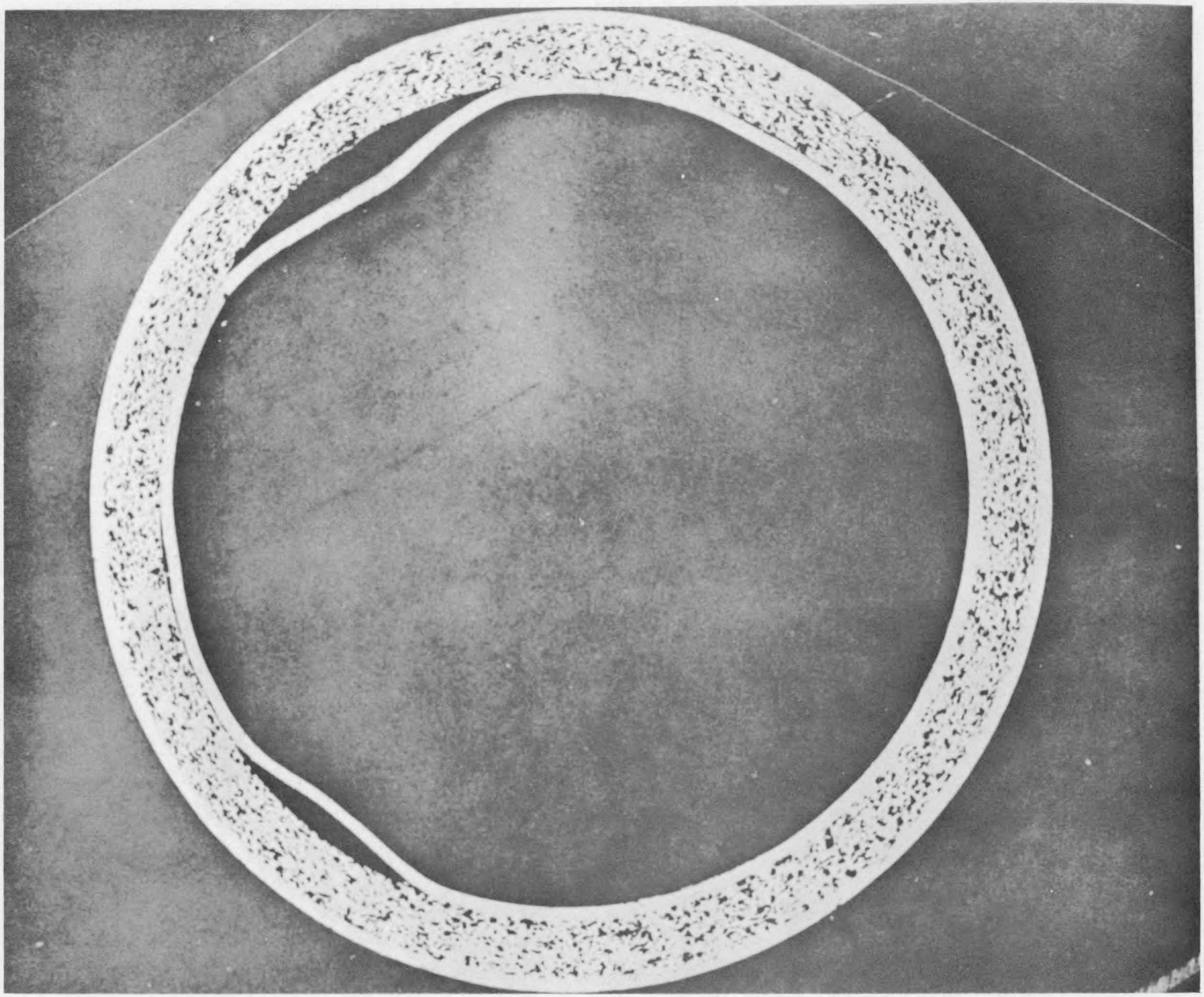

Fig. 5.3. Cross Section of Fuel Element Showing Unbonding of Inner Clad (Element 1029-3)

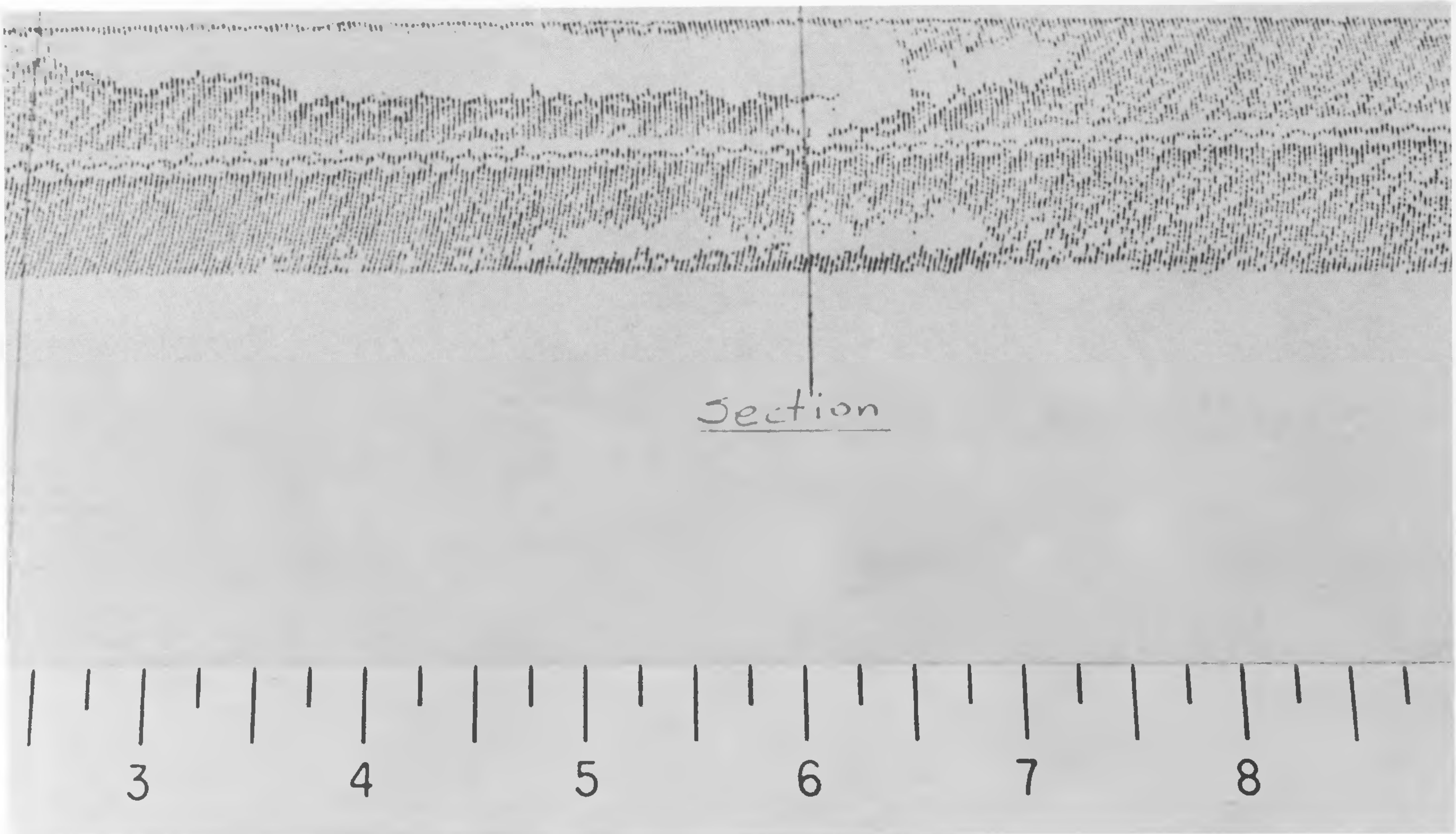

Fig. 5.4. DCP Recording Showing Unbonding of Inner Clad (Element 1029-3)

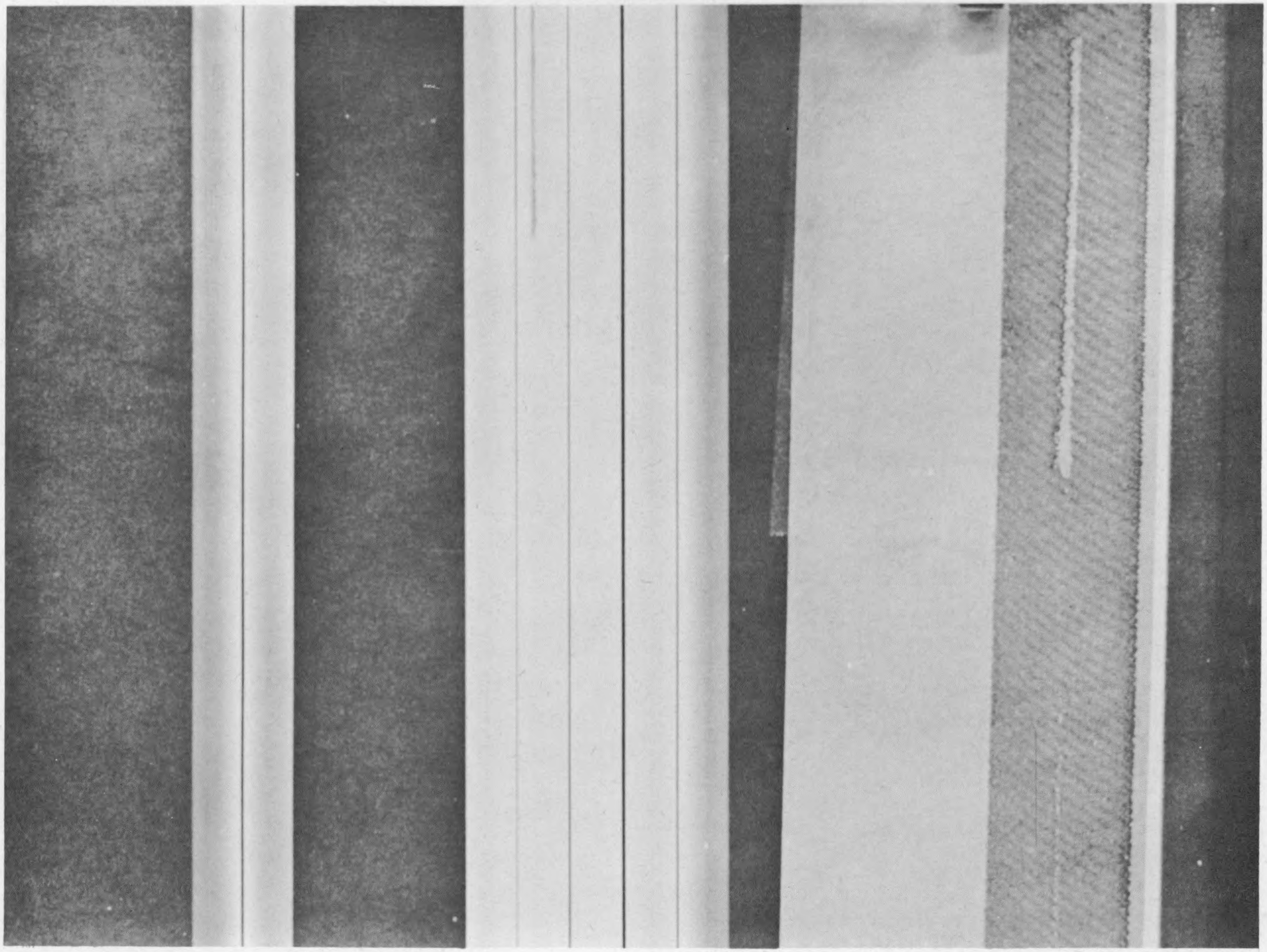

Fig. 5.5. Fuel Element and DCP Recording Showing Cracked Core Tube

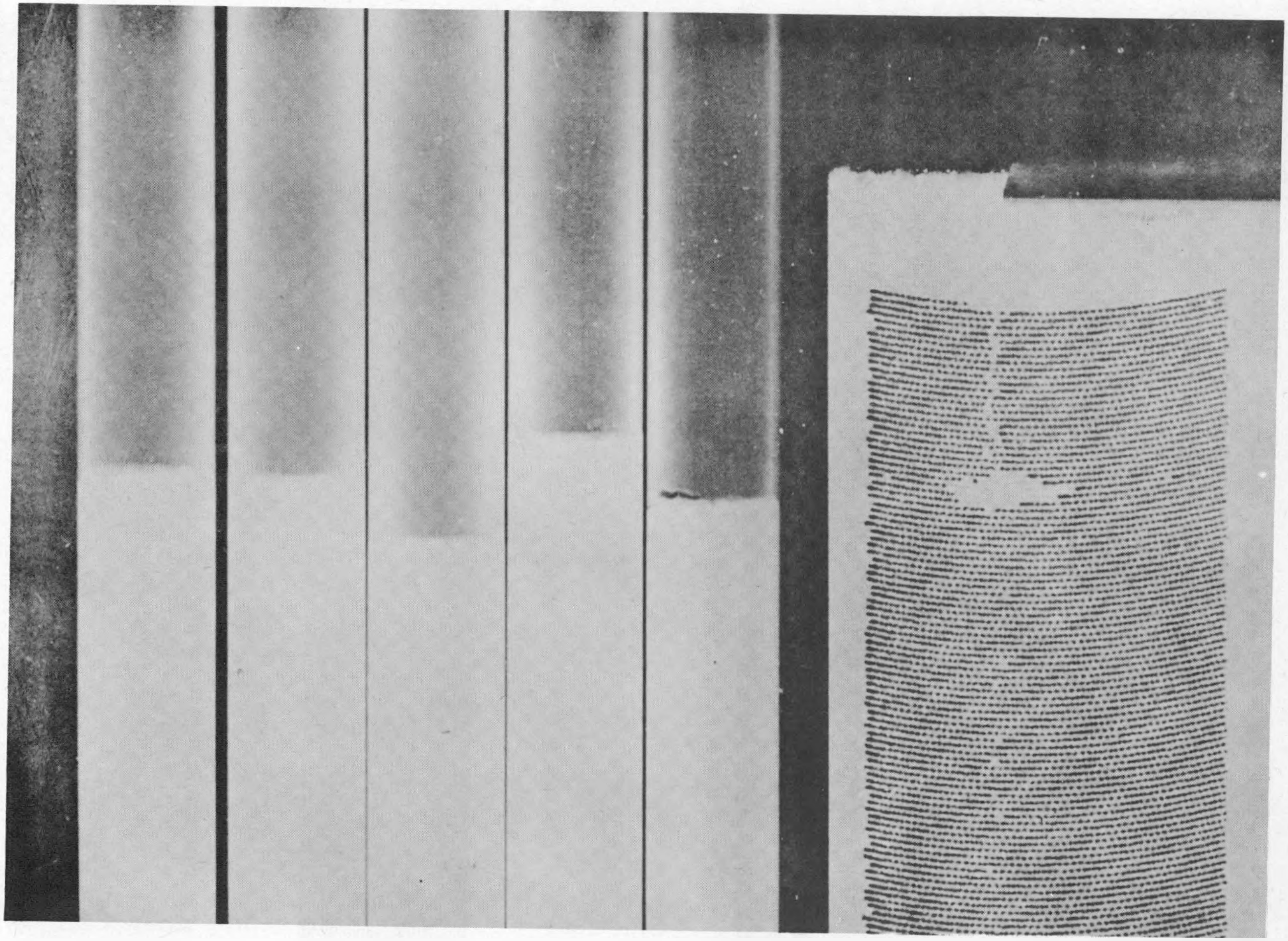

Fig. 5.6. Fuel Element and DCP Recording Showing Cracked Dead End Weld

3. Control of Burnable Poison

The effect of sintering time on boron loss was determined in several ways: (1) individual tests with the 0.38 B-stainless steel alloy and 302-B stainless steel run at different times and (2) a test with specimens of the alloy being removed at 3/4, 1-1/2, 3 and 4-1/2 hours. The results of the first test follow:

		Boron Loss (%)			
% Boron Alloy	% 302 Boron	3/4 Hour	1-1/2 Hours	3 Hours	6 Hours
100	0	0.010	0.030	0.039	0.045
75	25	0.025	0.026	0.046	
50	50	0.033	0.045	0.053	
25	75	0.034	0.036	0.045	
Average		0.026	0.037	0.046	

The results of remaining specimens of 100% 0.38 B-stainless steel alloy at various time intervals are as follows:

Sintering Time (hour)	Boron Loss (%)
3/4	0.019
1-1/2	0.038
3	0.060
4-1/2	0.098

In the first test, the boron loss appears to reach a certain point and then start to level out. In the second test, the boron loss increases with the longer time intervals; however, these greater losses may be due to the removal of the previous specimens during the furnace purge when the specimens are pulled into the cold zone for removal. It is possible that oxygen may have been picked up from the nitrogen during purging. Therefore, the resulting losses would become larger with an increased number of purgings.

Tests were run with various hydrogen flow rates to test the purity of the hydrogen. The dew point of the hydrogen on all tests was at least -75° C. The results of these tests follow:

% Boron Alloy	% 302 Boron	Boron Loss (%) Flow Rate 5 cfh	10 cfh	20 cfh	30 cfh
100	0	0.049	0.039	0.032	0.021
75	25	0.032	0.046	0.029	0.034
50	50	0.066	0.053	0.071	0.050
25	75	0.063	0.045	0.063	0.045
Average		0.055	0.046	0.049	0.038

The results reveal that there is very little difference in loss at the various hydrogen flows and indicate that hydrogen with a dew point of -75° C can be considered free of impurities in these tests.

A series of tests was made in production furnaces to compare rolled strip with compacted test specimens. It was found that the boron losses from both were equal if the dew point of the hydrogen was good; however, if the dew point was bad, there would be considerable loss from both test specimens.

4. Boron and Uranium Chemical Analysis

The boron analysis methods were tested in the 0.050 to 0.090% range. Type 304 steel containing 0.004% boron was used as the basic material for making synthetic samples. To a weighed quantity of this steel, a known quantity of boric acid solution was pipetted so that the final mixture was equivalent to 304 boron steel containing 0.050 to 0.090% boron. These samples were analyzed by the mercury cathode method, and the accuracy was found to be ± 0.002% boron.

A similar test was carried on for uranium. The synthetic samples were analyzed by the usual procedure (mercury cathode electrolysis, load reduction and ceric or dichromate titration). The accuracy was found to be four parts per thousand.

5. Stabilization of Rare Earth Oxides

During the past quarter, a preliminary study on the stabilization of rare earth oxides was conducted because the material for the control rods in the PM-1 core is Eu_2O_3. Tests were made on the stabilization of Nd_2O_3 and La_2O_3, which are both highly unstable in water. The results of the tests are applicable to Eu_2O_3, which was not used due to its high cost. A number of rare earth oxide based compounds were developed and found to be stable in various media, i.e., room temperature air, static water at room temperature, boiling water and high temperature-high pressure water. Compacts were made by sintering at 1400° C, 1500° C and 1600° C, but no apparent difference in compound stability at the different sintering temperatures was noted. The stability has been checked in air for 120 hours, in distilled water at room temperature for 48 hours, in boiling demineralized water for 67 hours and in an autoclave at 570° F and 1200 psi for 32 hours. The results of these tests are shown in Table 5.3 for those compacts sintered at 1600° C. The table reveals that a number of materials have shown a stabilizing effect. There is sufficient reason to believe that the same stabilizing effect can be obtained in a sintered compact of Eu_2O_3 and the admixture with stainless steel. Further tests will be conducted to qualify the preceding statement.

TABLE 5.3

Stability of Rare Earth Oxides

	Materials		Molecular (%)		Initial Weight	Weight After 120 hr in Air	Weight After 48 hr in Distilled H_2O at Room Temperature	Weight After 67 hr in Boiling H_2O (demineralized)	Weight After 32-hr Autoclave Test (570° F and 1200 psi)
1.	Nd_2O_3	$2SnO_2$ *	Nd_2O_3-33	SnO_2-67	2.3193	2.3193	2.3194	2.3194	2.3194
2.	Nd_2O_3	$2ZrO_2$	Nd_2O_3-33	ZrO_2-67	2.4863	2.4866	2.5147	decomposed------------------	
3.	Nd_2O_3	$2UO_2$	Nd_2O_3-33	UO_2-67	4.4863	4.4857	4.5197	4.5300	4.4750
4.	Nd_2O_3	$2CoO_2$	Nd_2O_3-33	CoO_2-67	3.2173	3.2173	3.2276	decomposed------------------	
5.	Nd_2O_3	$2TiO_2$	Nd_2O_3-33	TiO_2-67	1.8290	1.8317	1.8291	1.8285	1.8384
6.	Nd_2O_3	$3MoO_3$	Nd_2O_3-25	MoO_3-75	decomposed on firing------------------				
7.	Nd_2O_3	Al_2O_3	Nd_2O_3-50	Al_2O_3-50	2.8580	2.8578	decomposed------------------		
8.	Nd_2O_3	Fe_2O_3	Nd_2O_3-50	Fe_2O_3-50	2.7790	2.7788	2.7786	2.7762	2.7753
9.	Nd_2O_3	$2MnO_2$	Nd_2O_3-33	MnO_2-67	2.3491	2.3485	2.3474	2.3423	2.3383
10.	Nd_2O_3	Cr_2O_3	Nd_2O_3-50	Cr_2O_5-50	2.6250	2.6247	2.8566	decomposed------------------	
11.	Nd_2O_3		Nd_2O_3-100		1.8458	1.8484	decomposed------------------		
12.	Gd_2O_3		Gd_2O_3-100		2.0040	2.0040	2.0038	decomposed------------------	
13.	La_2O_3		La_2O_3-100		decomposed after pressing------------------				
14.	La_2O_3	Fe_2O_3	La_2O_3-50	Fe_2O_3-50	1.8342	not taken	1.8340	1.8330	1.8329

* Compacts sintered at 1600° C.

V. TASK 6--DUMMY CORE

The objective of this task is the fabrication of a dummy reactor core for flow tests and for a refueling demonstration. The task heading is chiefly an administrative convenience, since all experimental work is reported under Reactor Flow Studies, Subtask 2.3.

VI. TASK 7--FABRICATION AND ASSEMBLY OF THE PLANT

The objectives of this task are the procurement, fabrication and assembly of the PM-1 nuclear power plant and the necessary spare parts, special tools, and auxiliary equipment. Procurement action under this task will follow directly from development work on the control rod actuator (Subtask 2.5) and from preparation of specifications and bidding invitations to vendors for the 37 subsystems described in Task 4. Action on long-lead components, such as the reactor pressure vessel, was initiated late in the third project quarter. Action on most of the subsystems will commence during the next quarter.

VII. TASK 11--SITE PREPARATION AND INSTALLATION

Project Engineer--G. Zindler

The objectives of this task are to prepare the site for the orderly installation of PM-1 packages and to install and interconnect the packages into an operable nuclear power plant.

During this reporting period, no specific efforts are planned or required. General liaison with the various design groups was maintained to ensure the inclusion of the special requirements of the Warren Peak Site in the overall PM-1 design. It is the concensus of all expert opinion that the Sundance, Wyoming area is unsuitable for site work during the winter season.

During the next reporting period, design criteria will be prepared presenting the data necessary for the design of foundations, plant-operations area interconnects, roads and grading during site preparation and installation. The actual design of the PM-1 site will be initiated and integration of field work with the Corps of Engineers, Omaha District will be accomplished.

VIII. TASK 13--MANUALS

This task has the objective of preparation of the operating, maintenance and training publications required for the PM-1 nuclear power plant. The task will become active during the next project quarter.

The first effort will be compilation of training manuals to implement the training program (Subtask 13.2). During the next quarter, the Training Manual topical outline will be submitted to the USAEC for review under Task 14. When the outline is approved, work will commence with selection of the manual format.

IX. TASK 14--TRAINING

Project Engineer--F. McGinty

The objectives of this task are to develop and implement a program to train competent military personnel to supervise and conduct operation and maintenance on the PM-1 Nuclear Power Plant.

A. SUBTASK 14.1--TRAINING PROGRAM DEVELOPMENT

During this reporting period, as planned, the Training Manual topical outline and the training program course outlines were completed and submitted to the USAEC for review and approval. Drafts of the PM-1 Training Plan and training equipment list were also completed.

Efforts during the next quarter will be directed toward:

(1) Completing the Training Plan and submitting it to the USAEC for review and approval.

(2) Revising course outlines and the Training Manual topical outline if the USAEC review so indicates.

(3) Further development of the training equipment list.

The major area of work during the third quarter was course outline development. Outlines were prepared and submitted for:

(1) An 80-hr Plant Information Course.

(2) A 30-hr Electrical Specialty Training Course.

(3) A 116-hr Instrumentation Specialty Training Course.

(4) A 28-hr Mechanical Specialty Training Course.

(5) An 18-hr Process Control Specialty Training Course.

(6) A 40-hr Operating Procedures Course.

(7) A 40-hr Assemble and Disassembly Procedures Course.

(8) The Practical Training Phase.

(9) The On-The-Job Training Phase.

The format used in preparing items (1) through (7), above, was similar to that used by the U.S. Army Engineer School in preparing their Programs of Instructions (POI). The use of this format was to simplify the task of developing a POI for use in the military school. It also simplifies the review of the outlines submitted by The Martin Company.

The draft of the Training Plan, which was completed this quarter, contains statements relative to:

(1) The training objectives.

(2) The training concept.

(3) The training scope.

(4) The training program schedule.

(5) Training materials.

(6) Program administration and supervision.

(7) Program manpower requirements.

Special training equipment requirements are not critical at this time. The PM-1 will be available for training purposes at the factory. In addition, it is planned to use the refueling demonstration equipment and the prototype control rod actuating mechanism for training purposes. Simulated (nonanimated) control console panels, motor control center panels and switchgear panels will be prepared for classroom and familiarization training. These will be fabricated of plywood and panel photographs. Certain nuclear instrumentation modules will be purchased for demonstration and practical work purposes. The final selection of such items must await completion of the final design.

X. TASK 15--PROJECT SERVICES

Project Engineer--C. Fox

A. SUBTASK 15.1--FILM AND PHOTOGRAPHS

During the quarter, it was planned to obtain applicable progress photographs and film coverage of fabrication and test work, and to complete an outline of the project documentary film. These were accomplished and the film outline is being reviewed internally. Next quarter, it is planned to submit the completed outline to the AEC and to continue to obtain applicable photographic coverage of project progress.

B. SUBTASK 15.2--MODELS

During the quarter, it was planned to complete the PM-1 model specification for AEC approval and to begin model fabrication. This was accomplished. The model specification established the following requirements:

(1) All models will be identical and shall present the operating configuration rather than the shipping configuration.

(2) Scale of models will be: one inch = 2-2/3 ft.

(3) Overall size of each assembled model shall be approximately 3 ft by 4 ft.

(4) The terrain will be simulated to indicate site conditions.

(5) All housing facilities will be simulated and shall be constructed of transparent plexiglass and/or removable sections to reveal important interior details.

(6) The Primary System will be simulated in detailed reproduction utilizing transparent plexiglass and/or cutaway sections, where necessary, to reveal all major system units and components including the steam generator, pressurizer, reactor vessel, main coolant pump, demineralizer, charge pumps and shield water equipment in addition to supporting structure and fuel loading facilities. All major piping necessary for system operation will be simulated but all other piping incidental to system operation will be simulated only according to its size limitations. In general, piping of one-inch

diameter or smaller (actual size) will not be shown unless important to the function of the system.

(7) The Secondary System will be simulated in detail reproduction for major cycle equipment and components including the turbine-generator, condenser units, pumps, deaerator, heater, switchgear and motor control center cubicles, control console and plant maintenance equipment and facilities. Major and minor piping will be simulated subject to same conditions as stated in Item 6 for the Primary System.

(8) Valves, pipe elbows, tees, etc., will be simulated with a reasonable facsimile using commercial model components as may be necessary for all major systems throughout the facility.

(9) Suitable color coding of all equipment and service lines will be incorporated.

(10) Lighting effects will be primarily installed in the Primary System equipment tanks and the Secondary System housing facility to show major cycle equipment and components.

(11) The models will be packaged in carrying cases approximately 2 feet by 3 feet by 4 feet and will be mounted on roller casters for ease of handling.

A preliminary mockup of the overall facility base was constructed with simulated terrain contours prepared from site data. Model construction concentrated on the model base and terrain contours.

Effort will continue on the display models toward a scheduled completion date in April 1960. The model specification was submitted to the AEC for approval.

XI. TASK 16--CONSULTING

The purpose of this task is to secure technical services as required for the PM-1 Project.

The Gibbs and Hill Company provided project support in five main areas during this quarter:

(1) Review of the switchgear, motor control center, turbine-generator unit and condenser work performed by Westinghouse.

(2) Completion of the PM-1 general piping, electrical and welding specifications (MN-2003, MN-2004 and MN-2005, respectively).

(3) Completion of the preliminary Heat Transfer Apparatus Package equipment layout as a basis for the package test program (Task 1.1).

(4) Review of the secondary water chemical treatment system.

(5) Review of the primary loop configuration and erection procedure.

Work accomplished by Gibbs and Hill in the PM-1 steam-electric system area during this quarter is tabulated below:

(1) Completion of the following specifications for review by The Martin Company:

(a) Switchgear and Power Center Transformer--MN-8711

(b) Motor Control Center--MN-8700

(c) Deaerator--MN-8130

(d) D-C and Vital A-C Bus Equipment--MN-8650

(e) Condensate Pumps and Drivers--MN-8120

(f) Secondary System Process Instrumentation and Controls--MN-7601

(g) Evaporator-Reboiler--MN-7322

(h) Feedwater Heater--MN-7740

(i) Feedwater Pumps and Drivers--MN-7750

(j) 125-volt Battery--MN-8640

(k) Turbine Oil Conditioning Equipment--MN-8210

(l) Turbine-Generator Unit--MN-7900

(m) Lube Oil Cooler--MN-8211

(n) Chemical Treatment Equipment--MN-7720

(o) Air Cooled Condenser--MN-8100

(p) Miscellaneous Tanks--MN-8630.

(2) The layouts of the PM-1 Heat Transfer Apparatus Package were begun and are now about 85% complete. These layouts include equipment weights, pipe and valve weights and center of gravity details.

(3) Work continued on the flow diagram, heat balance diagram, control schematics and one-line electric diagram. These diagrams are now 90% complete.

(4) Preliminary reliability data on the secondary steam-electric equipment was completed and is now being reviewed by The Martin Company.

(5) Work continued on the switchgear package layout, general wire tray arrangement, dimensional pipe layout, bill of materials, conduit and cable schedule, tool (standard and nonstandard) list, valve and specialty list, general facility requirements and equipment test requirements. This work is about 50% complete.

During the next quarter, the consulting efforts of Gibbs and Hill will be:

(1) Review of condenser model test procedures.

(2) Development of a general thermal insulation specification.

(3) Review of general primary loop final design.

(4) The vendors for all secondary loop equipment will be selected.

(5) The detailed layout of the heat transfer package, switchgear package, condensers, turbine-generator unit, piping and wiring will be completed except for minor changes which will be required after the receipt of selected vendor certified drawings.

(6) The flow diagrams, heat balance diagrams, control schematics and one-line electrical diagrams will be completed.

(7) The bill of materials, conduit and cable schedule, tool list, general facility requirements, test requirements, valve and speciality list will be completed.

XII. TASK 17--REPORTS

The objective of this Task is to accomplish the timely preparation of reports required by the USAEC.

A. SUBTASK 17.1--HAZARDS REPORTS

G. Zindler

During this reporting period, the first submittal of the PM-1 Hazards Summary Report, MND-M-1853, was made to the USAEC. The document covered:

(1) PM-1 Nuclear Power Plant design summary.

(2) Site environment.

(3) PM-1 Nuclear Power Plant description.

(4) Shielding.

(5) PM-1 Nuclear Power Plant operating procedures.

(6) Hazards evaluation.

An evaluation has been made of the potential hazards associated with the operation of the PM-1 Nuclear Power Plant at Warren Peak, Wyoming. It is shown that the plant operating personnel are protected from radiation hazards through properly designed radiation shielding. The use of detailed operating and maintenance procedures provides a further means of significantly reducing any potential hazards.

The analysis shows the hazards to the general public following an extreme accident to be within generally accepted tolerances. In particular, the population of Sundance, Wyoming, is sufficiently distant so as not to be jeopardized.

As a result of these evaluations, it is believed that the PM-1 Nuclear Power Plant can be operated at the Warren Peak site without undue risk to the general public or to the Sundance Air Force Base personnel.

Following submittal of the hazards report, liaison has continued with the various agencies of the Government during their review of the document.

Anticipated Accomplishments for Next Quarter

No specific efforts are planned during the next quarter. It is expected that continued liaison will be required with the various governmental agencies.

B. SUBTASK 17.2--REPORTS OTHER THAN HAZARDS

E. H. Smith

This subtask includes all reports submitted to the AEC except those on hazards.

During the third project quarter:

(1) The PM-1 Parametric Study Report, MND-M-1852, was distributed.

(2) The PM-1 Preliminary Design Technical Report was completed and distributed.

(3) The second Quarterly Progress Report on the PM-1 Nuclear Power Plant Program, MND-M-1813, was prepared and distributed.

(4) PM-1 technical memoranda were published on the following topics:

   (a) "Packaging and Housing Plan," MND-M-1906

   (b) "Investigation of Reactor Pressure Vessel Materials," MND-M-1901

   (c) "Selection of 347 Stainless Steel for Use in the PM-1 Reactor Pressure Vessel," MND-M-1911.

(5) The program plan for reports was revised, with AEC approval, to substitute technical memoranda for five topical reports originally required. Eight formal topical reports remain on the list.

(6) A plan to report the final design effort in a series of 37 subsystem submittals received AEC approval. (See Task 4, Section III of this report for a list of subsystems.)

During the next project quarter:

(1) A thechnical memorandum on Incore Instrumentation will be prepared and delivered to the AEC.

(2) A topical report on controls and instrumentation will be prepared and distributed.

(3) The third quarterly progress report will be completed and delivered.